Lysozyme natif et chauffé à sec : perturbation de l'intégrité membranaire d'Escherichia coli

Melanie Derde

N° ordre : 2014-18
N° série : B-249

THÈSE/AGROCAMPUS OUEST

Sous le sceau de l'Université Européenne de Bretagne

Pour obtenir le diplôme de

DOCTEUR de l'INSTITUT SUPERIEUR DES SCIENCES AGRONOMIQUES, AGRO-ALIMENTAIRES, HORTICOLES ET DU PAYSAGE

Spécialité : «Science de l'aliment»

École doctorale : «Vie, Agronomie et Santé»

Présentée par :

Melanie DERDE

Lysozyme natif et chauffé à sec : perturbation de l'intégrité membranaire d'*Escherichia coli*

soutenue le 20 octobre 2014 devant la commision d'Examen

Composition du jury :

Véronique	Rosilio	Professeur, Université de Paris Sud, Institut Galien	Rapporteur
Laurent	Miclo	Maître de conférences, Université de Lorraine, INRA	Rapporteur
Françoise	Leroi	Chargée de recherches, IFREMER	Examinateur
Jean-François	Hubert	Professeur, Université de Rennes 1	Examinateur
Françoise	Nau	Professeur, Agrocampus Ouest, INRA	Directeur
Véronique	Vié	Maître de conférences, Université de Rennes 1, IPR	Co-directeur

What is a scientist after all ?
It is a curious man looking through a keyhole,
the keyhole of nature, trying to know what's going on.
Jacques-Yves Cousteau
(1973, Christian Science Monitor)

-

Remerciements

En premier lieu, je souhaite remercier Françoise Nau, directrice de cette thèse, pour son accompagnement tout au long de ces trois années d'aventure scientifique. J'ai beaucoup apprécié nos nombreuses discussions, extrêmement enrichissantes. Son regard critique, sa patience, son soutien et sa confiance m'ont aidée pour réaliser cette thèse. Elle m'a appris ce qu'est être une scientifique et c'est grâce à elle si je le suis devenue, je lui en suis pleinement reconnaissante. Je souhaite également remercier Véronique Vié, qui a particulièrement marqué mon parcours durant cette thèse. Elle m'a fait aimer la biophysique. Toujours prête à aider, rassurer et inventer de nouvelles expériences, elle a fait de mon séjour à l'IPR un vrai bonheur. Aussi, merci Françoise et Véronique pour avoir rendu belles et heureuses ces trois dernières années, pour m'avoir donné la liberté de mettre ma touche personnelle dans ce grand projet et, par-dessus tout, parce que grâce à vous j'ai pu m'épanouir dans mes recherches.

J'adresse également des remerciements à Valérie Lechevalier et Cathérine Guérin pour nos échanges plus qu'intéressants, leurs remarques pertinentes, leur disponibilité et leur gentillesse. Leurs encouragements m'ont toujours aidée à rebondir. Finalement, « ça a marché » !

Je veux également remercier Michel Gautier, Florence Baron et Sophie Jan pour leur encadrement et leur regard critique. Je remercie aussi Véronique Rosilio, Laurent Miclo, Françoise Leroi et François Hubert membres du jury de cette thèse et la région Bretagne pour le financement de ce projet.

Tout au long de ces trois ans, j'ai eu à travailler avec de nombreuses personnes au sein de notre laboratoire. Je veux donc remercier Marie-Françoise Cochet pour son aide et soutien au quotidien, sa gentillesse, pour m'avoir écoutée dans les moments difficiles et pour tous les bons moments passés ensemble. Je n'oublie naturellement pas Clarisse Techer, Noël Grosset et Fabienne Gonnet qui ont toujours été disponibles, avec lesquels j'ai passé de bons moments au laboratoire. Je remercie également Maryvonne Pasco et Claire Prioul pour leur aide, leur disponibilité, les superbes conversations et tous les moments de joie partagés. Je veux également adresser mes remerciements à Gilles Paboeuf. Grâce à lui, les manipulations à l'IPR sont devenues un jeu d'enfant. Sa gentillesse, sa bonne humeur constante ont été une vraie motivation dans le travail quotidien à l'IPR. Je remercie également Guillaume Raffy pour son travail de traitement d'images !

Et - ce n'est pas fini - merci à toutes les autres personnes du laboratoire STLO et de l'IPR qui ont participé à ce travail. Tant de personnes m'ont soutenue et ont marqué ces trois ans qu'il m'est malheureusement impossible de tous les citer ici. Je veux donc également dédier ces remerciements à tous ceux qui ont fait du laboratoire un endroit agréable pour travailler, pour les moments de détente, pour les journées de travail, pour les repas partagés, pour le soutien qu'ils ont pu m'apporter dans les moments difficiles. J'espère avoir pu apporter également un peu de bonne humeur de mon côté. Je n'oublie pas mes stagiaires Bérangère Guidici et Tanja Bertović, qui auront toutes les deux marqué ces trois années de thèse.

Finalement, je veux remercier ma famille. Sans mes parents, je n'aurai jamais pu être là. Leur éducation, la valeur travail qu'ils m'ont communiqué, leur amour et leur dévotion m'ont permis de réaliser des études à la hauteur de mes attentes. J'espère que ce travail les rendra fiers de leur fille comme je suis fière de les avoirs comme parents. En dernier, je remercie Nicolas, mon mari et l'amour de ma vie. Tu as été là aux moments les plus difficiles. Tu m'as poussée à être forte et à faire toujours mieux, à être toujours meilleure. L'aboutissement de ce travail n'est que le début de quelque chose encore plus beau.

Merci à tous pour ces trois années de bonheur, de plaisirs et de science de haut niveau !!!!

Table des matières

Abréviations

AFM	Microscopie à force atomique
AMP	Protéine ou peptide antimicrobien
ATP	Adénosine triphosphate
BAM	Microscopie à angle de Brewster
CAP	Protéine liée à la paroi
CEC	Chromatographie liquide d'échange de cations
CE-HPLC	Chromatographie liquide à haute pression d'échange de cations
CL	Cardiolipine
CMEC	Mélange de phosholipides de la membrane cytoplasmique d'*E. coli*
Conc.	Concentration
CW	Paroi cellulaire (Cell wall)
D8PG	Dioctanoyl-phosphatidylglycérol
DH-L	Lysozyme chauffé à sec
$DiSC_3$	3,3-dipropylthiadicarbocyanine iodide
DOPE	1,2-dioleoyl-sn-glycéro-3-phosphoéthanolamine
DOPG	1,2-dioleoyl-sn-glycéro-3-phospho-(1'-rac-glycérol)
DPC	Dodécylphosphocholine
DPPE	1,2-dipalmitoyl-sn-glycéro-3-phosphoéthanolamine
DPPG	1,2-dihexadécanoyl-sn-glycéro-3-phospho-(1'-rac-glycérol)
DTT	Dithiotréitol
EggPC	L-α-phosphatidylcholine de l'œuf de poule
EtBr	Bromide d'éthidium
Gal	Galactose
Glc	Glucose
GlcN	N-acétylglucosamine
GUV	Vésicules unilamellaires géantes
Hep	L-glycéro-D-manno heptose
HEPES	Acide 4-(2-hydroxyéthyl)-1-piperazineéthanesulfonique
HEWL	Lysozyme de l'œuf de poule
HP-nitrocefin	Produit d'hydrolyse de la nitrocéfine
IMP	Protéine membranaire interne
ISO-L	Fraction d'iso-aspartyles
KdO	Acide 3-désoxy-D-manno-octulosonique
KLA	Lipid A-$(KdO)_2$
LB	Langmuir Blodgett
LB	Luria Broth
LC	Liquide condensé
LE	Liquide expansé
LP	Lipoprotéine

LPS	Lipopolysaccharide
LTA	Acide lipotéichoïque
LUB	Grandes vésicules unilamellaires
Méso-A_2pm	Acide méso-diaminopimélique
MIP	Pression maximale d'insertion
MLV	Vésicules multilamellaires
MRSA	*Staphylococcus aureus* résistant à la méticilline
NAG	N-acétylglucosamine
NAM	Acide N-acétylmuramique
N-L	Lysozyme natif
NL-L	Fraction de lysozyme native-like
NPN	1-N-phénylnapthylamine
OM	Membrane externe
OMP	Protéine membranaire externe
ONP	Ortho-nitrophénol
ONPG	Ortho-nitrophénylgalactoside
PC	Phosphatidylcholine
PE	Phosphatidyléthanolamine
PG	Phosphatidylglycérol
PI	Iodure de propidium
PL	Phospholipide
PM	Membrane cytoplasmique
POPC	1-Palmitoyl-2-oleoylphosphatidylcholine
POPE	1-Palmitoyl-2-oleoylphosphatidyléthanolamine
POPG	1-Palmitoyl-2-oleoylphosphatidylglycérol
SCOP	Classification structurales des protéines
SDS	Dodécyl sulfate de sodium
SIMS	Spectométrie de masse à ions secondaires
SUC-L	Fraction de succinimides
SUV	Petites vésicules unilamellaires
TPP	Tetraphénylphosphonium
TSB	Tryptic soy broth
WTA	Acide téichoïque

Introduction générale et objectifs

De nombreuses molécules antimicrobiennes sont aujourd'hui connues et disponibles. Elles sont présentes dans notre vie quotidienne sous forme d'antibiotiques, de désinfectants, de conservateurs alimentaires... Mais plusieurs problématiques entourent ces molécules omniprésentes, justifiant la recherche de nouvelles solutions.

Dans le domaine médical et vétérinaire, le recours aux antibiotiques qui s'est fortement développé au cours des dernières décennies a contribué à l'apparition de multiples résistances chez des bactéries comme *Staphylococcus aureus*, *Klebsiella pneumoniae*, *Pseudomonas aeruginosa*, *Escherichia coli* et *Enterococcus faecium* (Figure 1). La résistance de ces microorganismes pathogènes rendent la guérison des pathologies dont ils sont responsables difficile, voire même impossible, et souvent coûteuse. Les infections dues à ces bactéries multi-résistantes conduiraient dans l'Union Européenne à des surcoûts liés aux soins et aux pertes de productivité estimés à 1.5 milliard € en 2007 ; 25000 décès seraient par ailleurs imputables annuellement aux infections dues à ces bactéries résistantes. Des pertes économiques dans le secteur agricole doivent également être prises en compte en raison de la mortalité croissante des animaux de rente suite à une infection bactérienne (European Centre for Disease Prevention and Control/European Medicines Agency joint working group, 2009; European commission, 2011). La recherche de nouvelles molécules antibactériennes constitue par conséquent un enjeu important en termes de santé publique, et en termes économiques. Or, depuis 1987, aucune nouvelle classe d'antibactériens n'a été commercialisée (Figure 2 ; Silver (2011)), en raison sans doute du relatif désintérêt des entreprises pharmaceutiques pour développer de nouvelles molécules de ce type. Malgré un marché mondial estimé à 40 milliard de dollars, le développement des antibiotiques est en effet peu intéressant pour ce secteur industriel. Les antibiotiques sont généralement prescrits pour de courtes durées, variant de 3 jours à 2 semaines et leur prescription est de plus évitée au maximum pour limiter le développement de résistance. Par ailleurs, les antibiotiques les plus efficaces actuellement sont presque tous disponibles sous forme de générique, rendant difficile la vente de produits plus chers, même si plus efficaces. Enfin, les essais cliniques sont plus lourds et les coûts de développement plus élevés que pour d'autres molécules pharmacologiques (Brogan & Mossialos, 2013). Il en résulte un manque avéré de développement de nouvelles molécules antimicrobiennes, alors même qu'il serait nécessaire de disposer de stratégies alternatives face aux résistances bactériennes, actuelles ou futures, vis-à-vis des molécules actuellement utilisées.

Dans le domaine alimentaire, les additifs en général, dont les conservateurs, inquiètent 66% des consommateurs européens (données 2010, TNS Opinion & Social (2010)). Les molécules issues de synthèses chimiques en particulier sont perçues négativement (Bruhn, 2002), malgré les procédures complexes d'évaluation mises en place par l'Union Européenne pour leur autorisation de mise sur le marché. Dans le même temps, les consommateurs sont demandeurs de produits alimentaires affichant des durées de conservation toujours plus longues. Or, des aliments sûrs et conservant toutes leurs qualités organoleptiques sur des durées longues nécessitent bien souvent l'addition de conservateurs. Le développement de molécules antimicrobiennes d'origine naturelle pourrait donc contribuer à concilier les attentes et objectifs, parfois contradictoires, de l'industrie alimentaire et du consommateur. Indirectement, ces molécules pourraient également permettre de diminuer les pertes et gaspillages qui représenteraient de 25 à 50 % des produits alimentaires, « de la fourche à la fourchette ». En effet, les pertes et gaspillages seraient moins importants pour les produits affichant une durée de conservation longue (Mena *et al.*, 2011).

La recherche et la caractérisation de nouvelles molécules antimicrobiennes apparaissent ainsi nécessaires. Et une priorité semble pouvoir être donnée aux molécules à la fois naturelles et limitant le risque de développement de résistance. Les protéines et peptides antimicrobiens, présents dans une extraordinaire diversité de milieux biologiques comme le venin d'abeille,

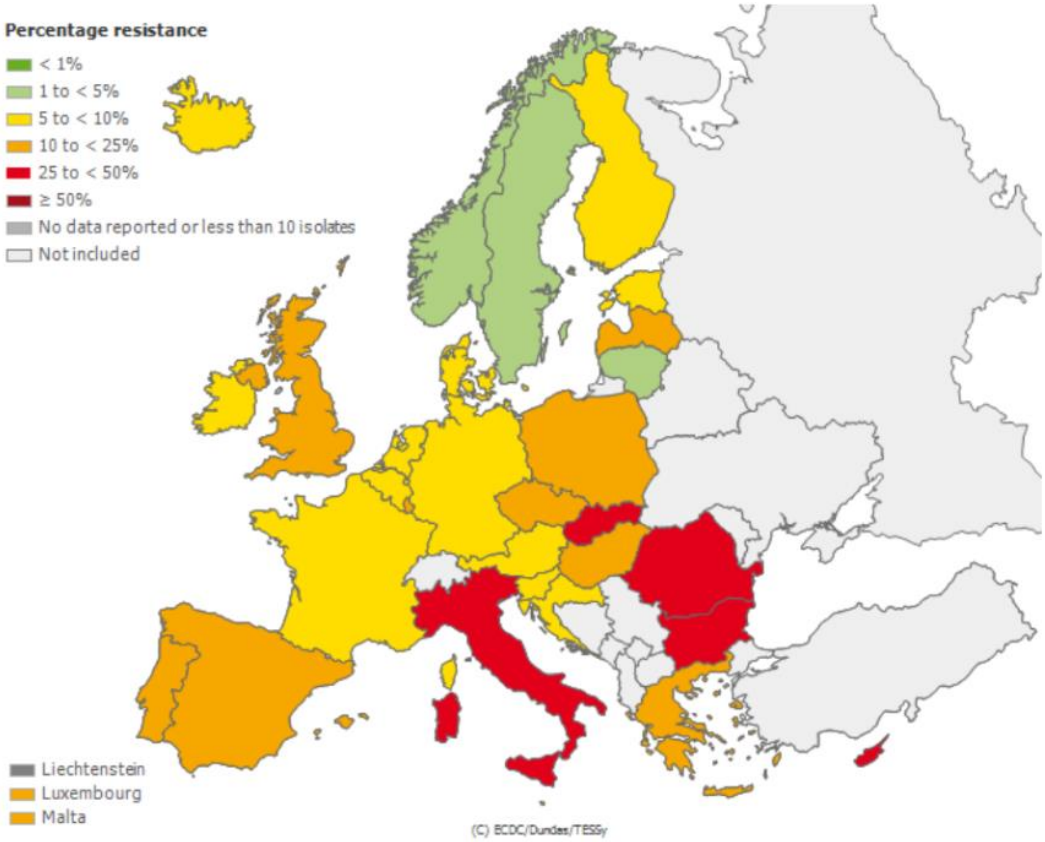

Figure 1 – Pourcentages de résistance aux céphalosporines de troisième génération mesurés en Europe parmi des souches isolées et invasives d'*Escherichia coli* (données 2012, European Centre for Disease Prevention and Control).

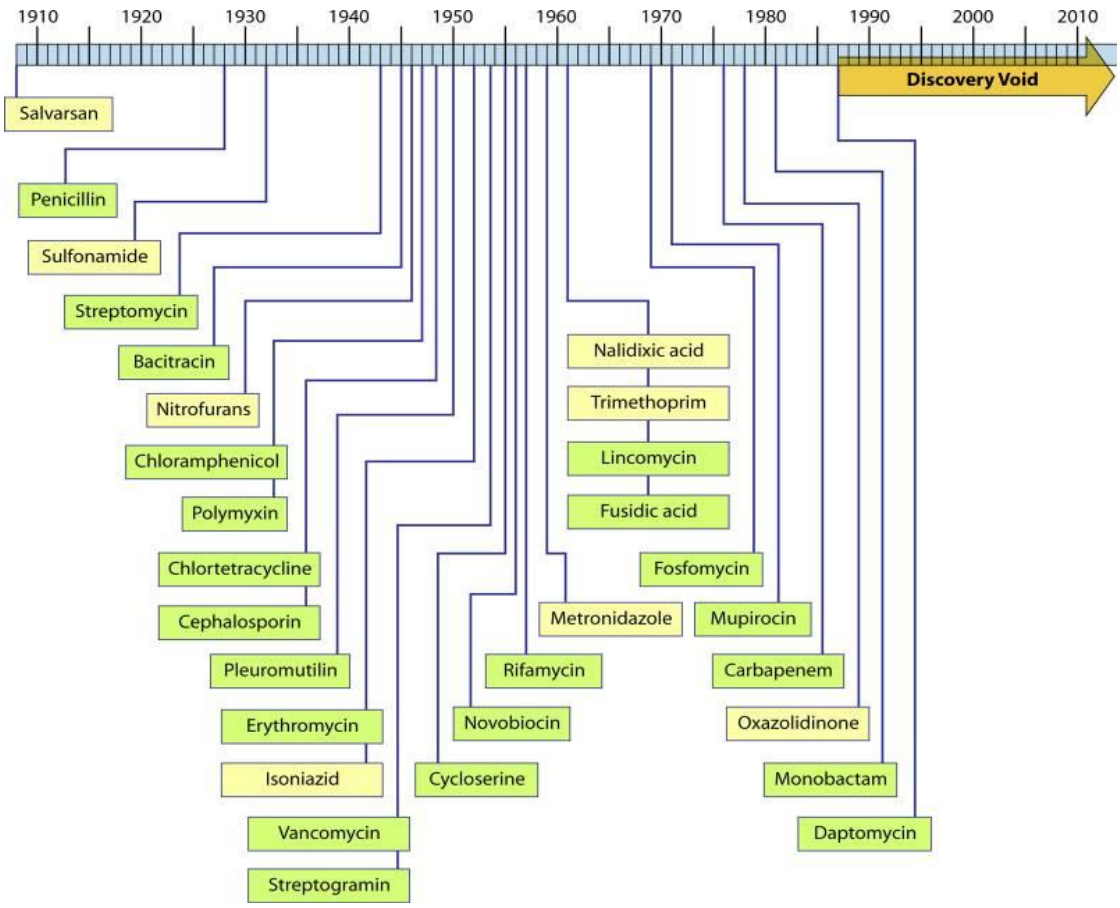

Figure 2 – Chronologie des découvertes de classes d'antibactériens commercialisés depuis 1900. Les dates indiquées sont celles de la première mention de chaque molécule et non celles des mises sur le marché (Silver, 2011).

la peau de grenouille, ou encore les larmes, sont a priori de bons candidats respectant ces conditions. En effet, le développement de résistances vis-à-vis de ces molécules devrait être limité, du fait de leurs modes d'action impliquant souvent la perturbation des membranes bactériennes, car pour la plupart des espèces bactériennes, il paraît difficile de mettre en place rapidement des stratégies de défense contre des attaques ciblant leurs membranes. Par ailleurs, les protéines et peptides antimicrobiens ont souvent un large spectre d'activité (Nguyen *et al.*, 2011).

La première protéine antimicrobienne fut découverte en 1922 par Fleming ; il s'agissait du lysozyme (Fleming, 1922; Nakatsuji & Gallo, 2012). Le lysozyme est une enzyme présente dans des tissus et de très nombreux fluides biologiques comme le lait, les larmes, ou encore le mucus nasal. Mais l'une des sources les plus riches en lysozyme est le blanc d'œuf, et c'est tout naturellement que le lysozyme du blanc d'œuf est le plus étudié depuis maintenant près d'un siècle. Les propriétés antibactériennes de cette protéine sont largement et depuis longtemps décrites dans la littérature. Elles sont également très utilisées dans des applications pharmaceutiques et alimentaires variées.

Par rapport aux autres types de lysozyme, celui extrait du blanc d'œuf de poule offre plusieurs avantages, dont le premier est sa disponibilité à l'échelle industrielle à un prix relativement modéré (100 €/kg). Par ailleurs, cette protéine est déjà référencée en tant que conservateur (E1105) et autorisée par l'Union Européenne (directive 95/2/EG) dans la fabrication de fromages et de vins. Ceci est a priori favorable à l'obtention d'autorisations d'usages pour d'autres produits alimentaires. Elle est également autorisée en applications pharmaceutiques, notamment pour le traitement de pathologies bénignes de la sphère buccale (Table 1).

Table 1 – Liste des produits pharmaceutiques à base de lysozyme autorisés en France (ANSM base de donnée des médicaments autorisés, 23/06/2014).

Nom commercial du produit	**Fabricant**
Lysopaine®	Boehringer Ingelheim
Oroseptol lysozyme®	GlaxoSmithKlein
Lyso6®	Pierre Fabre
Lysocalmspray®	Pierre Fabre

Pour ces applications alimentaires et pharmaceutiques, le lysozyme est utilisé en raison de son activité lytique vis-à-vis des liaisons entre l'acide N-acétylmuramique et la N-acétylglucosamine du peptidoglycane des bactéries. Cette activité est à l'origine de son pouvoir bactéricide vis-à-vis des bactéries à coloration de Gram positive (Masschalck & Michiels, 2003). Mais le lysozyme est également actif contre certaines bactéries à coloration de Gram négative, indépendamment de l'activité enzymatique évoquée ci-dessus. Plusieurs auteurs suggèrent entre autre que le lysozyme induit une perte de l'intégrité membranaire des bactéries (Düring *et al.*, 1999; Pellegrini *et al.*, 2000; Wild *et al.*, 1997), mais les modalités d'action restent largement méconnues.

L'action du lysozyme sur les bactéries à coloration de Gram négative est généralement de moindre ampleur par rapport à son activité hydrolytique vis-à-vis des bactéries à coloration de Gram positive (Pellegrini *et al.*, 1992). La littérature fait toutefois mention de modifications biochimiques du lysozyme susceptibles d'accroître son efficacité vis-à-vis des bactéries à coloration de Gram négative. Les modifications évoquées sont la fusion avec des groupes chimiques spécifiques (Ibrahim *et al.*, 1991, 1993, 1994a; Nakamura *et al.*, 1991, 1992), la protéolyse (Ibrahim *et al.*, 2001b; Mine *et al.*, 2004), ou encore la dénaturation thermique

(Ibrahim *et al.*, 1996a,b; Ibrahim, 1998). Elles impliquent toutes des modifications des caractéristiques physicochimiques du lysozyme. L'augmentation d'hydrophobie est notamment souvent évoquée comme l'un des paramètres expliquant l'accroissement de l'activité antibactérienne du lysozyme.

Le chauffage à sec, c'est-à-dire sous forme de poudre, est un procédé industriel classiquement utilisé pour diminuer la charge bactérienne et/ou virale d'un produit lorsque celui-ci ne permet pas aisément un traitement à l'état liquide. Ce type de procédé est ainsi appliqué au blanc d'oeuf en poudre, ainsi qu'à des produits médicamenteux divers (Hammershøj *et al.*, 2006; Roberts *et al.*, 2007; Skidmore *et al.*, 1990). Dans le cas du blanc d'œuf, il est également mis en oeuvre pour améliorer les propriétés techno-fonctionnelles du produit (pouvoir moussant et gélifiant) (Desfougères *et al.*, 2008; Kato *et al.*, 1990; Mine, 1996, 1997; Van der Plancken *et al.*, 2007). Dans ce cas, les traitements appliqués sont de l'ordre de quelques jours à 80°C environ. Lorsqu'un tel traitement (7 jours à 80°C) est appliqué au lysozyme, des modifications chimiques interviennent, aboutissant à un mélange d'isoformes de la protéine : « iso-aspartyles », « native-like » et « succinimides » (Desfougères *et al.*, 2011a). Ces isoformes du lysozyme ont des caractéristiques physicochimiques différentes de celles du lysozyme natif. Certaines présentent notamment une hydrophobie et une flexibilité supérieures, associées à des propriétés interfaciales accrues (Desfougères *et al.*, 2011a,b). L'augmentation de l'hydrophobie et de la flexibilité moléculaire permettent d'envisager une augmentation de l'activité antibactérienne des isoformes en question par rapport à la protéine native. La perturbation des membranes bactériennes par les protéines et peptides antimicrobiens est en effet généralement basée sur une cascade de phénomènes faisant intervenir une attraction électrostatique entre la protéine (ou le peptide) et la paroi bactérienne, nécessitant des modifications structurales facilitées par une flexibilité élevée et conduisant à l'insertion de la protéine dans les membranes bactériennes via des interactions hydrophobes (Nguyen *et al.*, 2011). Le chauffage à sec pourrait ainsi s'avérer être un procédé technologique simple permettant de moduler et/ou augmenter l'efficacité antibactérienne du lysozyme vis-à-vis des bactéries à coloration de Gram négative.

Afin d'explorer les possibilités d'utilisation du lysozyme en tant qu'agent antimicrobien contre les bactéries à coloration de Gram négative, il nous a semblé opportun d'approfondir l'hypothèse d'une action de cette protéine sur les membranes bactériennes. Le lysozyme est-il capable de perméabiliser ces membranes ? Sous quelles conditions ? Via quels mécanismes ? Par ailleurs, compte tenu des caractéristiques physicochimiques particulières des isoformes du lysozyme résultant du chauffage à sec, il nous a paru intéressant d'explorer les propriétés antibactériennes du lysozyme ainsi modifié. Ces modifications sont-elles à même de moduler et/ou amplifier les propriétés antibactériennes de la protéine ? Les formes modifiées du lysozyme interagissent-elles de façon différente et spécifique avec les membranes bactériennes ? Quelles sont les caractéristiques structurales et/ou physicochimiques à l'origine des différences éventuelles de comportement de la protéine vis-à-vis des membranes bactériennes ?

Ce travail s'inscrit ainsi dans la perspective d'une meilleure compréhension des mécanismes à la base des interactions moléculaires entre le lysozyme et les membranes des bactéries à coloration de Gram négative, que la protéine soit dans sa forme native ou sous des formes modifiées. Pour répondre à ces différentes questions, nous avons combiné des approches *in vivo*, c'est-à-dire sur les bactéries elles-mêmes, et des approches *in vitro*, c'est-à-dire sur des modèles membranaires à base de monocouches lipidiques. Nous avons également associé des méthodes microbiologiques, biochimiques et biophysiques. Cette stratégie, dont l'objectif était de répondre à des questionnements de type mécanistique, en lien avec des activités biologiques avérées, est schématisée ci-dessous (Figure 3). Le travail a ainsi été décomposé en trois grandes parties, abordant successivement 1) l'activité antimicrobienne du lysozyme vis-à-vis

d'*Escherichia coli* en lien avec la perte d'intégrité membranaire, 2) les interactions du lysozyme avec les monocouches lipidiques, modèles des membranes bactériennes et l'impact sur leur organisation, et 3) l'activité spécifique de chacune des isoformes constitutives du lysozyme chauffé à sec. En amont de la présentation et de la discussion des résultats obtenus au cours de cette étude, un état de l'art bibliographique a également été dressé, rappelant les éléments majeurs concernant d'une part le lysozyme, et d'autre part les membranes bactériennes, avec une attention particulière accordée aux méthodes décrites pour leur étude.

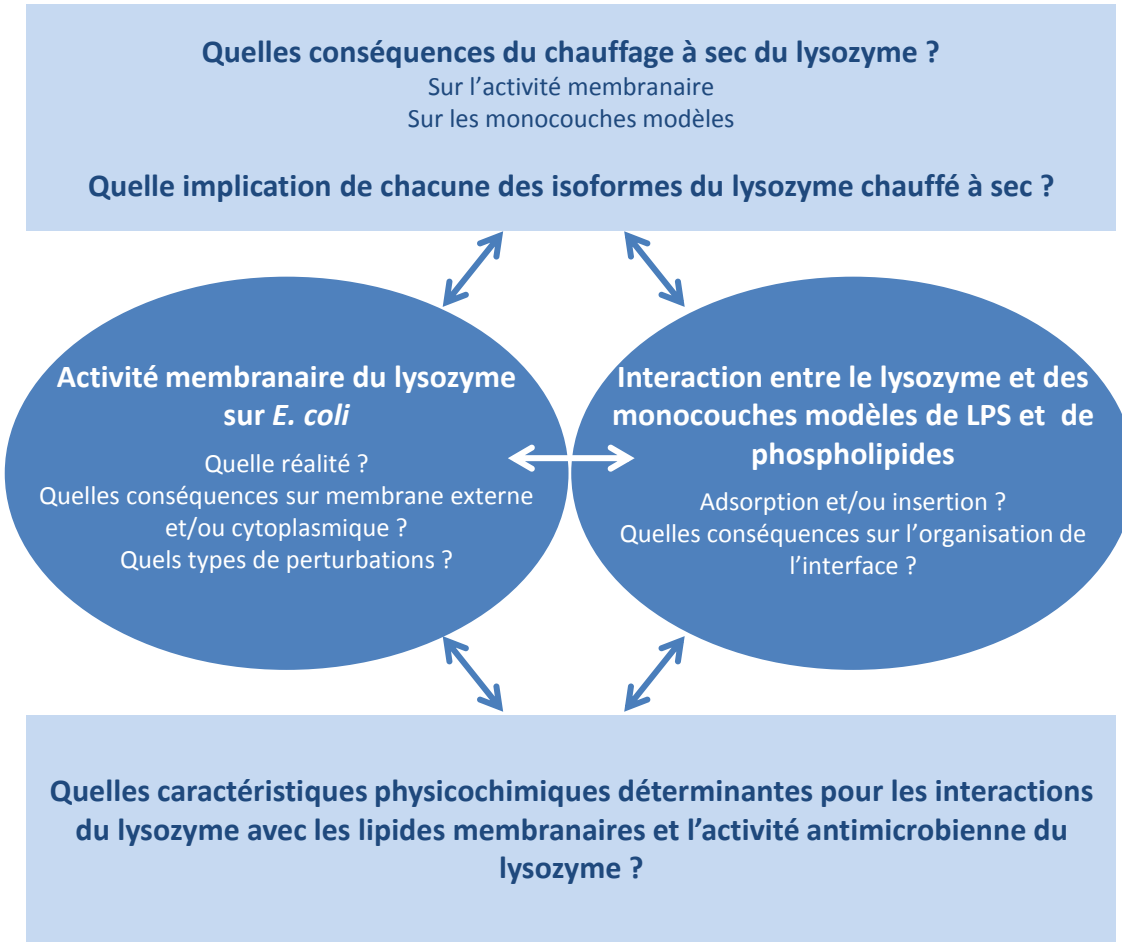

Figure 3 – Schématisation de la stratégie de recherche de cette étude.

Chapitre 1

Étude bibliographique

1.1 Protéines et peptides antimicrobiens

Les protéines et peptides antimicrobiens sont aujourd'hui largement étudiés car envisagés comme l'une des solutions possibles face aux souches bactériennes multirésistantes, alors même que le développement de nouvelles molécules antimicrobiennes est très limité depuis plus de 20 ans. La découverte des protéines et peptides antimicrobiens d'origine naturelle date de 1922 quand Alexander Fleming découvrit le lysozyme (Fleming, 1922; Nakatsuji & Gallo, 2012). Depuis, plus de 2000 protéines et peptides antimicrobiens naturels ont été décrits (Antimicrobial peptide database, (Wang, 2014)).

1.1.1 Caractéristiques physicochimiques et structurales des protéines et peptides antimicrobiens

Ces peptides et protéines sont généralement des molécules cationiques, amphiphiles, hydrophobes et flexibles (Brogden, 2005; Jenssen *et al.*, 2006; Melo *et al.*, 2009; Nguyen *et al.*, 2011). Les peptides antimicrobiens peuvent être classés, sur la base de leur structure secondaire, en cinq catégories : 1) les peptides à hélices α, 2) les peptides à feuillets β, 3) les peptides à épingles β ou boucles 4) les peptides cycliques et 5) les peptides « étendus » (Jenssen *et al.*, 2006; Melo *et al.*, 2009; Nguyen *et al.*, 2011; Seo *et al.*, 2012; Teixeira *et al.*, 2012).

Pour les peptides antimicrobiens avec une structure en **hélices** α, le caractère amphiphile est généralement déterminé par rapport à l'axe de l'hélice : l'une des faces de l'hélice est majoritairement hydrophobe alors que la face opposée est majoritairement hydrophile. Ces peptides sont de longueur semblable à l'épaisseur des bicouches membranaires (Nguyen *et al.*, 2011). La structure hélicoïdale est souvent présente uniquement lorsque le peptide est dans l'environnement membranaire, et absente lorsqu'il est en solution aqueuse (Seo 2012). La mélittine, la magainine et le peptide LL-37 sont des exemples de peptides de cette catégorie (Figure 1.1A).

La structure des peptides en **feuillets** β est stabilisée par au moins deux ponts disulfures. Ces ponts disulfures ne sont toutefois pas indispensables pour l'activité antimicrobienne de ces peptides (Nguyen *et al.*, 2011). La lactoferricine et la protégrine 1 font partie de cette famille de peptides (Figure 1.1B).

Les peptides dont la structure est caractérisée par la présence d'**épingles** β **ou de boucles** sont stabilisés dans leur conformation par un pont disulphure. Un exemple de peptide de ce type est la thanatine (Figure 1.1C) (Jenssen *et al.*, 2006; Seo *et al.*, 2012).

Les peptides **cycliques** sont caractérisés par la présence d'une cyclisation de leur chaîne peptidique. La gramicidine S et la polymyxine B sont des exemples de peptides de ce type (Teixeira *et al.*, 2012).

Les peptides dits « **étendus** » se caractérisent par l'absence de structures secondaires. Ils sont souvent riches en arginine, tryptophane, histidine ou proline (Nguyen *et al.*, 2011; Seo *et al.*, 2012). L'indolicidine est un exemple de ce type de peptide (Figure 1.1D).

En dehors de ces 5 catégories, il existe des protéines et peptides antimicrobiens associant plusieurs de ces structures.

1.1.2 Mécanismes à l'origine de l'activité antibactérienne

Les protéines et peptides antimicrobiens ont généralement des spectres d'activité larges. Ils peuvent avoir des activités antibactériennes, antifongiques et/ou antivirales. L'activité antibactérienne de ces molécules naturelles est principalement due à la rupture des membranes

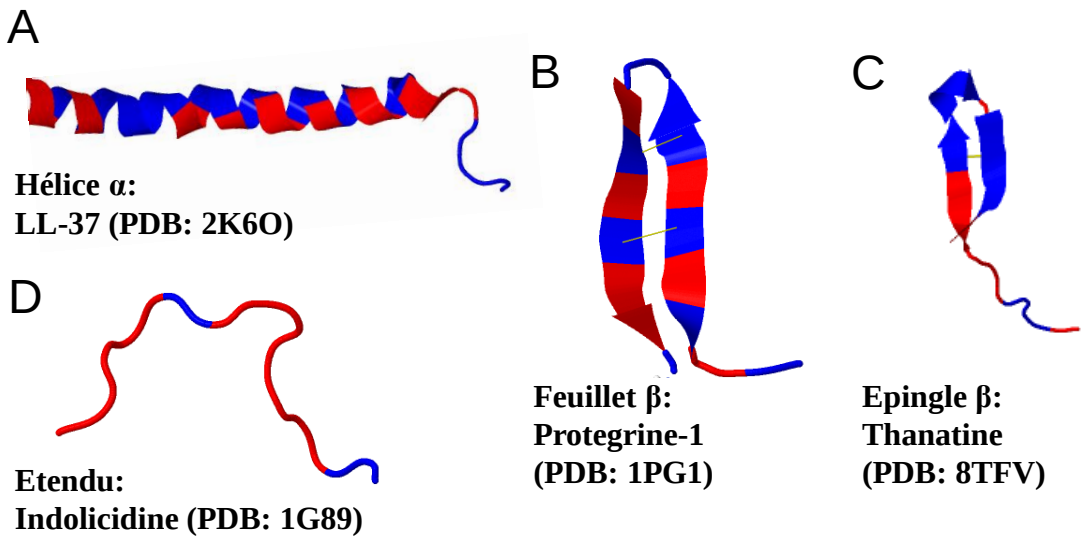

Figure 1.1 – Classes structurales des peptides antimicrobiens.(A) Peptides en hélices α représentés ici par la structure du peptide LL-37 (PDB 2K6O) en présence de micelles de dodécylsulfate de sodium (SDS) et de dioctanoyl-phosphatidylglycérol (D8PG) ; (B) Peptides en feuillets β représentés ici par la protegrine-1 (PDB 1PG1) en solution ; (C) Peptides en épingles β représentés ici par la thanatine (PDB 8TFV) en solution ; (D) Peptides étendus représentés ici par l'indolicidine (PDB 1G89) en présence de micelles de SDS et de dodecylphosphocholine (DPC). Les zones faiblement hydrophobes sont représentées en bleu, celles fortement hydrophobes en rouge (http ://www.uniprot.org/).

bactériennes qu'elles engendrent, parfois combinée à des effets sur des cibles intracellulaires. Les peptides étendus peuvent quant à eux traverser les membranes bactériennes sans perturber leur intégrité, pour ensuite interagir avec des cibles intracellulaires (Hancock & Sahl, 2006; Jenssen *et al.*, 2006; Nguyen *et al.*, 2011).

L'interaction entre les protéines ou peptides antimicrobiens et les membranes bactériennes fait intervenir quatre étapes successives (Brogden, 2005; Melo *et al.*, 2009; Zasloff, 2002) :

- **Attraction et fixation** : Chargés positivement au pH physiologique, du fait de leurs pI basiques, les protéines et peptides antimicrobiens sont attirés par les molécules électronégatives présentes à la surface des bactéries, qu'il s'agisse des lipopolysaccharides dans le cas des bactéries à coloration de Gram négative, ou des acides teichoïques dans le cas des bactéries à coloration de Gram positive. Les interactions électrostatiques seraient ainsi largement impliquées dans la fixation des protéines et peptides antimicrobiens sur les membranes bactériennes
- **Insertion et permeabilisation** : Chaque protéine ou peptide antimicrobien se caractérise par une concentration seuil en-deça de laquelle la molécule se fixe parallèlement à la membrane. Au-delà de cette concentration seuil, les protéines et peptides antimicrobiens peuvent dans certains cas s'insérer dans la membrane lipidique et la perméabiliser.

La perméabilisation membranaire peut se faire selon plusieurs mécanismes comme représenté dans la Figure 1.2 (Teixeira *et al.*, 2012; Nguyen *et al.*, 2011) ; ces mécanismes peuvent coexister pour un même peptide ou une même protéine. Les mécanismes se divisent en deux groupes selon qu'il y a ou non une activité membranolytique (Teixeira *et al.*, 2012). Les mécanismes membranolytiques incluent les pores « barrel-stave », les pores toroïdaux, les pores

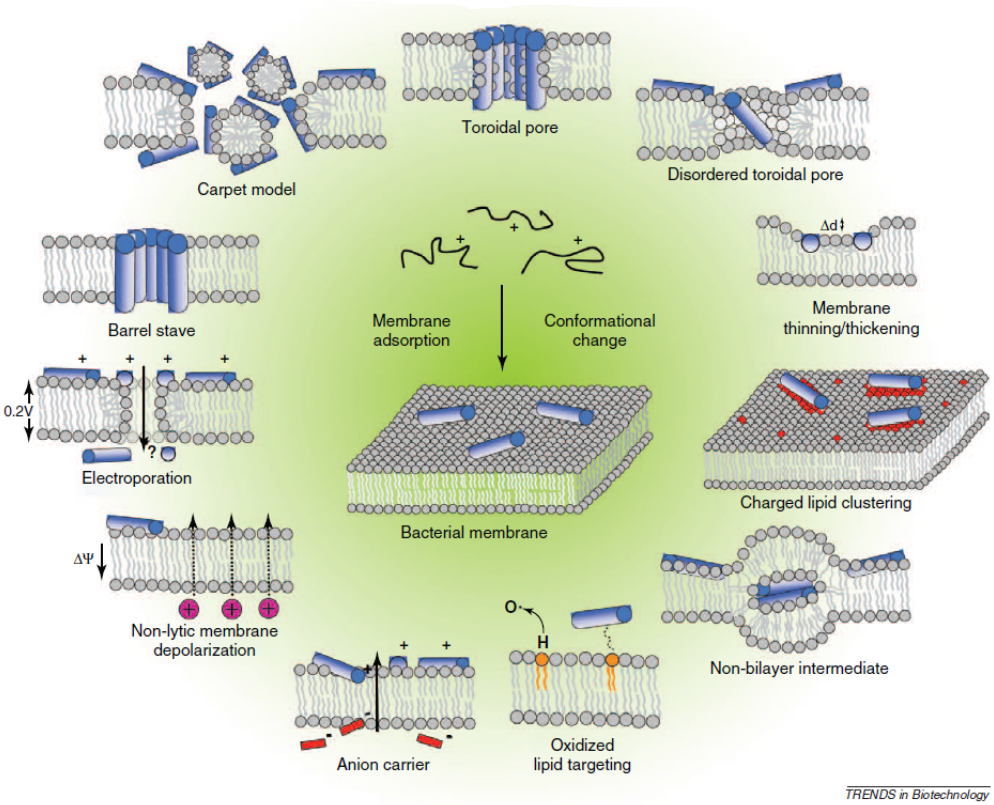

Figure 1.2 – Représentation des différents mécanismes d'action des peptides antimicrobiens vis-à-vis des membranes bactériennes (Nguyen *et al.*, 2011).

toroïdaux désordonnés et le modèle dit « carpet » :

- Les **pores « barrel-stave »** sont observés pour des peptides comme l'alaméthicine et la zervamicine. Après l'adsorption à la membrane, les peptides subissent un changement de conformation, déplacent les têtes lipidiques et induisent un amincissement local de la bicouche lipidique. La partie hydrophobe du peptide est alors insérée dans le premier feuillet de la membrane. Une fois la concentration seuil dépassée, les monomères peptidiques s'associent entre-eux et les agrégats ainsi formées s'insèrent profondément dans la membrane. L'association des peptides continue sous l'influence de la tension créée sur les lipides et du potentiel membranaire. Finalement, un pore transmembranaire est formé. Les parties hydrophobes des peptides sont orientées vers les chaines aliphatiques et les parties hydrophiles tapissent l'intérieur du pore (Teixeira *et al.*, 2012).

- Les **pores toroïdaux** sont identifiés pour les peptides comme les magainines, les protégrines et la mélittine. Les peptides se répartissent dans la membrane bactérienne : les parties hydrophiles des peptides s'associent avec les têtes polaires des lipides et induisent ainsi une courbure de la membrane. Le pore résultant est tapissé de peptides et de têtes lipidiques. Une continuité est créée entre les deux feuillets membranaires (Melo *et al.*, 2009; Teixeira *et al.*, 2012). Des simulations de dynamique moléculaire suggèrent une réevaluation du dernier modèle. Ces analyses réalisées pour des analogues des magainines et la mélittine montrent la formation de pores plus désordonés : les **pores toroïdaux désordonnés**. La courbure des lipides en présence des peptides résulte toujours de la liaison entre les deux feuillets membranaires ; en revanche, un ou deux peptides seraient positionnés à l'interieur du pore à la hauteur du feuillet externe de la membrane (Nguyen *et al.*, 2011).

- Dans le **modèle « carpet »**, les peptides couvrent la surface de la membrane, jusqu'à atteindre une concentration seuil. Les peptides s'insèrent alors dans la membrane, formant des pores toroïdaux transitoires, ce qui libère de la place pour l'adsorption d'autres peptides. Finalement, la membrane se désintègre en formant des micelles tapissées de peptides (Melo *et al.*, 2009; Nguyen *et al.*, 2011; Teixeira *et al.*, 2012). Ce modèle explique l'activité des cécropines, de la dermaseptine et de l'ovispirine.

Les mécanismes membranolytiques ne permettent pas pour d'expliquer l'activité antimicrobienne de tous les peptides. C'est pourquoi d'autres mécanismes, non-membranolytiques, sont proposés :

- Après adsorption, les peptides cationiques peuvent attirer des lipides anioniques. Le mécanisme est nommé **ségrégation lipidique ou « lipid clustering »**. La ségrégation lipidique conduit à des défauts membranaires et à la perméabilisation de la membrane. La présence des peptides à la surface de la membrane peut également induire une **dépolarisation membranaire** (Epand *et al.*, 2010; Teixeira *et al.*, 2012).
- Le peptide NK-lysin agit par un modèle d'**électroporation moléculaire**. Le peptide chargé s'adsorbe à la surface membranaire. Sa densité de charge est suffisante pour créer un potentiel électrostatique supérieur à 0.2 V de part et d'autre de la membrane, ce qui entraîne la perforation dans cette dernière (Miteva *et al.*, 1999).
- Certains peptides du système immunitaire inné des organismes multicellulaires comme les temporines B et L s'intercalent plus particulièrement entre les lipides oxydés, en raison probablement de la formation de bases de Schiff entre les acides aminés et les aldéhydes des lipides oxydés. Ce mécanisme est nommé **ciblage des lipides oxydés** L'oxydation lipidique pourrait entervenir durant la phagocytose à cause de la présence de l'oxygène réactif rendant ces peptides plus efficaces contre la bactérie (Mattila *et al.*, 2008).

En complément de leur action sur les membranes bactériennes, les protéines et peptides antibactériens peuvent également avoir des cibles intracellulaires (Brogden, 2005; Hancock & Sahl, 2006; Jenssen *et al.*, 2006; Nguyen *et al.*, 2011). L'interaction avec ces cibles peut entraîner selon les cas l'inhibition de la synthèse de la paroi bactérienne, l'inhibition de la formation du septum pendant la division cellulaire, l'activitation des autolysines, la fixation à l'ADN, l'inhibition de la synthèse de l'ADN/ARN ou de la synthèse protéique, ou encore l'inhibition d'enzymes intracellulaires.

1.1.3 Stratégies de résistance des bactéries face aux protéines et peptides antimicrobiens

Cibles privilégiées des protéines et peptides antimicrobiens, les membranes bactériennes sont des structures très conservées. La modification de leur organisation et de leur composition paraît difficile pour la plupart des espèces bactériennes (Lohner, 2009; Zasloff, 2002). De plus, l'action des protéines et peptides antimicrobiens est souvent très rapide, et les bactéries n'ont donc pas le temps de s'adapter au stress induit (Lohner, 2009). Si le développement de stratégies de résistance des bactéries contre les protéines et peptides antimicrobiens reste donc limité, il n'est toutefois pas impossible. Perron *et al.* (2006) ont par exemple démontré la mise en place de mécanismes de résistance au peptide antimicrobien pexiganane chez *Pseudomonas fluorescens* et *Escherichia coli*. Plusieurs formes de résistance naturelle ont en réalité été décrites (Brogden, 2005; Gruenheid & Le Moual, 2012) :

- **Dégradation protéolytique des protéines et peptides antimicrobiens** par des protéases localisées sur la membrane externe des bactéries, ou sécrétées. Après hydrolyse, les molécules antibactériennes s'avèrent inactives. *Staphylococcus aureus* produit ainsi l'aureolysine qui peut hydrolyser le peptide LL-37 (Sieprawska-Lupa, 2004). *E. coli* possède quant à lui dans la membrane externe des protéases comme OmpT ; chez *E. coli* K12, cette protéase est capable de dégrader la protamine (Stumpe *et al.*, 1998).

- **Écrantage de la surface bactérienne** : Certaines structures externes de l'enveloppe bactérienne comme les exopolysaccharides, les fimbriae ou les groupements O-antigènes des lipopolysaccharides peuvent piéger les protéines et peptides antimicrobiens. La concentration de molécules antimicrobiennes libres dans le milieu, et donc susceptibles d'atteindre les membranes bactériennes, se trouve alors diminuée. L'alginate, un exopolysaccharide de *Pseudomonas aeruginosa*, est ainsi capable d'inhiber l'activité bactéricide du peptide LL-37 en le séquestrant (Foschiatti *et al.*, 2009).

- **Modifications de la membrane bactérienne** : Plusieurs espèces bactériennes sont capables de modifier la charge globale de leur membrane. C'est le cas par exemple de *Staphylococcus aureus* dont la charge nette négative de la paroi bactérienne peut diminuer (Kristian *et al.*, 2003; Peschel, 2001). D'autres sont à même de modifier la nature de leurs lipides membranaires. Ainsi, *Salmonella typhimurium* peut changer les chaînes lipidiques du lipide A, renforçant la barrière que constitue la membrane externe (Guo, 1998).

- **Systèmes impliquant des transporteurs moléculaires** : Chez *Salmonella typhimurium*, la résistance à la mélittine et à la protamine fait intervenir la protéine SapABCDF, qui est un transporteur de la famille ABC (ATP-binding cassette) ; ce transporteur permet l'entrée de la protéine ou du peptide dans la bactérie. Deux hypothèses sont alors évoquées dans la littérature : les molécules antibactériennes seraient soit dégradées par des protéases intracellulaires, soient liées à un récepteur qui activerait une cascade de réactions à l'origine du mécanisme de résistance (Groisman, 1994). À l'inverse, chez d'autres espèces bactériennes comme *Neisseria gonorrhoeae*, des pompes à efflux de type RND (resistance nodulation cell division) seraient impliquées dans la résistance contre les protéines et peptides antimicrobiens (Nikaido, 2003; Shafer *et al.*, 1998) ; ces pompes permettraient l'excrétion des molécules antimicrobiennes ayant traversé les membranes bactériennes.

1.1.4 Limites à l'utilisation des protéines et peptides antimicrobiens

Même si les protéines et peptides antimicrobiens sont souvent présentés dans la littérature comme des molécules prometteuses, notamment en substitution ou complément des antibiotiques actuellement disponibles, très peu sont aujourd'hui en phase de tests cliniques (Tableau 1.1). Les protéines et peptides antimicrobiens présentent en effet un certain nombre d'inconvénients. Ainsi ils ne résistent pas au processus de digestion, limitant leur utilisation par voie orale (Seo *et al.*, 2012; Zasloff, 2002). Pour pallier cette difficulté, certains auteurs suggèrent d'incorporer dans leurs séquences des acides aminés rares, ou de substituer certains des acides aminés par leurs énantiomères D pour rendre les peptides ou protéines résistants à l'hydrolyse gastro-intestinale (Hamamoto *et al.*, 2002; Meng & Kumar, 2007). Par ailleurs, la purification des protéines et peptides à partir de leurs milieux biologiques d'origine est rarement simple, donc souvent coûteuse. Et les peptides synthétiques sont également souvent très couteux. Mais surtout, la toxicité potentielle pour l'homme de certaines de ces molécules pose question (Seo *et al.*, 2012; Zasloff, 2002). Des études de toxicité s'imposent donc dans tous les cas avant de pouvoir envisager des études cliniques avec ces molécules. Il convient cependant de souligner que, malgré tous ces inconvénients, des peptides antimicrobiens comme la gramicidine, la polymyxine et la daptomycine sont sur le marché depuis plusieurs années.

Table 1.1 – Peptides antimicrobiens en phase de tests cliniques ou en développement (Fox, 2013).

Peptide	Phase du test clinique	Indication
Pexiganane	3	Ulcère du pied chez les patients diabétiques
Omiganane	2	Rosaceae
OP-145	2	Infection bactérienne chronique de l'oreille moyenne
Novexatine	1/2	Mycose d'ongles de pied
Lyxitar	1/2	*Staphylococcus aureus* résistant à la méticilline (MRSA)
NVB302	1	*Clostridium difficile*
MU1140	préclinique	Bactéries à coloration de Gram positive (MRSA, *C. difficile*)
Arenicine	préclinique	Bactéries à coloration de Gram positive multirésistantes
Avidocine	préclinique	Antibiotique à spectre étroit
Purocine	préclinique	Antibiotique à spectre étroit
IMX924	préclinique	Antibiotique à large spectre

1.2 Le lysozyme, première protéine antibactérienne découverte

1.2.1 Structure du lysozyme d'œuf de poule

Le lysozyme du blanc d'œuf de poule (E.C. 3.2.1.17) est une petite protéine globulaire de 129 résidus d'acides aminés, d'une masse moléculaire de 14.3 kDa (Uniprot database, 2014). Généralement sous forme monomèrique, il existe également sous forme dimérique (Onuma & Inaka, 2008). Le lysozyme du blanc d'œuf de poule fait partie des lysozymes de type c et appartient à la famille des glycosyl hydrolases (Uniprot database, 2014). Son point isoélectrique est particulièrement élevé (10,7) en raison de la présence en grand nombre de résidus d'arginine et de lysine (Alderton *et al.*, 1945). À pH physiologique (pH $\approx$ 7), le lysozyme est donc chargé positivement. Cette protéine se caractérise également par sa très grande rigidité en raison des 4 ponts disulfures intramoléculaires (Cys^{6}-Cys^{127}, Cys^{30}-Cys^{115}, Cys^{64}-Cys^{80} et Cys^{76}-Cys^{94}) qui stabilisent sa structure tertiaire (Figure 1.3A) (Canfield & Liu, 1965).

La structure du lysozyme a été la première structure protéique résolue par diffraction des rayons X dès 1965 (Blake *et al.*, 1965), ensuite confirmée et précisée par plusieurs auteurs (Fischmann *et al.*, 1991; Moult *et al.*, 1976). Le lysozyme est une protéine ellipsoïdale de 3 x 3 x 4.5 nm (Figure 1.3C)(Diamond, 1974). Il appartient à la classe SCOP (Structural Classification Of Proteins) « $\alpha + \beta$ ». La région α comprend 4 hélices α et 1 hélice 3_{10} C-terminale. La région β comprend quant à elle 1 feuillet β avec 3 brins, 1 hélice 3_{10} et une longue boucle (Figure 1.3B).

1.2.2 Activité antibactérienne du lysozyme

Activité muramidase

Le lysozyme est avant tout connu pour son activité enzymatique. Cette enzyme hydrolyse les liaisons $\beta(1,4)$ entre l'acide N-acétylmuramique et la N-acétylglucosamine du peptidoglycane bactérien. Or, le peptidoglycane est une structure essentielle à la cellule bactérienne, qui maintient la forme cellulaire et protège la bactérie contre les différences de pression osmotique avec le milieu environnant. En hydrolysant ce maillage, le lysozyme ne permet donc plus à la bactérie de résister aux chocs osmotiques, conduisant à l'éclatement de la cellule et finalement à la mort bactérienne (Masschalck & Michiels, 2003).

Le site actif du lysozyme peut fixer un hexasaccharide (résidus A, B, C, D, E et F) dans 6 sous-sites de fixation. L'hydrolyse intervient entre les résidus D et E. Parmi les 12 résidus

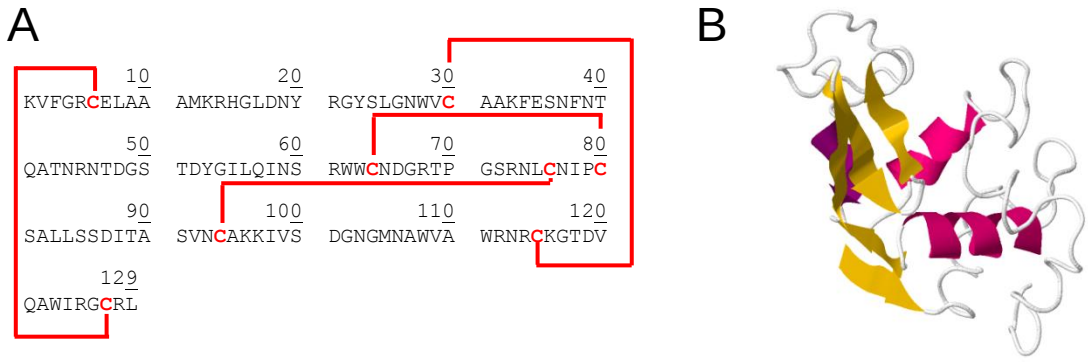

Figure 1.3 – Structure du lysozyme d'œuf de poule. (A) Séquence primaire (Swisprott P00698) sur laquelle les résidus cystéine et les ponts disulfures sont indiqués en rouge ; (B) Représentation 3D mettant en évidence les éléments de structures secondaires, figurant les hélices α en rose et les feuillets β en jaune (Uniprot : 1LYZ). (Uniprot database, 2014)

d'acides aminés impliqués dans la liaison avec le substrat, les deux résidus indispensables à l'hydrolyse sont Glu^{35} et Asp^{52}. Glu^{35} est localisé dans un environnement très apolaire, expliquant que le pKa de ce résidu soit déplacé vers les valeurs élevées. Le groupement carboxylique du Glu^{35} est de ce fait protoné sur une gamme étendue de pH dans laquelle le lysozyme est actif. En revanche, Asp^{52} se trouve dans un environnement polaire, avec un pKa proche de la valeur normale pour ce résidu ; il est chargé négativement au-delà de cette valeur. Quand l'hexasaccharide est lié au lysozyme au niveau des 6 sous-sites de fixation mentionnés ci-dessus, Glu^{35} transfère un proton vers l'atome d'oxygène de la liaison $\beta(1,4)$. Ceci crée une rupture de la liaison glycosidique C-O du résidu D. Un intermédiaire covalent entre le résidu D et Asp^{52} est formé. L'oligosaccharide en position E, correspondant aux résidus E à F est alors libéré. Le deuxième produit de la réaction enzymatique, correspondant aux résidus A à D de l'hexasaccharide est libéré lorsque Glu^{35} accepte un proton d'une molécule d'eau, l'ion OH^- produit réagissant avec l'intermédiaire covalent (Figure 1.4) (Osserman, 2012; Vocadlo *et al.*, 2001).

Autres modalités de l'activité antibactérienne

L'activité hydrolytique ne peut pas expliquer toute l'activité antimicrobienne du lysozyme, et d'autres mécanismes ont effectivement pu être mis en évidence. Ainsi, le lysozyme active la sécrétion d'autolysines chez les espèces *Streptococcus faecalis*, *Bacillus subtilis* et *Capnocytophaga gingivalis* (Iacono *et al.*, 1985; Ibrahim *et al.*, 2001a; Laible & Germaine, 1985). Ce mécanisme, indépendant de l'activité enzymatique de la protéine, induit la lyse cellulaire. D'autres modalités d'action, non-enzymatiques et non-lytiques, ont été décrites chez *Staphylococcus aureus*, *Listeria innocua*, *Escherichia coli*, *Klebsiella pneumoniae* et *Serratia marescens* (Ibrahim *et al.*, 2001a; Masschalck *et al.*, 2002; Pellegrini *et al.*, 1992, 1997). L'hypothèse de perturbations membranaires induites par le lysozyme est la plus probable. Elle a été en partie confirmée chez *E. coli*, notamment par Wild *et al.* (1997) et Pellegrini *et al.* (2000) qui ont mis en évidence la perturbation de la membrane externe de la bactérie. En revanche, la perturbation de la membrane cytoplasmique reste hypothétique (Düring *et al.*, 1999; Pellegrini *et al.*, 2000; Wild *et al.*, 1997). En plus de l'activation des autolysines et des perturbations membranaires, le lysozyme est également capable d'inhiber la synthèse d'ARN et d'ADN chez *E. coli* (Pellegrini *et al.*, 2000).

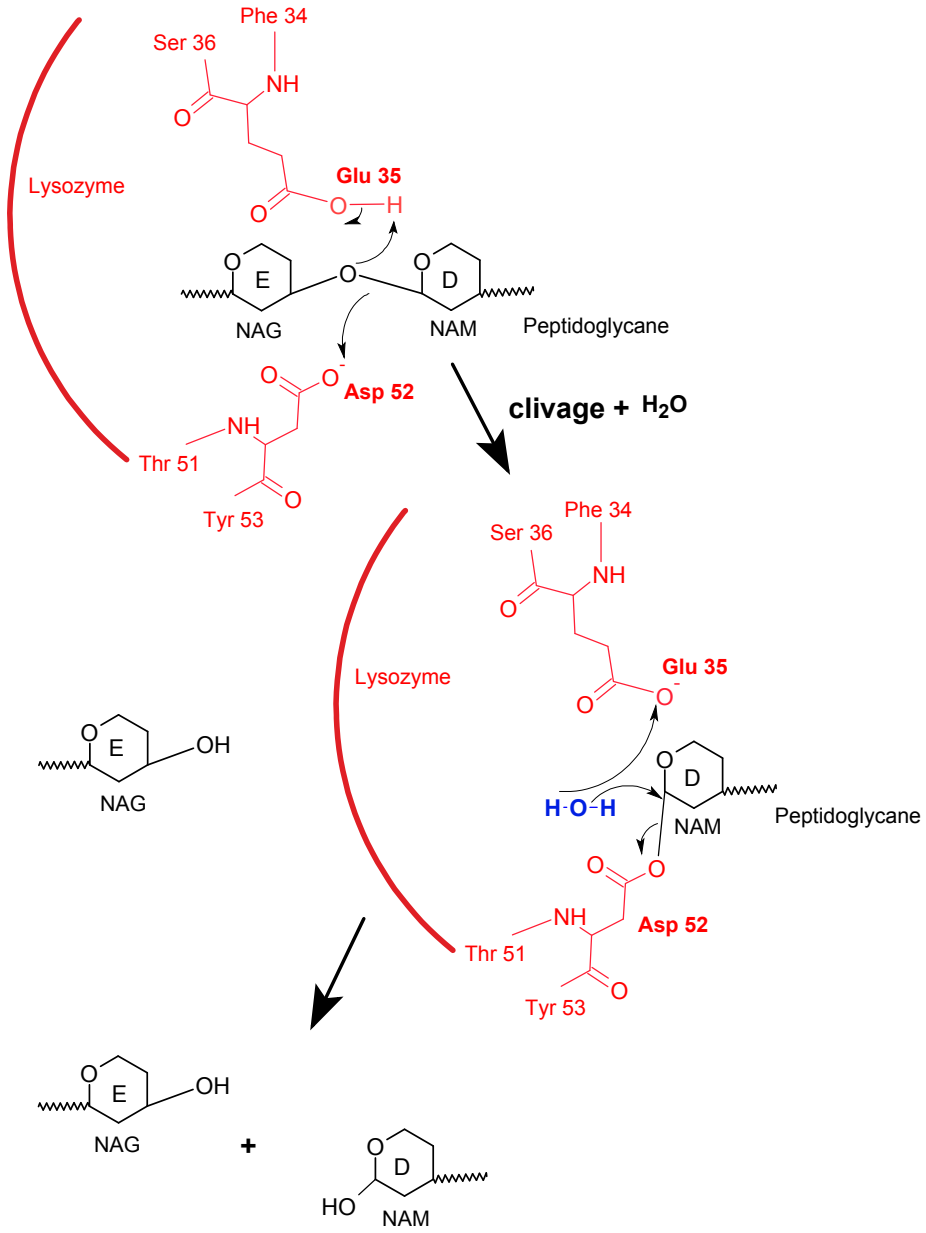

Figure 1.4 – Mécanisme réactionnel de l'hydrolyse enzymatique du peptidoglycane par le lysozyme au niveau des résidus D (NAM : acide N-acétylmuramique) et E (NAG : N-acétylglucosamine) (Selon (Osserman, 2012; Vocadlo *et al.*, 2001)).

Modifications du lysozyme pouvant augmenter son activité antibactérienne

En raison de son activité enzymatique contre le peptidoglycane, le lysozyme est très actif contre la plupart des bactéries à coloration de Gram positive, même s'il existe des cas de résistance au lysozyme chez ces bactéries. Ces résistances résultent de modifications de la structure moléculaire du peptidoglycane. Il peut s'agir d'O-acétylation de l'acide N-acétylmuramique comme observé chez plusieurs souches de *Staphylococcus aureus* (Bera *et al.*, 2005), de de-N-acétylation de la N-acétylglucosamine comme chez *Bacillus cereus*, *Bacillus anthracis* et *Streptococcus pneumoniae* (Araki *et al.*, 1972; Vollmer & Tomasz, 2002; Zipperle *et al.*, 1984), ou encore de l'augmentation du pontage entre les brins polysaccharidiques du peptidoglycane (Strominger & Ghuysen, 1967) ou de la présence d'autres types de polymères à la surface bactérienne comme chez certaines souches de *Streptococcus* (Krause & McCarty, 1961). La résistance au lysozyme reste cependant limitée parmi les bactéries à coloration de Gram positive. En revanche, les bactéries à coloration de Gram négative sont globalement plutôt résistantes au lysozyme. Leur membrane externe est en effet une protection efficace contre cette enzyme (Nikaido, 2003). De plus, certaines de ces bactéries, notamment parmi les *Enterobacteriaceae*, contiennent dans leur périplasme des inhibiteurs du lysozyme tels que les molécules Ivy ou MliC présentes chez *E. coli* (Callewaert *et al.*, 2005, 2008; Deckers *et al.*, 2004).

Cependant, la littérature fait état de la possibilité de modifier le spectre d'activité du lysozyme, et notamment d'augmenter son efficacité contre les bactéries à coloration de Gram négative, par la modification de ses caractéristiques physicochimiques. Quel que soit le procédé exploré, les modifications engendrées sur la protéine se traduiraient principalement par l'augmentation des interactions entre le lysozyme et les membranes bactériennes (Ibrahim *et al.*, 2002).

Un premier moyen d'augmenter l'activité antibactérienne du lysozyme est le greffage de groupements chimiques spécifiques. Les groupements utilisés peuvent être des acides gras, des polysaccharides, des périllaldéhydes, des acides organiques ou encore des peptides hydrophobes. La fusion entre le lysozyme et ces groupements est réalisée soit par réactions chimiques, soit par génie génétique. Différents exemples de fusions efficaces sont présentés dans le Tableau 1.2. Toutes ces nouvelles formes de lysozyme sont supposées perturber plus efficacement l'intégrité des membranes bactériennes que le lysozyme natif, en raison de propriétés physicochimiques modifiées. Cette hypothèse s'appuie sur des mesures de perméabilité *in vivo* sur cellules *E. coli*, et sur des mesures *in vitro* de perméabilisation et de perturbation du potentiel membranaire de liposomes.

L'hydrolyse enzymatique a également été utilisée pour augmenter l'activité antibactérienne du lysozyme. Pellegrini *et al.* (1997) ont ainsi montré que le fragment peptidique [98-112], issu de la protéolyse du lysozyme par la clostripaïne, est actif contre plusieurs espèces bactériennes à colorations de Gram positive et négative (Pellegrini *et al.*, 1997). Des mesures effectuées *in vivo* et sur liposomes ont démontré que ce peptide perméabilise les membranes externe et cytoplasmique d'*E. coli* (Ibrahim *et al.*, 2001b). Mine *et al.* (2004) ont également mis en évidence plusieurs peptides actifs produits par hydrolyse pepsique puis trypsique du lysozyme. Deux de ces peptides ont été séquencés : le fragment [98-108] s'est avéré avoir une action bacteriostatique contre *E. coli* et le fragment [15-21] contre *S. aureus*. L'hypothèse d'une action de ces deux peptides sur la paroi bactérienne est confortée par les observations faites en microscopie électronique sur les bactéries. Plusieurs peptides actifs contre *E. coli*, *S. aureus* et d'autres espèces bactériennes ont également été mis en évidence après hydrolyse pepsique du lysozyme à pH 4.0 (Ibrahim *et al.*, 2005). Ces peptides ont un effet bactéricide lié à leur capacité à perméabiliser les membranes bactériennes et perturber le potentiel membranaire. Enfin, Abdou *et al.* (2007) ont identifié parmi les peptides issus de l'hydrolyse partielle du

Table 1.2 – Exemples de greffages réalisés par voie chimique ou génétique et ayant permis d'augmenter l'activité antimicrobienne du lysozyme en modifiant ses propriétés physicochimiques.

Groupements chimiques	**Méthode de greffage**	**Propriétés physicochimiques modifiées**	**Espèces bactériennes sensibles au lysozyme modifié**	**Références**
Dextrane ou galactomannane	Réactions de Maillard contrôlées	Augmentation du caractère hydrophile, et de la tensio-activité	*Bacillus cereus* *Staphylococcus aureus* *Escherichia coli* *Aeromonas hydrophila* *Proteus mirabilis* *Klebsiella pneumoniae* *Vibrio parahaemolyticus*	Amiri *et al.* (2008) Nakamura *et al.* (1991) Nakamura *et al.* (1991)
Acides gras : C14 :0, C16 :0, C18 :0	Échange d'esters catalysé en milieu basique	Augmentation du caractère hydrophobe	*Escherichia coli*	Ibrahim *et al.* (1991) Ibrahim *et al.* (1993)
Périllaldéhyde	Formation de bases de Schiff puis réduction	Augmentation du caractère hydrophobe	*Escherichia coli* *Staphylococcus aureus*	Ibrahim *et al.* (1994a)
Acide caféique ou acide cinnamique	Réaction de condensation	Augmentation du caractère amphiphile	*Escherichia coli*	Bernkop-Schnurch *et al.* (1998)
Chloride oléolyle	*non définie*	Augmentation du caractère hydrophobe	*Escherichia coli*	Evran *et al.* (2010)
Pentapeptide : (FFVAP)	Génie génétique	Augmentation du caractère hydrophobe	*Escherichia coli*	Arima *et al.* (1997) Ibrahim *et al.* (1992) Ibrahim *et al.* (1993) Ibrahim *et al.* (1994b)
Peptides composés uniquement de résidus proline	Génie génétique	Augmentation du caractère hydrophobe	*Escherichia coli*	Ito *et al.* (1997)
Heptapeptides riches en résidus sérine	Génie génétique	Augmentation du Caractère hydrophobe	*Escherichia coli*	Xu *et al.* (2004)

lysozyme par la pepsine, des fragments actifs contre des espèces du groupe *Bacillus*.

Le traitement thermique en solution (0-30 min, 70-100°C, pH 5.0-8.0) s'est également avéré constituer une façon simple d'améliorer l'activité antibactérienne du lysozyme (Ibrahim *et al.*, 1996b,a). Parmi les nombreux barèmes mis en oeuvre, le traitement le plus efficace rapporté par ces auteurs est un chauffage de 20 min à 80°C et pH 6.0 (HLz80/6). L'action bactéricide du HLz80/6 sur *Staphylococcus aureus*, *E. coli* et *Salmonella* Enteritidis est indépendante de l'activité enzymatique mais dose-dépendante. La dénaturation du lysozyme dans ces conditions provoque la réduction de ponts disulfures intramoléculaires et la formation de ponts disulfures intermoléculaires. Les résidus Trp sont par ailleurs exposés en surface de la protéine augmentant son hydrophobie (Ibrahim *et al.*, 1996b,a; Ibrahim, 1998). La structure primaire du HLz80/6 est également affectée ; trois résidus Asn (Asn^{46}, Asn^{59}, Asn^{103}) sont désamidés et trois résidus Asp/Asn (Asn^{48}, Asp^{65}, Asp^{101}) sont transformés en leurs isoformes iso-aspartyles (Figure 1.5) (Ibrahim, 1998). L'activité bactéricide du HLz80/6 serait due à son action sur les membranes externe et cytoplasmique. HLz80/6 a en effet une affinité de fixation sur les LPS améliorée par rapport à la forme native de la protéine, et rentre en compétition avec les ions bivalents Ca^{2+} et Mg^{2+} qui forment les ponts ioniques entre les charges négatives des LPS. HLz80/6 est de plus capable de perméabiliser des liposomes phospholipidiques (Ibrahim *et al.*, 1997; Ibrahim, 1998).

La réduction des ponts disulfures du lysozyme par le dithiotréitol (DTT) (pH 8, 30°C, 0.5-4 h) augmente l'activité antimicrobienne du lysozyme vis-à-vis *Salmonella* Enteritidis (Touch *et al.*, 2004). Une réduction partielle (1.5 h) du lysozyme donne les meilleurs résultats. L'augmentation de l'activité antimicrobienne est due à une hydrophobie et une flexibilité accrues qui favoriseraient la perturbation membranaire. Ceci n'explique cependant pas pourquoi le lysozyme intégralement réduit, qui constitue la forme la plus hydrophobe, ne montre pas la plus forte activité. Touch *et al.* (2004) proposent que les modifications de structures secondaires et tertiaire après réduction seraient également importantes pour l'interaction membranaire.

1.2.3 Modifications induites par le chauffage à sec

Les conséquences du chauffage à sec pendant 7 jours à 80°C sur les caractéristiques physico-chimiques et les propriétés du lysozyme ont été étudiées par Desfougères et al. Aucune modification des structures secondaires ni de la structure tertiaire n'a été observée (Desfougères *et al.*, 2011a). Toutefois, l'activité enzymatique du lysozyme chauffé à sec est diminuée d'environ 35% par rapport au lysozyme natif. Par ailleurs, l'hydrophobie de surface, la flexibilité moléculaire, le pI apparent et la tensio-activité du lysozyme sont augmentés par le chauffage à sec (Desfougères *et al.*, 2011a,b).

Le lysozyme chauffé à sec est en réalité constitué de trois isoformes qui peuvent être séparées par chromatographie d'échange de cations : les iso-aspartyles, la forme « native-like » et les succinimides. Ces formes se distinguent par leur pI, leur hydrophobie et leur tensio-activité (Desfougères *et al.*, 2011a,b). La structure primaire du lysozyme est modifiée après chauffage à sec : de 1 à 5 résidus Asp ou Asn (Asp^{18}, Asp^{48}, Asp^{52}, Asp^{66}, Asp^{101} et/ou Asn^{103}) sont modifiés en résidus succinimidyles et/ou iso-aspartyles. Ces modifications sont le résultat respectivement d'une cyclisation et d'une cyclisation suivie d'une isomérisation (Figure 1.5).

Les formes iso-aspartyles sont les formes les moins abondantes dans le lysozyme chauffé à sec ; elles sont également les moins basiques. Les formes succinimides sont présentes à hauteur d'environ 50%. Le pI apparent, l'hydrophobie de surface, la flexibilité moléculaire et la tensio-activité des succinimides sont supérieurs à ceux du lysozyme natif et des autres isoformes. En revanche, l'activité enzymatique n'est que de 42% de celle du lysozyme natif. Les formes

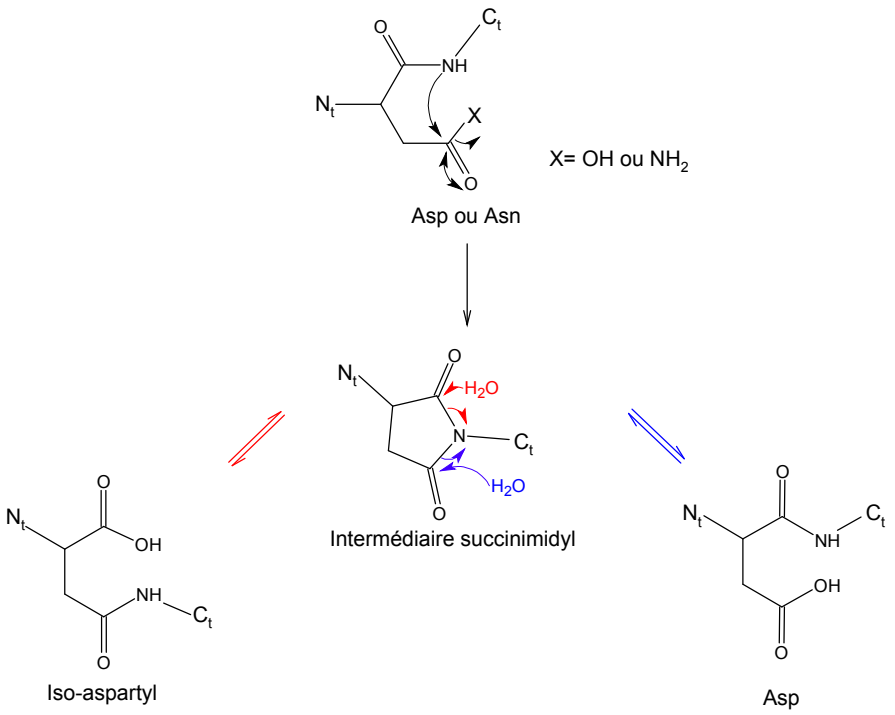

Figure 1.5 – Réaction de cyclisation et de désamidation des résidus Asn ou Asp (Selon Desfougères *et al.* (2011a); Ibrahim (1998)).

succinimides ne sont pas stables à pH supérieur à 6. La forme « native-like » ne diffère pas du lysozyme natif si l'on considère la séquence primaire ; elle a également un pI apparent équivalent, puisqu'éluée simultanément en chromatographie d'échange de cations. Jusqu'à présent, aucune différence structurale entre le lysozyme natif et la forme « native-like » n'a pu être démontrée. Toutefois, l'hydrophobie de surface, la flexibilité moléculaire et la tensio-activité de la forme « native-like » sont supérieures à celles du lysozyme natif (Desfougères *et al.*, 2011a,b).

Etant donné que les propriétés physicochimiques des protéines telles que la charge, l'hydrophobie et la flexibilité moléculaire sont mentionnées comme étant des caractéristiques importantes conditionnant leur interaction avec les membranes bactériennes, les modifications subies par le lysozyme au cours du chauffage à sec laissent donc envisager un impact sur ses propriétés antibactériennes. Au même titre que les différents procédés proposés jusqu'ici pour modifier les propriétés antibactériennes du lysozyme (cf § 1.2.2), le chauffage à sec pourrait donc apparaître comme un procédé simple permettant de produire de nouvelles formes dérivées du lysozyme, offrant des propriétés spécifiques. Mais jusqu'à aujourd'hui, aucune donnée dans la littérature ne permettait de confirmer ni d'infirmer cette hypothèse.

1.3 Les membranes bactériennes, cible des protéines et peptides antimicrobiens

1.3.1 Bactéries à coloration de Gram négative *vs* Gram positive

La coloration de Gram

La coloration de Gram, découverte en 1884 (Gram, 1884), est encore aujourd'hui largement utilisée pour différencier deux groupes de bactéries dites respectivement à coloration de Gram

positive et Gram négative. Ces deux groupes sont fondamentalement différents en termes de paroi bactérienne, ce qui explique qu'ils réagissent de manière différente au protocole de coloration/décoloration mis au point par Gram (Beveridge & Davies, 1983; Davies *et al.*, 1983; Salton, 1963). La coloration de Gram fait intervenir 4 étapes sur un frottis bactérien fixé :

- Première coloration au cristal violet ou gentiane violet ;
- Mordançage au lugol ;
- Décoloration à l'éthanol 95% ;
- Deuxième coloration à la safranine ou fuchsine.

Le cristal violet ($C_{25}H_{30}N_3Cl$) en solution est dissocié en $C_{25}H_{30}N_3^+$ et Cl^-. Le lugol est une solution d'iodure (I^- ou I_3^-) qui réagit avec les ions $C_{25}H_{30}N_3^+$ pour former des complexes iodure-cristal violet ($C_{25}H_{30}N_3I$). C'est au cours de l'étape de décoloration par l'éthanol que les deux groupes bactériens se différencient. L'éthanol déshydrate le peptidoglycane qui constitue la couche externe des bactéries à coloration de Gram positive ; ceci provoque la contraction du maillage du peptidoglycane qui piège alors les complexes $C_{25}H_{30}N_3I$ dans la paroi, colorant la cellule en violet. Chez les bactéries à coloration de Gram négative, l'éthanol provoque la perte de la membrane externe et la paroi est affaiblie. Ceci permet la décoloration. Le deuxième colorant appliqué (safranine ou fuchsine) est alors celui qui donne sa teinte à la bactérie qui devient rose (Smith & Hussey, 2005). Après coloration, lorsque l'échantillon est observé en microscopie optique, les bactéries à coloration de Gram positive et Gram négative apparaissent donc respectivement en violet et rose (Figure 1.6).

Dans certains cas, la coloration de Gram peut être ambiguë. Ainsi, les bactéries à coloration de Gram variable comme *Clostridium tetani* réagissent différemment au protocole de coloration en fonction des conditions de culture (Seltmann & Holst, 2002). Certaines bactéries atypiques comme les mycolata, à coloration de Gram positive, et les cyanobacteria, à coloration de Gram négative, constituent une autre exception, en raison de leur paroi bactérienne dont les caractéristiques sont intermédiaires entre les deux groupes définis ci-dessus (Seltmann & Holst, 2002).

Nature des différences au niveau de l'enveloppe entre les deux groupes de bactéries

L'enveloppe bactérienne est l'ensemble des structures qui délimitent la cellule bactérienne et la protège du milieu extérieur. La paroi bactérienne fait partie de cette enveloppe ; elle comprend l'ensemble des structures à l'exception de la membrane cytoplasmique.

L'enveloppe des bactéries à coloration de Gram négative est constituée de trois couches principales visualisées pour la première fois en microscopie éléctronique par Glauert & Thornley (1969) ; on distingue ainsi la membrane externe, le peptidoglycane et la membrane cytoplasmique ou membrane interne (Figure 1.7A) (Beveridge & Graham, 1991; Silhavy *et al.*, 2010). L'espace entre la membrane externe et la membrane cytoplasmique est nommé périplasme (Mitchell, 1961). Le peptidoglycane est principalement attaché à la membrane externe par des lipoprotéines de Braun (Braun, 1975; Silhavy *et al.*, 2010). Ces lipoprotéines s'insèrent d'un côté dans le feuillet interne de la membrane externe ; de l'autre côté, elles sont liées par liaison covalente aux ponts peptidiques du peptidoglycane.

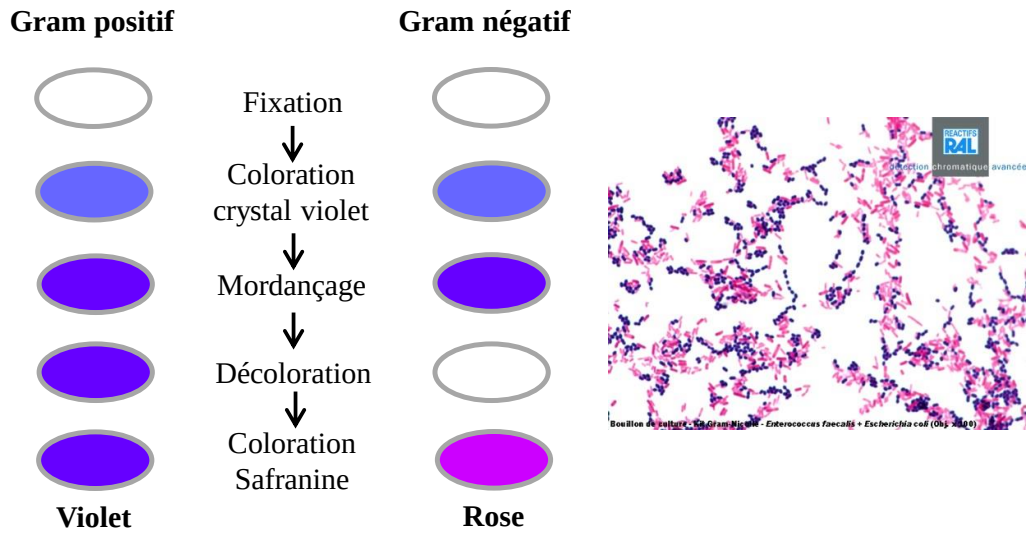

Figure 1.6 – Principe de la coloration de Gram pour la différenciation des bactéries en deux groupes (Photo de RAL reactifs).

L'enveloppe des bactéries à coloration de Gram positive est composée uniquement du peptidoglycane et de la membrane cytoplasmique (Figure 1.7B). La couche de peptidoglycane est ainsi directement en contact avec le milieu extérieur ; elle est en revanche plus épaisse (30 à 100 nm) que celle des bactéries à coloration de Gram négative (quelques nm) (Beveridge & Graham, 1991; Seltmann & Holst, 2002; Silhavy *et al.*, 2010). Des acides téichoïques et des acides lipotéichoïques sont insérés dans le peptidoglycane des bactéries à coloration de Gram positive. Parfois, des acides téichuroniques sont également présents dans le peptidoglycane. Les acides téichoïques sont attachés par liaison covalente au peptidoglycane, tandis que les acides lipoteichoïques sont reliés aux têtes polaires des phospholipides de la membrane cytoplasmique.

Les différences entre les bactéries à coloration de Gram négative et Gram positive sont présentées dans le Tableau 1.3 et visualisées dans la Figure 1.8. Dans les paragraphes suivants, la structure de l'enveloppe de la bactérie à coloration Gram négative *E. coli K12* sera spécifiquement détaillée. La description de cet organisme à été choisie, car c'est le modèle bactérien utilisé tout au long de ce travail.

1.3.2 Enveloppe cellulaire des bactéries à coloration de Gram négative : le modèle *E. coli* K12

La membrane externe

La membrane externe est une bicouche lipidique asymétrique. Le feuillet externe est constitué de lipopolysaccharides (LPS) et le feuillet interne de phospholipides (PL).

Les LPS sont des lipides spécifiques aux bactéries à coloration de Gram négative. Ces molécules sont des endotoxines et sont importantes pour le sérotypage, c'est-à-dire l'identification des bactéries par rapport aux antigènes (ici LPS) présents à la surface cellulaire. Les LPS sont des molécules amphiphiles, composées d'une partie hydrophobe (lipide A) et d'une partie hydrophile (Figure 1.9). Le lipide A est constitué d'un disaccharide de deux D-glucosamines (GlcN) liées par des liaisons $\beta(1,6)$, substitué avec des chaines lipidiques et deux groupements phosphate ; il porte deux charges négatives. L'un des deux résidus GlcN porte deux acides 3-désoxy-D-manno-octulosoniques (KdO) qui constituent le « noyau interne ». Une minorité

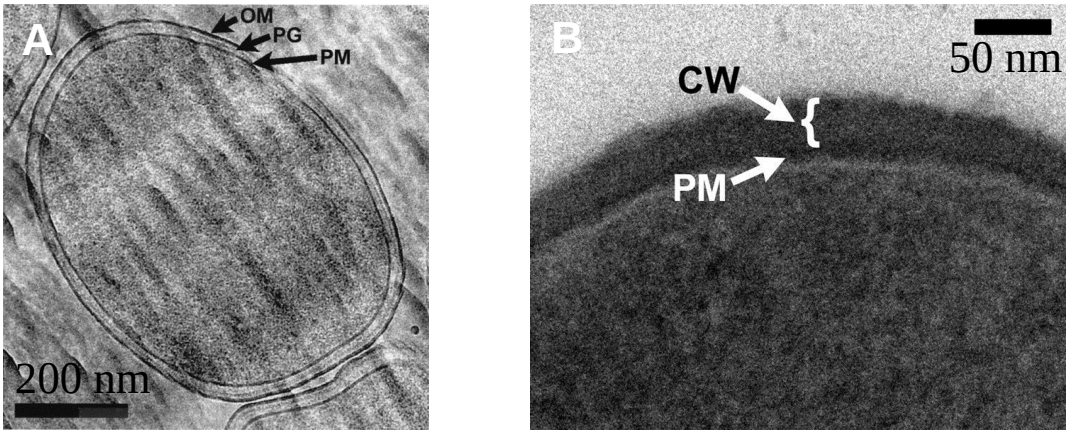

Figure 1.7 – (A) Image en microscopie électronique (cryo transmission) d'*E. coli* K12 montrant les trois couches de l'enveloppe des bactéries à coloration de Gram négative : la membrane externe (OM), le peptidoglycane (PG) et la membrane cytoplasmique (PM). (B) Image en microscopie électronique de *Staphylococcus aureus* montrant la paroi cellulaire (CW) et la membrane cytoplasmique (PM) (Selon Matias *et al.* (2003); Matias & Beveridge (2006)).

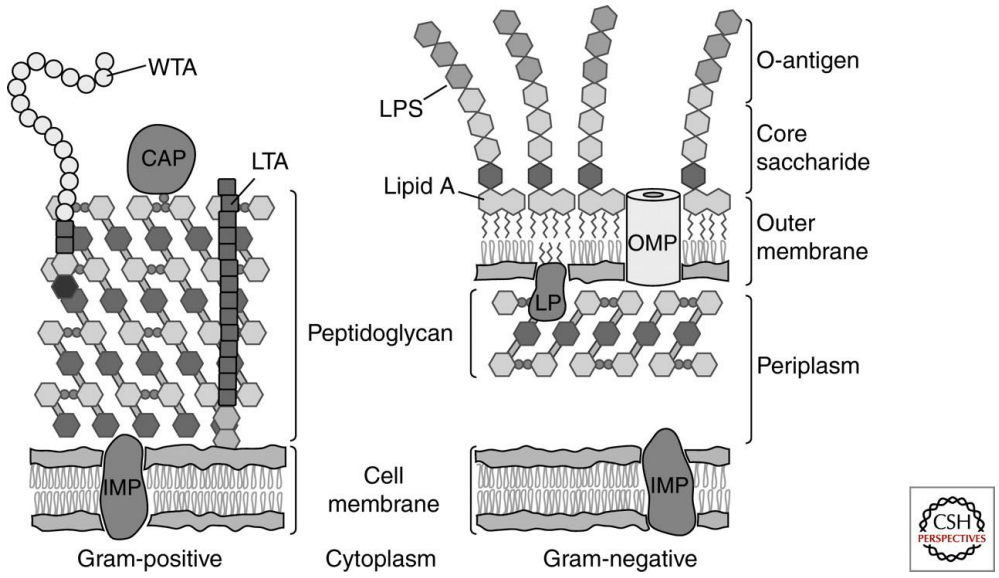

Figure 1.8 – Schémas de l'enveloppe bactérienne des bactéries à coloration de Gram positive et négative. Protéine membranaire interne, IMP ; Protéine membranaire externe, OMP ; Acide lipotéichoïque, LTA ; Acide téichoïque, WTA ; Lipopolysaccharides, LPS ; Lipoprotéine, LP ; Protéine liée à la paroi, CAP. (Silhavy *et al.*, 2010).

Table 1.3 – Enveloppes cellulaires des bactéries à coloration de Gram positive et Gram négative : principales différences entre les deux groupes bactériens (Selon Ghuysen & Hackenbeck (1994); Epand & Epand (2011). Phosphatidyléthanolamine, PE ; phosphatidylglycerol, PG ; cardiolipine, CL.

	Coloration de Gram positive	**Coloration de Gram négative**
Couche de surface cristalline	Parfois présente	Parfois présente
Membrane externe	Absente	Présente
Peptidoglycane	Épais	Mince
Acides téichoïques	Présents	Absents
Acides téichuroniques	Parfois présents	Absents
Lipopolysaccharides	Absents	Présents
Lipoprotéines	Absentes	Présentes
Membrane cytoplasmique	Présente	Présente
Acides lipotéichoïques	Présents	Absents
Phospholipides :		
PE	Absent ou non-majoritaire	Généralement majoritaire
PG	Présent	Présent
CL	Présent	Présent

de molécules LPS portent un troisième acide KdO chez cette souche d'*E. coli* (Nikaido, 2003; Raetz & Whitfield, 2002). Le « noyau externe » correspond à la partie de la molécule de LPS constituée d'un certain nombre d'hexoses. La composition du « noyau externe » varie beaucoup entre espèces ; celle correspondant à la souche *E. coli* K12 est présentée en Figure 1.9. A l'extrémité de la chaîne LPS, se trouve enfin la partie O-antigène, constituée de plusieurs unités répétables elles-mêmes composées de plusieurs monosaccharides. La longueur de l'O-antigène est variable ; par conséquent, la longueur de la chaîne polysaccharidique des LPS l'est également (Seltmann & Holst, 2002; Silhavy *et al.*, 2010)

La nature des PL qui composent le feuillet interne de la membrane externe varie en fonction de l'espèce, mais également des conditions environnementales comme la température par exemple. Chez *E. coli* K12, la composition suivante est observée à 37°C : 91% de phosphatidyléthanolamine (PE), 3% de phosphatidylglycérol (PG) et 6% de cardiolipine (CL) (Lugtenberg & Peters, 1976) (Figure 1.10). Les chaînes lipidiques sont à 55% insaturées dans ces conditions (Lugtenberg & Peters, 1976). La fraction lipidique compte pour 50% de la masse totale de la membrane externe dans laquelle on peut également trouver deux types de protéines : des lipoprotéines, dont la lipoprotéine de Braun, et des protéines transmembranaires avec une structure tonneau β. Les protéines transmembranaires permettent pour la plupart de rendre la membrane externe perméable aux nutriments essentiels à la survie de la bactérie et aux métabolites qui doivent être évacués. Ces protéines peuvent être classées en trois groupes : 1) les protéines formant des canaux spécifiques pour certains nutriments comme le maltose, 2) les récepteurs à forte affinité pour le transport de fer et de vitamine B12, et 3) les porines (Nikaido, 2003; Seltmann & Holst, 2002) ; les porines permettent la diffusion libre de molécules hydrophiles de masse moléculaire inférieure ou égale à 650 Da (Nikaido, 2003).

La membrane externe des bactéries à coloration de Gram négative a finalement avant tout une fonction de barrière. Aucune molécule hydrophile plus large que 650 Da ne peut diffuser librement dans le périplasme (Nikaido, 2003). Cette barrière est également très efficace contre les molécules hydrophobes, grâce aux ponts ioniques (Mg^{2+} et Ca^{2+}) entre les LPS et les chaînes lipidiques saturées des LPS qui réduisent la mobilité de la couche lipidique (Silhavy *et al.*, 2010).

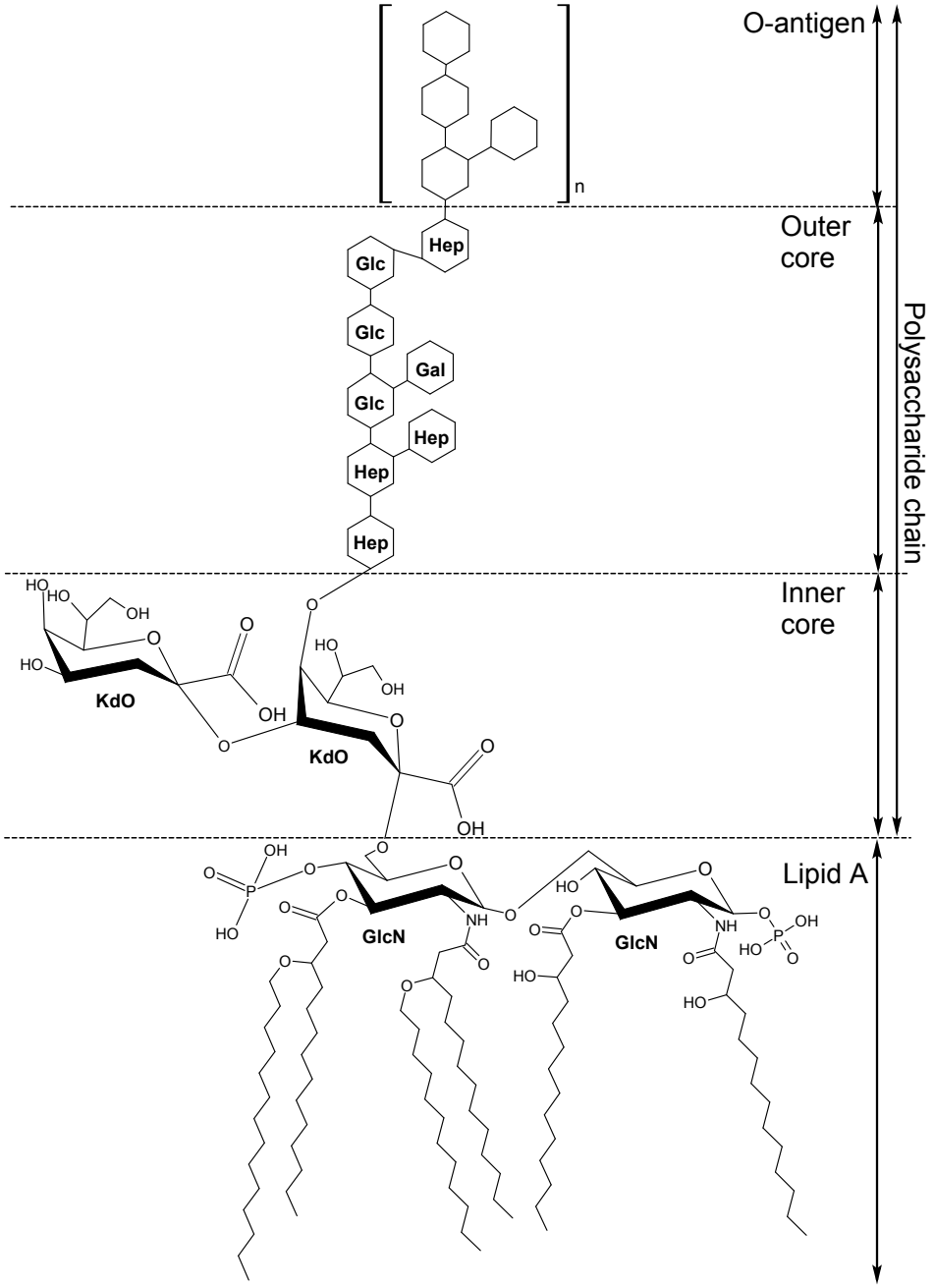

Figure 1.9 – Structure des lipopolysaccharides d'*E. coli* K12. N-acétylglucosamine, GlcN ; Acide 3-désoxy-D-manno-octulosonique, KdO ; L-glycéro-D-manno heptose, Hep ; Glucose, Glc ; Galactose, Gal

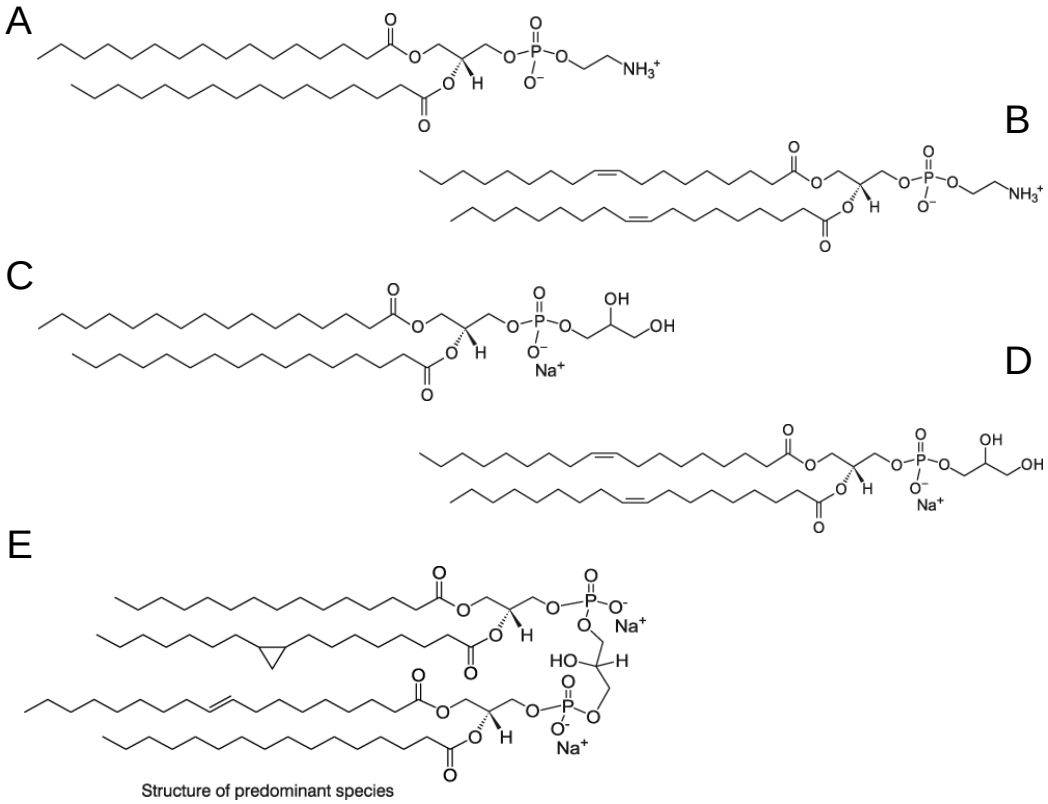

Figure 1.10 – Structures des phospholipides 1,2-dipalmitoyl-sn-glycero-3-phosphoéthanolamine (DPPE)(A), 1,2-dioleoyl-sn-glycéro-3-phosphoéthanolamine (DOPE) (B), 1,2-dihexadécanoyl-sn-glycéro-3-phospho-(1'-rac-glycérol) (DPPG) (C), 1,2-dioleoyl-sn-glycéro-3-phospho-(1'-rac-glycérol) (DOPG) (D) et cardiolipine (CL) (E) d'*Escherichia coli*.

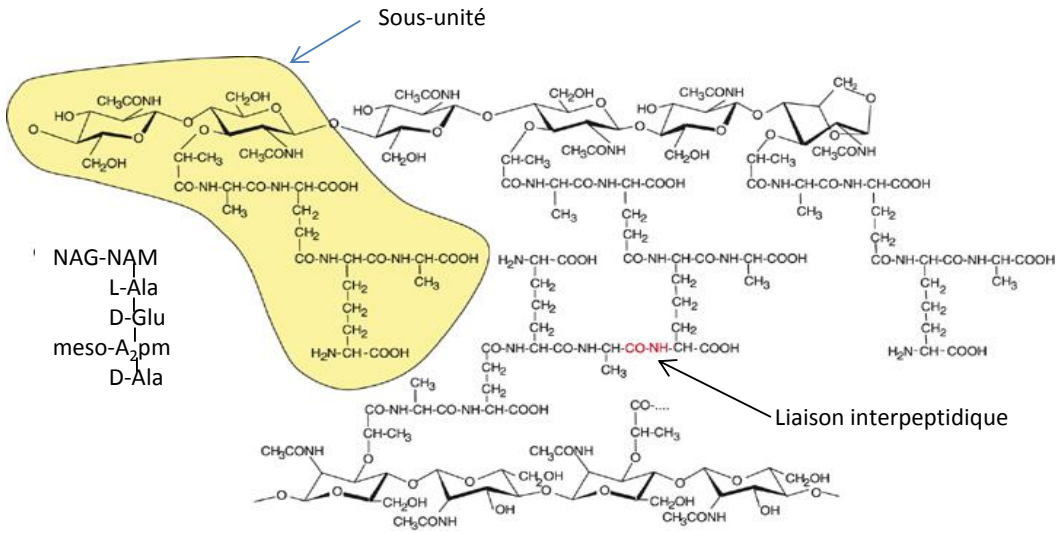

Figure 1.11 – Structure du peptidoglycane d'*E. coli*. Acide N-acétylmuramique (NAM), N-acétylglucosamine (NAG) (Mengin-Lecreulx & Lemaitre, 2005).

Le peptidoglycane

Le peptidoglycane est composé de brins polysaccharidiques reliés par des ponts peptidiques. Les brins polysaccharidiques sont composés de N-acétylglucosamine (NAG) et acide N-acétylmuramique (NAM) en alternance, liés par liaisons $\beta(1,4)$. Chez les bactéries à coloration de Gram négative, les brins se terminent par l'acide 1,6-anhydro-N-acétylmuramique (Vollmer & Bertsche, 2008; Vollmer *et al.*, 2008). Tous les groupements D-lactyle des NAM sont substitués par des structures peptidiques. Chez *E. coli*, les résidus d'acides aminés L-Ala, D-Glu, acide méso-diaminopimélique (meso-A_2pm) et D-Ala forment le tétrapeptide impliqué dans les ponts peptidiques ; la liaison interpeptidique entre deux tétrapeptides intervient directement entre l'acide méso-diaminopimélique et le résidu D-Ala, comme montré Figure 1.11 (Mengin-Lecreulx & Lemaitre, 2005; Vollmer & Bertsche, 2008; Vollmer *et al.*, 2008). Cette liaison peptidique relie les brins de peptidoglycane entre-eux. Le peptidoglycane d'*E. coli* fait partie de la classe A1γ selon Schleifer & Kandler (1972). Le degré de pontage est très variable selon les espèces. Chez *E. coli* les brins polysaccharidiques sont présents sous forme de monomères (environ 50%), de dimères (environ 40%) et une petite quantité d'oligomères (Vollmer *et al.*, 2008).

Le peptidoglycane assure la forme de la cellule et la protège contre les stress osmotiques. L'épaisseur du peptidoglycane d'*E. coli* est estimée entre 1.5 et 15 nm selon la technique d'analyse utilisée (Vollmer & Bertsche, 2008; Vollmer *et al.*, 2008). Le diamètre moyen des mailles du peptidoglycane est de 2.06 nm chez *E. coli* (Demchick & Koch, 1996). Des protéines globulaires de masse moléculaire entre 22 et 24 kDa seraient donc capables de traverser le peptidoglycane de cette espèce bactérienne (Vollmer & Bertsche, 2008).

La membrane cytoplasmique

La membrane cytoplasmique est une bicouche lipidique de phospholipides dont la composition dépend des conditions de culture, notamment de la température. A 37°C, la membrane cytoplasmique d'*E. coli* K12 est composée de 82% de phosphatidyléthanolamine (PE), 7% de phosphatidylglycérol (PG) et 12% de cardiolipine (CL) (Lugtenberg & Peters, 1976). La PE est un phospholipide zwitterionique, contrairement aux PG et cardiolipines qui sont des phos-

pholipides chargés négativement. Les chaînes lipidiques sont à 60% insaturées. Les structures des principaux phospholipides sont présentées Figure 1.10.

La membrane cytoplasmique est une structure très importante pour de nombreuses fonctions cellulaires. Les protéines insérées dans cette membrane participent à des voies métaboliques aussi essentielles et variées que la production d'énergie (force protomotrice), la biosynthèse de lipides, le transport de métabolites et de nutriments, la mobilité cellulaire ... (Silhavy *et al.*, 2010)

1.3.3 Méthodes d'investigation de l'état des membranes bactériennes

De nombreuses méthodes peuvent être utilisées pour évaluer l'état des membranes bactériennes. Certaines, basées sur la fluorimétrie ou la spectrophotométrie, permettent d'effectuer des observations et mesures directement sur la cellule bactérienne. D'autres, mettant en oeuvre des modèles membranaires, permettent d'aller plus loin dans la compréhension des mécanismes d'interaction entre les agents antimicrobiens et les lipides membranaires.

Études *in vivo* sur cellules bactériennes

La perméabilisation des membranes externe et cytoplasmique peut être évaluée en temps réel en utilisant le mutant *E. coli* ML-35p. Ce mutant est déficient en lactose perméase et exprime deux enzymes : la β-lactamase et la β-galactosidase, respectivement dans le périplasme et le cytoplasme (Figure 1.12) (Lehrer *et al.*, 1988). La nitrocéfine, substrat de la β-lactamase, ne peut pas pénétrer dans le périplasme si la membrane externe est intègre ; le produit de son hydrolyse par la β-lactamase, détectable à 486 nm, est donc un indicateur de la perméabilisation de la membrane externe. De même, l'hydrolyse de l'ortho-nitrophenylgalactoside (ONPG) par la β-galactosidase, libérant l'ortho-nitrophénol détectable à 420 nm, est un indicateur de la perméabilisation de la membrane interne. Pour ces deux réactions, les mesures d'absorbances, indicatives des quantités de produits libérés, sont directement proportionnelles aux concentrations de substrats (nitrocéfine et ONPG) pouvant entrer en contact avec les enzymes intra-cellulaires.

La détection de la perméabilisation des membranes telle que présentée ci-dessus ne permet toutefois pas de différencier une perméabilisation légère, de modifications plus sévères comme la formation de pores. En effet, lorsque les mesures d'absorbances sont réalisées sur une suspension de cellules bactériennes, l'ensemble des produits des réactions enzymatiques est détecté, que les produits soient à l'intérieur des cellules du fait de la diffusion des réactifs au travers des membranes, ou à l'extérieur des cellules dans le cas où les enzymes diffusent dans le milieu extérieur (Figure 1.12). C'est pourquoi, pour évaluer la formation éventuelle de pores, Lehrer *et al.* (1988) ont proposé de tester également le surnageant des cellules préalablement traitées par l'antimicrobien étudié. Dans le cas où des pores sont formés, l'enzyme (β-lactamase et/ou β-galactosidase, selon qu'il s'agit de la membrane externe et/ou cytoplasmique) est libérée dans le milieu extérieur à la cellule et est donc présent dans le surnageant de la suspension bactérienne. Mis en présence de nitrocéfine et/ou d'ONPG, le surnageant voit alors son absorbance à 486 nm et/ou 420 nm augmenter. La quantité d'enzyme libérée, proportionnelle à la quantité de pores formés, peut être comparée d'un échantillon à l'autre par comparaison des vitesses initiales de la réaction enzymatique.

Cependant, il est parfois préférable, voire indispensable, d'utiliser une souche sauvage d'*E. coli* plutôt qu'un mutant comme *E. coli* ML-35p. La perméabilisation de la membrane externe peut alors être mise en évidence à l'aide de la sonde fluorescente 1-N-phénylnatphtylamine

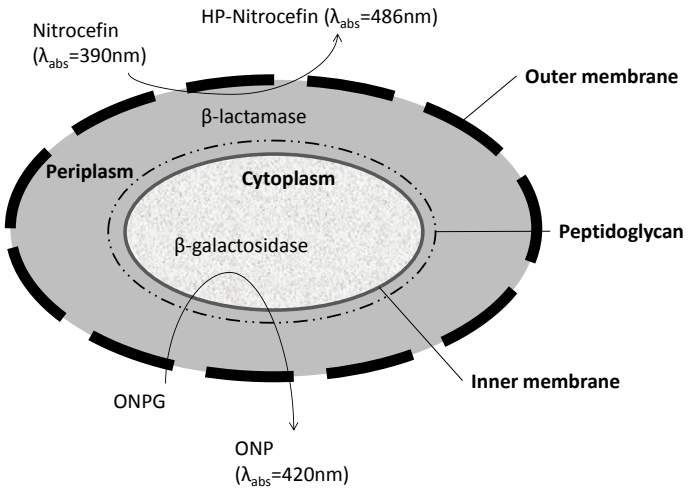

Figure 1.12 – Schéma de la cellule d'*E. coli* ML-35p figurant l'hydrolyse de la nitrocéfine et de l'ONPG par respectivement la β-lactamase et la β-galactosidase, après diffusion de ces deux réactifs par perméabilisation des membranes externe et cytoplasmique, respectivement.

(NPN). La sonde NPN est une sonde hydrophobe qui fluoresce dans un environnement hydrophobe tel que les membranes bactériennes, alors que sa fluorescence est faible en milieu aqueux (Trauble & Overath, 1973). Quand la membrane externe est intacte, la sonde NPN est exclusivement présente dans le milieu aqueux, exclue de l'environnnement hydrophobe de la membrane externe par les parties polysaccharidiques des LPS à la surface de la cellule bactérienne. En revanche, quand la membrane externe est endommagée, la sonde a accès à la partie hydrophobe de la membrane externe et fluoresce (Loh *et al.*, 1984; Helander & Mattila-Sandholm, 2000). D'autres sondes fluorophores comme le bromure d'éthidium (EtBr) et l'iodure de propidium (PI) permettent quant à elles de détecter la perméabilisation de la membrane cytoplasmique (Brehm-Stecher & Johnson, 2003; Miki & Hardt, 2013; Podda *et al.*, 2006). Ces fluorophores sont exclus des cellules dont la membrane cytoplasmique est intacte ; dans le cas contraire, ils parviennent jusqu'au cytoplasme où ils forment des complexes fluorescents avec l'ADN.

La perméabilisation des membranes externe et cytoplasmique peut également être détectée par ionométrie. L'ion lipophile tetraphénylphosphonium (TPP^+), ajouté à la suspension bactérienne, est incorporé dans le cytoplasme des bactéries sous l'influence du potentiel membranaire. Cette incorporation est dépendante de l'intégrité de la membrane externe : elle augmente quand la membrane externe est perméabilisée (Yasuda *et al.*, 2003). A l'inverse, la fuite du potassium cytosolique est un indicateur de la perte d'intégrité de la membrane cytoplasmique (Figure 1.13) (Johnston *et al.*, 2003; Lambert & Hammond, 1973; Orlov *et al.*, 2002; Yasuda *et al.*, 2003). Les suivis par ionomètrie de la disparition des ions TPP^+ d'une part, et de l'apparition des ions K^+ d'autre part dans le milieu extracellulaire indiquent donc respectivement une perméabilisation de la membrane externe et de la membrane cytoplasmique. Ces deux mesures peuvent naturellement être réalisées indépendamment.

La fuite d'autres composants du cytosol comme le phosphate et l'adénosine triphosphate (ATP) a également été utilisée pour évaluer la perte d'intégrité de la membrane cytoplasmique

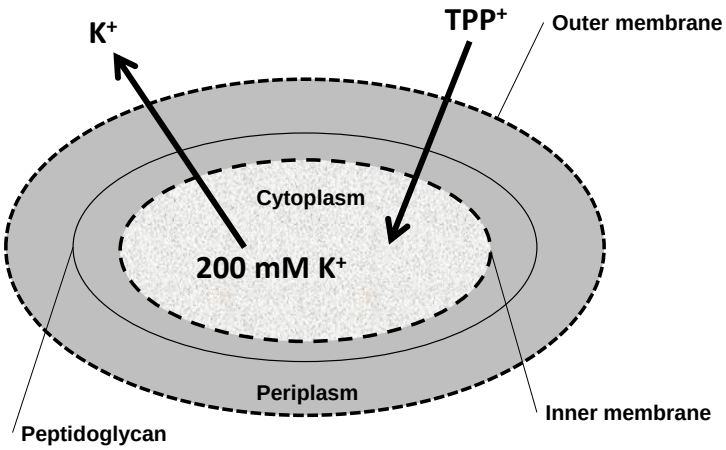

Figure 1.13 – Représentation de la fuite de potassium et de l'entrée des ions TPP^+ dans la cellule bactérienne après perméabilisation de la membrane cytoplasmique.

(Johnston *et al.*, 2003). La fuite des molécules les plus grandes comme l'ATP témoigne de dégâts sévères à la membrane (Johnston *et al.*, 2003). La fuite d'ATP peut être quantifiée par bioluminescence.

La détection de molécules libres de LPS dans le surnageant de cultures bactériennes indique quant à elle une désintégration de la membrane externe. Les LPS peuvent être détectés par électrophorèse SDS-PAGE (Helander *et al.*, 1998; Vaara, 1992).

Un autre critère important permettant de juger de l'état de la membrane cytoplasmique est le potentiel membranaire. Le potentiel membranaire ($\Delta\Psi$) résulte d'une différence de charges de part et d'autre de la membrane cytoplasmique (Breeuwer & Abee, 2004) ; avec le gradient de protons ; il constitue la force protomotrice qui intervient dans les phénomènes de transport cellulaire et de génération d'énergie. Quand la membrane est perméabilisée, ou que des molécules chargées s'adsorbent à la membrane, la différence de charges existant de part et d'autre de la membrane cytoplasmique est perturbée et le potentiel membranaire est modifié. Les modifications du potentiel membranaire peuvent être mises en évidence à l'aide de sondes fluorophores comme le 3,3'-dipropylthiadicarbocyanine iodide ($DiSC_3$) (Wu *et al.*, 1999). La sonde $DiSC_3$ est incorporée dans la cellule bactérienne sous l'influence du potentiel membranaire. Dans le cytoplasme, la sonde ne fluoresce pas en raison d'un phénomène d'autoquenching à forte concentration et du quenching par l'ADN (Wang *et al.*, 2011). Quand le potentiel membranaire de la bactérie est modifié, la sonde, préalablement internalisée par la cellule, est libérée dans le milieu où elle fluoresce (Figure 1.14).

Enfin, des observations microscopiques peuvent être réalisées pour visualiser les modifications morphologiques induites par les atteintes à la paroi bactérienne. La microscopie électronique offre une échelle d'observation pertinente, et est pour cette raison largement utilisée. Elle présente cependant l'inconvénient de nécessiter un traitement particulier de l'échantillon avant observation. Or, il est souvent difficile d'affirmer que ce traitement ne modifie pas lui-même l'aspect de la cellule. La microscopie à force atomique (AFM) est de ce point de vue plus adaptée pour observer les éventuels effets des antimicrobiens sur la paroi bactérienne ; aucun traitement préalable de l'échantillon avant observation n'est en effet nécessaire (Meincken

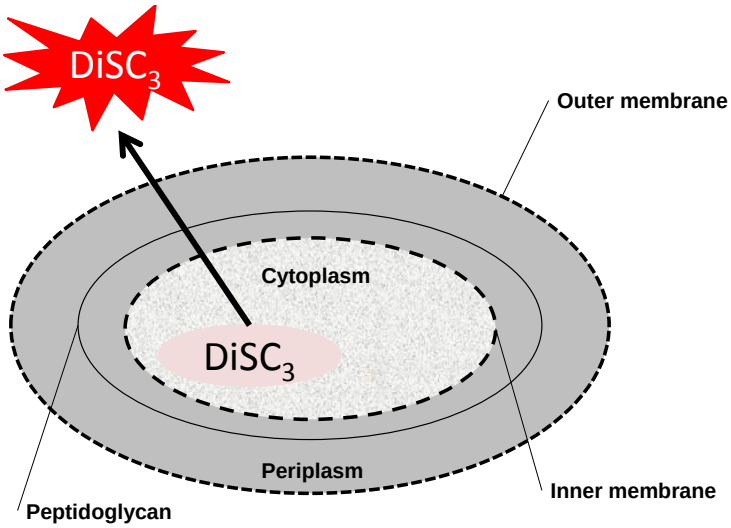

Figure 1.14 – Schéma de principe pour la détection de la modification du potentiel membranaire d'une bactérie par la sonde $DiSC_3$.

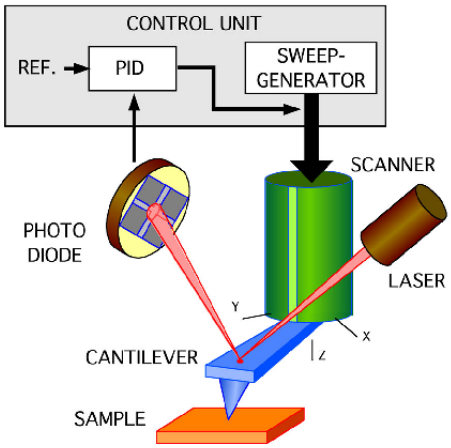

Figure 1.15 – Schéma de principe de la microscopie à force atomique (AFM) (Aström & Murray, 2012).

et al., 2005). L'AFM est une forme de microscopie à sonde locale. Les échantillons sont visualisés grâce à une pointe montée sur un micro-levier. La pointe scanne la surface de l'échantillon ; les mouvements de la pointe sont détectés par la reflexion d'un laser sur une photodiode et un scanner piézoélectrique. L'image est ensuite reconstituée à l'aide d'un ordinateur (Figure 1.15, Gaboriaud & Dufrêne (2007). Plusieurs modes peuvent être utilisés comme le mode contact et le mode tapping. En mode contact, la pointe et l'échantillon sont mis en contact et la pointe scanne simplement la surface donnant une image topographique de la surface de l'échantillon. En mode tapping, la pointe oscille à une fréquence proche de sa fréquence de résonance. Quand la pointe oscillante touche légèrement la surface, l'amplitude d'oscillation est diminuée. Cette reduction d'amplitude peut ensuite être convertie en information topographique (Gaboriaud & Dufrêne, 2007). L'interaction de la pointe avec l'échantillon induit également une différence de phase entre la phase imposée et la phase mesurée de l'oscillation de la pointe (Magonov *et al.*, 1997). Cette différence de phase donne des informations sur les propriétés de la surface de l'échantillon (Camesano *et al.*, 2000). Le mode tapping a comme avantage que la force latérale exercée sur l'échantillon est réduite.

Table 1.4 – Les différents types de vésicules (Eeman & Deleu, 2010).

Type de vésicule	**Taille (μm)**
Vésicules multilamellaires (MLV)	0.5-10
Grandes vésicules unilamellaires (LUV)	0.1-0.5
Petites vésicules unilamellaires (SUV)	< 0.05
Vésicules unilamellaires géantes (GUV)	5-100

Études *in vitro* sur modèles membranaires

Les techniques *in vivo*, telle que présentées précédemment, permettent uniquement d'étudier des phénomènes globaux d'interaction entre les protéines ou peptides antimicrobiens et les cellules bactériennes. La complexité du système que représente une bactérie ne permet pas d'appréhender ces interactions de manière « fine », c'est à dire à l'échelle supramoléculaire voire moléculaire. Pour ce faire, il est nécessaire de développer des stratégies expérimentales ne faisant intervenir que les membranes bactérienne. Il est possible de purifier des membranes biologiques pour les tester *in vitro*. Cependant, la composition de ces membranes est très complexe ; elles sont constituées d'une grande variété de lipides et de protéines. Il est de ce fait assez difficile d'émettre des hypothèses pour expliquer les mécanismes moléculaires impliqués. C'est pourquoi des modèles membranaires simplifiés sont couramment utilisés, notamment pour l'étude de phénomènes comme l'adsorption ou l'insertion protéique dans les membranes bactériennes (Eeman & Deleu, 2010; Maget-Dana, 1999).

Trois types de modèles membranaires sont utilisés : (1) les vésicules, (2) les monocouches et (3) les bicouches supportées (Figure 1.16). Les **vésicules** sont utilisées pour des études de fusion membranaire, de reconnaissance moléculaire, d'adhésion cellulaire, de « membrane trafficking » et de perméabilisation membranaire (Eeman & Deleu, 2010; Maget-Dana, 1999). Les vésicules sont des structures en bicouches mono- ou multilamellaires. A l'intérieur ou entre les lamelles des vésicules se trouve une solution aqueuse (Eeman & Deleu, 2010; Yeagle, 1993). La taille des vésicules varie de 0.05 à 100 μm (Tableau 1.4).

Les vésicules sont par exemple utilisées pour évaluer la perméabilisation membranaire sous influence de protéines ou peptides antimicrobiens. A l'intérieur des vésicules, un indicateur comme la calcéine peut être incorporé. La calcéine est une sonde fluorophore qui ne fluoresce pas à forte concentration, ce qui est le cas à l'intérieur des vésicules. En revanche, quand les vésicules sont perméabilisées la sonde fluoresce (Shimanouchi *et al.*, 2009). Les vésicules présentent un certain nombre inconvénients comme un rayon de courbure inférieur à ceux observés en conditions naturelles (SUV) ce qui peut modifier les phénomènes d'insertion membranaire. Par ailleurs seules certaines compositions lipidiques permettent la formation de vésicules. Enfin, une homogénéité de taille des vésicules est souvant difficile à obtenir (Maget-Dana, 1999).

Un autre modèle membranaire est **la monocouche lipidique**. Les monocouches lipidiques sont formées par dépôt de lipides à la surface d'une solution aqueuse. La partie hydrophobe (les chaînes lipidiques) se positionne dans l'air et la partie hydrophile (la tête polaire) s'étale dans la solution aqueuse (Yeagle, 1993). Les principaux avantages de ce modèle sont la possibilité de maîtriser la pression latérale entre les lipides (la pression superficielle), la composition lipidique, la température et la composition de la sous-phase (Brockman, 1999; Maget-Dana, 1999). Les monocouches lipidiques sont des modèles idéaux pour évaluer l'adsorption et l'insertion des molécules amphiphiles grâce à leur stabilité et leur homogénéité. De plus, de nombreux outils biophysiques peuvent être utilisés pour étudier ce modèle : mesure de la pression superficielle pour évaluer l'insertion des protéines, éllipsométrie pour évaluer l'adsorption protéique,

microscopie à angle de Brewster et à force atomique pour visualiser l'organisation lipidique ... (Eeman & Deleu, 2010; Brockman, 1999; Maget-Dana, 1999)

Un inconvénients des monocouches est naturellement l'absence du deuxième feuillet présent dans les membranes biologiques. Les **bicouches supportées** peuvent être utilisées pour pallier cet inconvénient. Dans ce modèle, des bicouches asymmétriques peuvent être formées contrairement aux vésicules. La bicouche peut être analysée par microscopie à force atomique, spectrométrie de masse à ions secondaires (SIMS), microscopie de fluorescence, ellipsométrie optique ... (Eeman & Deleu, 2010).

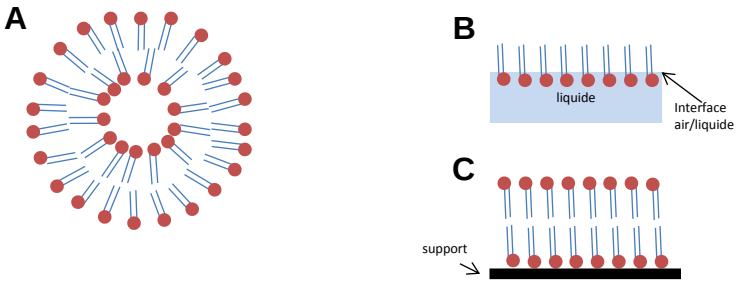

Figure 1.16 – Schématisation des différents modèles membranaires : (A) vésicule monolamellaire, (B) monocouche lipidique et (C) bicouche supportée. Les têtes polaires sont indiquées en rouge, les chaînes aliphatiques en bleu.

Chapitre 2

Activité antibactérienne du lysozyme vis-à-vis d'*Escherichia coli* : perte de l'intégrité membranaire

basé sur :

Derde M., Lechevalier V., Guérin-Dubiard C., Cochet MF., Jan S., Baron F., Gautier M., Vié V. & Nau F. (2013). Hen egg white lysozyme permeabilizes the *Escherichia coli* outer and inner membranes, *Journal of Agricultural and Food Chemistry*, 61(41) :9922-9929

Derde M., Guérin-Dubiard C., Lechevalier V., Cochet MF., Jan S., Baron F., Gautier M., Vié V. & Nau F. (2014). Dry-heating of lysozyme increases its activity against *Escherichia coli* membranes, *Journal of Agricultural and Food Chemistry*, 62(7) :1692-1700

2.1 Introduction

L'activité antimicrobienne du lysozyme contre les bactéries à coloration de Gram positive, basée sur l'activité enzymatique de cette protéine contre le peptidoglycane, est connue et décrite de très longue date (Berger & Weiser, 1957). En revanche, l'activité antimicrobienne du lysozyme contre les bactéries à coloration de Gram négative n'a été rapportée que récemment par plusieurs auteurs (Ellison & Giehl, 1991; Pellegrini *et al.*, 1992). Compte tenu de la protection que constitue la membrane externe qui, chez ces bactéries, protège naturellement le peptidoglycane, l'activité du lysozyme contre ce groupe bactérien peut paraître surprenante. En réalité, elle est indépendante de l'activité enzymatique du lysozyme (Düring *et al.*, 1999; Ibrahim *et al.*, 2001a). L'hypothèse d'une perte de l'intégrité membranaire des bactéries à coloration de Gram négative sous l'effet du lysozyme a été formulée, et partiellement confirmée dans le cas d'*E. coli* (Düring *et al.*, 1999; Pellegrini *et al.*, 2000; Wild *et al.*, 1997).

La perméabilisation membranaire par le lysozyme est une hypothèse séduisante si l'on considère la découverte relativement récente d'inhibiteurs du lysozyme (Ivy, MLiC) dans le périplasme de certaines *Enterobacteriaceae* comme *E. coli* (Abergel *et al.*, 2007; Callewaert *et al.*, 2005, 2008; Deckers *et al.*, 2004). Cette observation suggère en effet que le lysozyme peut franchir la barrière de la membrane externe, comme rapporté par Pellegrini *et al.* (2000) et Wild *et al.* (1997). Cependant, les effets du lysozyme sur les membranes bactériennes n'ont été que très peu explorés et caractérisés. Il n'existe notamment aucune preuve expérimentale de l'aptitude du lysozyme à agir directement, ou non, sur la membrane cytoplasmique des bactéries à coloration de Gram négative.

Plusieurs méthodes d'analyses peuvent être utilisées pour mettre en évidence l'activité anti-membranaire de molécules telles que les protéines et peptides antimicrobiens (cf Chapitre 1 § 1.3.3). Parmi ces méthodes, celle initialement développée par Lehrer (Lehrer *et al.*, 1988), puis adaptée aux échantillons de petite taille par Epand *et al.* (2010), s'avère particulièrement intéressante en raison de sa simplicité de mise en oeuvre - il s'agit d'une mesure spectrophotométrique -, et parce qu'elle permet d'investiguer l'état des membranes externe et cytoplasmique en temps réel. Cette méthode est basée sur l'utilisation de la souche mutante *E. coli* ML-35p qui exprime la β-lactamase dans le périplasme, la β-galactosidase dans le cytoplasme, et est déficiente en lactose perméase (cf Chapitre 1 § 1.3.3 et Figure 1.12).

La perméabilisation de la membrane externe d'*E. coli* sous l'effet du lysozyme a pu être démontrée par Pellegrini *et al.* (2000) grâce à la méthode de Lehrer. Ces auteurs confirmaient ainsi les hypothèses de Wild *et al.* (1997) et Düring *et al.* (1999), basées respectivement sur des observations en microscopie électronique et sur des mesures de fluorescence de l'iodure de propidium. Mais ces travaux n'ont pas permis de conclure avec certitude quant aux effets potentiels du lysozyme sur la membrane cytoplasmique des bactéries.

L'hypothèse que nous avons émise est que la durée d'observation pratiquée par Pellegrini *et al.* (2000) ne permettait pas de mettre en évidence la perméabilisation de la membrane cytoplasmique d'*E. coli* par le lysozyme. En effet, ces auteurs ont limité leurs observations à une durée de mise en contact lysozyme - bactéries de 2 h, durée classiquement utilisée pour évaluer l'efficacité de peptides antimicrobiens comme la mélittine ; pour la plupart de ces peptides, 2 h est en effet une durée suffisante pour mettre en évidence, le cas échéant, la perméabilisation des membranes externe et cytoplasmique. Mais dans le cas d'une protéine comme le lysozyme, il est imaginable que les interactions avec les membranes bactériennes se mettent en place plus lentement qu'avec des peptides. En effet, la structure plus complexe et/ou plus rigide d'une protéine par rapport à un peptide implique que les changements conformationnels, nécessaires à la mise en place d'interactions avec les membranes bactériennes, soient plus

lents (Gorbenko *et al.*, 2007; Nguyen *et al.*, 2011). Cette hypothèse paraît d'autant plus probable que le lysozyme est décrit comme une protéine hautement structurée et particulièrement rigide, en raison notamment des 4 ponts disulfures intramoléculaires qui stabilisent sa structure (Canfield & Liu, 1965). C'est pourquoi il nous est paru opportun de mettre en œuvre la méthode de Lehrer sur des durées supérieures à 2 h pour mettre en évidence l'éventuelle perméabilisation de la membrane cytoplasmique d'*E. coli* par le lysozyme. Nous nous sommes alors heurtés à l'instabilité des mesures d'absorbance traduisant la formation des produits des deux réactions enzymatiques à la base de cette méthode, ainsi qu'au problème d'évaporation au sein des échantillons en cours de dosage. Une adaptation de la méthode de Lehrer s'est donc avérée indispensable en amont de l'étude de la perméabilisation des membranes externe et cytoplasmique d'*E. coli* par le lysozyme.

2.2 Hen egg white lysozyme permeabilizes the *Escherichia coli* outer and inner membranes

Derde M., Lechevalier V., Guérin-Dubiard C., Cochet MF., Jan S., Baron F., Gautier M., Vié V. & Nau F.

(*Journal of Agricultural and Food Chemistry* 2013, vol. 61, pp. 9922-9929)

2.2.1 Abstract

Natural preservatives answer the consumer demand for long shelf life foods, synthetic molecules being perceived as a health risk. Lysozyme is already used because of its muramidase activity against Gram-positive bacteria. It is also described as active against some Gram-negative bacteria; membrane disruption would be involved, but the mechanism remains unknown. In this study, a spectrophotometric method using the mutant *Escherichia coli* ML-35p has been adapted to investigate membrane disruption by lysozyme for long durations. Lysozyme rapidly increases the permeability of the outer membrane of *E. coli* due to large size pore formation. A direct delayed activity of lysozyme against the inner membrane is also demonstrated, but without evidence of perforations.

2.2.2 Materials and methods

If not stated otherwise, chemicals were obtained from Sigma-Aldrich (Saint-Quentin, France).

Bacterial strains

The bacterial strain *E. coli* ML-35p, which is lactose permease deficient and expresses β-lactamase and β-galactosidase in the periplasm and cytoplasm, respectively, was kindly provided by Destoumieux-Garzon, initially supplied by Lehrer. *E. coli* ML-35p was grown overnight (18 h) in tryptic soy broth (TSB) (AES, Bruz, France) with 50 μg/mL ampicillin at 37 °C under stirring (130 rpm). The bacterial culture was washed twice in Tris-HCl buffer (50 mM, pH 7.0). The absorbance of the final suspension was around 1.0 at 620 nm, corresponding to about 10^9 CFU/mL. The 10^8 and 10^7 CFU/mL solutions were prepared by appropriate 10-fold dilutions of the previous culture.

Signal stability of the substrates and products of β-lactamase and β-galactosidase

To evaluate the signal stability of ortho-nitrophenylgalactoside (ONPG), orthonitrophenol (ONP), and nitrocefin (Merck Chemicals, Darmstadt, Germany), solutions of 1, 0.07, and 0.015 g/L of these three reagents, respectively, were prepared in 50 mM Tris-HCl buffer, pH 7.0. The hydrolysis product of nitrocefin (HP-nitrocefin) was produced by the enzymatic reaction (1 h, 25 °C) between nitrocefin (0.015 g/L) and penicillinase from *Bacillus cereus*

(3.5 g/L) in 50 mM Tris-HCl buffer, pH 7.0. Three hundred microliter aliquots of each solution (ONPG, ONP, nitrocefin, HP-nitrocefin) were dispensed into microplate wells. The absorbance of the four substances was subsequently measured by a spectrophotometer Spectramax M2 (Molecular Devices, UK) for 10 h, after sealing or not the microplates with a Clear Seal film (4titude, Surrey, UK). The stability of ONPG and ONP was determined by ONP absorbance at 420 nm. The stability of nitrocefin and HP-nitrocefin was determined by absorbance at 390 and 486 nm, respectively.

Outer and inner membrane permeability

Melittin from bee venom (85% purity) was used as a positive control in the membrane permeability experiments. Melittin is a small peptide, constituted of 26 amino acids (Terwilliger & Eisenberg, 1982). This peptide is active on biological membranes and shows antimicrobial activity; it is especially known to form pores in bacterial membranes and to permeabilize the outer and inner membranes (Epand *et al.*, 2010; Lee *et al.*, 2013).

Melittin and lysozyme (Liot, Annezin, France) activity against the outer and inner membranes was measured. The sample solutions to measure their activity contained either 0.015 mg/mL melittin or 0.05 mg/mL up to 10 mg/mL of lysozyme. The sample solutions were inoculated with 10^7 or 10^8 CFU/mL of *E. coli* ML-35p. A negative control sample consisted of solutions prepared as described above, but without melittin or lysozyme.

To test outer membrane permeability, 0.015 mg/mL nitrocefin (substrate of β-lactamase) was added to the sample solutions. When the outer membrane was permeabilized, the periplasmic β-lactamase came into contact with its substrate nitrocefin, resulting in HP-nitrocefin release (Figure 1.12). HP-nitrocefin absorbance was measured at 486 nm, at 37 °C under stirring.

This reaction could result from nitrocefin entrance into the bacteria and/or from β-lactamase leakage. To test the assumption of β-lactamase leakage in the presence of lysozyme, a 0.25 mg/mL lysozyme solution was inoculated with 10^7 CFU/mL *E. coli* ML-35p and incubated at 37 °C for 5 h before centrifugation (5000g, 10 min); the β-lactamase activity was then measured in the supernatant by adding 0.05 mg/mL nitrocefin. HP-nitrocefin absorbance was measured at 486 nm at 25 °C under stirring.

To test inner membrane permeability, 0.7 mg/mL ONPG (substrate of β-galactosidase) was added to the sample solutions. When the inner membrane was permeabilized, the cytoplasmic β-galactosidase came into contact with its substrate ONPG, resulting in ONP release (Figure 1.12). ONP absorbance was measured at 420 nm at 37 °C under stirring. Similarly to what was described above, to test the assumption of β-galactosidase leakage from bacteria cells in the presence of lysozyme, a 0.25 mg/mL lysozyme solution was inoculated with 10^7 CFU/mL *E. coli* ML-35p and incubated at 37 °C for 5 h before centrifugation (5000g, 10 min); the β-galactosidase activity was then measured in the supernatant by adding 1 mg/mL ONPG. ONP absorbance was measured at 420 nm at 25 °C under stirring.

Quantification of membrane permeabilization

The absorbance responses *versus* time, resulting from experiments of outer and inner membrane permeabilization, were analyzed to quantify the antibacterial efficiency of melittin and lysozyme. Absorbance curves for both outer and inner membrane permeabilization are the result of an enzymatic reaction between a substrate and the respective enzyme, which becomes accessible when the membranes are permeabilized.

For outer membrane permeabilization, the maximal slope ($\Delta AU_{486\ nm}$/30 min) was considered to quantify the velocity of the enzymatic reaction. Because the substrate concentration was fixed, this velocity was relied only on the concentration of accessible enzyme; an increase of the accessible enzyme quantity was indicative of a more severe membrane disruption. Then, the higher is the maximal slope, the more intense is the outer membrane permeabilization.

For inner membrane permeabilization, the maximal slope ($\Delta AU_{420\ nm}$/30 min) was considered to quantify the intensity of the inner membrane disruption, in a similar way as described above. Moreover, the lag time before the absorbance signal increase was considered indicative of the delay between outer and inner membrane permeabilization. The lag time was determined as the intersection between the baseline and the tangent of the curve at the maximal slope (Figure 2.1).

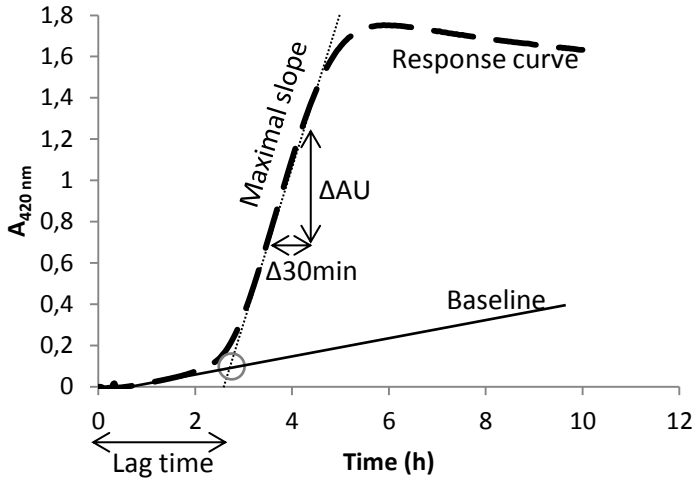

Figure 2.1: Quantification of inner membrane permeabilization using maximal slope and lag time.

Statistical analysis

All experiments were at least performed in triplicates. Statistical analysis was performed with R 2.15.2. Significance levels were at least 95%. Data from the normal distribution and with equal variances were treated with parametric tests. In this case, for the comparison of means the Student t test was used. Data from other distributions or with unequal variances were treated with nonparametric tests. In this case, for the comparison of means the Wilcoxon rank sum test was used.

2.2.3 Results

Preliminary protocol improvements for reliable measurements of outer and inner membrane disruption for long durations

Extension of Lehrer's method to long durations implies that substrates and products of β-lactamase and β-galactosidase are time-stable. Nitrocefin and ONPG absorbances were both stable at 37 °C for durations as long as 10 h (data not shown). On the contrary, the absorbances of HP-nitrocefin (Figure 2.2A) and ONP (Figure 2.2B) were not stable.

Sealing the microplate improved ONP stability from an 80% decrease to only 26% decrease of absorbance. Similarly, HP-nitrocefin absorbance decreased only 12% under sealed

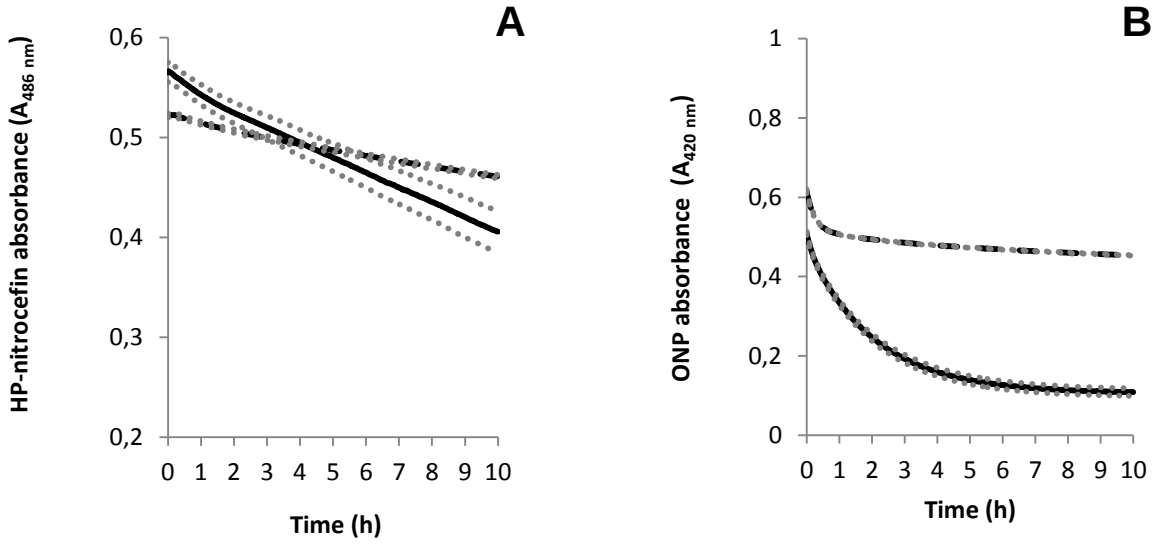

Figure 2.2: Absorbance stability of the reaction products of β-lactamase and β-galactosidase in non-sealed (full line) and sealed (dashed line) microplates. (A) HP-nitrocefin is detected by absorbance at 486 nm. (B) ONP is detected by absorbance at 420 nm. Standard deviation was calculated from triplicates (gray dotted line). Results were not corrected with a reference measurement, meaning that the absorbance values include the absorbance of the microplate and the buffer solution.

conditions compared to 28% under nonsealed conditions. To prove the relevance of sealing microplates, melittin has been used as a reference antibacterial agent. When the outer membrane permeabilization was measured by melittin, the maximum absorbance was higher under sealed conditions, compared to nonsealed ones (Figure 2.3A). Moreover, a higher maximal slope was observed with a sealed microplate (Figure 2.3C). When the inner membrane permeabilization was measured (Figure 2.3B), the absorbance signal corresponding to ONP release was dramatically different, depending on whether the microplate was sealed or not. Especially, during the first 3 h, the slope of the absorbance curve was much higher under sealed conditions. Because of this initial discrepancy, and despite an equivalent maximal slope between 3 and 5 h, the maximum absorbance was lower under nonsealed conditions (Figure 2.3B). With regard to the latter results, experiments with lysozyme will be performed only with sealed microplates.

Lysozyme activity against outer and inner membranes of *E. coli*

Lehrer's method was applied to test hen egg white lysozyme (HEWL) activity, including the modifications as described above. The results exhibited that 0.25 mg/mL HEWL disturbed the outer membrane of *E. coli* because β-lactamase activity was measured after around 0.5 h of incubation, whereas no absorbance was measured in the negative control, that is, without lysozyme (Figure 2.4A). Despite HP-nitrocefin content subsequently increasing in the negative control, it remained much lower than in the presence of 0.25 mg/mL lysozyme, throughout the 10 h experiment. Moreover, the supernatant of the bacterial suspension treated with lysozyme contained β-lactamase activity, unlike the supernatant of the negative control (Figure 2.4C).

During the first 2 h, a slight β-galactosidase activity was also measured, but in a similar way in samples with and without lysozyme (Figure 2.4B). On the contrary, when the experiment was extended to durations as long as 2.7 h and longer, β-galactosidase activity was much more extensive in the presence of 0.25 mg/mL HEWL, compared to the negative control (Figure 2.4B). However, the supernatant of the bacterial suspension treated with lysozyme did not

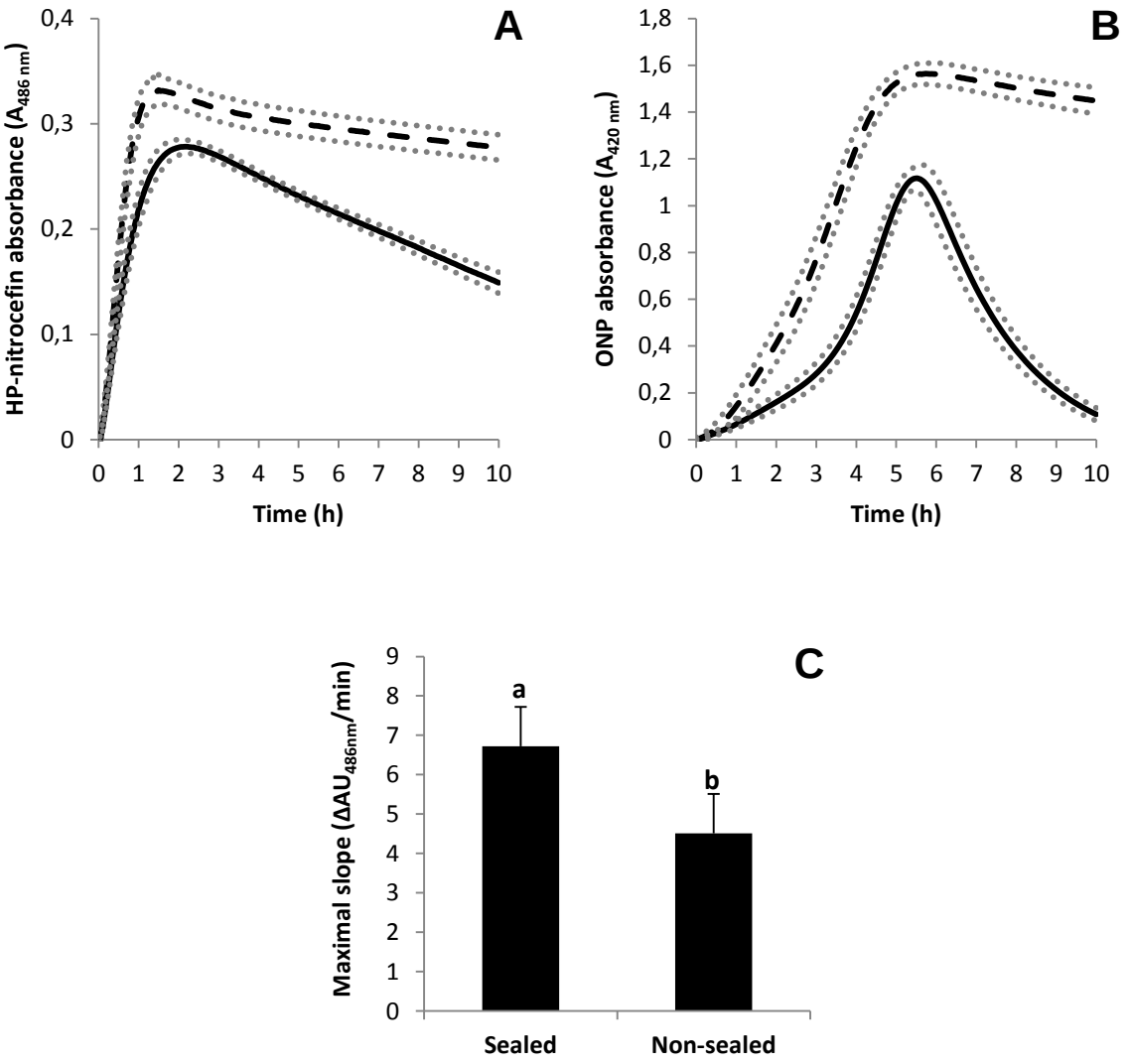

Figure 2.3: Permeabilization of the outer membrane (A) and inner membrane (B) of *E. coli* ML-35p (10^7 CFU/mL) by melittin (15 μg/mL) in nonsealed (full line) and sealed (dashed line) microplates, as evidenced by HP-nitrocefin and ONP release, respectively. Standard deviations were calculated from nine replicates (gray dotted line). Results were corrected with a reference absorbance including the absorbance of the microplate and the buffer solution. (C) Comparison of the maximal slopes for outer membrane permeabilization with and without sealing. Different letters (a,b) indicate significant difference ($p < 0.05$, Student t test).

contain β-galactosidase activity (data not shown).

Membrane permeabilization depending on lysozyme concentration and *E. coli* inoculum

When 10^7 CFU/mL *E. coli* was inoculated, β-lactamase activity, that is, outer membrane permeabilization, remained unchanged whatever the lysozyme concentration was, from 0.05 to 10 mg/mL (maximal slope around 0.0025 $\Delta AU_{486\ nm}$/min; Figure 2.5A). On the contrary, when the inoculum was 10^8 CFU/mL, the intensity of outer membrane permeabilization increased when lysozyme concentration increased from 0.05 to 0.5 mg/mL; above 0.5 mg/mL HEWL, the intensity of outer membrane permeabilization decreased when the lysozyme concentration increased (Figure 2.5A).

For both inocula levels, β-galactosidase activity, that is, inner membrane permeabilization, increased when lysozyme concentration increased (higher maximal slope; Figure 2.5B). Moreover, the higher inoculum showed systematically higher maximal slopes. Considering the lag time, when 10^7 CFU/mL was inoculated, lag time strongly decreased when lysozyme concentration increased (Figure 2.5C). On the contrary, with 10^8 CFU/mL inoculum, the lag time first remained stable between 0.05 and 0.5 mg/mL HEWL and then slightly decreased when lysozyme concentration increased over 0.5 mg/mL HEWL (Figure 2.5C). Lag time was systematically shorter with 10^8 CFU/mL inoculum compared to 10^7 CFU/mL.

2.2.4 Discussion

Membrane permeabilization is a major mechanism involved in the activity of many antimicrobial molecules, especially antimicrobial peptides and proteins (Ibrahim *et al.*, 2001b; Mine *et al.*, 2004). Most of the studies aiming to highlight such bacterial membrane disruption are limited to short-time experiments (<2 h). However, it is conceivable that membrane permeabilization could sometimes need more time, especially when proteins are concerned. Indeed, mechanisms described to explain the antimicrobial activity of peptides and the interaction between lysozyme and lipid bilayers generally suppose conformational modifications (Gorbenko *et al.*, 2007; Nguyen *et al.*, 2011). Then, protein structure changes at the water/cell membrane interface might be slower than with peptides, because proteins are generally much more rigid molecules compared to peptides. Especially, HEWL is known as a particularly rigid protein crosslinked by four disulfide bridges (Canfield & Liu, 1965). The extension to long durations of the traditional methods to investigate bacterial membrane permeabilization by proteins is then a relevant challenge. The popular and simple spectrophotometric method developed by Lehrer has here been selected for such an adaptation (Lehrer *et al.*, 1988).

Sealing microplates is an efficient way to improve the reliability of Lehrer's method for long experiments

To extend Lehrer's method to durations longer than 2 h, the substrates (ONPG and nitrocefin) and the products (ONP and HP-nitrocefin) of both enzymatic reactions need to be stable at 37 °C. This condition was not fulfilled for ONP, even for shorttime experiments (Figure 2.2B), and to a lesser extent for HP-nitrocefin (Figure 2.2A). ONP, which results from ONPG hydrolysis by β-galactosidase, turns out to be especially unstable when nonsealed plates are used (Figure 2.2B). This is likely the result from the high volatility of this compound at 37 °C, because the ONP signal decrease is largely limited with sealed microplates. In these conditions, only a slight decrease is observed at the very beginning of the experiment (Figure 2.2B), probably due to the partial evaporation of ONP in the gas phase, between the liquid phase and the film, until the gas/liquid equilibrium was reached for this chemical compound. This observation suggests that a minimal headspace between the liquid phase and the film should

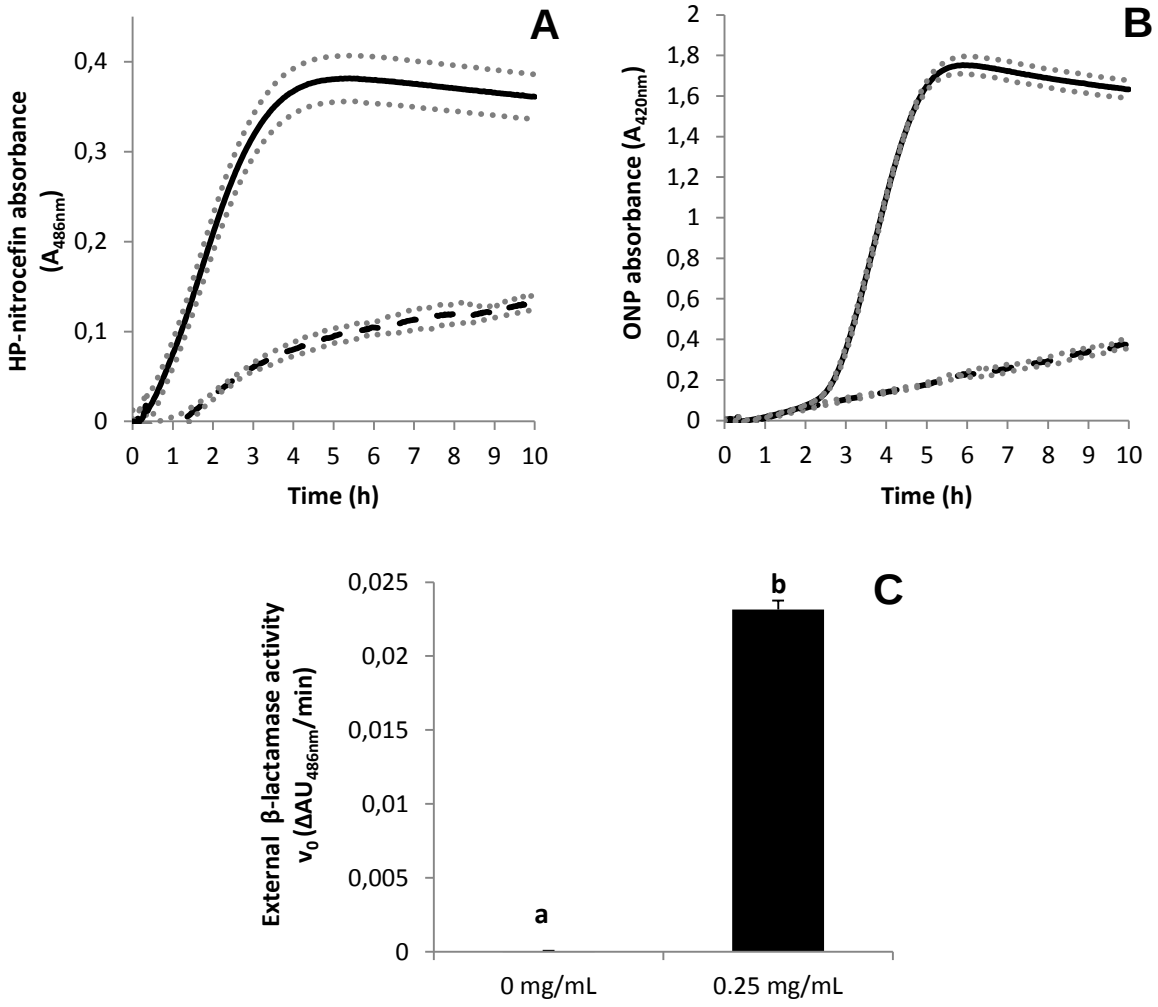

Figure 2.4: Permeabilization of outer membrane (A) and inner membrane (B) of *E. coli* ML-35p (10^7 CFU/mL) for 10 h, in the presence of 0.25 mg/mL HEWL (full line), and without lysozyme (dashed line). Standard deviations were calculated from triplicates (gray dotted line). Results were corrected with a reference absorbance including the absorbance of the microplate and buffer solution. (C) Externalization of β-lactamase in the absence and presence of 0.25 mg/mL of lysozyme measured by supernatant enzyme activity. Results stem from six replicates. Different letters (a,b) indicate significant difference ($p < 0.01$, Wilcoxon rank sum test).

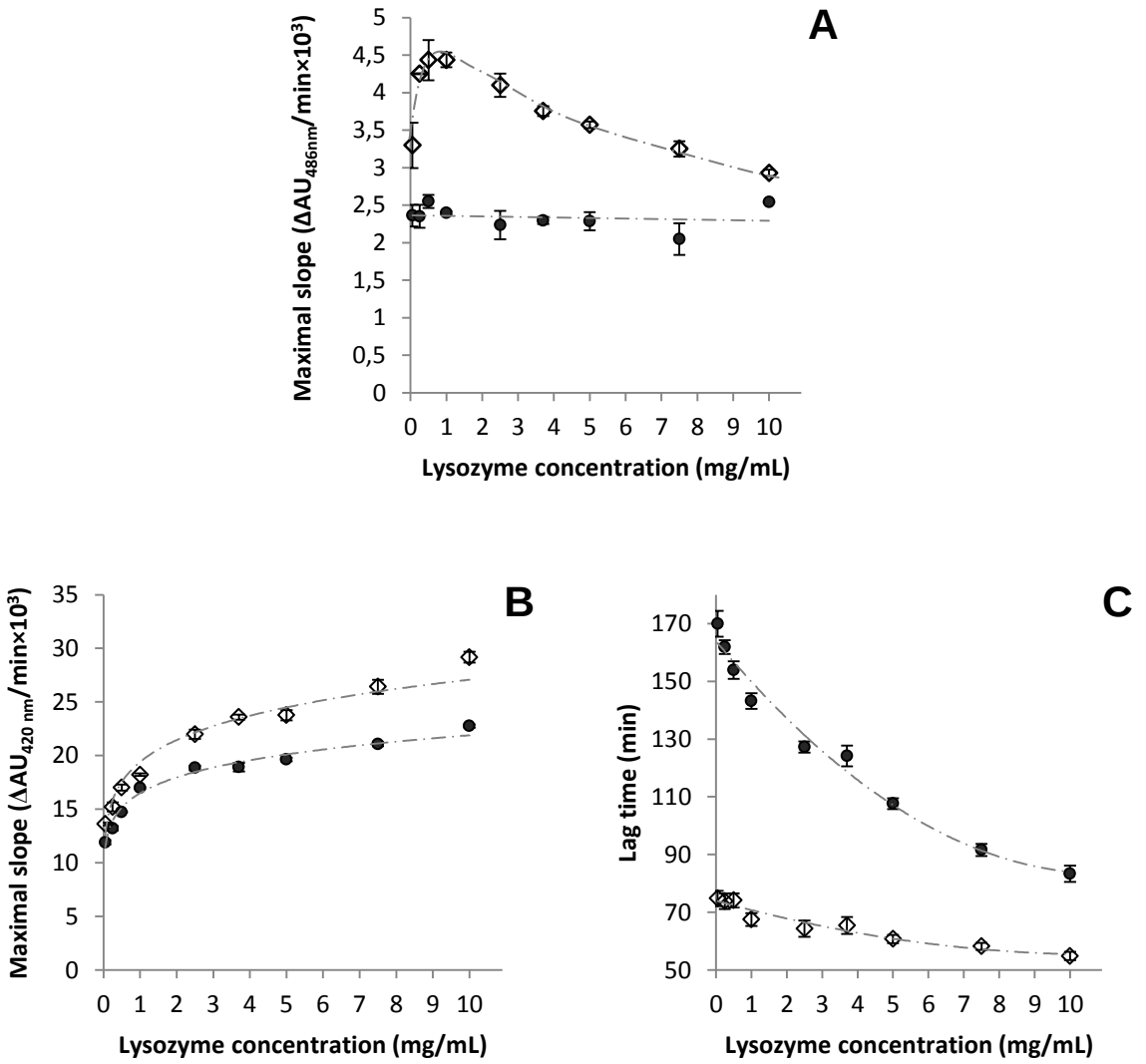

Figure 2.5: Membrane permeabilization as a function of lysozyme concentration for 10^7 CFU/mL (•) and 10^8 CFU/mL (◊) inocula: (A) outer membrane permeabilization as evidenced by β-lactamase activity; inner membrane permeabilization as evidenced by (B) β-galactosidase activity and (C) lag time between outer and inner membrane permeabilization. Standard deviations were calculated from triplicates.

be preferred; however, it cannot be reduced to zero, because of practical considerations such as sealing difficulty and risk of cross-contamination between adjacent wells. Although much less significant than for ONP, the HP-nitrocefin signal also decreases throughout the 10 h experiment when performed without sealing; this decrease is smaller when microplates are previously sealed (Figure 2.2A). Sealing microplates as proposed in this study appears then to be an easy and efficient way to improve the reliability of Lehrer's method when time extension up to 10 h is needed. Moreover, sealing avoids cross-contamination between wells, which can happen because of microplate stirring.

When the modified method (sealing microplates) was performed to measure the melittin antibacterial activity against *E. coli*, the results were significantly improved compared to the original method: higher initial rates were measured for both outer and inner membrane permeabilization (Figure 2.3). This indicates that the technical adjustments proposed in this study solve the underestimation induced by the original protocol. This underestimation is quite moderate for outer membrane permeabilization (Figure 2.3A), but a huge difference exists for the measurement of the inner membrane permeabilization (Figure 2.3B). In the latter case, the use of sealed microplates appears absolutely necessary, even for short-time experiments. Indeed, even in the very first moments of the test, because an extensive and quick disappearance of ONP occurs -simultaneously with ONP enzymatic release, the initial rate of permeabilization is underestimated by 80% when nonsealed microplates are used.

HEWL disrupts outer and inner membranes of *E. coli*

The method adjustments proposed above enabled the investigation of lysozyme membrane activity for durations as long as 10 h. With such long experiments, the ability of HEWL to permeabilize both outer and inner membranes of *E. coli* was demonstrated. Indeed, both β-lactamase and β-galactosidase activities were detected when HEWL (0.25 mg/mL) was added to an *E. coli* culture, as indicated by HP-nitrocefin and ONP release, respectively (Figure 2.4). The weak absorbance signals obtained with the negative control likely result from the spontaneous lysis of bacteria that occurs during the 10 h experiments. However, both β-lactamase and β-galactosidase activities were higher when HEWL was added, undoubtedly proving the membrane permeabilization induced by lysozyme.

Outer membrane permeabilization has already been described by Wild *et al.* and Pelligrini *et al.* for a similar HEWL concentration (Pellegrini *et al.*, 2000; Wild *et al.*, 1997). These authors observed the outer membrane permeabilization using electron microscopy and Lehrer's membrane permeabilization assay, respectively. The original Lehrer method enabled this because outer membrane permeabilization occurs after around 30 min, for 0.25 mg/mL lysozyme. However, these authors conclude that no inner membrane permeabilization occurs due to the direct action of HEWL.

The present study highlights that, when Lehrer's method is extended to long durations, HEWL induces inner membrane permeabilization, too, but this is only detectable after 2.7 h of incubation with 0.25 mg/mL HEWL and 10^7 CFU/mL *E. coli* inoculum. It is then a slow phenomenon, compared to what is usually observed with antibacterial peptides. The delay necessary for the detection of the inner membrane permeabilization could be explained by the succession of hurdles that HEWL has to get over: passing through the outer membrane, peptidoglycan hydrolysis or diffusion through the peptidoglycan network (Vollmer & Bertsche, 2008), and finally disturbance of the inner membrane.

To ensure that the inner membrane permeabilization is not the result of cell lysis caused by peptidoglycan disintegration, the presence of β-galactosidase was investigated in the su-

pernatant of the *E. coli* cells (10^7 CFU/mL) treated with 0.25 mg/mL lysozyme (as explained under section 2.2.2). β-Galactosidase would be present in the supernatant when peptidoglycan disintegration and thus cell lysis occur (Silhavy *et al.*, 2010). However, no β-galactosidase activity could be measured in the supernatant, demonstrating that this enzyme was not leaking out of the cytoplasm; then, there was no cell lysis, and the β-galactosidase activity detected when *E. coli* cells are in the presence of lysozyme resulted from the diffusion of ONPG into the cell. This confirms that HEWL directly acts on the inner membrane of *E. coli*, modifying its permeability, and independent of the lysozyme enzymatic activity on peptidoglycan.

It is noticeable that, in opposition to β-galactosidase, β-lactamase activity was measured in the supernatant of *E. coli* cells treated with 0.25 mg/mL lysozyme (Figure 2.4C). This proves that HEWL disrupts the outer membrane in such a way that this enzyme of 28.9 kDa can leak out of the periplasm. Large size pores inside the outer membrane are thus induced by HEWL.

HEWL acts by a two-step process: saturation of the outer membrane before entrance into the cell and permeabilization of the inner membrane

The extent of the outer membrane permeabilization, quantified by the β-lactamase activity (Figure 2.5A), was unchanged between 0.05 and 10 mg/mL HEWL with inoculation of 10^7 CFU/mL. On the contrary, the outer membrane permeabilization increased when HEWL concentration increased from 0.05 to 0.5 mg/mL with inoculation of 10^8 CFU/mL. This suggests that a critical ratio for outer membrane saturation should be 0.05 mg/mL HEWL:10^7 CFU/mL *E. coli*. Indeed, β-lactamase activity did not increase when $>$0.05 mg/mL lysozyme was added to 10^7 CFU/mL. Moreover, the maximum β-lactamase activity when 10^8 CFU/mL was inoculated was reached at a ratio 0.5 mg/mL lysozyme:10^8 CFU/mL, that is, the same ratio as 0.05 mg/mL HEWL:10^7 CFU/mL.

As far as the inner membrane is concerned, a dose-response effect occurred for 0.05-10 mg/mL HEWL at both *E. coli* inocula (10^7 and 10^8 CFU/mL). The extent of the inner membrane permeabilization increased when HEWL concentration increased (Figure 2.5B). The maximal slopes obtained with 10^8 CFU/mL inoculum were systematically higher than those obtained with 10^7 CFU/mL. This is consistent with the higher quantity of β-galactosidase potentially accessible to ONPG when the bacterial inoculum was higher. Simultaneously, the lag time decreased when the HEWL concentration increased, for both *E. coli* inocula (Figure 2.5C). Because the lag time is the delay needed for the release of detectable quantities of ONP, a lag time decrease indicates a faster increase of ONP concentration, related to a higher β-galactosidase activity. Therefore, the lag time is consistently shorter with 10^8 CFU/mL *E. coli* compared to 10^7 CFU/mL.

When the inoculum was 10^7 CFU/mL *E. coli*, the lag time regularly and strongly decreased when HEWL increased from 0.05 to 10 mg/mL. This suggests that the higher the HEWL concentration in the bulk, the higher the quantity of HEWL reaching the inner membrane. The lag time decrease is then consistent with the assumption of the outer membrane saturation with HEWL concentration of 0.05 mg/mL or higher and 10^7 CFU/mL *E. coli*. Indeed, because of such a saturation, each additional HEWL molecule added in the bulk remains 'free' (not entrapped into the outer membrane), able to cross over the disrupted outer membrane and to reach the inner membrane.

When 10^8 CFU/mL *E. coli* was inoculated, the lag time was constant between 0.05 and 0.5 mg/mL HEWL. Because the outer membrane would not be saturated with HEWL molecules in these conditions, as suggested above, each additional HEWL molecule added in

the bulk would then be essentially entrapped inside the outer membrane and then unavailable for deeper penetration into the bacteria cell. On the contrary, with HEWL concentrations > 0.5 mg/mL, meaning when outer membrane saturation is achieved, the lag time decreased when HEWL concentration increased, similarly to what was observed when 10^7 CFU/mL *E. coli* was inoculated; in these conditions, each additional HEWL molecule remains 'free' and able to enter into the cell. However, even with the highest lysozyme concentration, that is, 10 mg/mL, the lag time remained >50 min; this could be the minimal delay for lysozyme entrance into the cell and interaction with the inner membrane.

Outer membrane permeabilization is reduced when *E. coli* inoculum and HEWL concentration are simultaneously high

At high inoculum levels, quorum sensing can play a major role in bacterial resistance against antimicrobial agents (Mah & O'Toole, 2001). Quorum sensing is a cell-to-cell communication between bacteria by excretion of signal molecules, which can be detected by other bacteria of the same or other species (Waters & Bassler, 2005). In *E. coli* K12, AI-2 is one of those signal molecules that up-regulates several genes related to the outer membrane such as rfaY; rfaY controls the LPS-core biosynthesis. Stress induction of AI-2 has been demonstrated due to the addition of glucose, Fe^{3+}, NaCl, and dithiothreitol (DeLisa *et al.*, 2001a,b). Thus, quorum sensing can be a stress-induced phenomenon.

In the present study, it is noticeable that *E. coli* outer membrane permeabilization decreased when HEWL concentration exceeds 1 mg/mL and when 10^8 CFU/mL was inoculated, but this was not observed when inoculum was 10^7 CFU/mL (Figure 2.5A). The assumption of a lysozyme stress (≈ 1 mg/mL) could be proposed. This stress could activate quorum sensing between bacterial cells, in a dose-dependent manner. In these conditions, that is, high inoculum and high HEWL concentration, the outer membrane permeabilization of some bacterial cells may induce the expression of signal molecules, which could activate defense mechanisms by the sister cells. These defense mechanisms could include changes in the outer membrane composition, thus decreasing permeabilization by lysozyme. However, more investigations are needed to prove such hypothetical mechanisms.

2.3 Bilan de l'étude de l'activité du lysozyme natif sur les membranes d'*E. coli*

Parce que nous avons émis l'hypothèse que l'action d'une protéine rigide telle que le lysozyme, sur les membranes externe et cytoplasmique d'*E. coli*, pouvait nécessiter des temps plus longs que ceux habituellement testés dans le cas des petits peptides antimicrobiens, la méthode de Lehrer devait être adaptée pour des observations sur une durée supérieure à celle proposée par cet auteur. La difficulté est que les produits des réactions enzymatiques à la base de la méthode (ONP et HP-nitrocéfine) ne sont pas stables à 37°C au-delà de 2 h. De plus, à la température à laquelle la méthode est appliquée (37°C), l'évaporation des échantillons est conséquente. La solution que nous avons testée pour résoudre ces difficultés a simplement consisté à fermer hermétiquement les microplaques utilisées pour réaliser le test, à l'aide d'un film transparent, limitant d'une part l'évaporation et stabilisant d'autre part les produits de la réaction enzymatique. Cette adaptation de la méthode de Lehrer permet effectivement de réaliser un suivi spectrophotométrique de suspensions bactériennes sur une durée d'au moins 10 h. La prolongation de l'analyse nous a ainsi permis de confirmer la perméabilisation de la membrane externe d'*E. coli* par le lysozyme et, pour la première fois, de démontrer expérimentalement la perméabilisation de la membrane cytoplasmique de cette même bactérie. Dans les conditions mises en œuvre ici (inoculation d'*E. coli* à 10^7 CFU/mL en présence de

0.25 mg/mL de lysozyme), le temps nécessaire pour détecter la perméabilisation de la membrane interne est d'environ 2.7 h. Ceci confirme que des mesures sur une durée plus longue que celles habituellement pratiquées peuvent être nécessaires pour analyser la perméabilisation des membranes bactériennes par des protéines.

La méthode de Lehrer ainsi adaptée nous a permis d'investiguer les différentes étapes à l'origine de l'activité anti-membranaire du lysozyme (Figure 2.6). Ainsi, la membrane externe piège les molécules de lysozyme en solution jusqu'à un niveau de saturation atteint pour une concentration en lysozyme de 0.05 mg/L lorsque la population bactérienne est de 10^7 CFU/mL. L'adsorption du lysozyme sur la membrane externe induit la formation de pores dans cette membrane, pores dont la taille est suffisante pour permettre la diffusion de la β-lactamase dans le milieu extérieur. Ces pores permettent également aux molécules de lysozyme libres en solution, c'est-à-dire non adsorbées sur la membrane externe, d'accéder au périplasme où elles hydrolysent et/ou traversent le peptidoglycane, pour finalement arriver au niveau de la membrane interne dont elles provoquent la perméabilisation, sans toutefois qu'il y ait formation de pores.

L'action directe du lysozyme sur les membranes externe et cytoplasmique d'*E. coli* étant établie, la question des caractéristiques physicochimiques à l'origine de cette action se pose. Et par analogie d'une part avec les peptides antimicrobiens dont on sait qu'ils sont généralement caractérisés par une charge électropositive et un caractère hydrophobe importants (cf Chapitre 1 § 1.1.1), et d'autre part avec les modifications du lysozyme permettant d'augmenter son efficacité antibactérienne (cf Chapitre 1 § 1.2.2), nous avons souhaité exploré les conséquences éventuelles du chauffage à sec sur l'activité du lysozyme vis-à-vis d'*E. coli*. En effet, ce procédé simple à mettre en œuvre, tant au niveau laboratoire qu'à l'échelle industrielle, augmente l'hydrophobie, la tensio-activité, le point isoélectrique et la flexibilité du lysozyme (Desfougères *et al.*, 2011a,b). Or, tous ces changements sont a priori favorables à l'augmentation du potentiel de perturbation des membranes bactériennes par le lysozyme, et par conséquent à son activité contre les bactéries à coloration de Gram négative. C'est cette hypothèse que nous avons voulu tester ici en étudiant l'effet du lysozyme chauffé à sec sur les membranes d' *E. coli*, en comparaison du lysozyme natif.

2.4 Dry-heating of lysozyme increases its activity against *Escherichia coli* membranes

Derde M., Guérin-Dubiard C., Lechevalier V., Cochet MF., Jan S., Baron F., Gautier M., Vié V. & Nau F.

(*Journal of Agricultural and Food Chemistry* 2014, vol. 62, pp. 1692-1700)

2.4.1 Abstract

For food as well as for medical applications, there is a growing interest in novel and natural antimicrobial molecules. Lysozyme is a promising candidate for the development of such molecules. This protein is largely studied and known for its muramidase activity against Gram-positive bacteria, but it also shows antimicrobial activity against Gram-negative bacteria, especially when previously modified. In this study, the activity of dry-heated lysozyme (DH-L) against *Escherichia coli* has been investigated and compared to that of native lysozyme (N-L). Whereas N-L only delays bacterial growth, DH-L causes an early-stage population decrease. The accompanying membrane permeabilization suggests that DH-L induces either larger pores or more pores in the outer membrane as compared to N-L, as well as more ion channels in the inner membrane. The strong morphological modifications observed by optical microscopy and atomic force microscopy when *E. coli* cells are treated with DH-L are consistent with the

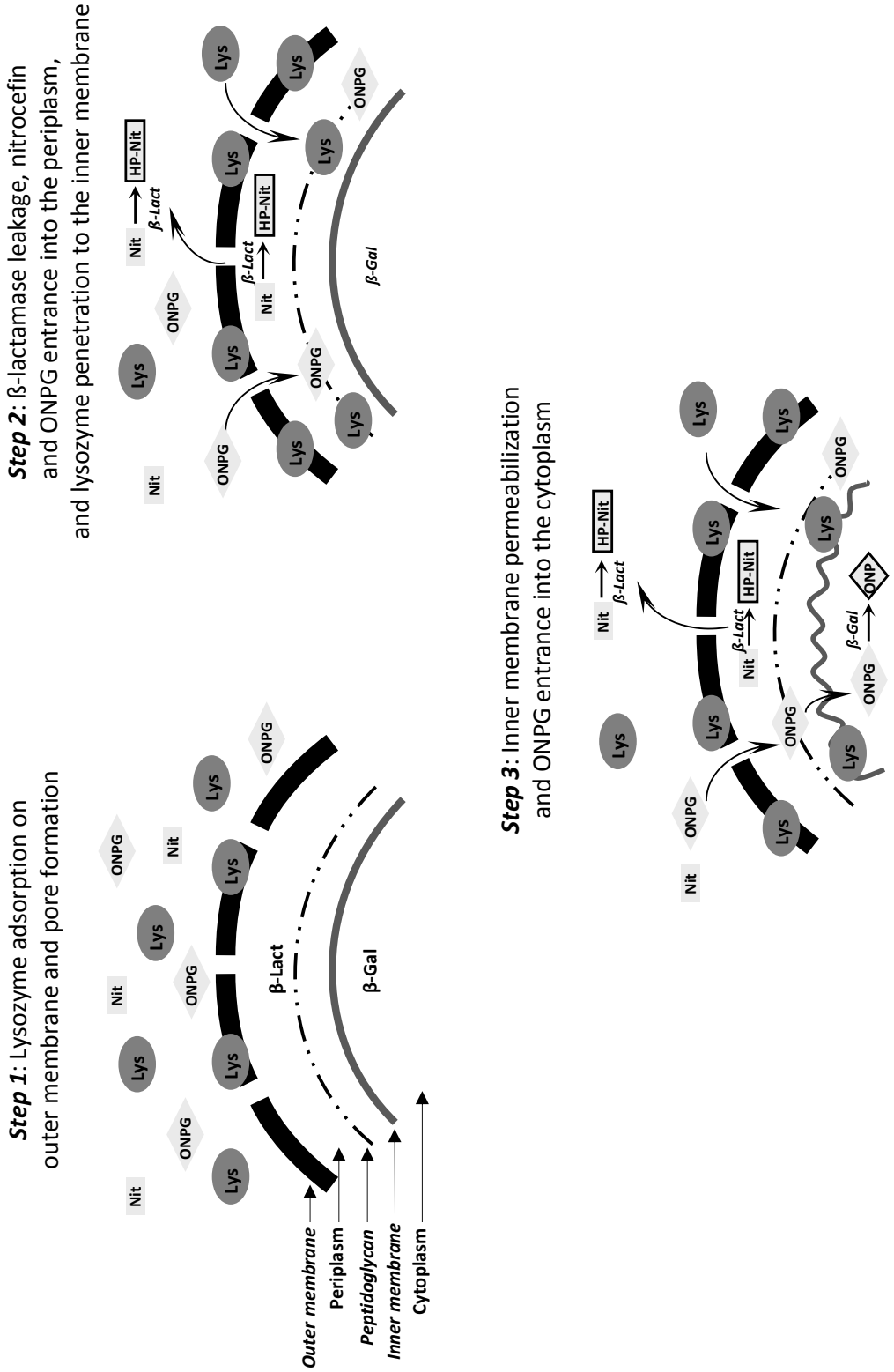

Figure 2.6: Hypothetical sequential events explaining the action of HEWL on outer and inner membranes of *E. coli*. Lys, lysozyme; β-Lact, β-lactamase; β-Gal, β-galactosidase; Nit, nitrocefin, and HP-Nit, HP-nitrocefin, substrate and product of β-lactamase, respectively; ONPG and ONP, substrate and product of β-galactosidase, respectively.

suggested disturbances of membrane integrity. The higher hydrophobicity, surface activity, and positive charge induced by dry-heating could be responsible for the increased activity of DH-L on the *E. coli* membranes.

2.4.2 Materials and methods

Materials

Native lysozyme powder (pH 3.2) was obtained from Liot (Annezin, 62-France); it was heated for 7 days at 80 °C in hermetically closed glass tubes to obtain dry-heated lysozyme. Micrococcus lysodeikticus, ATCC no. 4698, Trisma base, potassium phosphate monobasic, potassium phosphate dibasic, potassium chloride, ampicillin, chloramphenicol, (o-nitrophenyl)-galactoside (ONPG), 3,3′-dipropylthiadicarbocyanine iodide ($DiSC_3$), 4-(2-hydroxyethyl)-1-piperazineethanesulfonic acid (HEPES), and glucose were obtained from Sigma-Aldrich (Saint-Quentin, France). Nitrocefin, a standard solution of potassium (1000 mg/L), casein peptone, and yeast extract were obtained from Merck Chemicals (Darmstadt, Germany). Tryptic soy broth (TSB) was from AES (Bruz, France).

Bacterial strains

Three different *E. coli* strains have been used (Table 2.1). *E. coli* K12 was obtained from the Institut Pasteur (Paris, France). *E. coli* MG1655 ivy::Cm was kindly provided by C. Michiels (Centre of Food and Microbial Technology, KU Leuven, Belgium); this bacterial strain no longer expresses the lysozyme inhibitor Ivy. The bacterial strain *E. coli* ML-35p ($LacI^-$ $LacY^-$ $LacZ^+$, plasmid pBR322) was kindly provided by R. Lehrer (Department of Medicine, University of California, Los Angeles) and transmitted to our laboratory by D. Destoumieux-Garzon (UMR 5119, Ecologie des systèmes marins côtiers, University of Montpellier, France). *E. coli* ML-35p lacks lactose permease and expresses β-lactamase and β-galactosidase in the periplasm and cytoplasm, respectively.

Table 2.1: Presence (+) or absence (−) of Ivy, β-lactamase, β-galactosidase, and lactose permease in the different bacterial strains used for the present study.

	Ivy	**β-lactamase**	**β-galactosidase**	**Lactose permease**
***E. coli* K12**	+	-	+	+
***E. coli* ML-35p**	+	+	+	-
***E. coli* MG1655 ivy::Cm**	-	-	+	+

Growth assays with *E. coli* K12 and *E. coli* MG1655 ivy::Cm

The bacterial culture *E. coli* K12 or *E. coli* MG1655 ivy::Cm was grown overnight (18 h) at 37 °C under stirring (130 rpm) in TSB containing no antibiotics or 50 μg/mL ampicillin and 30 μg/mL chloramphenicol, respectively. After the incubation period, the cultures contained about 10^9 CFU/mL *E. coli*, from which 10^5 CFU/mL bacterial suspensions were prepared by performing four 10-fold serial dilutions in LB05 (Luria broth containing 10 g/L peptone of casein, 5 g/L yeast extract, and 0.5 g/L NaCl). After solubilization in demineralized water, lysozyme (native or dry-heated) was added at 0.25 or 3.7 g/L to the bacterial suspension, before incubation at 37 °C under stirring (130 rpm) for 24 h; 3.7 g/L is the natural concentration of lysozyme in hen egg white. Cell enumeration was performed by colony count after 2, 4, 6, and 24 h as previously described by Baron *et al.* (2006). The results for cell counts are based on nine replicates (three biological replicates, each with three technical replicates).

Outer and inner membrane permeability measurements

Outer and inner membrane permeability was measured using the Lehrer method (Lehrer *et al.*, 1988), modified as described by Derde *et al.* (2013). The *E. coli* ML-35p culture was grown overnight (18 h) in TSB containing 50 μg/mL ampicillin at 37 °C under stirring (130 rpm). The bacterial culture was washed twice in 50 mM Tris−HCl buffer, pH 7.0 (5000g, 10 min), and diluted to obtain about 10^7 CFU/mL in solutions containing 0.25 or 3.7 g/L native or dry-heated lysozyme.

To test outer membrane permeability, 0.015 mg/mL nitrocefin (substrate of β-lactamase) was added to the sample solutions. When the outer membrane was permeabilized, the periplasmic β-lactamase hydrolyzed nitrocefin into the hydrolysis product of nitrocefin (HP-nitrocefin). HP-nitrocefin absorbance was measured at 486 nm (Spectramax M2, Molecular Devices, United Kingdom), at 37 °C under stirring.

To test inner membrane permeability, 0.7 mg/mL ONPG (substrate of β-galactosidase) was added to the sample solutions. When the inner membrane was permeabilized, the cytoplasmic β-galactosidase hydrolyzed ONPG into o-nitrophenol (ONP). ONP absorbance was measured at 420 nm (Spectramax M2, Molecular Devices, United Kingdom), at 37 °C under stirring.

Two parameters could then be determined: maximal slope and lag time. The maximal slope determined the maximal velocity of the enzymatic reaction of either β-lactamase or β-galactosidase. The maximal velocity is directly related to the concentration of accessible enzyme and thus to the permeability of the outer or inner membrane, respectively. The lag time was the time between outer and inner membrane permeabilization, estimated by the delay between both enzymatic reactions.

The results of lysozyme activity on membrane permeability are based on three replicates. The results were corrected for reference absorbance, i.e., the absorbance of the microplate and of the buffer solution.

Detection of β-lactamase and β-galactosidase leakage out of bacterial cells

After overnight growth (18 h) in TSB containing 50 μg/mL ampicillin at 37 °C under stirring (130 rpm), the *E. coli* ML-35p culture was washed twice with 50 mM Tris−HCl buffer, pH 7.0 (5000g, 10 min), and diluted to obtain 10^7 CFU/mL bacterial suspensions. These suspensions were added with lysozyme (0.25 or 3.7 g/L, native or dry-heated lysozyme) and incubated for 5 h at 37 °C under stirring, before centrifugation at 5000g for 10 min. β-lactamase and β-galactosidase activities were then tested in the supernatants by adding 0.05 g/L nitrocefin and 1 g/L ONPG, respectively. The initial reaction rates of both enzymatic reactions (v_0 = ΔAU/min) were determined at 25 °C from absorbance curves (Multiskan Go, Thermo Fisher Scientific, Illkirch, France) at 486 and 420 nm, respectively.

Measurement of the bacterial membrane potential disruption

The disruption of the bacterial membrane potential was measured according to the method proposed by Wu *et al.* (1999). The *E. coli* K12 culture was grown for 3.5 h in TSB at 37 °C under stirring (130 rpm) to reach a midlog phase. The culture was washed twice with 5 mM HEPES buffer at pH 7.2 containing 5 mM glucose (5000g, 10 min) and diluted to obtain an absorbance of around 0.06 at 620 nm. A 1 μM concentration of $DiSC_3$ and 100 mM KCl were added to the diluted bacterial suspension, before incubation for 1 h at 30 °C in the dark. Then lysozyme (0.25 or 3.7 g/L, native or dry-heated) was added to the bacterial cells, and

the samples were incubated for 30 min at 30 °C in the dark. Fluorescence was then measured at 670 nm with a fluorimeter, Perkin-Elmer LS55 (Perkin-Elmer, Courtaboeuf, France), after excitation at 622 nm; the slit width was 2.5 nm/2.5 nm, and the integration time was 6.2 s. The results are based on nine replicates (three biological replicates, each with three technical replicates).

Potassium leakage measurement

The measurement of potassium leakage was performed according to the method described by Orlov *et al.* (2002). After overnight growth (18 h) in TSB at 37 °C under stirring (130 rpm), the *E. coli* K12 culture was washed twice with 10 mM Tris−acetate buffer, pH 7.0, containing 100 mM NaCl (5000g, 10 min), and diluted to obtain 10^8 CFU/mL bacterial suspensions. Lysozyme (0.25 or 3.7 g/L, native or dry-heated) was added to the bacterial solutions, and then the samples were incubated for 3 h at 37 °C under stirring, centrifugated (5000g for 10 min), and filtered with 0.22 μm filters. The K^+ concentration was measured in the filtrates using a potassium-selective electrode (DX239-K) coupled to an S50 SevenMulti meter (Mettler Toledo, Viroflay, France) and recorded with an ISE meter previously calibrated with six standard solutions containing 5.15, 10.3, 77.6, 103, 1330, and 11700 μM potassium, respectively. Calibration and measurements were performed at 25 °C.

Optical microscopy and atomic force microscopy (AFM)

The *E. coli* K12 culture was grown overnight (18 h) in TSB at 37 °C under stirring (130 rpm). After the incubation period, the culture contained about 10^9 CFU/mL *E. coli*, from which 10^5 CFU/mL bacterial suspensions were prepared by performing four 10-fold serial dilutions in LB05. Then lysozyme (0.25 or 3.7 g/L, native or dry-heated) was added to the bacterial suspension before incubation at 37 °C under stirring (130 rpm) for 24 h. Samples were washed in a 0.85% NaCl solution (3000g, 10 min) before optical microscopy and AFM were performed.

Optical microscopy observations were performed with an Olympus BX51 (enlargement 100×). Images were taken with a digital camera, Olympus Camedia C-5050.

Samples were deposited on freshly cleaved mica. To avoid accumulation of bacteria, a dipper (Nima Technology, Cambridge, U.K.) was used to gently remove the mica from the sample solution at 2 mm/min while the solution was being stirred. The mica plate was then dried at room temperature, and shortly after that, AFM imaging was performed. Images were recorded with a Pico-plus atomic force microscope (Molecular Imaging, Phoenix, AZ) operating in tapping mode. A scanner of 100 μm was used for the measurements. Topographic and phase images, illustrating cell topography and cell heterogeneity (Camesano *et al.*, 2000), were acquired simultaneously using silicon nitride tips (AppNano, Silicon Valley, CA) with a resonance frequency of 145−230 kHz and a nominal spring constant of 20−95 mN/m. Transversal cross sections of the bacteria were performed to illustrate height and surface roughness. The images presented in the present study are representative of several samples.

Statistical analysis

All experiments were performed at least in triplicate. Statistical analysis was performed with R 2.15.2. Significance levels were at least 95%. Data from the normal distribution and with equal variances were treated with parametric tests. In this case, for the comparison of means the Student t test was used. Data from other distributions or with unequal variances were treated with nonparametric tests. In this case, for the comparison of means the Wilcoxon rank sum test was used.

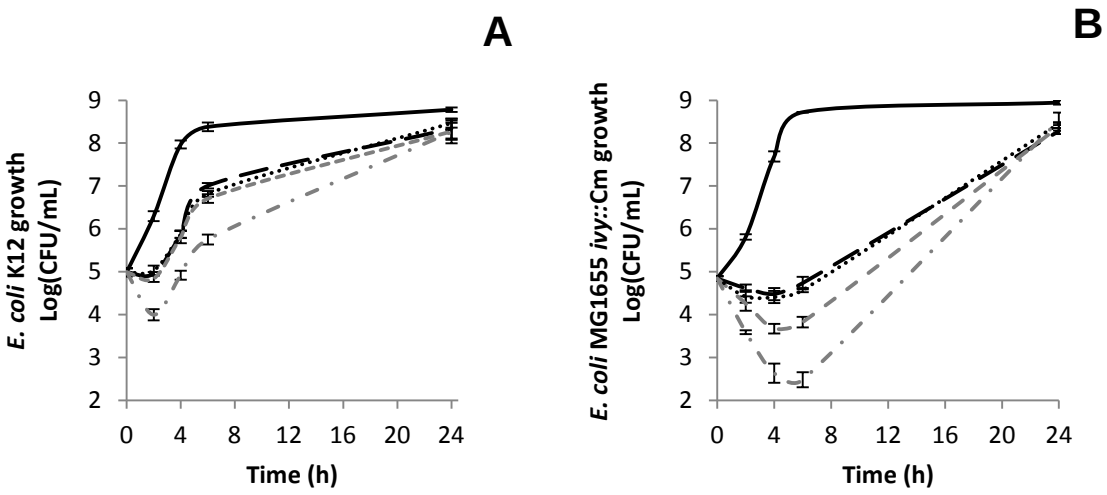

Figure 2.7: Growth curves of *E. coli* K12 (A) and of *E. coli* MG1655 ivy::Cm (B) in LB05 medium in the absence of lysozyme (—) or in the presence of 0.25 g/L N-L (— —), 0.25 g/L DH-L (· · ·), 3.7 g/L N-L (- -) or 3.7 g/L DH-L (- · -). The results are based on nine replicates.

2.4.3 Results

Growth of *E. coli* in the presence of lysozyme

The growth of *E. coli* K12 is disturbed in the presence of both native (N-L) and dry-heated (DH-L) lysozyme during the first hours of growth (Figure 2.7A), but after 24 h of incubation at 37 °C, no significant difference is observed between the samples with or without lysozyme. The growth of *E. coli* K12 shows the same pattern when N-L is added, whatever the concentration (0.25 or 3.7 g/L), and when DH-L is added at low concentration (0.25 g/L): the bacterial growth is inhibited for 2 h, before it recovers, and cell counts similar to those in the control sample (without lysozyme) are finally reached. On the contrary, the addition of 3.7 g/L DH-L induces a different pattern of the *E. coli* K12 growth: 1 log reduction of the bacterial cells is observed after 2 h of incubation, after which the growth rate recovers; with up to 6 h of incubation, the *E. coli* K12 population remains lower than in the other samples (control sample and samples with N-L or low-concentration DH-L).

When the same tests are performed on the *E. coli* MG1655 ivy::Cm strain, which lacks the periplasmic lysozyme inhibitor Ivy, the impact of lysozyme on the bacterial growth pattern is stronger as compared to that for *E. coli* K12, for both N-L and DH-L and both concentrations (0.25 and 3.7 g/L) (Figure 2.7B). The modification of the growth pattern is dose-dependent: the higher the N-L or DH-L concentration, the higher the population decrease observed in the first hours of incubation. At high concentration (3.7 g/L), DH-L causes a population decrease which is 1.3 log higher than that of N-L, whereas no difference is observed between both types of lysozyme at low concentrations (0.25 g/L). However, the number of bacterial cells suitable for growth is the same after 24 h of incubation with N-L and DH-L.

Membrane state of *E. coli* in the presence of lysozyme

N-L and DH-L induce similar overall permeabilization of the outer membrane whatever the concentration, as measured by the total β-lactamase activity (Figure 2.8A), but externalized β-lactamase activity, i.e., activity in the supernatant resulting from centrifugation of the bacterial culture incubated with lysozyme, is higher with DH-L than with N-L at both lysozyme concentrations (Figure 2.8B). Moreover, it is noticeable that a high concentration (3.7 g/L)

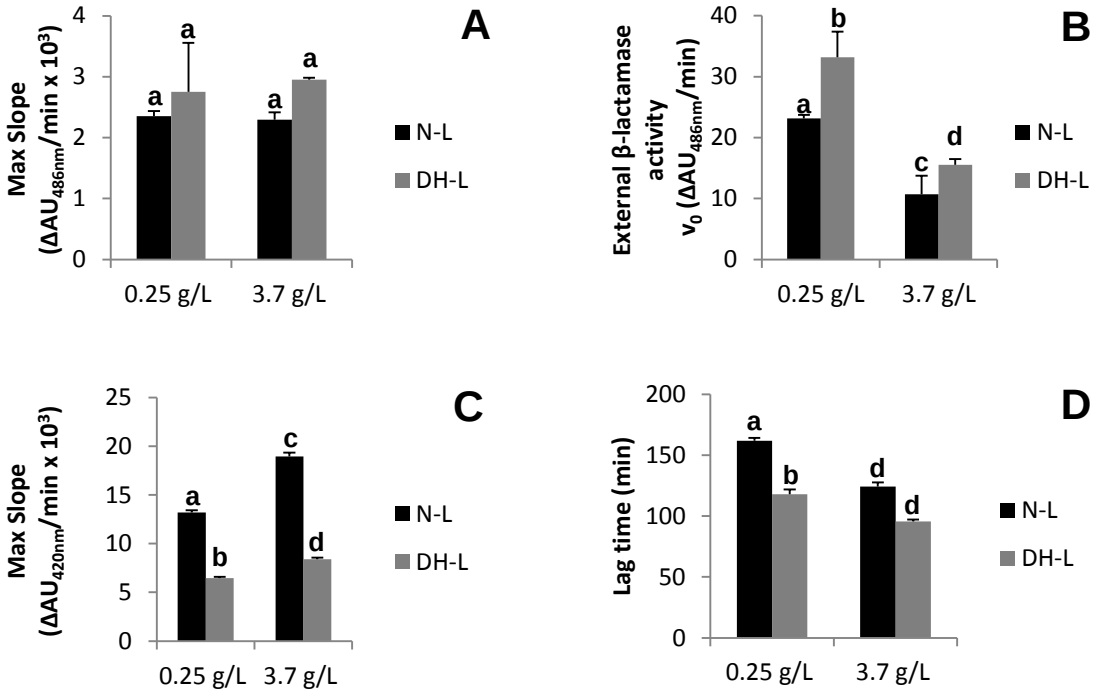

Figure 2.8: Comparison of the permeabilization of *E. coli* ML-35p outer (A, B) and inner (C, D) membranes by native (N-L) or dry-heated (DH-L) lysozyme as evidenced by β-lactamase and β-galactosidase activity, respectively. Different letters (a, b, c, d) indicate significant difference obtained from the Student t test (A, C, D) ($p < 0.01$) or Wilcoxon rank sum test (B) ($p < 0.01$).

of N-L and DH-L causes lower externalized β-lactamase activity than a low concentration (0.25 g/L) (Figure 2.8B).

Figure 2.8C shows that permeabilization of the inner membrane is stronger with N-L than with DH-L at either 0.25 or 3.7 g/L. On the other hand, the lag time before detection of the inner membrane permeabilization is shorter with DH-L than with N-L at both concentrations (Figure 2.8D). The intensity of inner membrane permeabilization and lag time are lysozyme concentration-dependent for both N-L and DH-L.

Disturbance of the inner membrane has also been investigated by measurement of changes of the membrane potential. N-L and DH-L similarly disturb the membrane potential of *E. coli* when added at 0.25 g/L in the bacterial culture. On the contrary, at higher concentration (3.7 g/L lysozyme), DH-L causes a stronger disruption of the membrane potential than N-L, as indicated by the 2-fold higher relative fluorescence of $DiSC_3$ (Figure 2.9A). For both N-L and DH-L, a dose-response effect is observed.

Finally, the measurement of intracellular K^+ leakage has been used as an indicator of inner membrane disruption. K^+ leakage is not detectable in *E. coli* cultures containing 0.25 g/L N-L or DH-L (data not shown), but significant K^+ leakage is measured in the presence of 3.7 g/L lysozyme. The extent of the K^+ leakage is 75% higher with DH-L than with N-L (Figure 2.9B).

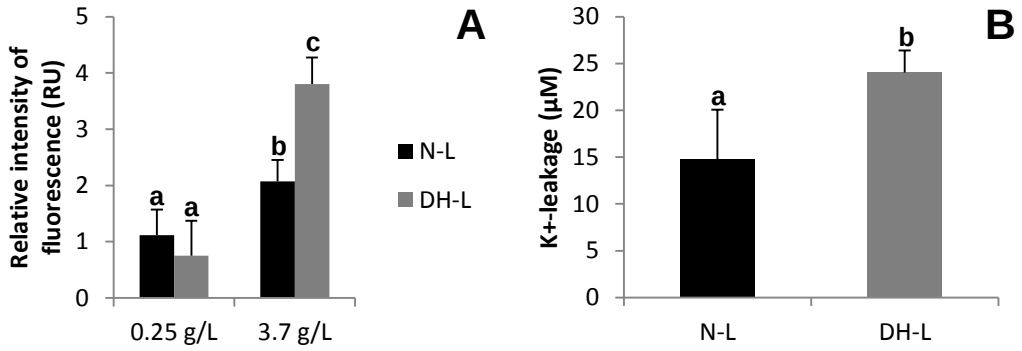

Figure 2.9: (A) Disruption of the membrane potential of *E. coli* K12 caused by native (N-L) or dry-heated (DH-L) lysozyme at 0.25 and 3.7 g/L. Different letters (a, b, c) indicate significant difference obtained from the Student t test ($p < 0.01$). Results are based on nine replicates. (B) K^+ leakage of *E. coli* K12 in the presence of 3.7 g/L N-L or DH-L after 3 h of incubation. Different letters (a, b) indicate significant difference obtained from the Student t test ($p < 0.01$). Results are based on six replicates.

Morphology of *E. coli* K12 in the presence of lysozyme

E. coli K12 incubated for 24 h in the presence of 0.25 g/L lysozyme exhibits differences in cell morphology in comparison to the control sample, as shown by optical microscopy images (Figure 2.10). Abnormally elongated bacterial cells are observed after treatment with lysozyme; such modified bacteria are present in a larger number when DH-L is added as compared to N-L (Figures 2.10B, C). These elongated cells could not be observed at high concentration (3.7 g/L) of N-L and DH-L (data not shown).

Topographic AFM enables determination of the size and characterization of the shape and the surface topology of bacteria. Non-treated bacteria are about 2 μm long, with a diameter of 500 nm; the surface is smooth and regular, and flagella are observed (Figure 2.11A). When bacteria are treated with N-L, the size is not modified (Figures 2.11B, D), whereas abnormally elongated cells without a visible septum are observed when the bacteria are treated with 0.25 g/L DH-L (Figure 2.11C). With high-concentration N-L treatment (Figure 2.11D), depressions can be observed on the bacterial cells, but the bacterial morphology is more strongly disturbed when the bacteria are treated with DH-L (Figures 2.11C, E), with an especially irregular cell surface and depressions; the depth and the diameter of these depressions increase when the DH-L concentration increases: around 15 nm depth at 0.25 g/L DH-L *versus* around 26 nm at 3.7 g/L and around 128 nm diameter *versus* 160 nm. When the bacteria are treated with either 3.7 g/L N-L or both concentrations of DH-L, cell debris is also observed (data not shown).

Phase AFM enables visualization of homogeneity or heterogeneity of the cell surface composition. (Camesano *et al.*, 2000) Thus, the non-treated bacteria appear homogeneous (Figure 2.12A), whereas heterogeneity can be observed with all the treated samples, with either N-L or DH-L, and at both concentrations (Figures 2.12B-E). However, higher heterogeneity is observed when the bacteria are treated with DH-L as compared to N-L.

2.4.4 Discussion

The capability of native hen egg white lysozyme to permeabilize the outer and inner membranes of *E. coli* has been previously established by Derde *et al.* (2013). Moreover, some structural modifications of lysozyme proved to be efficient to enhance the antibacterial activity

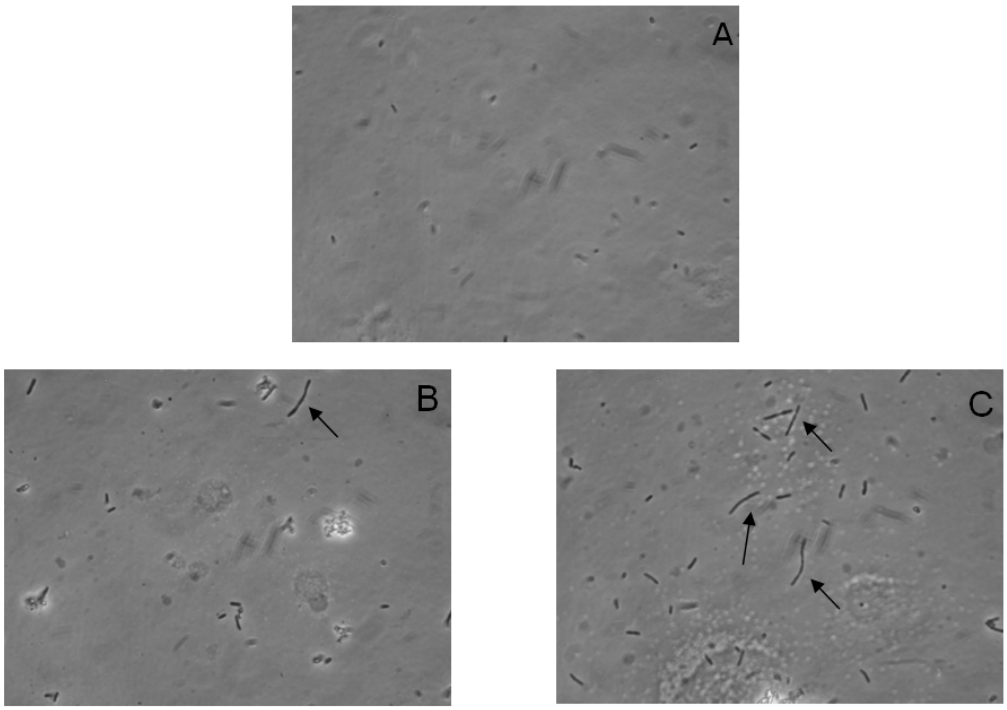

Figure 2.10: Observations of *E. coli* K12 with optical microscopy after 24 h of incubation in the absence of lysozyme (A) and in the presence of 0.25 g/L native lysozyme (N-L) (B) and dry-heated lysozyme (DH-L) (C).

of this protein (Masschalck & Michiels, 2003). Modifying lysozyme to design a novel antimicrobial with enhanced membrane activity and thus improved antibacterial activity against *E. coli* then seems relevant. Because membrane activity of antimicrobial proteins or peptides is highly dependent on the physicochemical properties of the molecules, dry-heating could be an interesting process for lysozyme design. Indeed, dry-heated lysozyme is more hydrophobic and more surface-active, and it contains isoforms that are more positively charged than native lysozyme (Desfougères *et al.*, 2011a). To test the hypothesis that dry-heated lysozyme is more active than native lysozyme against *E. coli*, because of an increased membrane activity, a comparative study is proposed.

Native lysozyme causes *E. coli* K12 growth latency

In the presence of low and high concentrations of N-L, the inhibition of *E. coli* K12 growth is observed for 2 h (Figure 2.7A). Lysozyme is undoubtedly the cause of this phenomenon, regarding the fact that the control sample (without lysozyme) does not induce any lag time before bacterial growth starts (Figure 2.7A). However, the N-L effect is rather short, and bacterial growth resumes. A bacterial concentration similar to that in the control sample is reached after 24 h of incubation (Figure 2.7A). This could be explained by several hypotheses: damage repair by the bacteria, activation of adaptation and defense mechanisms, and/or depletion of lysozyme in the growth medium by irreversible interaction with the bacteria.

The first possibility is that N-L causes minor damage to the bacterial cells. This damage does not lead to cell death, but the bacterial cell needs to repair the obtained cell structures. For these repair mechanisms, energy is needed and cell growth is thus retarded.

E. coli also have several defense mechanisms. The first defense mechanism of Gram-negative bacteria is the outer membrane. However, lysozyme has been shown to cross this

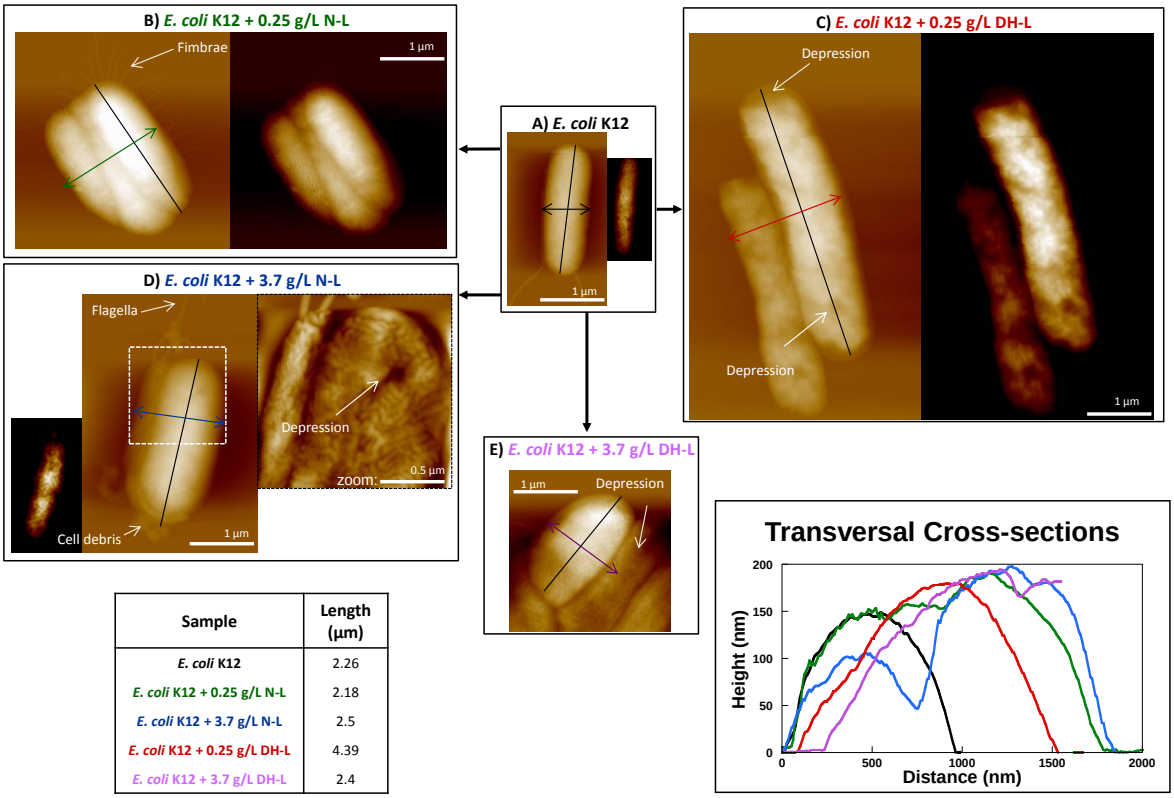

Sample	Length (µm)
E. coli K12	2.26
E. coli K12 + 0.25 g/L N-L	2.18
E. coli K12 + 3.7 g/L N-L	2.5
E. coli K12 + 0.25 g/L DH-L	4.39
E. coli K12 + 3.7 g/L DH-L	2.4

Figure 2.11: Topographical AFM observations: nontreated *E. coli* K12 cells (A); cells treated with native lysozyme at 0.25 g/L (B) or 3.7 g/L (D); cells treated with dry-heated lysozyme at 0.25 g/L (C) or 3.7 g/L (E). Topographical AFM images have a z-range from 0 to 400 nm for full-scale images and from 0 to 15 nm for the 3.7 g/L N-L zoom. Bacterial lengths and cross sections are measured as indicated by full lines on the AFM images. AFM images shown here are representative of the whole sample.

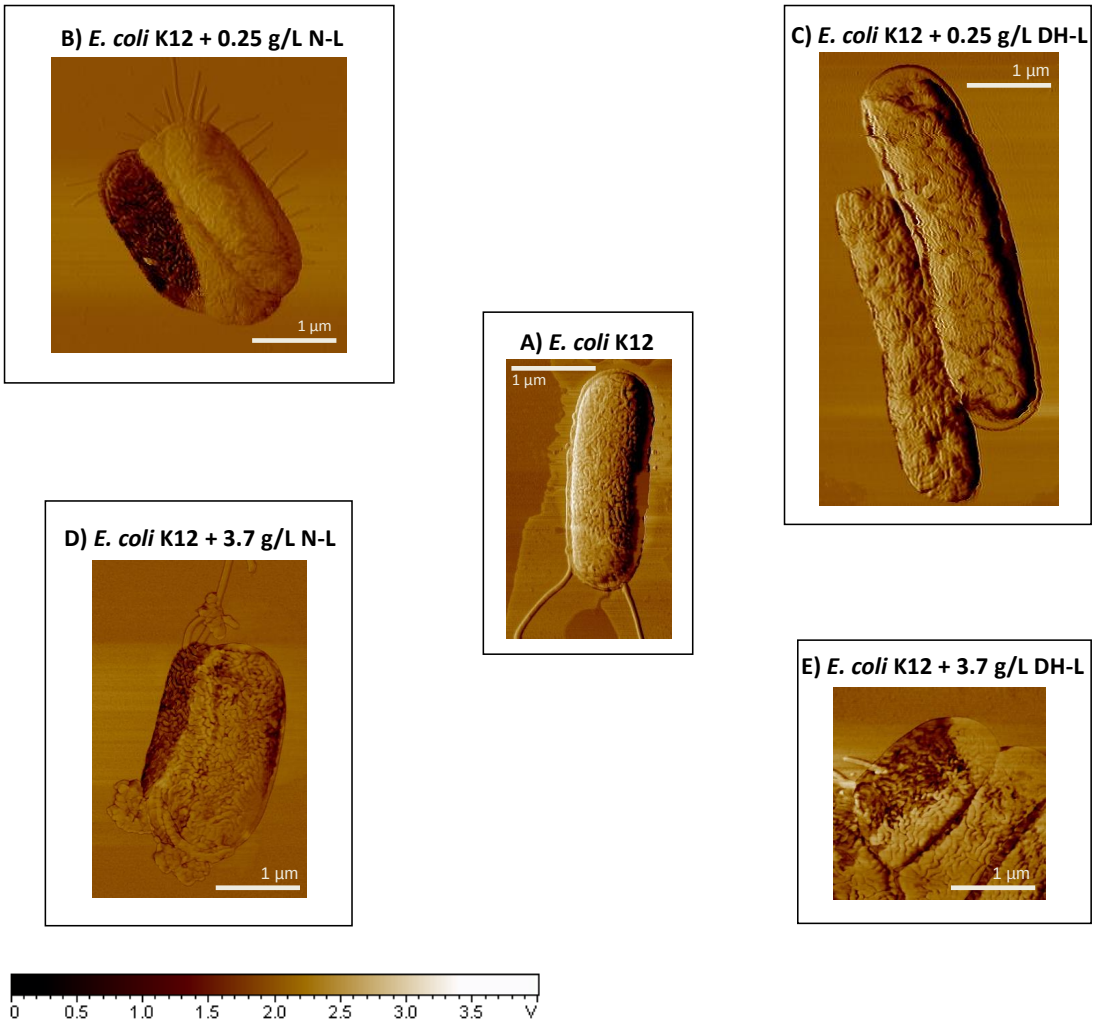

Figure 2.12: AFM phase imaging: nontreated *E. coli K12* cells (A); cells treated with native lysozyme at 0.25 g/L (B) or 3.7 g/L (D); cells treated with dry-heated lysozyme at 0.25 g/L (C) or 3.7 g/L (E). The z-range is from 0 to 4 V. AFM images shown here are representative of the whole sample.

hurdle (Derde *et al.*, 2013). Another present defense mechanism in *E. coli* is the lysozyme inhibitor Ivy, which neutralizes N-L in the periplasm (Abergel *et al.*, 2007). When N-L reaches the periplasm of *E. coli*, Ivy binds to N-L. This makes N-L harmless for the *E. coli* cells (Figure 2.7). *Enterobacteriaceae* are also known for the presence of proteases on their outer membrane. *E. coli* K12 carries a protease, OmpT, which combines characteristics of serine and aspartate proteases. The OmpT of *E. coli* K12 has been reported to degrade the antimicrobial peptide protamine. (Gruenheid & Le Moual, 2012) It is thus possible that OmpT also hydrolyzes lysozyme molecules. Besides the above-mentioned defense mechanisms, *E. coli* is also able to modify the lipopolysaccharides of the outer membrane, protecting the outer membrane from permeabilization and neutralizing negative charges of the lipid A moiety (Gruenheid & Le Moual, 2012). Finally, all these defense mechanisms could protect *E. coli* from N-L and would delay the bacterial growth in the first moments after N-L addition.

Another assumption is that lysozyme concentration in the culture medium progressively decreases until it drops below a critical concentration, because of irreversible interaction between the protein and the bacterial cell membranes (Derde *et al.*, 2013). Because of its amphiphilic nature, and its surface-active properties, N-L could insert itself into the outer bacterial membrane, in which it could be irreversebly entrapped, causing depletion of N-L in the medium. Moreover, regarding the N-L molecules that could pass the outer membrane, binding to the peptidoglycan and/or to the inner membrane could decrease the lysozyme concentration in the culture medium. When this decrease results in a lysozyme concentration lower than the lowest active concentration, bacterial growth will resume.

Dry-Heated lysozyme at high concentration (3.7 g/L) causes an early-stage population decrease

At low concentration (0.25 g/L), DH-L acts similarly to N-L at low and high concentrations: *E. coli* growth is inhibited whether Ivy is present or not (Figure 2.7), but bacterial growth resumes afterward, and the same bacterial levels as in the control sample are attained after 24 h. As suggested above, three assumptions can be proposed: damage repair by the bacteria, activation of defense and adaptation mechanisms, and/or depletion of lysozyme in the growth medium by irreversible interaction with bacteria.

On the contrary, high-concentration DH-L (3.7 g/L) causes a population decrease ($\approx$ 1 log) in the early stages of growth. Thus, it is noticeable that whereas the presence of the Ivy inhibitor completely removes the population decrease observed when *E. coli* is treated with 3.7 g/L N-L, a slight decrease is still observed in the presence of the Ivy inhibitor when *E. coli* is treated with 3.7 g/L DH-L, even when the muramidase activity of DH-L is 22% lower than that of N-L (data not shown). This indicates that the Ivy inhibitor is not enough to defend *E. coli* cells against the effect of DH-L and that DH-L undoubtedly acts in different way compared to N-L. The physicochemical differences between both lysozymes could be responsible for such different activities. Especially, DH-L has been described more surface-active, more positively charged, and more hydrophobic than N-L (Desfougères *et al.*, 2011a). This indicates that DH-L is more membrane active than N-L. To confirm this hypothesis, the *E. coli* membrane state has been tested in the presence of either DH-L or N-L.

Membrane disruption differs between native and dry-heated lysozyme

Both N-L and DH-L pass the outer bacterial membrane and reach the periplasm, consistently with the increased lysozyme effect in the absence of the lysozyme inhibitor Ivy (Figure 2.7B). Actually, the passage of N-L through the outer bacterial membrane has already been described (Derde *et al.*, 2013). In the present study, it is demonstrated that N-L and DH-L permeabilize the outer membrane (Figure 2.8A), but when *E. coli* is treated with DH-L, more β-lactamase

is released from the bacterial cell than when it is treated with N-L (Figure 2.8B), meaning that DH-L causes either larger pores or more pores in the outer membrane as compared to N-L.

Outer membrane permeabilization intensity is independent of the concentration of N-L or DH-L administered to the bacteria (Figure 2.8A), but higher concentrations of N-L or DH-L (3.7 g/L) cause less β-lactamase leakage in the medium (Figure 2.8B). This could result from a large insertion of lysozyme molecules into the outer membrane and/or surrounding of the bacteria in high-concentration conditions, causing more difficult diffusion of β-lactamase.

The permeabilization of the inner membrane by DH-L is less intense as compared to that by N-L when measured by the maximal rate of β-galactosidase activity (Figure 2.8C), but permeabilization occurs faster with DH-L than with N-L (Figure 2.8D). In both cases, β-galactosidase activity could not be observed in the medium (data not shown), meaning that neither N-L nor DH-L causes pores large enough in the inner membrane to release this cytoplasmic enzyme. High-concentration DH-L also causes higher membrane potential disturbance and K^+ leakage than N-L (Figure 2.9). Inner membrane disruption is also dose-dependent: the higher the lysozyme concentration, the more severe (Figures 2.8C and 2.9) and the faster (Figure 2.8D) the inner membrane disruption.

It thus seems that, at high concentration, the DH-L activity on *E. coli* could be related to its enhanced activity on the outer and inner membranes. DH-L forms large and/or a lot of pores in the outer membrane; afterward it penetrates into the periplasm where it could either hydrolyze the peptidoglycan layer or diffuse through this layer to finally reach the inner membrane. Once it has arrived at the inner membrane, DH-L causes severe membrane potential disturbance and cytosol leakage (K^+ leakage). These latter phenomena suggest ion channel formation, which has already been reported for native lysozyme and lysozyme-derived peptides by Kimelberg & Papahadjopoulos (1971) and Ibrahim *et al.* (2001b), respectively. The presented study thus suggests that DH-L forms more ion channels in the cytoplasm membrane than N-L. Moreover, membrane potential disturbance is known to cause cellular division disturbance (Strahl & Hamoen, 2010). In combination with the pore formation, this could explain the morphological modifications observed here.

The impact of DH-L on the membrane integrity of *E. coli* is confirmed by severe morphological modifications observed *in vivo*

Not only can the effect of lysozyme, and especially of DH-L, on the membrane integrity of *E. coli* be shown *in vitro* as described above, it can also be highlighted *in vivo*. DH-L causes severe disruptions of cellular division observed by optical and atomic force microscopy: elongated cells of about 4.5 μm long could be observed without any sign of septum formation (Figures 2.10 and 2.11), as well as depressions which could be pores in the outer membrane and lateral depression which can be related to the activity of an antimicrobial as reported by Meincken *et al.* (2005) and Li *et al.* (2007). (Figure 2.11). DH-L also homogenizes the ribs present on the bacterial cell surface at high concentrations (3.7 g/L), which could be the result of protein insertion into the bacterial cell wall as seen for *E. coli* cells treated with PGLa (Meincken *et al.*, 2005). Then cell division and cell morphology are known to depend on the proton motive force, which itself depends on the bacterial membrane integrity (Strahl & Hamoen, 2010). In Figure 2.12, it is also noticeable that N-L or DH-L (0.25 and 3.7 g/L) alters the bacterial surface heterogeneity, resulting in the appearance of more rigid zones (Camesano *et al.*, 2000; Meincken *et al.*, 2005).

These morphological modifications are consistent with the membrane integrity disturbances. Thus, the depressions formed in the presence of DH-L (Figure 2.11) are consistent

with the higher leakage of β-lactamase, as compared to that in bacterial cells treated with N-L (Figure 2.8B). Perturbated cell division (Figures 2.10 and 2.11) is consistent with membrane potential disruption (Figure 2.9A), as recently reported by Strahl & Hamoen (2010).

2.5 Bilan de l'étude comparative de l'activité du lysozyme natif *vs* chauffé sur les membranes d'*E. coli*

Le chauffage à sec améliore donc considérablement l'activité antimembranaire du lysozyme vis-à-vis d'*E. coli*. Le lysozyme chauffé induit en effet des perturbations membranaires plus sévères que la protéine dans son état natif, avec notamment des pores plus grands et/ou plus nombreux dans la membrane externe, une perméabilisation plus rapide de la membrane interne, une forte dépolarisation membranaire et la formation de canaux ioniques qui entraînent des fuites du cytosol. Le cumul de ces multiples dégâts résulte en une diminution de la population bactérienne à forte concentration (3,7 g/L) de lysozyme chauffé, alors que seule une inhibition de croissance est observée avec le lysozyme natif.

Les différences entre le lysozyme natif et le lysozyme chauffé à sec étant exclusivement de nature physicochimique, il apparaît clairement que les propriétés physicochimiques de la protéine sont déterminantes pour l'interaction du lysozyme avec les membranes bactériennes. Il est essentiel de comprendre les mécanismes qui régissent ces interactions pour pouvoir, à terme, imaginer (« designer ») des formes particulièrement bactéricides de lysozyme. L'approche mécanistique, nécessaire à ce niveau de compréhension, nous a conduits à étudier le comportement du lysozyme, dans ses formes native et modifiée, à des interfaces modèles représentatives des membranes bactériennes.

En Bref

- Le lysozyme natif perméabilise les membranes externe et cytoplasmique d'*E. coli* par un mécanisme en plusieurs étapes :
  - Saturation de la membrane externe pour un ratio critique de 0.05 mg/mL de lysozyme pour 10^7 CFU/mL d'*E. coli* ;
  - Perforation de la membrane externe et diffusion du lysozyme dans le périplasme ;
  - Perméabilisation de la membrane interne sans perforation (formation de canaux ioniques).
- Le chauffage à sec augmente l'activité antimicrobienne du lysozyme (diminution de la population bactérienne *vs* latence de croissance).
- Le chauffage à sec augmente l'activité membranaire du lysozyme :
  - Perforations dans la membrane externe en plus grand nombre et/ou de plus grand diamètre ;
  - Perturbation du potentiel membranaire plus sévère et augmentation de la fuite du cytosol indiquant la formation d'un plus grand nombre de canaux ioniques ;
  - Apparition de défauts morphologiques sévères dont la perturbation de la division cellulaire.

Chapitre 3

Interactions des lysozymes natif et chauffé avec des monocouches lipidiques, modèles des membranes externe et cytoplasmique d'*Escherichia coli*

basé sur une publication et un projet de publication :

Derde M., Nau F., Lechevalier V., Guérin-Dubiard C., Paboeuf G., Jan S., Baron F., Gautier M. & Vié V. (2015) Native and dry-heated lysozyme interactions with membrane lipid monolayers : lateral reorganization of a lipopolysaccharide monolayer, model of the *Escherichia coli* outer membrane, *BBA biomembranes*, 1848 : 174-183

Derde M., Nau F., Guérin-Dubiard C., Lechevalier V., Paboeuf G., Jan S., Baron F., Gautier M. & Vié V. Native and dry-heated lysozyme interactions with membrane lipid monolayers : lipid packing modifications of a phospholipid monolayer, model of the *Escherichia coli* cytoplasmic membrane, soumis *BBA biomembranes*, en revision

3.1 Introduction

Les études *in vivo* ont montré que le lysozyme, qu'il soit natif ou chauffé à sec, perturbe l'intégrité des membranes bactériennes d'*E. coli* (cf Chapitre 2). Sous ces deux formes, le lysozyme interagit donc incontestablement avec les lipides membranaires. Les interactions entre le lysozyme natif et les lipides membranaires ont déjà été décrites dans la littérature (Al Kayal *et al.*, 2012; Arnold *et al.*, 1992; Brandenburg *et al.*, 1998; Gorbenko *et al.*, 2007; Ioffe & Gorbenko, 2005; Matsumura & Dimitrova, 1996; Mudgil *et al.*, 2006; Ohno & Morrison, 1989; Ohno *et al.*, 1991; Posse *et al.*, 1990, 1994; Trusova, 2012; Vechetti *et al.*, 1997; Yuan *et al.*, 2007; Zschornig *et al.*, 2000, 2005). Elles sont présentées comme étant impliquées dans les propriétés antimicrobiennes de la protéine (Trusova, 2012). L'association du lysozyme avec les membranes résulterait d'un mécanisme en plusieurs étapes : 1) adsorption sur la bicouche membranaire par attraction électrostatique et/ou par liaisons hydrogènes, 2) modifications conformationelles du lysozyme, 3) réorganisation de la phase lipidique, 4) insertion partielle du lysozyme entre les chaînes lipidiques de la bicouche par interactions hydrophobes (Al Kayal *et al.*, 2012; Gorbenko *et al.*, 2007; Trusova, 2012).

L'interaction du lysozyme natif avec les lipides membranaires dépend de plusieurs facteurs comme le pH, la force ionique et la nature des lipides en présence (Bergers *et al.*, 1993; Posse *et al.*, 1994; Trusova, 2012; Zschornig *et al.*, 2005). Parce que le pH et la force ionique ont un impact majeur sur les interactions électrostatiques, ces deux paramètres gouvernent l'adsorption du lysozyme sur des vésicules (LUV) (Zschornig *et al.*, 2005) ; l'augmentation du pH ou de la force ionique diminue la charge nette positive et augmente l'écrantage des charges du lysozyme, diminuant son adsorption. La nature des lipides membranaires est également un facteur clé. Le lysozyme, chargé positivement au pH physiologique, interagirait de préférence avec les phospholipides anioniques (Trusova, 2012). Il a ainsi une affinité forte pour les cardiolipines (CL) et les phosphatidylglycérols (PG) (Sankaram & Marsh, 1993), présents dans les membranes bactériennes.

Bien que de nombreuses études aient été menées pour comprendre le comportement du lysozyme natif à l'interface lipidique, rares sont celles utilisant des modèles membranaires mimant la composition naturelle des membranes bactériennes. Dans le travail présenté ici, deux modèles membranaires ont été mis en œuvre pour étudier les interactions du lysozyme avec les lipides membranaires. D'une part, des monocouches de lipopolysaccharides extraits d'*E. coli* ont été utilisées pour modéliser la membrane externe de cette bactérie ; d'autre part, des monocouches constituées à partir d'un mélange de phospholipides basé sur la composition de la membrane cytoplasmique d'*E. coli* K12 ont été utilisées pour modéliser cette membrane. La complexité des interactions entre lipides et protéines impose que les études de modélisation soient réalisées dans des conditions aussi proches que possible des conditions réelles, tant en termes de composition lipidique que d'environnement physicochimique. Dans cette étude, un tampon HEPES de pH et de force ionique proches des conditions physiologiques a été utilisé (pH 7.0, 155 mM).

Les interactions entre le lysozyme et les lipides membranaires seraient majoritairement dirigées par des interactions électrostatiques et hydrophobes (Ohno & Morrison, 1989; Ohno *et al.*, 1991; Trusova, 2012; Zschornig *et al.*, 2005). Le lysozyme chauffé à sec ayant des propriétés physicochimiques modifiées par rapport à la protéine native, à savoir une charge électropositive et une hydrophobie plus élevées (cf Chapitre 1 §1.2.3), nous avons émis l'hypothèse que les interactions du lysozyme avec les lipides membranaires seraient impactées par le chauffage à sec. C'est pourquoi nous avons décidé de comparer le comportement des lysozymes natif et chauffé aux interfaces lipidiques modèles présentées ci-dessus. Cette comparaison pouvait en effet permettre d'identifier les facteurs clés de l'augmentation de l'activité antimicrobienne et

des perturbations membranaires induites par le lysozyme chauffé, par rapport à la protéine native (cf Chapitre 2).

3.2 Native and dry-heated lysozyme interactions with membrane lipid monolayers: lateral reorganization of a lipopolysaccharide monolayer, model of the *E. coli* outer membrane.

Derde M., Nau F., Lechevalier V., Guérin-Dubiard C., Paboeuf G., Jan S., Baron F., Gautier M. & Vié V. (*BBA biomembranes* 2015, vol. 1848, pp. 174-183)

3.2.1 Abstract

Lysozyme is mainly described active against Gram-positive bacteria, but is also efficient against some Gram-negative species. Especially, it was recently demonstrated that lysozyme disrupts *E. coli* membranes. Moreover, dry-heating changes the physicochemical properties of the protein and increases the membrane activity of lysozyme. In order to elucidate the mode of insertion of lysozyme into the bacterial membrane, the interaction between lysozyme and a LPS monolayer mimicking the *E. coli* outer membrane has been investigated by tensiometry, ellipsometry, Brewster Angle Microscopy and Atomic Force Microscopy. It was thus established that lysozyme has a high affinity for the LPS monolayer, and is able to insert into the latter as long as polysaccharide moieties are present, causing reorganization of the LPS monolayer. Dry-heating increases the lysozyme affinity for the LPS monolayer and its insertion capacity; the resulting reorganization of the LPS monolayer is different and more drastic than with the native protein.

3.2.2 Material and methods

Proteins and lipids

Native lysozyme (N-L) powder (pH 3.2) was obtained from Liot (Annezin, 62-France). It was heated for 7 days at 80°C in hermetically closed glass tubes to obtain dry-heated lysozyme (DH-L). Lysozyme (N-L or DH-L) was solubilized (around 0.5 g/L) in 5 mM 4-(2-hydroxyethyl)-piperazine-1-ethanesulfonic acid (HEPES) buffer (Sigma Aldrich, Saint-Quentin, France), pH 7.0, 150 mM NaCl (Fluka, Saint-Quentin, France). The concentration of the lysozyme stock solution was precisely determined by absorbance at 280 nm (extinction coefficient = 2.6 L/g) (Expasy SIB Swiss, 2014; Gasteiger *et al.*, 2005). The protein solution was then diluted in the HEPES buffer to obtain the desired concentration for used lysozyme solutions.

The lipopolysaccharides (LPS) of *E. coli* K12 were obtained from Invivogen (Toulouse, France). The LPS were solubilized in 2:1 chloroform/methanol mixture at 0.5 g/L. Lipid A-$(KdO)_2$ (KLA) were purchased by Avanti Polar Lipids (Alabaster, Alabama, USA) and were solubilized in a 2:1 chloroform/methanol mixture at 0.67 g/L.

Lipid/protein monolayers

The experiments were performed in a homemade TEFLON® trough of 8 mL. Before each use, the trough was thoroughly cleaned with successively warm tap water, ethanol, demineralized water, and then boiled for 15 minutes in demineralized water. After cooling the TEFLON® trough was then filled with 8 mL HEPES buffer. The LPS or KLA were spread with a high precision Hamilton microsyringe at the clean air/liquid interface to obtain an initial surface

pressure between 18 and 30 mN/m. After 1 h to allow the solvent to evaporate and the lipids to organize, 50 μL N-L or DH-L solution were injected in the subphase with a Hamilton syringe to obtain a final protein concentration of 0.02, 0.03, 0.05, 0.1, 0.2, 0.3 or 1 μM.

Surface pressure measurements

The surface pressure was measured following a Wilhelmy method using a 10 mm x 22 mm filter paper as plate (Whatman, Velizy-Villacoublay, France) connected to a microelectronic feedback system (Nima PS4, Manchester, England). The surface pressure (π) was recorded every 4 s with a precision of $\pm$ 0.2 mN/m. The measured surface pressure is the result of the surface tension of water (72.8 mN/m at 20°C) minus the surface tension of the lipid film (Vargaftik *et al.*, 1983).

Ellipsometry

Measurements of the ellipsometric angle value were carried out with an in-house automated ellipsometer in a "null ellipsometer" configuration (Azzam & Bashara, 1977; Berge & Renault, 1993). A polarised He-Ne laser beam (λ=632.8 nm, Melles Griot, Glan-Thompson polarizer) was reflected on the surface of the trough. The incidence angle was 52.12°, i.e. Brewster angle for the air/water interface minus 1°. After reflection on the liquid surface, the laser light passed through a $\lambda/4$ retardation plate, a Glan-Thompson analyser, and a photomultiplier. The analyser angle, multiplied by two, yielded the value of the ellipsometric angle (Δ), i.e. the phase difference between parallel and perpendicular polarisation of the reflected light. The laser beam probed the 1 mm^2 surface with a depth in the order of 1 μm. Initial values of the ellipsometric angle (Δ_0) and surface pressure (π_0) of buffer solutions were recorded for at least half an hour to assure that the interface is clean. Only in the case of a stable minimal signal, experiments were performed. Values of Δ were recorded every 4 s with a precision of $\pm$ 0.5°. When measuring the pressure increase induced by lysozyme at the air/liquid interface, a lysozyme solution at 0.1 μM is deposited in the trough. When the pressure increase induced by lysozyme is measured at the LPS/liquid interface, a LPS monolayer is first created as formerly described.

For the detection of local ellipsometric angle values, an imaging ellipsometer EP3 (Nanofilm, Göttingen, Germany) in "null ellipsometer" configuration was used with a 10X objective. A solid-state laser (λ=532 nm) was used as a light source. Delta/Psi maps were recorded with the EP3 software for a 450 μm x 390 μm surface. For delta and psi maps, a polarizer and analyzer range of 20° was used. Delta/psi maps were based on 20 images taken at different polarizer and analyzer angles.

Brewster angle microscopy

An ellipsometer EP3 (Nanofilm, Berlin, Germany) with a polarized incident laser (λ = 532.0 nm) was used with a 10X objective in a Brewster angle configuration (angle of incidence was 53.1°). The images represented a 450 μm x 390 μm surface. Different zones of each sample were evaluated; the images here shown are representative of the whole samples.

AFM sample preparation and AFM imaging

Experiments were performed with a computer-controlled and user-programmable Langmuir TEFLON®-coated trough (type 601BAM) equipped with two movable barriers and of total surface 90 cm^2 (Nima Technology Ltd., England). Before starting the experiments, the trough was cleaned successively with ultrapure water (Nanopure-UV), ethanol, and finally ultrapure water. The trough was filled with 5 mM HEPES buffer pH 7 150 mM NaCl. LPS were spread over the clean air/liquid interface at a surface pressure of 25 mN/m or 30 mN/m. The solvent

was then left to evaporate for 1 h. Then, a Langmuir-Blodgett transfer was performed onto freshly cleaved mica plates at constant surface pressure by vertically raising (1 mm/min) the mica through the air/liquid interface to obtain a sample of the initial LPS monolayer. The LPS monolayer stability was assured during the Langmuir-Blodgett transfer allowing the injection of lysozyme in the subphase.

Then, 0.1 μM lysozyme was injected in the subphase of the previously sampled LPS monolayer with a Hamilton syringe. Surface pressure variations were recorded until a stable surface pressure was reached (after $\approx$1 h). Then, a second Langmuir-Blodgett transfer was performed onto freshly cleaved mica as described above to obtain the sample of the LPS monolayer after lysozyme interaction. AFM imaging of Langmuir Blodgett films was performed in contact mode using a Pico-plus atomic force microscope (Agilent Technologies, Phoenix, AZ) under ambient conditions with a scanning area of 20x20 μm^2 and 5x5 μm^2. Topographic images were acquired using silicon nitride tips on integral cantilevers. The forces were controlled along the imaging process. Different zones of each sample were scanned; the images here shown are representative of the whole samples.

3.2.3 Results

Insertion capacity of lysozyme into a LPS monolayer

The insertion capacity of N-L and DH-L into a LPS monolayer was determined by independent tensiometry experiments at different protein concentrations. Insertion can be detected by a surface pressure increase ($\Delta\pi = \pi_{final} - \pi_{initial}$). Here, lysozyme was injected under a LPS monolayer with an initial surface pressure ($\pi_{initial}$) of 18 mN/m.

In both cases (N-L and DH-L), a surface pressure increase is demonstrated indicating lysozyme insertion into the LPS monolayer for protein concentrations above 0.02 μM (Figure 3.1A). Below 0.05 μM, no difference can be observed between both lysozymes, while above this protein concentration, DH-L induces a higher surface pressure increase than N-L (Figure 3.1A). When increasing the lysozyme subphase concentration, a $\Delta\pi$-plateau is obtained at a lysozyme concentration of 0.2 μM for both N-L and DH-L, indicating saturation of the interface in these conditions. However, the maximum $\Delta\pi$ value is higher for DH-L than for N-L (12 mN/m and 8 mN/m, respectively; Figure 3.1A). For further investigation of the insertion capacity of lysozyme, 0.1 μM N-L or DH-L has been used. At this concentration, differences exist between both proteins, and lipid protein interactions can be observed, while minimizing protein-protein interactions in the bulk solution (aggregation) or at the lipid interface.

Affinity of lysozyme for LPS monolayers

To evaluate the affinity of both N-L and DH-L for the LPS monolayer, $\Delta\pi$ was determined after lysozyme injection (0.1 μM) under LPS monolayers previously formed at different initial surface pressures ($\pi_{initial}$). Supplementary experiments demonstrated that no phase transition occurs in the π-range here used (supplementary data S3, § 3.2.5) comparisons are then valuable. Linear regression analysis of the $\Delta\pi$ values *vs* $\pi_{initial}$ allows calculation of three binding parameters of lysozyme: maximal insertion pressure (MIP), synergy factor, and $\Delta\pi_0$ (Figure 3.1B) (Boisselier *et al.*, 2012; Calvez *et al.*, 2009, 2011). MIP is the intercept of the straight line with x-axis after extrapolation; it is thus the initial surface pressure for which no surface pressure increase occurs when lysozyme is injected in the subphase. The synergy factor is determined as the slope of the linear regression +1. . The synergy factor provides information on the affinity of the protein for the lipid monolayer. High positive synergy values indicate the existence of strong protein/lipid interactions, since it means that the protein is able to insert into the lipid film even when initial surface pressure is high. $\Delta\pi_0$ is the intercept of the

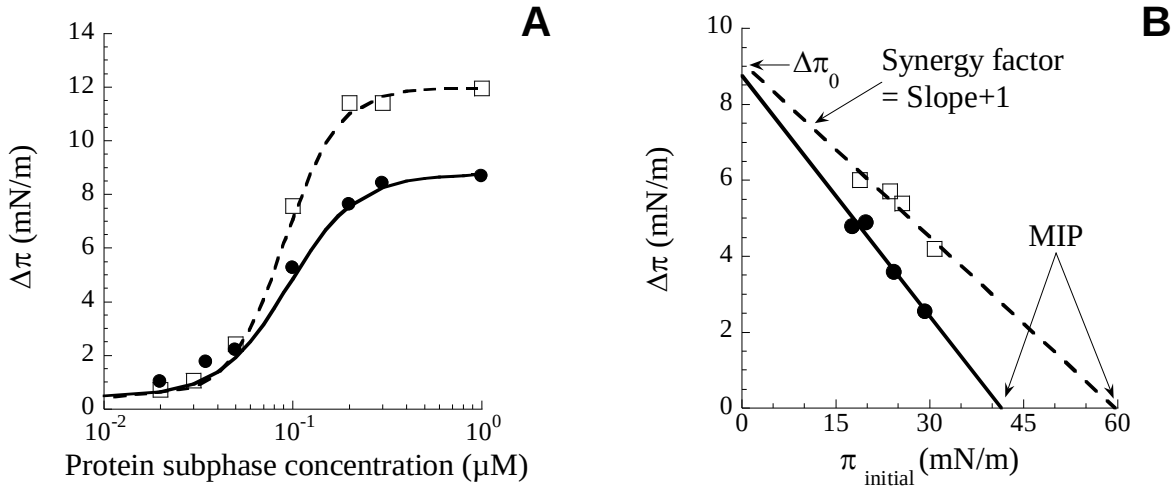

Figure 3.1: (A) Surface pressure increase ($\Delta\pi$) of a LPS monolayer (π_{initial}=18 mN/m) induced by different subphase concentrations of native lysozyme (N-L) (•) and dry-heated lysozyme (DH-L) (□); (B) Surface pressure increase of a LPS monolayer induced by 0.1 μM N-L (•) and DH-L (□), depending on the initial surface pressure (π_{initial}); the maximal insertion pressure (MIP) and the theoretical pressure increase in the absence of lipids ($\Delta\pi_0$) are indicated by arrows.

straight line with y-axis after extrapolation; it is thus the theoretical pressure increase in the absence of lipids (π_{initial} = 0 mN/m).

Linear regression for N-L and DH-L resulted in equations 3.1 and 3.2, respectively, with respective determination coefficients (R^2) of 0.96 and 0.91.

$$y = -0.21x + 8.75 \tag{3.1}$$

$$y = -0.15x + 9.10 \tag{3.2}$$

The MIP is higher with DH-L than with N-L (59.6 and 41.5 mN/m, respectively; Table 3.1). The synergy factor as introduced by Calvez *et al.* (2011) and Boisselier *et al.* (2012) is also higher with DH-L than with N-L, and is positive for both proteins (0.85 and 0.79, respectively; Table 3.1). Oppositely, the $\Delta\pi_0$ are similar for N-L and DH-L (8.75 and 9.10 mN/m, respectively; Table 3.1). It is noticeable that these latter values are lower than the experimental surface pressure increase observed for N-L and DH-L lysozymes at the air/liquid interface at the same subphase concentration (10 and 11 mN/m, respectively).

The rate constant of adsorption k_{ads} ($M^{-1} \cdot s^{-1}$) of a lysozyme solution with a concentration (c) of 0.1 μM at the air/liquid interface and the LPS/liquid interface can be evaluated by fitting the Langmuir equation (3.3 and 3.4) for adsorption to the surface pressure measurements. The rate constant of desorption k_{des} ($M^{-1} \cdot s^{-1}$) can here be considered negligible.

$$\pi(t) = \pi_{final} \cdot (1 - exp(-\sigma \cdot t)) \tag{3.3}$$

$$\sigma = k_{ads} \cdot c + k_{des} \tag{3.4}$$

At the air/liquid interface, N-L and DH-L have a k_{ads} value of $6.6 \cdot 10^2$ $M^{-1} \cdot s^{-1}$ and $6.4 \cdot 10^2$ $M^{-1} \cdot s^{-1}$, respectively. The rate constants of adsorption for N-L and DH-L at the

LPS/liquid interface of $1.7 \cdot 10^3$ $M^{-1} \cdot s^{-1}$ and $1.3 \cdot 10^3$ $M^{-1} \cdot s^{-1}$, respectively, are higher than the rate constants of adsorption at the air/liquid interface. Thus, lysozyme adsorption at the air/liquid interface is slower than adsorption at the LPS/liquid interface. The differences in k_{ads} for N-L and DH-L for both the air/liquid and the LPS/liquid interface are not significant.

Table 3.1: Binding parameters calculated for N-L and DH-L adsorption at a LPS monolayer: maximal insertion pressure (MIP), synergy factor, and theoretical pressure increase in the absence of lipids ($\Delta\pi_0$); these parameters were extrapolated from the $\Delta\pi$ *vs* $\pi_{initial}$ plots for 0.1 μM lysozyme. For comparison, the surface pressure increase resulting from 0.1 μM lysozyme adsorption at the air/liquid interface is indicated ($\Delta\pi_{final}$).

		N-L	**DH-L**
air/lipid interface	**MIP (mN/m)**	41.5	59.6
	Synergy factor	0.79	0.85
	Theoretical $\Delta\pi_0$ (mN/m)	8.75	9.10
air/liquid interface	**$\Delta\pi_{final}$ (mN/m)**	10	11

Changes of surface pressure (π) and ellipsometric angle (Δ) of LPS monolayer in the presence of lysozyme

Kinetics of the π and Δ changes after injection of N-L and DH-L in the subphase were recorded using a LPS monolayer with an initial surface pressure of 25 mN/m and 30 mN/m, respectively. Different initial surface pressures of the LPS monolayers were chosen because of the different insertion capacities of N-L and DH-L for this experiment. The aim of this study was to evaluate the effects of N-L or DH-L on the LPS monolayer after a similar insertion of proteins, i.e. a similar $\Delta\pi$. The initial surface pressures which correspond to this prerequisite is 25 mN/m and 30 mN/m for a concentration of 0.1 μM N-L and DH-L, respectively (Figure 3.1B); more so, LPS monolayers with an initial surface pressure of 25 mN/m and 30 mN/m have similar Δ values (supplementary data S1, § 3.2.5). The injection of N-L and DH-L under the LPS monolayer in these conditions results in a surface pressure increase of 2.9 mN/m and 3.5 mN/m, respectively (Figure 3.2A), and induces an increase of ellipsometric angle of 8° and 12°, respectively (Figure 3.2B).

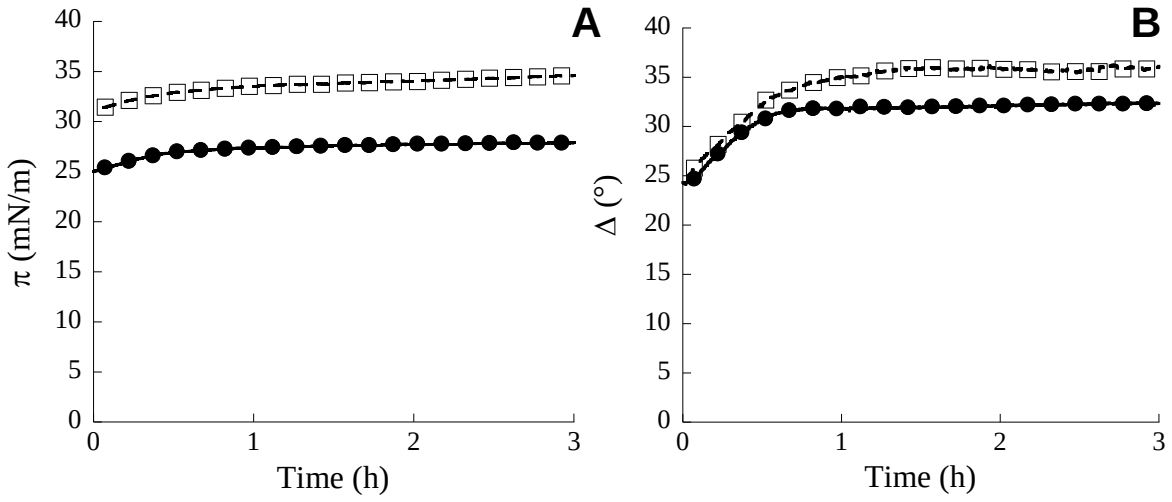

Figure 3.2: Surface pressure π (A) and ellipsometric angle Δ (B) changes during N-L (•) and DH-L (□) adsorption at a LPS monolayer having an initial surface pressure of 25 mN/m and 30 mN/m, respectively.

Changes of surface pressure (π) and ellipsometric angle (Δ) of KLA monolayer in the presence of lysozyme

To estimate the influence of the polysaccharide moieties on lysozyme interactions with LPS monolayer, KLA lipids were used. KLA lipids are derivative forms of LPS from which the polysaccharide moiety besides two 3-deoxy-D-manno-octulosonic acid (KdO) groups are missing (Figure 3.3). The use of KLA was also relevant to test the role of electrostatic interactions between lysozyme and the negative charge at the interface by making the access to the charge easier. KLA monolayers are homogeneous lipid films on the contrary to LPS monolayers. This was confirmed by AFM imaging (Supplementary data S2, § 3.2.5).

Kinetics of the π and Δ changes after injection of N-L and DH-L in the subphase were recorded for a KLA monolayer with an initial surface pressure of 25 mN/m and 30 mN/m, respectively. For N-L, the surface pressure of the KLA monolayer is stable for the first half hour and then decreases (-2.1 mN/m) (Figure 3.4A). Oppositely, DH-L injection induces an immediate and more intense decrease (-5 mN/m after 3 h) (Figure 3.4A). Both N-L and DH-L interact with the KLA monolayer in such a way that the ellipsometric angle increases slightly after injection of both proteins: $+0.65°$ and $+1.5°$ after 3 h, respectively (Figure 3.4B). Thus, both N-L and DH-L adsorb onto the KLA monolayer.

Microscopic observations of LPS monolayer in the presence of lysozyme

Brewster angle microscopy (BAM) and ellipsometry were performed to visualize the LPS monolayer organization on a μm-scale before and after lysozyme injection in the subphase. BAM-images give information on the thickness and refraction index of the LPS monolayer. Thick and/or high refraction index zones will appear lighter (white) than thin and low index zones (black). Delta maps show the same information as the BAM images, but the differences in height and/or refraction index are more precisely measured. Blue is the baseline color of the delta maps and correspond to a small delta value. High delta zones are represented from green till red.

Before lysozyme injection, the LPS monolayer is heterogeneous, with black and white zones, at both initial surface pressures (25 mN/m and 30 mN/m), as evidenced by BAM-imaging (Figures 3.5A and 3.5E). In the absence of literature references, The black colored zones are assumed to correspond to LPS with short polysaccharide chains (low refractive index and low thickness), while the white regions are assumed to correspond to LPS with long polysaccharide chains (high refractive index and high thickness). Such domain-organization is likely considering the optimal thermodynamic configuration that suggests segregation of LPS with similar polysaccharide chain lengths. The same information is provided by the delta-maps (Figures 3.5C and 3.5G).

One hour after injection of 0.1 μM N-L, the BAM-images and delta-maps do not show any significant change of the heterogeneity as compared to the initial LPS monolayer (Figures 3.5B and 3.5D), despite a slight increase of the background Δ-value in the delta-map (Figure 3.5D). On the contrary, after injection of DH-L, an unequivocal change of the LPS monolayer organization is observed in both BAM-images and delta-maps (Figures 3.5F and 3.5H). Especially, the small high Δ-domains make place for bigger ones, and the background Δ-value increases (Figure 3.5H).

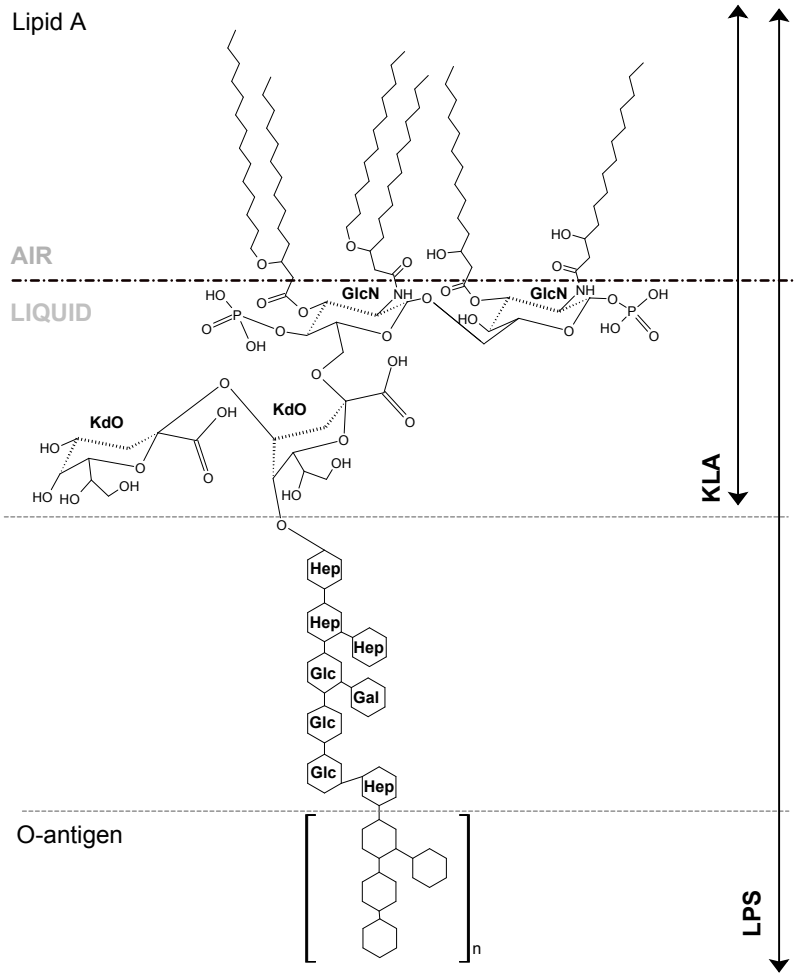

Figure 3.3: Schematic representation of *E. coli* K12 LPS and KLA lipids. GlcN (N-acetylglucosamine); KdO (3-deoxy-D-manno-octulosonic acid); Hep (L-gycero-D-manno heptose); Gal (galactose); Glc (glucose).

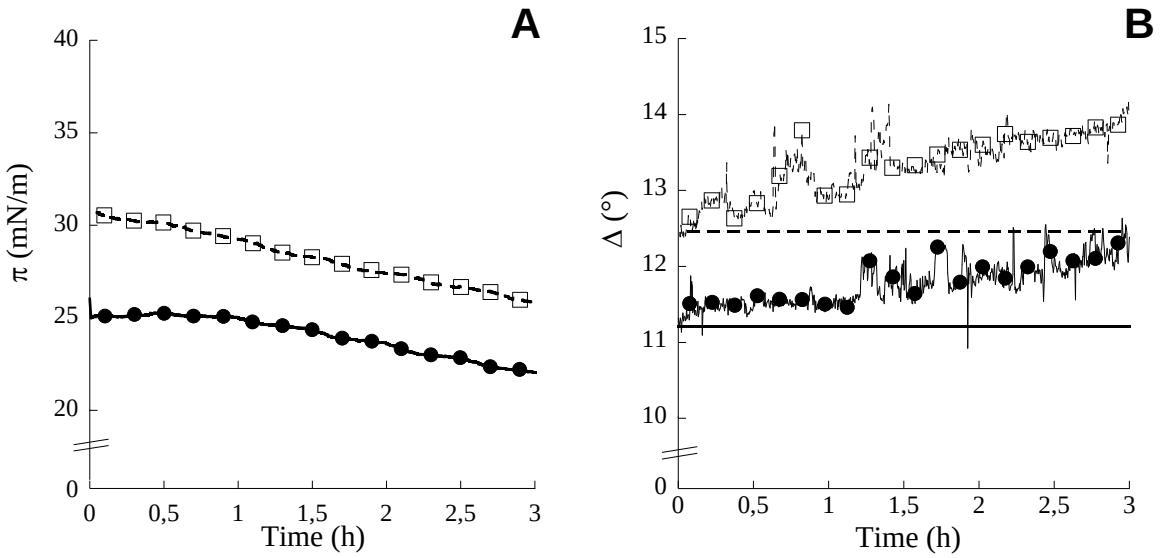

Figure 3.4: Surface pressure π (A) and ellipsometric angle Δ (B) changes during N-L (•) and DH-L (□) adsorption at a KLA monolayer having an initial surface pressure of 25 mN/m and 30 mN/m, respectively. The initial Δ values of the KLA lipids at 25 mN/m and 30 mN/m are shown as a full and dashed line, respectively.

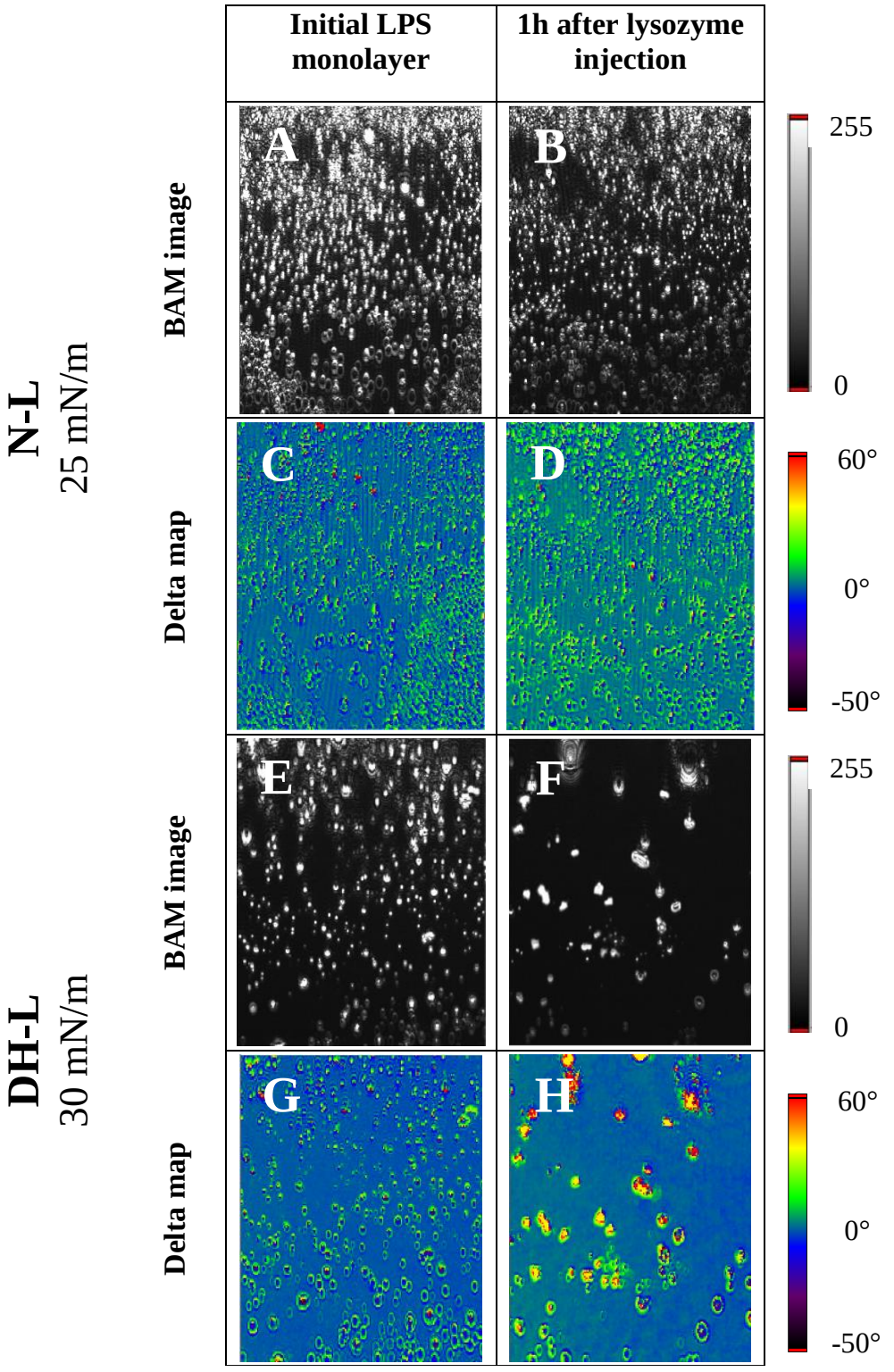

Figure 3.5: BAM-images and delta-maps (450 μm x 390 μm) before (A, C, E, G) and after N-L (B, D) or DH-L (F, H) injection under the LPS monolayer. The initial surface pressure was 25 mN/m or 30 mN/m, for N-L or DH-L, respectively.

Atomic force microscopy (AFM) enables to investigate the LPS monolayer at a nanoscale with a high resolution. Thus, this technique was used to study more precisely the organization of the lipid monolayer observed in the background of BAM-images (black zones). The resulting AFM-images show the heterogeneity of the initial LPS monolayer at a nanoscale at both initial surface pressures (25 mN/m and 30 mN/m; Figures 3.6A, 3.6C, 3.6E and 3.6G). The height difference between the lower (zone 1) and higher (zone 2) lipid zones is 1.2 to 2.0 ± 0.2 nm. By grating the LPS (data not shown), the monolayer thickness could be measured and corresponds to 5 nm. The monolayer thickness is in coherence with the one found by Le Brun *et al.* (2013).

The impact of N-L and DH-L on the lipid monolayer can also be studied by AFM, enabling to study more carefully the reorganization of the low Δ-domains present in the BAM-images. AFM shows that the injection of 0.1 μM N-L or DH-L does not significantly modify the heterogeneous appearance of the LPS monolayer (Figures 3.6B, 3.6D, 3.6F and 3.6H). However, the insertion and adsorption of 0.1 μM N-L gives rise to the formation of small domains (object 1) with a height of 1.4 ± 0.4 nm (Figures 3.6B and 3.6D). The height of these domains is equivalent to the height of the dense domains observed in absence of lysozyme (Figures 3.6A and 3.6C). The adsorption and insertion of 0.1 μM DH-L induces the formation of two types of clusters (object 2 and 3 with a height of 25 ± 5 and 57 ± 12 nm, respectively) and small domains (object 4) (1.4 ± 0.3 nm height) (Figures 3.6F and 3.6H).

Topographical information shown in the AFM images is representative for the whole sample. However, the size and shape of the different domains is irregular and heterogeneously distributed over the sample, making it impossible to quantify the effect of lysozyme on the domain size and shape.

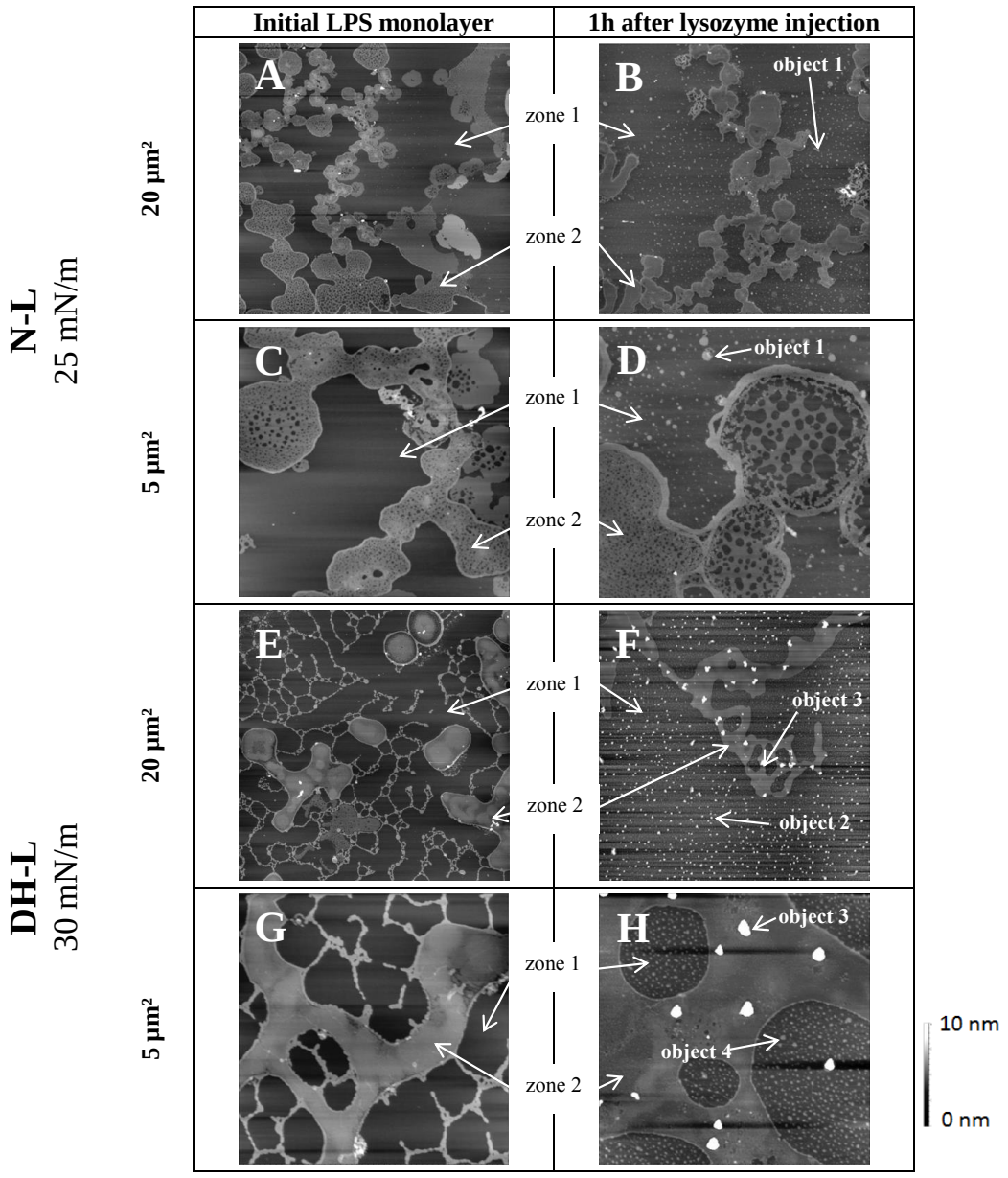

Figure 3.6: Topographic AFM-images before (A ,C, E, G) and after N-L (B, D) or DH-L (F, H) injection under the LPS monolayer. The initial surface pressure was 25 mN/m or 30 mN/m, for N-L or DH-L, respectively. The Z-range is 10 nm.

3.2.4 Discussion

Native lysozyme (N-L) has been shown active against Gram-negative bacteria such as *E. coli* (Derde *et al.*, 2014; Pellegrini *et al.*, 1992). Membrane permeabilization has been suggested as one of the mechanisms responsible for this activity (Pellegrini *et al.*, 2000; Wild *et al.*, 1997). This assumption was recently confirmed in our group who demonstrated that N-L causes the formation of pores and ion channels in the outer and cytoplasmic membranes, respectively (Derde *et al.*, 2013, 2014). Pore formation due to N-L implies that interactions occur between the protein and the *E. coli* outer membrane. Nevertheless, the mode of insertion of lysozyme into the outer membrane remains unknown.

Moreover, dry-heated lysozyme (DH-L) has a higher antimicrobial activity and higher membrane disruption potential than N-L (Derde *et al.*, 2014). This improved activity is related to the modified physico-chemical properties of DH-L. DH-L is more hydrophobic, flexible and surface active than N-L, but its secondary and tertiary structure remains intact (Desfougères *et al.*, 2011a,b). It is thus interesting to study the interaction differences of native and dry-heated lysozyme with lipopolysaccharides, the lipid components of the outer leaflet of the outer membrane of Gram negative bacteria.

Interfacial monolayers are considered as good models to study interactions between antimicrobial peptides and bacterial membranes (Brockman, 1999; Roes *et al.*, 2005). In the presently reported study, a LPS monolayer was used to mimic the outer leaflet of the *E. coli* K12 outer membrane, in order to explore the first step of lysozyme interaction with bacterial membrane. It is noticeable that wild-type LPS was here used for the first time to investigate protein-LPS interactions at a macroscopic and mesoscopic level, using biophysical tools such as tensiometry, ellipsometry, AFM and BAM.

The affinity of N-L for LPS is very high and makes possible the insertion of the protein into a LPS monolayer

For the first time, protein insertion into a wild-type LPS monolayer is here demonstrated. Until now, protein insertion into LPS or LPS-derivative monolayers was only recorded for LPS-derivative monolayers and lung surfactant protein D (Wang *et al.*, 2008). The surface pressure increase measured when N-L is injected into the subphase demonstrates that N-L is able to insert into a LPS monolayer (Figure 3.1A). The ability of lysozyme to interact with LPS is consistent with the surface activity of the protein at the air/liquid interface (Desfougères *et al.*, 2011b). However, insertion of N-L into the LPS monolayer remains lower than for antimicrobial peptides such as temporin L, as suggested by the lower surface pressure increase (Table 3.2). The larger molecular size and higher rigidity of lysozyme (Canfield & Liu, 1965), as compared to peptides, could be responsible for the lower efficiency of the protein.

The maximal insertion pressure (MIP), determined from measurements of N-L insertion at different initial pressures, is high (41.5 mN/m, Table 3.1) and similar to MIP recorded for antimicrobial peptides and phospholipid monolayers (25-45 mN/m) (Calvez *et al.*, 2009; Giacometti *et al.*, 2006). Especially, it is remarkable that the MIP value is higher than the lateral pressure which is supposed to exist in natural membrane systems in eukaryotic cells (≈30 mN/m) (Marsh, 1996). Unfortunately, no measurements or theoretical deductions of lateral pressure in the outer and cytoplasmic membranes of prokaryotes are mentioned in literature and therefore no comparison is possible with the here observed MIP value. Moreover, the N-L synergy factor (0.79, Table 3.1) is extremely high as compared to reported values for protein insertion into phospholipid monolayers (from 0.3 to 0.5) (Boisselier *et al.*, 2012). It can thus be concluded the protein has a high affinity for LPS interface between 18 and 30 mN/m, and strinkingly lysozyme insertion is almost not impacted by the lateral cohesion of

the LPS molecules. These observations suggest a mode of action that is unusual compared to the interaction between proteins and phospholipids. This could result from the LPS inherent molecular structure and from the specificities of a LPS monolayer compared to a phospholipid monolayer; the LPS molecules have heterogeneous polysaccharide chains in length, thus the monolayer has a variable thickness induced by the auto-assemblage of similar LPS molecules observed by BAM and AFM microscopy (figures 3.5 and 3.6). Indeed, a LPS monolayer can be divided into two distinct zones, i.e. a polysaccharide zone and a phospholipid-like zone, on the contrary to a phospholipid monolayer which is composed of a unique zone.

Table 3.2: Surface pressure increase ($\Delta\pi$) of LPS or LPS-derivative monolayers measured after adsorption of antimicrobial peptides and N-L or DH-L. The initial surface pressure was 18 mN/m for both peptides and protein.

	Peptide or protein	Conc. (μM)	$\Delta\pi$ (mN/m)	Bacterial species	LPS type	Reference
Peptides	Polymyxin B (1.4 kDa)	0.5	17.5	*Salmonella enterica*	Re-LPS	Zhang *et al.* (2000a)
	Polymyxin E1 (1.2 kDa)	0.5	21			
	Colymycin (1.8 kDa)	0.5	0.5			
	Gramicidin S (1.1 kDa)	0.15	17			
Lysozyme (14.3 kDa)	Temporin L (1.6 kDa)	0.1	7.5	*Escherichia coli*	Wild-type LPS	Giacometti *et al.* (2006)
	N-L	0.1	5.2	*Escherichia coli*	Wild-type LPS	This study
	N-L	0.1	-2.1		KLA	
	DH-L	0.1	7.8		Wild-type LPS	
	DH-L	0.1	-5		KLA	

The polysaccharide moieties of LPS are needed for N-L insertion

When LPS molecules are depleted from their polysaccharide moieties (KLA), lysozyme is no longer able to insert into the lipid monolayer, since no increase of the surface pressure occurs (Figure 3.4A). However, lysozyme adsorption is evidenced by the increase of the ellipsometric angle (Δ) (Figure 3.4B). Lysozyme adsorption could involve hydrogen bonds between the protein and the remaining two sugar moieties, or electrostatic interactions between the positive lysozyme and the negative KLA. The latter assumption is reinforced by the immediate and higher adsorption of DH-L which is more positively charged than N-L (Figure 3.2B). It is also in accordance with Brandenburg *et al.* (1998) who reported electrostatic interactions between *Salmonella minnesota* Re-LPS and lysozyme in solution; Re-LPS are natural KLA purified from bacteria.

Here, the ellipsometric angle increases (figure 4), meaning that rather than a solubilization of the KLA monolayer, a reorganization of the KLA head groups takes place leading to a relaxation of the lipid film. Lysozyme molecules are trapped beneath the KLA monolayer caused by strong electrostatic attractive forces between lysozyme and the KLA lipids.

Actually, while N-L adsorption is proceeding for 3 h (Figure 3.4B), the surface pressure of the lipid monolayer is decreasing (Figure 3.4A). This could be due to a destabilization and partial solubilization of the lipid monolayer as has been previously described for with the antimicrobial peptide protegrin-1 at a lipid A monolayer (Ishitsuka *et al.*, 2006); another hypothesis is the a reorganization or reorientation of the lipid headgroups induced by lysozyme presence beneath the monolayer, similarly to what has been previously reported for a dystrophin subdomain R20-24 at a DOPC/DOPS monolayer (Vié *et al.*, 2010). If a partial solubilization of the KLA occurs, this should be reflected by a decrease of the ellipsometric angle (Δ), due to the loss of matter at the interface. Here, the ellipsometric angle increases (Figure 3.4), meaning that rather than a solubilization of the KLA monolayer, a reorganization of the KLA head groups takes place leading to a relaxation of the lipid film. Lysozyme molecules are trapped beneath the KLA monolayer caused by strong electrostatic attractive forces between lysozyme and the KLA lipids.

On the contrary, when N-L interacts with a LPS monolayer, i.e. including polysaccharide moieties, surface pressure and ellipsometric angle simultaneously increase (Figures 3.2A and 3.2B). Undoubtedly, N-L is thus able to insert deeply in the interface, up to the hydrophobic zone of the LPS monolayer. A hypothesis can be the effect of steric hindrance of the polysaccharides which prevents total coverage of the interface by the lipid headgroups, thus leaving free space for lysozyme insertion. Moreover, the polysaccharide chains can also cause simultaneously partial shielding of the negative charges on the headgroups and therefore prevent the entrapment of the positive lysozyme molecules at the level of these negative charges as it is the case for KLA lipids. The decreased interaction of the negative charges with positive lysozyme could enable the insertion of the protein between the LPS headgroups. At last, lysozyme and the polysaccharide moieties could interact and create compact zones as LPS/lysozyme domains and complexes (Figure 3.6) resulting in lesser density in other areas enabling the remaining free lysozyme. Such strong hydrophobic interactions have already been reported between LPS and lysozyme in solution (Ohno & Morrison, 1989), and LPS/lysozyme complexes have been observed (Brandenburg *et al.*, 1998; Ohno *et al.*, 1991).

N-L interaction with LPS causes a slight reorganization of the LPS monolayer

At the same time as the surface pressure increases when N-L is injected under a LPS monolayer, a strong increase of the ellipsometric angle Δ ($+7°$, Figure 3.2B) is observed, which is higher than the ellipsometric angle increase for protein/phospholipid monolayers (Sarkis *et al.*, 2011). This unusually high Δ increase can be explained by the LPS/lysozyme complex formation, polysaccharide reorganization, and/or the presence of N-L at the interface, since the ellipsometric angle depends on the refraction index and the film thickness.

BAM and AFM imaging were performed to evaluate the different hypotheses explaining the Δ increase. BAM and AFM imaging show the heterogeneity of the initial LPS monolayer at micrometer and nanometer scale, respectively (Figures 3.5A, 3.5C, 3.6A and 3.6C), as a result of the variable lengths of the polysaccharide chains. After N-L injection and interaction with LPS, this heterogeneity is maintained as can be observed in the BAM (Figures 3.5B and 3.5D) and AFM images (Figures 3.6B and 3.6D). But N-L injection also results in a slight increase of the background Δ-value in the delta-map (Figure 3.5D), and in the formation of small domains on the background zones in AFM-imaging (Figures 3.6B and 3.6D). It can thus be concluded that N-L reorganizes the LPS monolayer, even if this reorganization remains limited. The reorganization of the LPS monolayer and the formation of LPS/lysozyme complexes could possibly be the preliminary steps for pore formation by N-L as observed by Derde *et al.* (2013).

DH-L has a stronger affinity for LPS than N-L, and causes more radical reorganization of the LPS monolayer

Similarly to N-L, DH-L insertion into the LPS monolayer is enabled by the polysaccharide moieties, and DH-L reorganizes the LPS monolayer. However, differences in the behavior of DH-L *vs* N-L can be noticed. This modified behavior could be related to its different physicochemical properties such as increased hydrophobicity, surface-activity, positive charge and flexibility (Desfougères *et al.*, 2011a,b).

DH-L insertion into the LPS monolayer is more efficient than N-L at concentrations higher than 0.05 μM (Figure 3.1A). This could be due to the higher flexibility of DH-L as compared to N-L (Desfougères *et al.*, 2011a), which could allow more DH-L molecules to insert into the LPS monolayer, and/or to restructure more efficiently the interface. The increased insertion capacity of DH-L is consistent with its slight increased interfacial behavior (π_{final}, Table 3.1). Especially, it is noticeable that the surface pressure increase induced by DH-L insertion into the LPS monolayer is similar to that measured with an antimicrobial peptide, i.e. temporin L, in equivalent conditions (Table 3.2). DH-L has also more affinity for the LPS monolayer than N-L, demonstrated by its higher MIP and synergy factor (59.6 mN/m and 0.85, respectively; table 3.1) (Boisselier *et al.*, 2012; Calvez *et al.*, 2009). The drastically different reorganization of the LPS monolayer by DH-L is highlighted by BAM and AFM imaging (Figures 3.5 and 3.6). The BAM-images show that the many small domains with a high Δ-value visible in the presence of N-L (Figures 3.5B and 3.5D) are replaced by larger and fewer high Δ-value domains in the presence of DH-L (Figures 3.5F and 3.5H). Concurrently, more or less thick, and more or less large clusters appear in the presence of DH-L, as evidenced by AFM images (Figures 3.6F and 3.6H). These clusters could be protein aggregates caused by high local concentration of DH-L at the LPS monolayer, consistently with the higher sensitivity to aggregation of DH-L as compared to N-L, previously established by Desfougères *et al.* (2011b). It should be noticed that the minor modifications of DH-L have a major impact on the interactions with LPS monolayer. The increased interactions of DH-L with the LPS monolayer compared to N-L is consistent with the improved antimicrobial activity and increased outer membrane disruption potential described by Derde *et al.* (2014) *in vivo*.

3.2.5 Supplementary data

S1: Analysis of the ellipsometric angle of LPS monolayer

The ellipsometric angle of a LPS monolayer is significantly higher than the usual ellipsometric angle of a phospholipid monolayer which is about 10° (Sarkis *et al.*, 2011). On the contrary of phospholipid monolayers, the ellipsometric angle of a LPS monolayer depends on the initial surface pressure of the monolayer. For a surface pressure lower than 20 mN/m, the ellipsometric angle Δ is about 13° (Figure 3.7). When increasing the surface pressure between 20 mN/m and 24 mN/m, the ellipsometric angle Δ increases. Between 24 mN/m and 32 mN/m, the ellipsometric angle value is constant (Figure 3.7). The ellipsometric angle is thus independent of the surface pressure at these higher surface pressure values. This is probably due to a slight reorientation and reorganization of the polysaccharide moieties. This reorientation and reorganization does not modify the film thickness.

S2: Atomic force images of LPS and KLA monolayers

The heterogeneity of the LPS molecules is here visualized by AFM-imaging after compression of the lipids up to a surface pressure of 26 mN/m (Figure 3.8A). The length of the O-antigen chain is naturally variable and thus gives rise to a distribution of chain lengths within the LPS extract. In the topographical images, high and low domains can be noticed. The organization of the monolayer is thus complex. The mean thickness (background to mica) of the monolayer

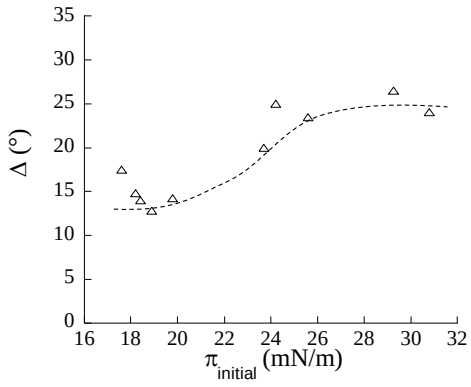

Figure 3.7: The ellipsometric angle Δ of a LPS monolayer at different initial surface pressure between 16 and 32 mN/m.

is about 5 nm for LPS monolayers. On the other hand, KLA monolayer is a more uniform sample caused by the use of one unique lipid molecule. One can observe a height difference of 1.15 ± 0.1 nm between the background (dark zones) and higher zones (light zones). .

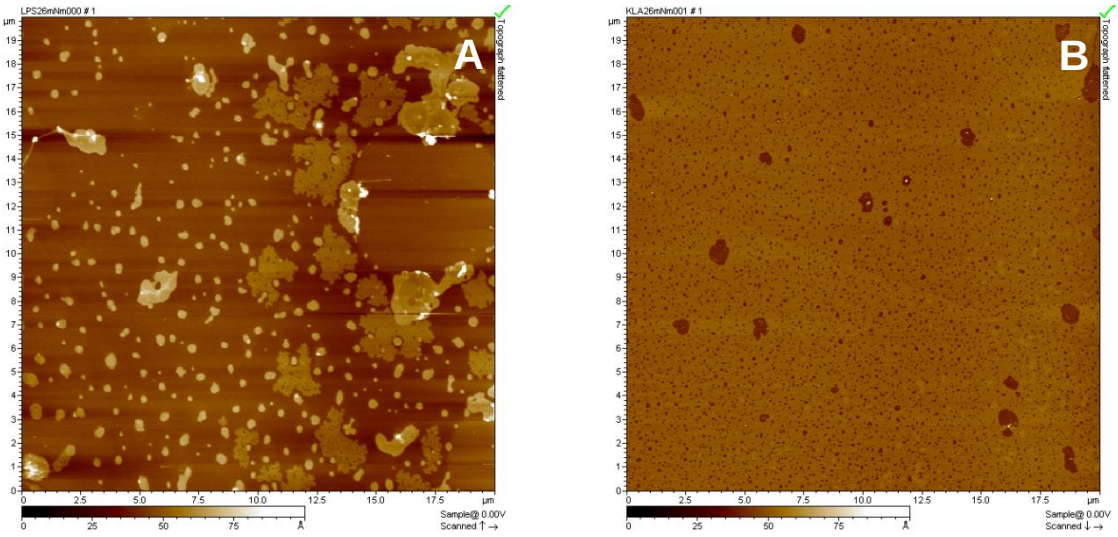

Figure 3.8: Topographical images (20 μm^2) of LPS monolayer (A) and KLA monolayer (B) at 26 mN/m.

S3: Isothermal compression of LPS and KLA monolayers

π normalized-area isotherms were recorded for both LPS and KLA monolayers (Figure 3.9). Because LPS is a natural extract, it contains different LPS molecules with variable polysaccharide chain lengths and thus variable molecular weights. Therefore, molecular area and compressibility modulus cannot be calculated.

To visualize both isotherms of LPS and KLA monolayers, a normalized area was here used. The absence of any plateau in the compression curves suggests that no phase transition occurs (LE-LC), probably due to the presence of a large head group compared to the fatty acyl chains, that prevents the ordering the hydrocarbon chains.This is in accordance with GIXD-experiments performed on *E. coli* Re-LPS. These experiments showed no diffraction even up till 30 mN/m meaning no lateral ordering of the hydrocarbon chains in the absence of Ca^{2+} and chelating agents (Oliveira *et al.*, 2010).

The compression isotherms of LPS and KLA monolayers only show a slight change in slope at 13.2 and 13.3 mN/m, respectively. This could indicate the reorientation of the molecules at the interface. It is noticeable that the slope changes are at a similar surface pressure for LPS and KLA monolayers; this could be due to the mutual lipid A component.

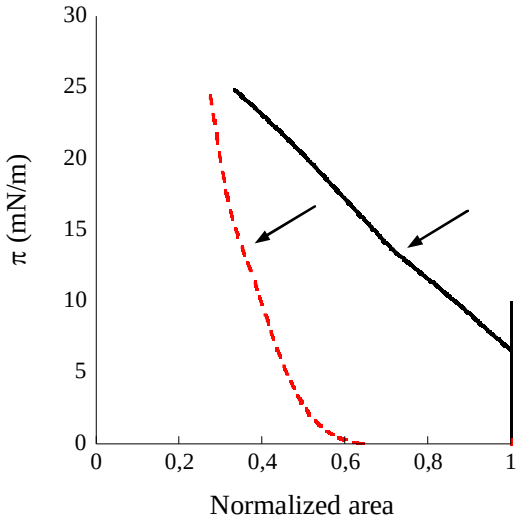

Figure 3.9: π-Area Langmuir isotherms of LPS (—) and KLA (– –) monolayers.

3.3 Native and dry-heated lysozyme interactions with membrane lipid monolayers: lipid packing modifications of a phospholipid monolayer, model of the *E. coli* cytoplasmic membrane.

Derde M., Nau F., Guérin-Dubiard C., Lechevalier V., Paboeuf G., Jan S., Baron F., Gautier M. & Vié V. (soumis à *BBA biomembranes, en revision*)

3.3.1 Abstract

Today's society is confronted with an important public health issue: antimicrobial resistance. The need for novel antimicrobial compounds is thus growing. The novel, ideal antimicrobial compounds should try to limit this antimicrobial resistance. Antimicrobial peptides or proteins such as hen egg white lysozyme are promising molecules acting on the bacterial membranes. Hen egg white lysozyme has recently by identified as active on Gram negative bacteria due to its intervenance with the outer and cytoplasmic membranes integrity. Moreover, dry-heating (7 days at 80°C) improves the membrane activity of lysozyme resulting in higher antimicrobial activity. These *in vivo* findings thus suggest interactions between lysozyme and the membrane lipids. This is consistent with the findings of several authors which have shown the lysozyme interaction with bacterial phospholipids such as phosphatidylglycerol and cardiolipin. However, up till now the mechanism of interaction between lysozyme and the cytoplasmic phospholipid mixture remains to be discovered. In the here presented study, the use of a monolayer model with a realistic bacterial phospholipid composition and in physiological conditions is proposed. The lysozyme/phospholipid interactions have been studied by surface pressure measurement, ellipsometry and atomic force microscopy. Native lysozyme revealed to be able to adsorb onto and insert into a bacterial phospholipid monolayer resulting in a lipid packing reorganization and a lateral cohesion decrease between the phospholipids. Dry-heating of lysozyme increased the insertion capacity and the ability to induce lipid packing modifications. These *in vitro* findings are then consistent with the increased membrane disruption potential of dry-heated lysozyme *in vivo* compared to native lysozyme. Moreover, lysozyme/phospholipid interactions have been shown specific for bacterial cytoplasmic membranes.

3.3.2 Materials and methods

Proteins and lipids

Native lysozyme (N-L) powder (pH 3.2) was obtained from Liot (Annezin, 62-France). It was heated for 7 days at 80°C in hermetically closed glass tubes to obtain dry-heated lysozyme (DH-L). Lysozyme (N-L or DH-L) was solubilized (around 0.5 g/L) in 5 mM 4-(2-hydroxyethyl)piperazine-1-ethanesulfonic acid (HEPES) buffer (Sigma Aldrich, Saint-Quentin, France), pH 7.0, 150 mM NaCl (Fluka, Saint-Quentin, France). The concentration of the lysozyme stock solution was precisely determined by absorbance at 280 nm (extinction coefficient = 2.6 $g^{-1} \cdot L$) (Gasteiger *et al.*, 2005; Expasy SIB Swiss, 2014). The protein solution was then diluted in the HEPES buffer to obtain the desired lysozyme concentration.

A mixture of different lipids (Avanti Polar Lipids, Alabaster, USA) was prepared to mimic the cytoplasmic membrane of *E. coli* (CMEC) as described by Lugtenberg & Peters (1976); it contained 2.6% 1,2-dioleoyl-sn-glycero-3-phospho-(1'-rac-glycerol) (DOPG), 3.9% 1,2-dihexadecanoyl-sn-glycero-3-phospho-(1'-rac-glycerol) (DPPG), 11.8% cardiolipin (CL), 32.3% 1,2-dioleoyl-sn-glycero-3-phosphoethanolamine (DOPE) and 49.4% 1,2-dipalmitoyl-sn-glycero-3-phosphoethanolamine (DPPE). This lipid mixture was prepared in 2:1 chloroform/

methanol mixture at 0.25 mM. Hen egg L-α-phosphatidylcholine (eggPC) (Avanti Polar Lipids, Alabaster, USA) was also prepared in 2:1 chloroform/methanol mixture at 1 mM.

Lipid/protein monolayers

The experiments were performed in a homemade TEFLON® trough of 8 mL. Before each use, the trough was thoroughly cleaned with successively warm tap water, ethanol, demineralized water, and then boiled for 15 min in demineralized water. After cooling the TEFLON® trough was filled with 8 mL HEPES buffer. The CMEC mixture was spread with a high precision Hamilton microsyringe at the clean air/liquid interface to obtain an initial surface pressure of 20 or 30 mN/m. The eggPC were spread as described for the CMEC to obtain an initial surface pressure of 30 mN/m. After 15 min, i.e. a duration necessary to allow solvent evaporation and lipid organization, 50 μL N-L or DH-L solution were injected in the subphase with a Hamilton syringe to obtain a final protein subphase concentration between 0.02 and 3 μM.

Surface pressure measurements

The surface pressure was measured following a Wilhelmy method using a 10 mm x 22 mm filter paper as plate (Whatman, Velizy-Villacoublay, France) connected to a microelectronic feedback system (Nima PS4, Manchester, England). The surface pressure (π) was recorded every 4 s with a precision of $\pm$ 0.2 mN/m. The measured surface pressure is the result of the surface tension of water (72.8 mN/m at 20°C) minus the surface tension of the lipid film (Vargaftik *et al.*, 1983).

Ellipsometry

Measurements of the ellipsometric angle value were carried out with an in-house automated ellipsometer in a "null ellipsometer" configuration (Azzam & Bashara, 1977; Berge & Renault, 1993). A polarized He–Ne laser beam (λ=632.8 nm, Melles Griot, Glan-Thompson polarizer) was reflected on the liquid surface. The incidence angle was 52.12°, i.e. Brewster angle for the air/water interface minus 1°. After reflection on the liquid surface, the laser light passed through a $\lambda/4$ retardation plate, a Glan-Thompson analyser, and a photomultiplier. The analyser angle, multiplied by two, yielded the value of the ellipsometric angle (Δ), i.e. the phase difference between parallel and perpendicular polarization of the reflected light. The laser beam probed the 1 mm^2 surface with a depth in the order of 1 μm. Initial values of the ellipsometric angle (Δ_0) and surface pressure (π_0) of buffer solutions were recorded for at least half an hour to assure that the interface is clean. Only in the case of a stable and minimal signal, experiments were performed. Values of Δ were recorded every 4 s with a precision of $\pm$ 0.5°.

AFM sample preparation and AFM imaging

Experiments were performed with a computer-controlled and user-programmable Langmuir TEFLON®-coated trough (type 601BAM) equipped with two movable barriers and of total surface 90 cm^2 (Nima Technology Ltd., England). Before starting the experiments, the trough was cleaned successively with ultrapure water (Nanopure-UV), ethanol, and finally ultrapure water. The trough was filled with 5 mM HEPES buffer pH 7 150 mM NaCl. CMEC mixture was spread over the clean air/liquid interface at a surface pressure of 20 mN/m. The solvent was then left to evaporate for 15 min. Then, a Langmuir-Blodgett (LB) transfer was performed onto freshly cleaved mica plates at constant surface pressure by vertically raising (1 mm/min) the mica through the air/liquid interface to obtain a sample of the initial CMEC monolayer. To investigate the influence of lysozyme on the CMEC monolayer, two lysozyme subphase concentrations (0.1 and 0.3 μM) were used. After lysozyme injection with a

Hamilton syringe, surface pressure variations were recorded until a stable surface pressure was reached to obtain the lysozyme adsorption kinetics onto the CMEC monolayer. Then, a LB transfer of the lysozyme/lipid film was performed onto freshly cleaved mica as described above.

AFM imaging of LB films was performed in contact mode using a Pico-plus atomic force microscope (Agilent Technologies, Phoenix, AZ) under ambient conditions with scanning areas of 5 μm^2. Topographic images were acquired using silicon nitride tips (Bruker, CA, USA) on integral cantilevers with a nominal spring constant of 60 mN/m. The forces were controlled and minimized along the imaging process. Three different areas were imaged for each sample to assure that the images here shown are representative for the whole sample.

3.3.3 Results

Insertion capacity of lysozyme into CMEC monolayers

The insertion capacity of lysozyme was evaluated by injecting different concentrations of native lysozyme (N-L) or dry-heated lysozyme (DH-L) into the subphase of CMEC monolayers with an initial surface pressure ($\pi_{initial}$) of 20 mN/m. The surface pressure was continuously measured until a stable surface pressure was reached. A surface pressure increase $\Delta\pi$ ($\Delta\pi = \pi_{max}$ - $\pi_{initial}$) indicates lysozyme insertion into the CMEC monolayer.

N-L inserts into a CMEC monolayer when the lysozyme subphase concentration is higher than 0.2 μM (Figure 3.10). Above this concentration, the $\Delta\pi$ value increases when the N-L concentration increases in the subphase, up to a $\Delta\pi$-plateau value of 6 mN/m. This plateau is reached at 1 μM N-L, indicating that no more N-L insertion is possible from this subphase concentration onwards.

DH-L inserts into the CMEC monolayer at lysozyme subphase concentrations higher than 0.03 μM, and a $\Delta\pi$-plateau value of 8 mN/m is attained at 0.3 μM DH-L in the subphase. It is thus noticeable that DH-L inserts into the CMEC monolayer and reaches a $\Delta\pi$-plateau at lower concentration than N-L, and DH-L leads to a $\Delta\pi$-plateau value which is 2 mN/m higher than that of N-L.

For the further investigation of lysozyme insertion and adsorption kinetics, and of the impact on the lipid organization, two subphase concentrations (0.1 μM and 0.3 μM) are chosen. These subphase concentrations are chosen so that differences exist between both proteins, and lipid-protein interactions can be observed, while minimizing protein-protein interactions in the bulk solution (aggregation) or at the lipid interface.

Changes of ellipsometric angle (Δ) and surface pressure (π) of CMEC monolayer in the presence of lysozyme

The ellipsometric angle and surface pressure were monitored during 3 h after 0.1 μM lysozyme subphase injection, to evaluate the adsorption and insertion of N-L and DH-L onto and into a 20 mN/m CMEC monolayer, respectively (Figure 3.11).

After, a 0.1 μM N-L subphase injection the surface pressure remains stable for the first hour. It is thus obvious that N-L does not insert into a 20 mN/m CMEC monolayer, when injected in the subphase at 0.1 μM (Figure 3.11A). However, a slight ellipsometric angle increase (+0.3°) is observed after 30 min indicating lysozyme adsorption (Figure 3.11A). After 1 h, the surface pressure decreases severely until 16.7 mN/m is reached, and remains stable afterwards (Figure 3.11A). Meanwhile, the ellipsometric angle decreases slightly, but remains

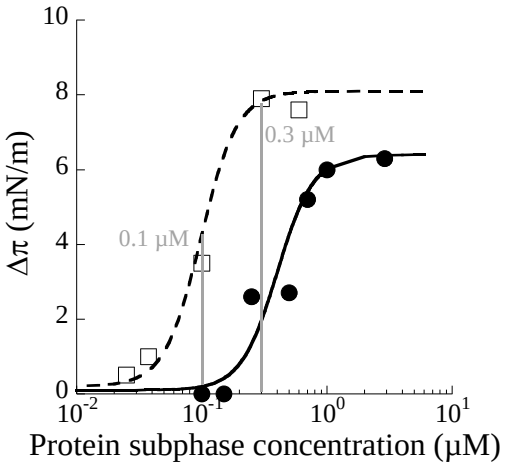

Figure 3.10: Surface pressure increase ($\Delta\pi$) of a CMEC monolayer (π_{initial} = 20 mN/m) induced by different subphase concentrations of native (N-L) (•) or dry-heated lysozyme (DH-L)(□).

stable at 9.7° from 1 h to 3 h (Figure 3.11A). It should be noticed that the ellipsometric angle is never lower than the ellipsometric angle of the CMEC monolayer before lysozyme injection.

On the contrary, a surface pressure increase (+4.3 mN/m) is observed 1h after injection of 0.1 μM DH-L, demonstrating that DH-L inserts into a 20 mN/m CMEC monolayer (Figure 3.11B). Simultaneously, the ellipsometric angle increases with +1.5°. Beyond 1h after DH-L subphase injection, the surface pressure decreases, while the ellipsometric angle remains constant (Figure 3.11B).

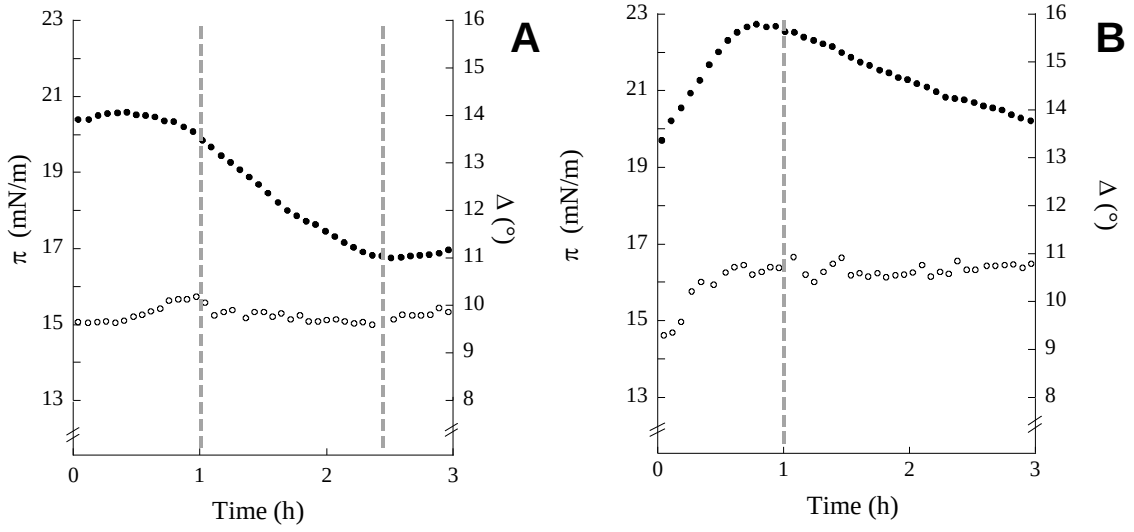

Figure 3.11: Surface pressure (π) and ellipsometric angle (Δ) measurements for a 20 mN/m CMEC monolayer after 0.1 μM N-L (A) or DH-L (B) subphase injection. The full circles (•) and open circles (○) represent surface pressure and ellipsometric angle measurements, respectively.

When increasing the concentration of N-L or DH-L in the subphase (0.3 μM *vs* 0.1 μM), the ellipsometric angle increases (+0.8° and +2.8°, respectively), indicating more lysozyme adsorption onto the CMEC monolayer. Simultaneously, surface pressure increases are observed

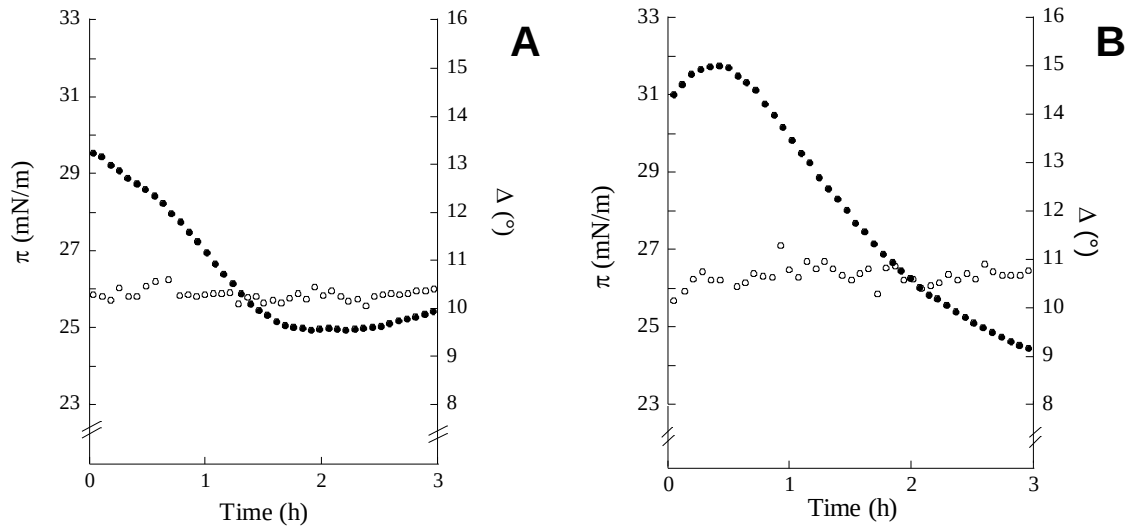

Figure 3.12: Surface pressure (π) and ellipsometric angle (Δ) measurements for a 30 mN/m CMEC monolayer after 0.1 μM N-L (A) or DH-L (B) subphase injection. The full circles (•) and open circles (○) represent surface pressure and ellipsometric angle measurements, respectively.

(+1.8 and +7.7 mN/m, respectively), indicating insertion into CMEC monolayer with initial surface pressure of 20 mN/m (Figure 3.10). Similarly, to the kinetics obtained with 0.1 μM N-L and DH-L, surface pressure decreases beyond 1 h of lysozyme injection is detected for 0.3 μM lysozyme (data not shown). At the same time, the ellipsometric angle remains constant (data not shown), indicating that no matter is lost at the interface.

To evaluate the influence of the initial surface pressure of CMEC monolayer, a 30 mN/m CMEC monolayer was used. In these conditions, no insertion is detected for 0.1 μM subphase concentration of N-L. Even more, surface pressure decreases immediately after N-L subphase injection (Figure 3.12A). However, the ellipsometric angle measurements increase slightly (+ 0.4°) 0.5 h after the 0.1 μM N-L subphase injection indicating that N-L adsorbs onto CMEC monolayer. Afterwards the ellipsometric angle decreases slightly, but the Δ-value is never lower than the initial value. On the contrary, DH-L induces a surface pressure increase (+1.1 mN/m), meaning that DH-L insertion still occurs in these conditions. Simultaneously, DH-L also induces an ellipsometric angle increase (+ 0.7°), indicating DH-L adsorption occurs (Figure 3.12B). After 0.5 h the surface pressure increase induced by DH-L is maximal and decreases afterwards; the ellipsometric angle remains constant after 0.5 h (Figure 3.12B).

Atomic force microscopy observations of CMEC monolayers in the presence of lysozyme

AFM imaging is a highly sensitive technique, allowing the visualization of the topographic surface of transferred interfacial films. Thus, in a 20 mN/m CMEC monolayer, lighter domains are visible on a dark background, indicating that two lipid phases coexist (Figure 3.13A). The lighter domains, having a diameter between 0.9 and 1.7 μm, correspond to a liquid condensed (LC) phase, while the dark background corresponds to a liquid expanded (LE) phase. The height difference between these two phases is 1.1 ± 0.1 nm (Figures 3.13A and 3.13A') (Harkins *et al.*, 1940).

Two lysozyme subphase concentrations were used to investigate the effect of N-L and DH-L on the CMEC monolayer. A general view of the topographic images of each protein subphase

concentration shows that the phase co-existence is still present. The height difference between the two phases is similar to the initial CMEC monolayer (Figures 3.13A'-E'). Nevertheless, changes in the size and shape of the LC domains can be noticed after N-L and DH-L interaction.

After injection of 0.1 μM N-L in the subphase (Figure 3.13B), diameter changes of the LC domains can clearly be observed with a repartition into two groups. The largest ones have a diameter between 0.6 and 4.0 μm, and the smallest ones have a diameter between 0.1 and 0.3 μm. It is also noticeable that the domains are more circular than in the initial situation. A 0.3 μM N-L injection (Figure 3.13D and 3.13D') induces no change in the LC domains size compared to the initial situation (diameter between 0.7 and 2.1 μm). But a high number of small objects with a height of 1.2 $\pm$ 0.1 nm and a diameter of 31 $\pm$ 13 nm appear in the LE phase. It should be noticed that these small objects only appear at the higher N-L subphase concentration (0.3 μM *vs* 0.1 μM) and that lysozyme insertion occurs at this subphase concentration (Figure 3.10). The small objects could thus be lysozyme/phospholipid clusters.

When the subphase concentration is 0.1 μM DH-L, the LC domain size increases up to a diameter 7.3 μm, and many small objects (1.4 $\pm$ 0.8 nm height; 66 $\pm$ 20 nm diameter) appear in the LE phase (Figures 3.13C and 3.13C'). The most spectacular modifications of the CMEC monolayer organization are observed after injection of 0.3 μM DH-L. Here, the edges of the domains are smooth, and long objects with a height of 2.5 $\pm$ 0.5 nm are observed in the LE phase; small objects (2.6 $\pm$ 0.6 nm height; 45 $\pm$ 10 nm diameter) are also visible in the LC phase domains (Figures 3.13E and 3.13E'). Small and large objects are observed at both DH-L subphase concentration and DH-L insertion occurs in both cases. The observed objects could be lysozyme/phospholipid clusters. Finally, it should be noticed that the repartition of the small objects between the LE and LC phases is different at a 0.1 or 0.3 μM DH-L in the subphase: at the lower concentration the small objects are only observed in the LE phase, contrary to the higher concentration where in both LE and LC phases objects can be observed (Figures 3.13C and 3.13E).

Changes of the surface pressure (π) and ellipsometric angle (Δ) eggPC monolayer in the presence of lysozyme

Phosphatidylcholine (PC) is the most abundant phospholipid in eukaryotic cells and is absent in the model bacteria *E. coli* (Lugtenberg & Peters, 1976; Teixeira *et al.*, 2012; van Meer *et al.*, 2008). EggPC monolayer is here used as a simplified model for the eukaryotic plasma membrane. The initial surface pressure of the eggPC monolayer was 30 mN/m, which is the theoretical initial surface pressure of the eukaryotic plasma membrane according to Marsh (1996). It is important to test the insertion and adsorption capacities of N-L and DH-L into and onto an eggPC monolayer model, to evaluate the selectivity of the antimicrobial proteins against bacterial cell membranes. The highest concentration used in this study (0.3 μM) was tested, because a higher concentration is more prone to induce interactions with the phospholipid monolayer. The surface pressure and ellipsometric angle changes were thus recorded after injection of 0.3 μM lysozyme (N-L and DH-L) in the eggPC monolayer subphase.

Surface pressure (π) remains stable after lysozyme injection for both N-L and DH-L, meaning both lysozymes are unable to insert into eggPC monolayer (Figure 3.14). Similarly, the ellipsometric angle Δ stays constant, equal to the initial value (7.8°) measured for the eggPC monolayer, meaning that both N-L and DH-L do not adsorb onto the eggPC monolayer (Figure 3.14).

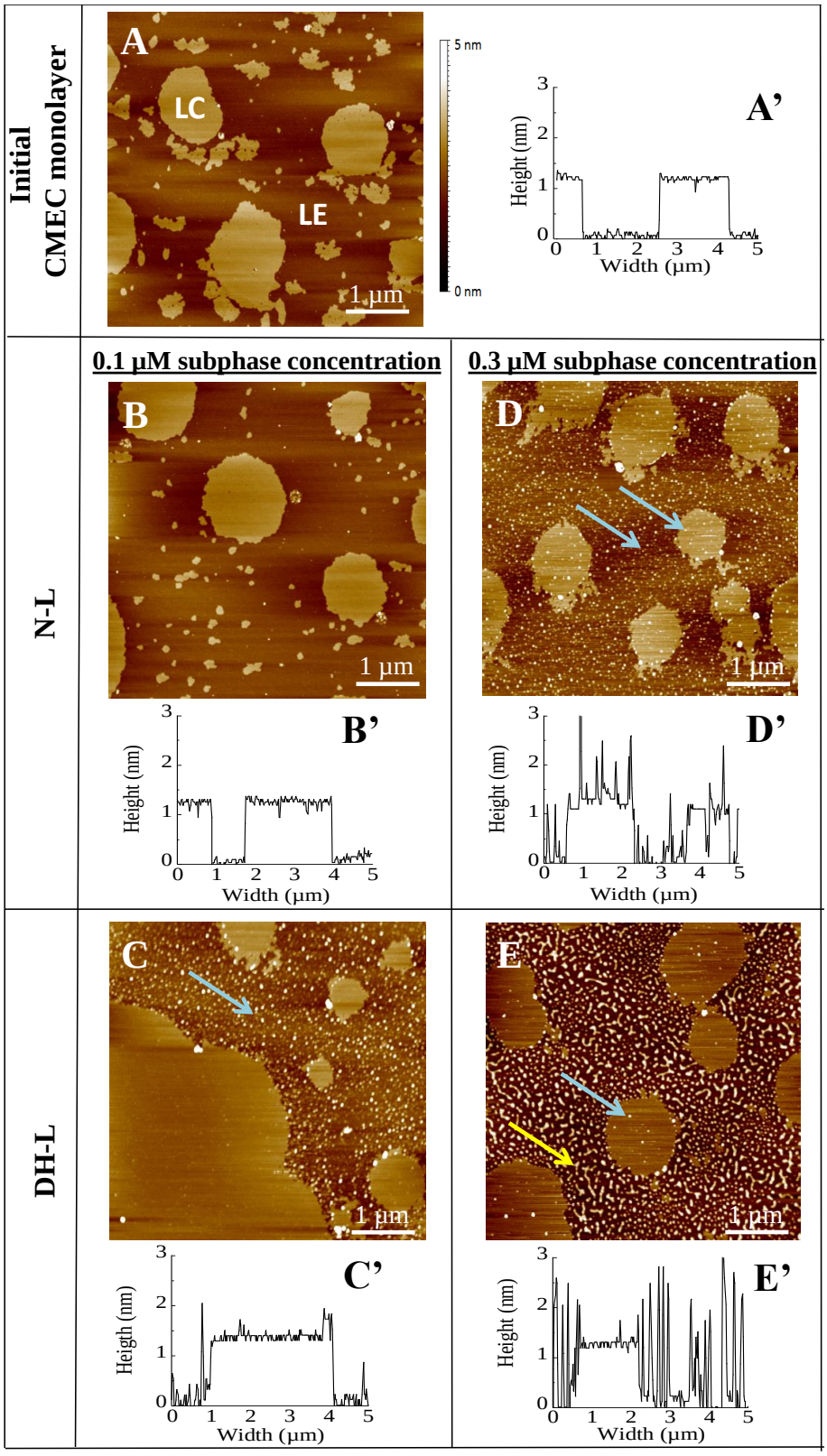

Figure 3.13: AFM topographical images (5 μm^2) of CMEC monolayers without lysozyme (A) and with lysozyme after 0.1 μM N-L (B) or DH-L subphase injection (C) and after 0.3 μM N-L (D) or DH-L subphase injection (E). Transversal cross-sections of the CMEC monolayers without (A') and with lysozyme after 0.1 μM N-L (B') or DH-L subphase injections (C') and after 0.3 μM N-L (D') or DH-L subphase injection (E'). Small and large objects are respectively indicated with blue and yellow arrows.

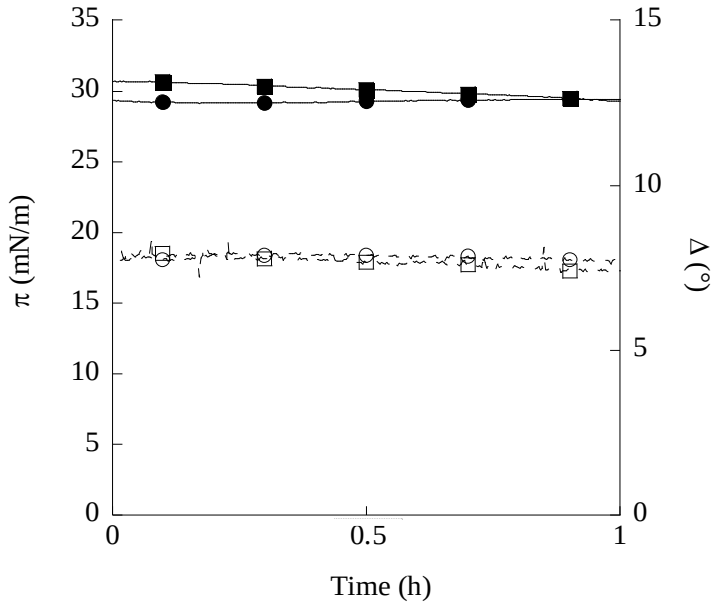

Figure 3.14: Surface pressure (π), represented as full symbols and full lines, and ellipsometric angle (Δ), represented as open symbols and dashed lines, changes after injection of 0.3 μM N-L (circels) and DH-L (squares) in the subphase of a eggPC monolayer with an initial surface pressure of 30 mN/m.

3.3.4 Discussion

Native lysozyme (N-L) has been shown active against Gram-negative bacteria such as *E. coli* (Derde *et al.*, 2013, 2014; Pellegrini *et al.*, 1992). Membrane permeabilization has been suggested as one of the mechanisms responsible for this activity (Pellegrini *et al.*, 2000; Wild *et al.*, 1997). This assumption was recently confirmed by Derde *et al.* who demonstrated that N-L interacts with the outer membrane of *E. coli*, causing the formation of pores (Derde *et al.*, 2013, 2014). Consistently, N-L has been proven able to insert into LPS monolayer, i.e. a model of the *E. coli* outer membrane, and then to reorganize the LPS monolayer (§ 3.2). N-L has also been shown active on the cytoplasmic membrane of *E. coli*, but without pore formation; the formation of ion channels is assumed (Derde *et al.*, 2013, 2014). This suggests that N-L interacts with the phospholipids of the cytoplasmic membrane, despite the mechanism of interaction remains unknown.

Moreover, the limited antimicrobial activity of native lysozyme can be increased by dry-heating (7 days, 80°C). This increased activity is the result of an increased membrane disruption potential due to the modified physicochemical properties of dry-heated lysozyme (DH-L) (Derde *et al.*, 2014). It is then interesting to compare the interactions of native and dry-heated lysozymes on the bacterial cytoplasmic phospholipids to get a better understanding of the interaction mechanism on the one hand and to identify major lipid interaction factors inducing antimicrobial activity on the other hand.

Interfacial monolayers are considered as good models to study interactions between antimicrobial proteins and bacterial membranes, because the initial lateral pressure can be controlled and multiple lipid compositions can be used (Brockman, 1999; Roes *et al.*, 2005). In the here presented study, a monolayer model build out of a complex phospholipid mixture is proposed. The composition of this mixture is based on the phospholipid composition of the cytoplasmic membrane of *E. coli* K12 (CMEC); it contains unsaturated and saturated phosphatidylethanolamine, phosphatidylglycerol and cardiolipin in proportions suggested by Lugtenberg & Peters (1976). The use of such a complex mixture is a key point because of the

complexity of electrostatic and hydrophobic interactions between the different phospholipids, and the impact of the lipid geometry and structure on the lateral lipid packing (Israelachvili & Mitchell, 1975). In order to investigate the mechanisms of lysozyme activity on cytoplasmic membrane, the interactions between the phospholipid monolayer described above and N-L or DH-L have been studied using biophysical tools such as surface pressure measurements, ellipsometry and AFM.

Hen egg white lysozyme is able to insert into the CMEC monolayer

Native lysozyme insertion into the complex bacterial phospholipid mixture mimicking the *E. coli* cytoplasmic membrane is here demonstrated by means of surface pressure measurements; it is noticeable that lysozyme insertion is concentration-dependent (Figure 3.10). This result completes earlier work on the interactions between antimicrobial peptides and monolayer of pure (DPPG or DPPC), simpler bacterial phospholipid mixtures (POPE:POPG, PG/CL, PE/PG) and complex bacterial phospholipid mixtures (PE/PG/CL) (Coccia *et al.*, 2011; Gidalevitz *et al.*, 2003; Krishnakumari & Nagaraj, 2008; Zhang *et al.*, 2000a,b).

However, the surface pressure increase due to lysozyme insertion into CMEC monolayer remains moderate compared to similar experiments with antimicrobial peptides as bombinins, protegrin 1, Phd 1 or 2, or Gramicidin S (Table 3.3) (Coccia *et al.*, 2011; Gidalevitz *et al.*, 2003; Krishnakumari & Nagaraj, 2008; Zhang *et al.*, 2000a,b). Most of the results obtained for these antimicrobial peptides could however be biased when the highly simplified monolayer models were used. Indeed, it should be noticed that the highest surface pressure increases are obtained with the monolayer models in which only or high proportions of negatively charged phospholipids (PG and CL) are used. This emphasizes the need to use phospholipid mixtures which mimick the composition of bacterial cytoplasmic membranes, as true-to-nature as possible.

Finally, the here obtained results for native lysozyme interactions with a CMEC monolayer and results from Mudgil *et al.* (2006) with PE or PG monolayers can be compared. Native lysozyme inserts at a subphase concentration of 0.1 μM into PE or PG monolayers ($\pi_{\text{initial}} =$

Table 3.3: Surface pressure increase ($\Delta\pi$) of bacterial cytoplasmic phospholipid monolayers ($\pi_{initial}$ = 20 mN/m) measured after insertion of antimicrobial peptides.

	Peptide or protein	Conc. (μM)	$\Delta\pi$ (mN/m)	Phospholipid composition	Reference
Peptides	Protegrin 1 (2.2 kDa)	0.05	24	DPPG	Gidalevitz *et al.* (2003)
		0.05	2	DPPE	
	Phd 1 (2.1 kDa)	0.6	10	POPE:POPG (7:3)	Krishnakumari & Nagaraj (2008)
		0.15	8	POPE:POPG (7:3)	
	Phd 2 (2.2 kDa)	0.6	6	POPE:POPG (7:3)	Krishnakumari & Nagaraj (2008)
	Bombinin H2 (1.9 kDa)	1	18	PG/CL (6:4)	Coccia *et al.* (2011)
		1	15	PE/PG (7:3)	
	Gramicidin S (1.2 kDa)	0.1	17	PE/PG/CL (8:0.5:1.5)	Zhang *et al.* (2000a)
		0.8	24	PG	
		0.8	6	POPE	
		0.8	18	CL	
	Polymyxin B (1.4 kDa)	0.7	8	PG	Zhang *et al.* (2000a)
		0.7	7	CL	
	Polymyxin E1 (1.2 kDa)	0.8	8	PG	Zhang *et al.* (2000a)
		0.8	7	CL	
	Polyphemusin 1 (2.4 kDa)	0.1	2	POPC/PG/CL (8:0.5:1.5)	Zhang *et al.* (2000a)
		1	7	POPC/PG/CL (8:0.5:1.5)	
		0.4	13	PG	
		0.4	5	CL	
Lysozyme (14.3 kDa)	N-L	0.1	2	PG	Mudgil *et al.* (2006)
		0.1	3	PE	Mudgil *et al.* (2006)
		0.1	-	PE/PG/CL (8.2:0.6:1.2)	This study
		0.3	2	PE/PG/CL (8.2:0.6:1.2)	This study
	DH-L	0.1	4	PE/PG/CL (8.2:0.6:1.2)	This study
		0.3	8	PE/PG/CL (8.2:0.6:1.2)	

20 mN/m) inducing a surface pressure increase of 2 and 3 mN/m, respectively (Table 3.3). On the contrary, at a subphase concentration of 0.1 μM N-L does not insert into CMEC monolayer. This could be explained by the lower negative charge density of CMEC compared to the pure PG monolayer of Mudgil *et al.* (2006). However, our results are not in agreement with the insertion of 0.1 μM N-L into the pure PE monolayer reported by Mudgil *et al.* (2006).

Native lysozyme decreases the lateral cohesion of CMEC monolayer

At low N-L concentration (0.1 μM), only adsorption (Δ increase) and no insertion (π constant) occurs at the CMEC/liquid interface (Figure 3.11A). After adsorption step, a severe decrease of surface pressure is observed, and this without matter loss from the CMEC/liquid interface as evidenced by the ellipsometric angle (Δ) which never drops below its initial value (Figure 3.11A). Adsorption followed by surface pressure decrease is observed similarly when the initial surface pressure of the CMEC monolayer is 20 mN/m as well as 30 mN/m (data not shown). When increasing N-L concentration (0.3 μM), adsorption and insertion occur in the first hour after lysozyme injection under CMEC monolayer. The subsequent surface pressure decrease proves that lysozyme adsorption affects the lateral cohesion of the CMEC lipids and causes lipid headgroups reorganization as described by Vié *et al.* (2010) for the dystrophin subdomain R20-24 at a DOPC/DOPS monolayer. These findings are then consistent with the results reported by Ioffe & Gorbenko (2005): the lysozyme induces lipid packing density change of cardiolipin/phosphatidylcholine bilayers. The reorganization of CMEC lipid headgroups observed in the presence of lysozyme is independent of the initial surface pressure (20 or 30 mN/m) and of lysozyme insertion ($\Delta\pi \geq 0$). The hypothesis that the surface pressure decrease indicates the lipid monolayer solubilization by lysozyme is excluded thanks to the combined use of ellipsometry and surface pressure measurements.

Changes in the lipid packing could also be confirmed by AFM topographical images. When N-L adsorbs onto the CMEC monolayer without insertion (0.1 μM N-L injected in the subphase), larger LC phase domains are visible (Figure 3.13B) compared to the initial CMEC monolayer (Figure 3.13A). When an increased N-L concentration is used (0.3 μM), making insertion into CMEC monolayer possible, small objects are visible on the AFM image (Figure 3.13D). These objects are assumed to be lysozyme aggregates or phospholipid-lysozyme complexes. Lysozyme aggregation upon membrane binding has already been observed by Gorbenko *et al.* (2007) and Trusova (2012).

These measurements and observations enable to conclude that N-L adsorbs onto CMEC monolayer, thus changing lipid packing of the monolayer, but in different ways depending if insertion occurs or not, i.e. depending on N-L concentration in the subphase. These findings are consistent with *in vivo* findings of ion channel formation and membrane depolarization (Derde *et al.*, 2014). When N-L adsorbs onto the cytoplasmic membrane and forms lipid-protein clusters, more permeable zones could be created causing ion channel formation as suggested by potassium leakage. Moreover, N-L is a positively charged molecule and thus its adsorption onto the cytoplasmic membrane could cause the disturbance of the transversal charge equilibrium of the membrane, resulting in a membrane potential dissipation.

Dry-heated lysozyme highly adsorbs onto and inserts into CMEC monolayer

DH-L insertion into a 20 mN/m CMEC monolayer is detectable for lysozyme concentration 6 times lower than for N-L insertion (Figure 3.10). Moreover, DH-L generates a higher $\Delta\pi$-plateau value than N-L (Figure 3.10). Then, dry-heating increases the lysozyme insertion capacity: either it is possible that more DH-L molecules than N-L molecules insert into the CMEC monolayer, or DH-L spreads out more easily than N-L at the CMEC/liquid interface,

creating higher lateral pressure at the interface. The latter assumption is consistent with the higher flexibility of DH-L compared to N-L (Desfougères *et al.*, 2011a). Moreover, the higher surface hydrophobicity of DH-L compared to N-L (Desfougères *et al.*, 2011a), may favor the insertion of the hydrophobic parts of the protein between the lipid chains of the CMEC monolayer.

DH-L also adsorbs more efficiently than N-L onto CMEC monolayer, as evidenced by ellipsometric angle increase (Figure 3.11); this is independent of initial surface pressure and lysozyme concentration. This can be explained by the more basic character of DH-L compared to N-L (Desfougères *et al.*, 2011a). DH-L is thus more positively charged than N-L at physiological pH, and electrostatic interactions between DH-L and the negatively charged CMEC monolayer could be increased compared to N-L, resulting in higher protein adsorption at the CMEC/liquid interface.

Dry-heated lysozyme induces severe lipid packing modifications in CMEC monolayer

Similarly to N-L, DH-L subphase injection induces a surface pressure decrease, while adsorbing onto the CMEC monolayer. This indicates that DH-L decreases the lateral cohesion of CMEC lipids after adsorption and insertion (Figure 3.11B). Severe packing defects can be evidenced by AFM. At low concentration, DH-L induces fusion of liquid condensed (LC) domains (Figure 3.13C), suggesting preferential insertion of lysozyme into liquid expanded (LE) phase of the CMEC monolayer (Figure 3.13C). This preferential insertion into LE phase could be due to the higher fluidity of this phase compared to the LC phase. This finding is interesting considering the equal repartition of negative charges into the LC and LE phases. DH-L insertion is thus not only guided by electrostatic attractions between DH-L and negative phospholipid charge, but also by the local phospholipid packing.

At high concentration, DH-L induces the formation of high and long objects (Figure 3.13E) which could be the evidence of protein clusters or lipid/protein complexes in LE phase. It could be that the positively charged DH-L recruits the anionic lipids (PG or CL) for subsequent lipid-protein cluster formation. Moreover, objects are visible in both phospholipid phases. This suggests that DH-L insertion is no longer guided by lipid packing at high concentration.

Overall, DH-L disrupts more severely the organization of CMEC monolayer. This could be due to its modified physicochemical properties such as higher basic character, hydrophobicity and surface activity compared to N-L (Desfougères *et al.*, 2011a,b). Derde *et al.* (2014) demonstrated that DH-L also disrupts more efficiently the cytoplasmic membrane of *E. coli* than N-L in *in vivo* conditions. The here displayed results are consistent with these *in vivo* findings.

Native and dry-heated lysozymes adsorb and insert specifically to bacterial monolayer models

Subphase injection of 0.3 μM N-L or DH-L beneath an eggPC monolayer does not modify the surface pressure and ellipsometric angle values (Figure 3.14). N-L and DH-L do neither insert into nor adsorb onto eggPC monolayer. These findings are consistent with the findings of Mudgil *et al.* (2006) and Matsumura & Dimitrova (1996), who observed no insertion of lysozyme into DPPC monolayer (20 mN/m) and eggPC monolayer (30 mN/m), respectively. Phosphatidylcholines are zwitterionic phospholipids making the net charge of eggPC monolayer nul at physiological pH. This suggests electrostatic attraction is essential for first interaction between lysozyme and a phospholipid monolayer model, consistently with earlier

findings of Zschornig *et al.* (2005) who established the importance of electrostatic interactions between lysozyme and anionic phospholipid vesicles.

The lack of interaction between N-L and DH-L on the one hand, and eggPC on the other hand, is a promising property for the development of novel antimicrobial drugs. Indeed, interaction between antimicrobial molecules and eukaryotic cell walls is unwanted to limit cell toxicity. The specificity of the antimicrobial proteins for bacterial membranes is thus essential for their further development for medical purposes.

3.4 Conclusions

Clairement, les lysozymes natif et chauffé à sec interagissent avec les lipides membranaires des membranes externe et cytoplasmique d'*E. coli* K12. Le lysozyme natif a une forte affinité pour la monocouche LPS dans laquelle il s'insère. Nos résultats montrent également que la partie polysaccharidique des LPS est essentielle à l'insertion du lysozyme entre les lipides A. Cette insertion induit une réorganisation de la monocouche LPS qui pourrait être une étape préliminaire à la formation des pores observés *in vivo* (cf Chapitre 2 § 2.4.4).

Après avoir franchi la membrane externe, le lysozyme se trouve en présence des phospholipides de la membrane cytoplasmique. Nos expérimentations *in vitro* montrent que le lysozyme peut s'adsorber à la monocouche CMEC et s'y insérer. Toutefois, la capacité d'insertion est plus faible que dans la monocouche LPS, ce qui est cohérent avec l'absence de pores dans la membrane cytoplasmique tel qu'observé *in vivo*, contrairement à ce qui se passe à la membrane externe. Quand le lysozyme s'adsorbe à la monocouche CMEC sans qu'il y ait pour autant insertion (0.1 μM N-L), la cohésion latérale entre les lipides s'amoindrit, mais n'entraîne pas de solubilisation lipidique. Une réorganisation des têtes lipidiques et la formation de clusters lysozyme/phospholipides anioniques seraient donc à la base de ce phénomène, indiquant un mécanisme de « lipid clustering » comme proposé par Epand *et al.* (2010). Ces résultats permettent d'expliquer les données *in vivo* (cf Chapitre 2) de la perméabilisation de la membrane cytoplasmique et de la perturbation du potentiel membranaire par le lysozyme qui agirait *via* un phénomène de ségrégation lipidique.

Le chauffage à sec s'est avéré un procédé efficace pour améliorer l'activité antimicrobienne du lysozyme mesurée *in vivo*, et pour augmenter sa capacité de perméabilisation des membranes bactériennes. Les propriétés physicochimiques du lysozyme chauffé, sensiblement différentes de celles de la protéine native, seraient à l'origine de ces différences d'activité antibactériennes et antimembranaires. *In vitro*, nous avons pu montrer que les interactions lysozyme/lipides membranaires sont également impactées par le chauffage à sec. Le lysozyme chauffé présente une plus forte capacité d'insertion que le lysozyme natif dans les deux modèles membranaires utilisés (monocouches LPS et CMEC). Ceci peut être expliqué par l'augmentation d'hydrophobie et de flexibilité de la protéine chauffée par rapport à la protéine native ; ces caractéristiques faciliteraient respectivement l'insertion entre les chaînes aliphatiques et les modifications conformationelles nécessaires au positionnement efficace de la protéine à l'interface. De plus, l'organisation des monocouches LPS et CMEC est sévèrement modifiée en présence de lysozyme chauffé. Ces résultats sont de nouveau cohérents avec les observations *in vivo* de formation de pores plus nombreux et/ou plus grands dans la membrane externe, ainsi que de canaux ioniques plus nombreux dans la membrane cytoplasmique.

Globalement, le lysozyme chauffé interagit donc plus fortement avec les lipides membranaires que le lysozyme natif. Cependant, le lysozyme chauffé est un mélange d'isoformes ayant chacune des propriétés physicochimiques différentes. La prochaine étape est d'étudier les in-

teractions membranaires pour chacune d'entre elles.

En Bref

- Le lysozyme natif s'insère dans des monocouches de LPS et CMEC.
- Les polysaccharides des LPS sont essentiels pour l'insertion du lysozyme dans la monocouche.
- Le lysozyme natif modifie l'organisation lipidique des monocouches de LPS et CMEC.
- Le chauffage à sec augmente la capacité d'insertion du lysozyme dans les monocouches de LPS et CMEC.
- Le lysozyme chauffé entraîne une réorganisation latérale sévère des monocouches de LPS et CMEC.

Chapitre 4

Le lysozyme chauffé : un mélange efficace d'isoformes ayant des activités membranaires différentes et complémentaires

basé sur le projet de publication :

Derde M., Vié V., Lechevalier V., Guérin-Dubiard C., Cochet MF., Paboeuf G., Bertović T., Jan S., Baron F., Gautier M. & Nau F. Dry-heated lysozyme, a mixture of complementary lysozyme isoforms acting on the *Escherichia coli* membranes, soumis *International Journal of Biological Macromolecules*, en revision

4.1 Introduction

Nous avons montré précédemment que le chauffage à sec est un procédé simple permettant d'augmenter l'activité antimicrobienne du lysozyme vis-à-vis d'*E. coli* (cf Chapitre 2 § 2.4.4). Cette plus grande efficacité antibactérienne du lysozyme chauffé a pu être expliquée par les propriétés physicochimiques modifiées de la protéine qui augmentent sa capacité d'interaction avec les lipides membranaires *in vitro* (cf Chapitre 3 § 3.2.4 et 3.3.4) et avec les membranes bactériennes *in vivo* (cf Chapitre 2 § 2.4). Mais le lysozyme chauffé à sec est en réalité un mélange d'isoformes du lysozyme : les formes iso-aspartyles, la forme « native-like » et les formes succinimides (cf. Chapitre 1 § 1.2.3, Desfougères *et al.* (2011a)). Ces isoformes se distinguent par leur charge nette, leur hydrophobie, leur flexibilité moléculaire et leur tensio-activité (Desfougères *et al.*, 2011a,b). Les formes iso-aspartyles et succinimides diffèrent de la forme native du lysozyme dans leur structure primaire même. De un à cinq résidus aspartate ou asparagine (Asp^{18}, Asp^{48}, Asp^{52}, Asp^{66}, Asp^{101} et/ou Asn^{103}) sont modifiés respectivement en leurs formes iso-aspartate ou succinimides (Desfougères *et al.*, 2011a). Ainsi, les formes succinimides sont plus chargées positivement à pH 7 et plus hydrophobes que le lysozyme natif, alors que les formes iso-aspartyles sont plus acides que la protéine native ; les formes succinimides sont également les plus flexibles et les plus tensio-actives des isoformes du lysozyme chauffé (Desfougères *et al.*, 2011a,b). La forme « native-like » présente quant à elle une charge nette égale à celle du lysozyme natif, mais offre un comportement différent à l'interface air-eau (Desfougères *et al.*, 2011b).

Les caractéristiques de charge et d'hydrophobie constituant des paramètres importants pour l'activité antimicrobienne des protéines et peptides en général, et du lysozyme en particulier (cf. Chapitre 1 § 1.1.1 et 1.2.2), il nous a paru pertinent d'évaluer et de comparer les isoformes du lysozyme chauffé à sec dans leur activité antimicrobienne vis-à-vis d'*E. coli*, en lien avec leur action sur les membranes bactériennes. La double approche proposée ici, associant des études *in vivo* (sur cellules bactériennes vivantes) et *in vitro* (sur modèles membranaires), vise d'une part à évaluer l'impact des interactions lysozyme-membranes dans un système complexe, et d'autre part à explorer les mécanismes moléculaires à l'origine de l'interaction entre les lipides membranaires et le lysozyme, qu'il soit natif ou sous l'une de ses isoformes.

4.2 Dry-heated lysozyme, a mixture of lysozyme complementary isoforms acting on the *Escherichia coli* membranes

Derde M., Vié V., Lechevalier V., Guérin-Dubiard C., Cochet MF., Paboeuf G., Bertović T., Jan S., Baron F., Gautier M. & Nau F., (soumis à *International Journal of Biological Macromolecules*, en revision)

4.2.1 Abstract

Antimicrobial resistance has become an important public health problem caused by decades of misuse of the antimicrobial compounds. This results in difficult and expensive disease treatment. Today, research for novel antimicrobial compounds limiting antimicrobial resistance development is highly stimulated. Antimicrobial proteins acting on the bacterial cell membranes can be one of those novel antimicrobial compounds. Hen egg white lysozyme has been identified to interact with both the outer and cytoplasmic membranes of Gram negative bacteria such as *E. coli*. However, its antimicrobial effect on those Gram negative bacteria remains limited. Dry-heating of lysozyme increases its antimicrobial and membrane activity against *E. coli*. But dry-heated lysozyme is a mixture of isoforms, iso-aspartyle lysozyme,

native-like lysozyme and succinimide lysozyme, of which the individual effects on *E. coli* and its membranes are still to be discovered.

In the here presented study, the effect of each component of dry-heated lysozyme has been investigated *in vivo* and *in vitro*. Dry-heated lysozyme appears to be an efficient mixture of complementary isoforms, which induces antimicrobial activity and membrane disruption. The positive charges of the isoforms seem to be a key parameter for their interaction with the outer and cytoplasmic membranes. However, hydrophobicity and molecular flexibility could also have an influence on the isoform/membrane interactions.

4.2.2 Material and methods

Materials

Native lysozyme (N-L) powder (pH 3.2) was obtained from Liot (Annezin, 62-France); it was heated for 7 days at 80°C in hermetically closed glass tubes to obtain dry-heated lysozyme (DH-L).

Trisma base, potassium phosphate monobasic, potassium phosphate dibasic, ortho-nitrophenylgalactoside (ONPG), 3,3'-dipropylthiadicarbocyanine iodide ($DiSC_3$), 4-(2-hydroxyethyl) -1-piperazineethanesulfonic acid (HEPES) and glucose were obtained from Sigma Aldrich (Saint-Quentin, France). Nitrocefin, casein peptone and yeast extract were obtained from Merck Chemicals (Darmstadt, Germany). Tryptic soy broth (TSB) was purchased from AES (Bruz, France).

The *E. coli* K12 lipopolysaccharides (LPS) were obtained from Invivogen (Toulouse, France) and solubilized at 0.5 g/L in 2:1 chloroform/methanol mixture. A mixture of different lipids (Avanti Polar Lipids, Alabaster, USA) was prepared at 0.25 mM in 2:1 chloroform/methanol mixture to mimic the cytoplasmic membrane of *E. coli* (CMEC) as described by Lugtenberg & Peters (1976); it contained 2.6% 1,2-dioleoyl-sn-glycero-3-phospho-(1'-rac-glycerol) (DOPG), 3.9% 1,2-dihexadecanoyl-sn-glycero-3-phospho-(1'-rac-glycerol) (DPPG), 11.8% cardiolipin (CL), 32.3% 1,2-dioleoyl-sn-glycero-3-phosphoethanolamine (DOPE) and 49.4% 1,2-dipalmitoyl-sn-glycero-3-phosphoethanolamine (DPPE).

Bacterial strains

Escherichia coli K12 was obtained from Institut Pasteur (Paris, 75-France). *Escherichia coli* ML-35p ($LacI^-$ $LacY^-$ $LacZ^+$, plasmid pBR322) was kindly provided by R. Lehrer (Department of medicine, UCLA, USA), and transmitted to our laboratory by D. Destoumieux-Garzon (UMR 5119, Ecologie des systèmes marins côtiers, University of Montpellier, France). *E. coli* ML-35p lacks lactose permease, and expresses β-lactamase and β-galactosidase in the periplasm and cytoplasm, respectively.

Purification of lysozyme isoforms

The different isoforms of lysozyme generated by dry-heating were purified from DH-L by cation exchange liquid chromatography (CEC). DH-L solution (2 g/L) was prepared in 60 mM phosphate buffer, pH 7.0, and injected onto an S-HYPERD F column (Biosepra®, Pall corporation, St-Germain-en-Laye, France) previously equilibrated with the same buffer, using a Varian ProStar chromatography system (Spectralab Scientific Inc., Markham, Canada). Elution was performed using a NaCl gradient from 0 to 0.5 M in 180 min, in a 60 mM phosphate buffer pH 7.0 at 10 mL/min. Protein detection was followed by spectrophotometry at 280 nm (Varian Prostar UV/VIS detector, Spectralab Scientific Inc., Markham, Canada). Three different protein fractions were collected: iso-aspartyle lysozyme fraction (ISO-L), native-like lysozyme

fraction (NL-L) and succinimide lysozyme fraction (SUC-L). The pH of the SUC-L fraction was adjusted to 4.0 immediately after elution in order to avoid succinimide rings hydrolysis. All the protein fractions were then dialyzed using a cellulose membrane with a molecular weight cut off of 3500 Da (Cellu-Sep T1, Texas, USA) and lyophilized using a lyophilizer S.G.D. Serial Cirp CS 10-0.8 (Serial, Le Coudray Saint Germer, France).

The composition of each collected fraction was determined by cation exchange high pressure liquid chromatography (CE-HPLC) using a device consisting of a Waters 2695 separation module and a Waters 2487 dual absorbance detector. The column used was an S-HYPERD 10 (Biosepra, Pall corporation, St-Germain-en-Laye, France). Elution was performed using a NaCl gradient from 0 to 1 M in 44 min, in a 20 mM sodium acetate buffer pH 5.0 at 1 mL/min, as described by Desfougères *et al.* (2011a). The absorbance of the eluent was followed at 214 and 280 nm. The relative proportion of each protein isoform was estimated from the area corresponding to each peak as determined by the Empower 2 software.

Escherichia coli growth assays

Growth assays were performed based on the method described by Derde *et al.* (2014). The *E. coli* K12 cultures were grown overnight (18 h) at 37°C under stirring (130 rpm) in TSB. After the incubation period, the cultures contained about 10^9 CFU/mL *E. coli*, from which 10^5 CFU/mL bacterial suspensions were prepared by performing 4 tenfold serial dilutions in LB05 (Luria Broth containing 10 g/L peptone of casein, 5 g/L yeast extract, and 0.5 g/L NaCl). After solubilization in demineralized water, 3.7 g/L N-L, 3.7 g/L DH-L, 0.19 g/L ISO-L, 1.9 g/L NL-L or 1.7 g/L SUC-L were added to the bacterial suspension, before incubation at 37°C under stirring (130 rpm). For the control sample only demineralized water was added to the bacterial suspension followed by incubation at 37°C under stirring (130 rpm). Cell enumeration was performed by colony count after 2 h as previously described by Baron *et al.* (2006). The results for cell counts were based on 9 replicates (3 biological replicates, each with 3 technical replicates).

Outer and cytoplasmic membrane permeability measurements

Outer and cytoplasmic membrane permeability was measured using the Lehrer method (Lehrer *et al.*, 1988), modified as described by Derde *et al.* (2013). The *E. coli* ML-35p culture was grown overnight (18 h) in TSB containing 50 μg/mL ampicilline at 37°C under stirring (130 rpm). The bacterial culture was washed twice in 50 mM Tris-HCl buffer pH 7.0 (5000g, 10 min) and diluted to obtain about 10^7 CFU/mL in solutions containing 3.7 g/L DH-L, 0.19 g/L ISO-L, 1.9 g/L NL-L or 1.7 g/L SUC-L.

To test outer membrane permeability, 0.015 mg/mL nitrocefin (substrate of β-lactamase) was added to the sample solutions. When the outer membrane was permeabilized, the periplasmic β-lactamase hydrolyzed nitrocefin into the hydrolysis product of nitrocefin (HP-nitrocefin). HP-nitrocefin absorbance was measured at 486 nm (Multiscan Go, Thermo Fisher Scientific, Illkirch, France), at 37°C under stirring. The maximal slope, which is the maximal velocity of the enzymatic reaction was chosen as the quantitative indicator of membrane permeabilization, since the maximal velocity is directly related to the concentration of accessible enzyme.

To test cytoplasmic membrane permeability, 0.7 mg/mL ONPG (substrate of β-galactosidase) was added to the sample solutions. When the cytoplasmic membrane was permeabilized, the cytoplasmic β-galactosidase hydrolyzed ONPG into ortho-nitrophenol (ONP). ONP absorbance was measured at 420 nm (Multiscan Go, Thermo Fisher Scientific, Illkirch, France),

at 37°C under stirring. The maximal slope was determined similarly to what has been described above for outer membrane permeabilization.

The results of lysozyme activity on membrane permeability were based on 3 replicates.

Detection of β-lactamase and β-galactosidase leakage out of bacterial cells

The method for the detection of β-lactamase and β-galactosidase leakage was based on a method proposed by Derde *et al.* (2013, 2014). allowing the detection of pore formation in the outer and cytoplasmic membrane, respectively. After overnight growth (18 h) in TSB containing 50 μg/mL ampicilline at 37°C under stirring (130 rpm), the *E. coli* ML-35p culture was washed twice with 50 mM Tris-HCl buffer pH 7.0 (5000 g, 10 min) and diluted to obtain 10^7 CFU/mL bacteria suspensions. Lysozyme (3.7 g/L DH-L, 0.19 g/L ISO-L, 1.9 g/L NL-L or 1.7 g/L SUC-L) was added to these suspensions before incubation for 5 h at 37°C under stirring, then centrifugation at 5000 g for 10 min. β-lactamase and β-galactosidase activities were then tested in the supernatants by adding 0.05 g/L nitrocefin and 1 g/L ONPG, respectively. The initial reaction rates of both enzymatic reactions (v_0=ΔAU/min) were determined at 25°C from absorbance curves (Multiskan Go, Thermo Fisher Scientific, Illkirch, France) at 486 nm and 420 nm, respectively. The results were based on 3 replicates.

Measurement of the bacterial membrane potential dissipation

The dissipation of the bacterial membrane potential was measured according to the method proposed by Wu *et al.* (1999). The *E. coli* K12 culture was grown for 3.5 h in TSB at 37°C under stirring (130 rpm) in order to reach a mid-log phase. The culture was washed twice with 5 mM HEPES-buffer at pH 7.2 and containing 5 mM glucose (5000g, 10 min), and then diluted to obtain an absorbance of around 0.06 at 620 nm. One μM $DiSC_3$ and 100 mM KCl were added to the diluted bacteria suspension, before incubation for 1 h at 30°C in the dark. Then, lysozyme (3.7 g/L DH-L, 0.19 g/L ISO-L, 1.9 g/L NL-L or 1.7 g/L SUC-L) was added to the bacteria suspension before incubation for 30 min at 30°C in the dark. Fluorescence was then measured at 670 nm with a fluorimeter Perkin Elmer LS55 (Perkin Elmer, Courtaboeuf, France), after excitation at 622 nm; slit width was 2.5/2.5 and integration time was 6.2 s. The results were based on 6 replicates (2 biological replicates, each with 3 technical replicates).

Lipid monolayers and surface pressure measurements

The experiments were performed in a homemade 8 mL TEFLON® trough. Before each use the trough was thoroughly cleaned with successively warm tap water, ethanol, demineralized water and then boiled for 15 min. The Teflon® trough was then filled with 8 mL HEPES-buffer. The LPS or CMEC were spread with a high precision Hamilton microsyringe at the clean liquid/air interface to obtain an initial surface pressure around 20 mN/m. After 1 h or 15 min of solvent evaporation for LPS or CMEC, respectively, 50 μL of DH-L, ISO-L, NL-L or SUC-L solutions were injected in the subphase with a Hamilton syringe to obtain a final protein concentration of 1.4 mg/L. This concentration has been chosen based on the $\Delta\pi$ *vs* lysozyme subphase concentration plots for LPS/lysozyme and CMEC/lysozyme interactions (data not shown). An example of such a $\Delta\pi$ *vs* protein subphase concentration plot can be found in Figure 4.1. To avoid protein-protein interactions in the bulk solution (aggregation) and to enable the evaluation of lipid-protein interactions, a concentration in the linear zone of $\Delta\pi$ *vs* protein concentration plot is chosen as usually done for monolayer techniques (Figure 4.1). Thus, the proportional concentrations of the isoforms as they are present in the DH-L mixture cannot be used because of the previously explained technical limits. DH-L and its isoforms are then tested at similar concentrations.

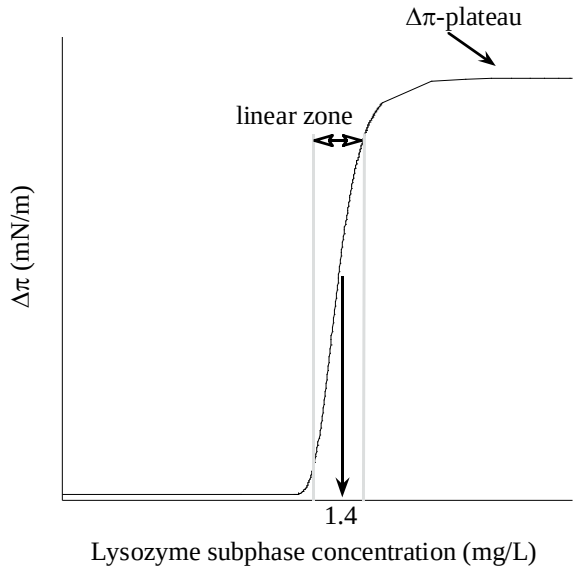

Figure 4.1: Example of a $\Delta\pi$ *vs* protein subphase concentration plot.

The surface pressure was measured following a Wilhelmy method using a 10 mm x 22 mm filter paper as plate (Whatman, Velizy-Villacoublay, France) connected to a microelectronic feedback system (Nima PS4, Manchester, England). The surface pressure (π) was recorded every 4 s with a precision of ± 0.2 mN/m until the equilibrium surface pressure. The results were based on 3 replicates.

Statistical analysis of data

Statistical analysis was performed with R 3.0.3. Data from the normal distribution and with equal variances were treated with parametric tests. In this case, for the comparison of means the ANOVA Tukey multiple comparisons were used. Data from other distributions or with unequal variances were treated with non-parametric tests. In this case, for the comparison of means the Wilcoxon rank sum test was used. Differences described in this manuscript were significant with $p<0.05$.

4.2.3 Results

Purification and characterization of the lysozyme fractions

The limits determined to discriminate between the different lysozyme isoforms when dry-heated lysozyme (DH-L) is analyzed by cation exchange high pressure liquid chromatography (CE-HPLC) have been determined according to Desfougères *et al.* (2011a). Thus, DH-L consists of a mixture of 7% iso-aspartyle lysozyme, 49% native-like lysozyme, and 44% succinimide lysozyme (Figure 4.2). Three lysozyme fractions (ISO-L, NL-L, SUC-L) have been purified from DH-L by cation exchange chromatography on a pilot scale, and using the latter limits. The analysis by CE-HPLC of the collected fractions enabled to estimate their composition as follows: ISO-L consists of 100% iso-aspartyle lysozyme, NL-L consists of 9% iso-aspartyle lysozyme and 91% native-like lysozyme, and SUC-L consists of 7% iso-aspartyle lysozyme, 14% native-like lysozyme and 78% succinimide lysozyme (Figure 4.2).

Growth of *E. coli* K12 in the presence of DH-L and its fractions

To estimate the antimicrobial activity of DH-L and its fractions, *E. coli* K12 growth assays were performed in the presence of the different lysozyme samples. Native lysozyme (N-L) and

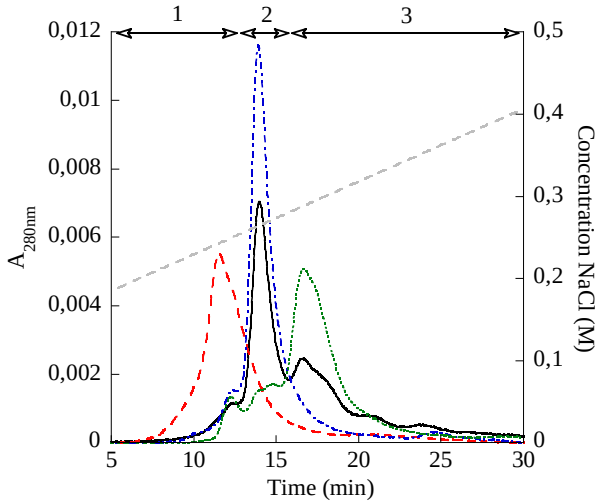

Figure 4.2: Cation exchange HPLC on S-HYPER D10 in 20 mM acetate buffer pH 5.0 of 1 mg/mL DH-L (—), ISO-L (– –), NL-L (- - -) and SUC-L (· · ·). Iso-aspartyle lysozyme, native-like lysozyme and succinimide lysozymes are indicated with 1, 2, and 3, respectively.

DH-L were tested at 3.7 g/L, the natural concentration of lysozyme in hen egg white. In order to mimic the relative proportions of isoforms originally determined in DH-L, the fractions were tested at 0.19 g/L, 1.9 g/L and 1.7 g/L for ISO-L, NL-L and SUC-L, respectively, i.e. 5%, 50% and 45% of 3.7 g/L.

The control sample, without addition of lysozyme, and ISO-L fraction enable *E. coli* growth resulting in respectively +1.3 log CFU/mL and +0.5 log CFU/mL after 2 h incubation (Figure 4.3). On the contrary, DH-L and SUC-L induce a population decrease after 2 h incubation, resulting in -1.0 log CFU/mL and -0.6 log CFU/mL, respectively (Figure 4.3). DH-L is thus the most efficient lysozyme sample for *E. coli* destruction. The slight population decrease observed with NL-L (-0.3 log CFU/mL) does not significantly differ from that observed with N-L (-0.2 log CFU/mL) after 2 h incubation (Figure 4.3).

Membrane state of *E. coli* ML-35p in the presence of DH-L and its fractions

E. coli ML-35p is an *E. coli* mutant allowing the detection of the outer and cytoplasmic membrane permeabilization by enzymatic reactions of β-lactamase and β-galactosidase, respectively. The absorbance of the enzymatic reaction products is measured in time by spectrophotometry at 486 nm and 420 nm for the outer and cytoplasmic membranes, respectively. The maximal slope of the absorbance *vs* time plot directly relates to the overall permeabilization of the bacterial cell membranes as described by Derde *et al.* (2013). However, this enzymatic reaction can take place either only inside the cell by diffusion of the reactants from outside, or inside and outside the cell if the reactants and the enzymes diffuse through the cell membranes. In order to distinguish between these two possible situations, the amount of enzyme leakage has been evaluated as described by Derde *et al.* (2013). The externalized enzyme activity is related to the amount and to the size of pores formed into the bacterial membrane.

DH-L and the fractions ISO-L, NL-L and SUC-L induce an overall permeabilization of the outer membrane of *E. coli*, as evidenced by the overall β-lactamase activity (Figure 4.4A). It is noticeable that all the fractions permeabilize the outer membrane more severely than DH-L, and that SUC-L is the more efficient fraction (Figure 4.4A). Oppositely, the measurement of externalized β-lactamase activity highlights that DH-L is more efficient than each fraction

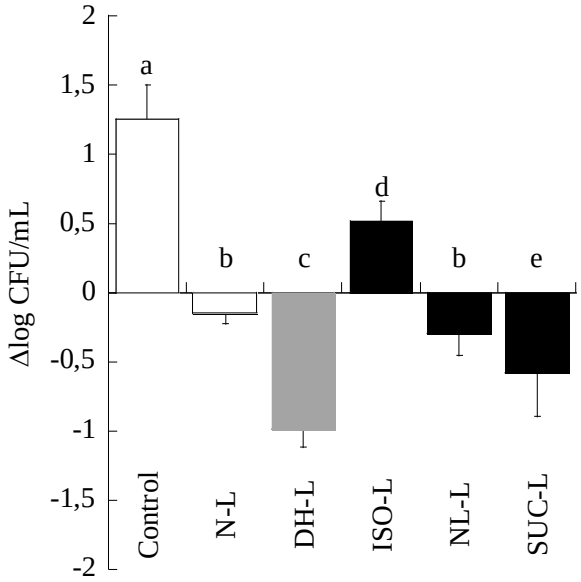

Figure 4.3: *E. coli* K12 growth or destruction after 2 h incubation at 37°C in the absence (control sample) and the presence of 3.7 g/L N-L, 3.7 g/L DH-L, 0.19 g/L ISO-L, 1.9 g/L NL-L and 1.7 g/L SUC-L. Different letters indicate significant difference obtained from the ANOVA analysis combined with Tukey multiple comparisons (n=9, $p < 0.05$).

separately to release the enzyme out of the bacteria cells (Figure 4.4B).

The overall permeabilization of the *E. coli* cytoplasmic membrane induced by DH-L is more severe than that induced by the fractions, as evidenced by β-galactosidase activity (Figure 4.5A). NL-L is proved to be the less efficient fraction according to this criterion. It should be noticed that no externalized β-galactosidase activity could be detected for DH-L or its fractions (data not shown).

The cytoplasmic membrane state was also investigated by the measurement of membrane potential dissipation. It shows that DH-L disturbs the membrane potential more strongly than all the fractions, and that ISO-L induces the lowest disturbance compared to the other fractions (Figure 4.5B).

Interaction of DH-L and its fractions with outer and cytoplasmic membrane models

To investigate the molecular interactions of DH-L and each of its fractions with the *E. coli* membrane lipids, monolayer models were used. To mimic the *E. coli* outer membrane, these lipid monolayers were composed of lipopolysaccharides (LPS) extracted from *E. coli* K12. To mimic the *E. coli* cytoplasmic membrane, the lipid monolayers consisted of a phospholipid mixture with a lipid composition based on the analysis of *E. coli* cytoplasmic membrane (CMEC) performed by Lugtenberg & Peters (1976). The lipids were spread at the buffer surface until a lateral surface pressure of 20 mN/m was reached. This initial surface pressure was chosen based on similar experiments performed by Zhang *et al.* (2000a), Gidalevitz *et al.* (2003) and Coccia *et al.* (2011).

An increase of the surface pressure ($\Delta\pi = \pi_{\text{equilibrium}} - \pi_{\text{initial}}$) after lysozyme injection into the subphase indicates that lysozyme inserts into the lipid monolayer. The lysozyme concentration used for these experiments was 1.4 mg/L whatever the protein sample, for technical

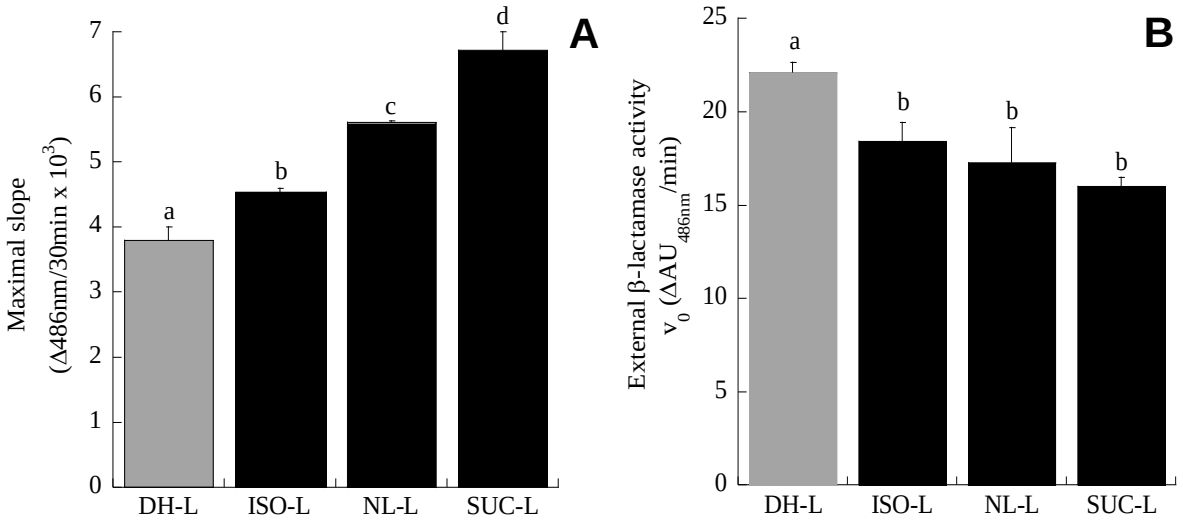

Figure 4.4: Permeabilization of the *E. coli* ML-35p outer membrane by 3.7 g/L DH-L, 0.19 g/L ISO-L, 1.9 g/L NL-L or 1.7 g/L SUC-L as evidenced by the overall (A) and externalized (B) β-lactamase activity. Different letters indicate significant difference obtained from the ANOVA analysis combined with Tukey multiple comparisons (n=3, $p < 0.05$).

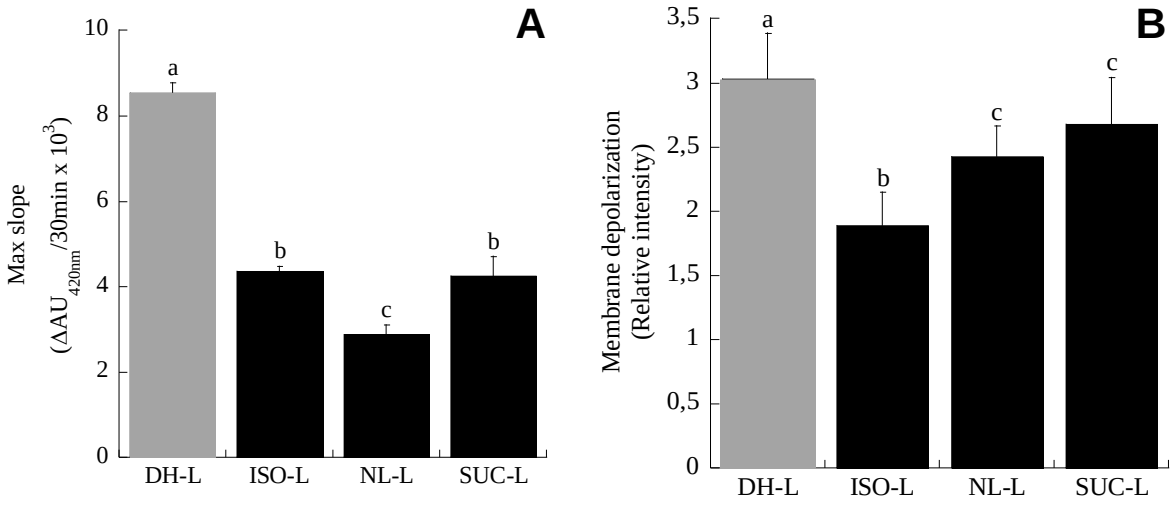

Figure 4.5: Permeabilization of the *E. coli* ML-35p cytoplasmic membrane as evidenced by the β-galactosidase activity (A) and dissipation of the membrane potential of *E. coli* K12 (B) induced by 3.7 g/L DH-L, 0.19 g/L ISO-L, 1.9 g/L NL-L or 1.7 g/L SUC-L. Different letters indicate significant difference obtained from the ANOVA analysis combined with Tukey multiple comparisons (n=3, $p < 0.05$).

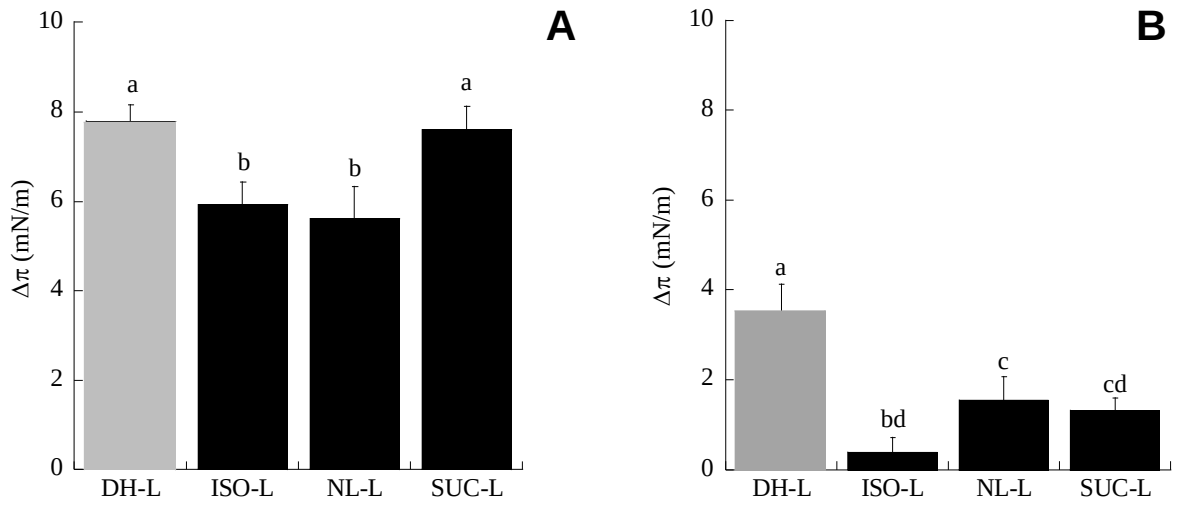

Figure 4.6: Overpressure ($\Delta\pi$) induced by insertion of DH-L or its fractions into a LPS monolayer (A) and into a CMEC monolayer (B) after a subphase injection of 1.4 mg/L lysozyme. The initial surface pressure $\pi_i initial$ was 20 mN/m for both monolayers. Different letters indicate significant difference obtained from the ANOVA analysis combined with Tukey multiple comparisons (n=3, $p < 0.05$).

reasons explained in the material and methods section.

The surface pressure increase after DH-L injection indicates that DH-L inserts into the LPS monolayer and a monolayer of an *E. coli* cytoplasmic phospholipid mixture (CMEC). Moreover, DH-L inserts more efficiently into both the LPS (Figure 4.6A) and CMEC (Figure 4.6B) monolayers compared to all the fractions, except SUC-L that is as efficient as DH-L in LPS monolayer. Among the fractions, SUC-L induces higher $\Delta\pi$ values than NL-L and ISO-L in LPS monolayer (Figure 4.6A), whereas NL-L and SUC-L are equivalent in CMEC monolayer (Figure 4.6B).

The rate constants of adsorption k_{ads} ($M^{-1} \cdot s^{-1}$) of lysozyme solutions at the air/liquid interface, the LPS/liquid interface, and the CMEC/liquid interface have been evaluated by fitting the Langmuir equation (4.1 and 4.2) for adsorption to the surface pressure measurements. The rate constants of desorption k_{des} ($M^{-1} \cdot s^{-1}$) can be considered negligible for the DH-L fractions when estimating that their interfacial behavior is comparable to DH-L for which desorption is negligible (data not shown).

$$\pi(t) = \pi_{final} \cdot (1 - exp(-\sigma \cdot t)) \tag{4.1}$$

$$\sigma = k_{ads} \cdot c + k_{des} \tag{4.2}$$

The k_{ads} values are systematically lower (or equivalent) at the air/liquid interface as compared to LPS/liquid and CMEC/liquid interfaces (Table 4.1). Thus, whatever the sample, lysozyme adsorption is slower at the air/liquid interface, suggesting lysozyme has higher affinities for the LPS and CMEC monolayers. Moreover, it is noticeable that significantly higher values of k_{ads} are measured at the CMEC/liquid interface, as compared to the LPS/liquid interface. At last, significantly different adsorption rates at the CMEC monolayer are observed between the fractions: ISO-L adsorbs much more quickly than SUC-L, whereas DH-L and NL-L are the slowest fractions for adsorption at the CMEC monolayer (Table 4.1). On the contrary, the adsorption rates at the LPS monolayer were not significantly different for DH-L, ISO-L, and SUC-L, whereas a slightly higher value is obtained for NL-L.

Table 4.1: Rate constants of adsorption (k_{ads}) at the air, LPS monolayer and CMEC monolayer interfaces determined from surface pressure measurements performed after injection in the subphase of 1.4 mg/L N-L, DH-L, ISO-L, NL-L and SUC-L.

	k_{ads} (10^3 $M^{-1} \cdot s^{-1}$)			
	DH-L	ISO-L	NL-L	SUC-L
air/liquid	0.8±0.2	0.9 ±0.1	0.5±0.1	1.3 ±0.3
LPS/liquid	1.3±0.1	1.5 ±0.0	2.3±0.4	1.4 ±0.4
CMEC/liquid	5.5±0.3	30.0±0.3	5.0±0.4	11.6±0.4

4.2.4 Discussion

The enhanced effect of DH-L compared to N-L on the *E. coli* outer and cytoplasmic membranes was previously established by Derde *et al.* (2014). DH-L creates pores in the outer membrane, and strongly affects the cytoplasmic membrane as evidenced by an increased permeability and membrane potential dissipation. It can be assumed that it results from the modified physicochemical properties of DH-L compared to N-L. However, DH-L is actually a mixture of different isoforms: isoaspartyle lysozyme, native-like lysozyme, and succinimide lysozyme, each exhibiting specific physicochemical properties (Desfougères *et al.*, 2011a). Thus, the question arises of the relative involvement of each isoform in the increased antibacterial activity of DH-L. To answer this question, the here presented study aimed to evaluate the antimicrobial and membrane activity of each lysozyme isoform induced by dry-heating. Further, these isoforms were also compared to DH-L.

The positive charge, flexibility and hydrophobicity of lysozyme isoforms are key parameters for *E. coli* membrane disruption

At a physiological pH, the three lysozyme isoforms are positively charged. Then, positive charge of proteins and peptides is reported as an important prerequisite for interaction with bacterial membranes, and eventually for antimicrobial activity (Melo *et al.*, 2009; Nguyen *et al.*, 2011). But ISO-L, NL-L and SUC-L differ in pI as shown by cation exchange chromatography (Figure 4.2). And it is noticeable that SUC-L, which has the highest positive charge at neutral pH, exhibits the highest outer membrane activity *in vivo* (Figure 4.4A) and *in vitro*, (Figure 4.6A). SUC-L also permeabilizes more efficiently the cytoplasmic membrane compared to the NL-L fraction (Figure 4.5A), and SUC-L adsorbs more rapidly at the CMEC monolayer (Table 4.1), even though insertion into the CMEC monolayer is similar for both fractions (Figure 4.6B). The attraction of the highly positively charged SUC-L for the negatively charged cytoplasmic membrane could be responsible for the more rapid adsorption to the membrane surface and the higher permeabilization. Thus, the positive charge of SUC-L could be related to the higher efficiency of this fraction for membrane disruption, and then for bacteria destruction since severe membrane disruption can lead to bacterial cell death (Matsuzaki *et al.*, 1997; Wu *et al.*, 1999). Indeed, bacteria counts after 2 h incubation highlight that the higher population decrease is obtained with the highest positively charged fraction (SUC-L), whereas a slight population decrease is obtained with the lower positively charged NL-L fraction (Figure 4.3). Moreover, NL-L and N-L fractions, equally charged as evidenced by their simultaneous elution in cation exchange chromatography (data not shown, Desfougères *et al.* (2011b)), exhibit equivalent antimicrobial activity (Figure 4.3). The antimicrobial activity of the lysozyme fractions appears thus correlated with the charge of the main component of each fraction: the higher the pI, the higher the antimicrobial activity.

Additionally, the lysozyme isoforms not only differ in pI, but also in hydrophobicity and flexibility as previously demonstrated by Desfougères (2009). SUC-L is the most positively

charged molecule, but also the most hydrophobic and flexible one. It is thus conceivable that the increased flexibility favors the conformational changes necessary for membrane-protein interactions (Jenssen *et al.*, 2006). Moreover, the increased hydrophobicity could favor the insertion in a hydrophobic environment such as the lipid chains.

Similarly, despite a lower positive charge and at lower concentration, ISO-L is as efficient as SUC-L considering cytoplasmic membrane permeabilization (Figure 4.5A). Moreover, ISO-L has the highest adsorption rate onto the negative CMEC monolayer (Table 4.1), whereas it is the less basic isoform. It could be assumed that besides electrostatic attraction, diffusion kinetics can play a role. Protein diffusion is dependent on the friction coefficient determined by the protein size and shape (Erickson, 2009). Since iso-aspartyle isoforms are more rigid than succinimides (data not shown), it is thus imaginable that iso-aspartyle lysozyme is a more compact protein than succinimide lysozyme; then, ISO-L would diffuse more quickly to the cytoplasmic membrane despite slightly lower electrostatic attractions.

Strikingly, it should be noticed that despite the high rate of adsorption of ISO-L onto CMEC monolayer (Table 4.1), this fraction poorly inserts between the CMEC lipids (Figure 4.6B). ISO-L is thus adsorbing onto the lipid monolayer, but remains beneath the latter. It can be assumed that the rigidity of ISO-L does not allow the needed structural modifications for insertion between the phospholipids. However, ISO-L is able to permeabilize the cytoplasmic membrane, even at low concentrations (Figure 4.5A). Protein insertion is thus not a prerequisite for membrane permeabilization. ISO-L adsorption onto the cytoplasmic membrane could induce lipid clustering leading to membrane permeabilization, similarly to what has been already described for magainin analogs and arginine-rich peptides by Epand & Epand (2011).

These results emphasize the complexity of the phenomena leading to the interaction between lysozyme and bacterial membranes. But clearly, slight physicochemical differences such as those discriminating iso-aspartyle, native-like and succinimide lysozymes suffice to induce different interactions with bacterial membranes.

Antimicrobial activity of DH-L results from the complementarity between the lysozyme isoforms

Bacteria counts after 2 h incubation in the presence of lysozyme show that DH-L has a higher antimicrobial effect on *E. coli* than each fraction (Figure 4.3). This result demonstrates that the DH-L effect on *E. coli* cells is not due to one single isoform. Actually, DH-L is an efficient mixture of complementary isoforms.

The cooperation of the DH-L isoforms is also observed when evaluating the DH-L effect on the *E. coli* membranes. Both DH-L and the isoforms disrupt the outer and cytoplasmic membranes of *E. coli*, with and without pore formation, respectively. When comparing the effect of DH-L and its fractions on the outer membrane, it can be noticed that DH-L causes a higher externalization of β-lactamase than its fractions (Figure 4.4B). This result proves that DH-L disrupts the outer membrane in such a way that β-lactamase, an enzyme of 28.9 kDa, can leak out of the periplasm in a larger extent than that induced by each fraction. On the contrary, the 3 fractions cause a higher overall permeabilization of the outer membrane without enzyme leakage (Figures 4.4A and 4.4B). In other words, the 3 fractions induce a higher porosity than DH-L, but the created pores must be too small to enable enzyme diffusion. Hence, the 3 fractions form a high number of small pores compared to DH-L which would form a small number of larger pores. Despite a lower overall permeabilization due to DH-L compared to the fractions, the bacterial population decrease (Figure 4.3) is more severe

with DH-L, suggesting that damages caused by few large pores are more deleterious for the bacteria than multiple small pores.

Similarly, the cytoplasmic membrane is more severely disrupted by DH-L compared to its isolated fractions as shown by β-galactosidase activity and membrane potential measurements (Figures 4.5A and 4.5B). It is noticeable that, opposite to outer membrane perforation, no pore formation into the cytoplasmic membrane by DH-L or its fractions has been detected. Thus, the *in vivo* experiments suggest that the combination of lysozyme isoforms is needed to obtain an efficient outer and cytoplasmic membrane disruption. To confirm this hypothesis of cooperation between the different lysozyme isoforms, monolayer models for the outer and cytoplasmic membranes have been used. These membrane models, with similar lipid compositions as the bacterial membranes, give us a higher understanding of the molecular interaction mechanism between lysozyme and bacterial membranes.

It can be established that DH-L and each fraction insert into each monolayer model. At equal concentration (1.4 mg/L), DH-L inserts more or equally than each fraction in monolayers, whatever the monolayer nature (Figure 4.6). It should be noticed that each isoform consists only of 5 to 50% of the DH-L mixture. The $\Delta\pi$-values corresponding to each fraction would thus be lower than those here measured if tested at the concentrations representative of those originally found in DH-L. In other words, the $\Delta\pi$-values measured for ISO-L, NL-L and SUC-L fractions (Figure 4.6) are overestimated as compared to the $\Delta\pi$-value induced by DH-L mixture. Thus, DH-L insertion into LPS and CMEC monolayers clearly results from cooperation between the different lysozyme isoforms. This cooperative effect of the isoforms is the most pronounced for the CMEC monolayer. This can be due to the differences in k_{ads} for each isoform fraction. Clearly, ISO-L, with the highest k_{ads}, would adsorb first onto the CMEC monolayer (Table 4.1). This adsorption of iso-aspartyle lysozyme onto the CMEC monolayer could modify the membrane in such a way that the adsorption and insertion of native-like and succinimide lysozymes is facilitated. This phenomenon could then result in the cooperative effect highlighted in the DH-L mixture.

Finally, both *in vivo* and *in vitro* experiments indicate a complementary effect between the lysozyme isoforms, which explains the higher efficiency of DH-L on *E. coli* cells.

4.3 Conclusions

Cette étude suggère que la charge nette positive est un facteur clé pour l'interaction entre les isoformes du lysozyme chauffé à sec et les membranes bactériennes, tant *in vivo* qu'*in vitro*. Cependant, l'hydrophobie et la flexibilité moléculaire sont des caractéristiques physicochimiques qui ne doivent pas être négligées. Ainsi, les formes succinimides, qui sont les plus chargées positivement, mais aussi les plus hydrophobes et les plus flexibles, expriment la plus forte activité antimicrobienne vis-à-vis d'*E. coli*, et induisent les plus fortes perturbations de l'intégrité membranaire. Toutefois, les interactions entre protéines et membranes bactériennes sont des phénomènes complexes que les différences de propriétés physicochimiques ne permettent pas toujours d'expliquer. Ainsi, les formes iso-aspartate du lysozyme adoptent des comportements particuliers aux interfaces modèles étudiées ici, qu'il ne nous a pas été possible d'expliquer totalement.

L'un des résultats marquants de cette étude est que les différences de comportement observées entre les isoformes du lysozyme semblent complémentaires, conférant au mélange qu'est le lysozyme chauffé à sec une activité antimicrobienne supérieure à celle de chacune des isoformes prise isolément. Les perturbations membranaires induites par le lysozyme chauffé sont en effet globalement plus sévères que celles induites par chaque isoforme individuellement.

On peut émettre l'hypothèse que l'interaction initiale entre l'une des isoformes et les membranes change les propriétés de cette dernière, facilitant alors l'insertion des autres isoformes et augmentant l'ampleur des perturbations membranaires. Les dégâts causés par le mélange des isoformes deviendraient alors difficilement surmontables par la bactérie, conduisant à la mort bactérienne.

En Bref

- La charge nette positive est un facteur déterminant pour l'interaction entre le lysozyme et les membranes bactériennes.
- L'hydrophobie et la flexibilité moléculaire joueraient également des rôles importants pour l'interaction avec les membranes ; elles favoriseraient l'insertion entre les chaînes aliphatiques des lipides membranaire.
- Le lysozyme chauffé à sec est un mélange d'isoformes agissant de manière complémentaire sur les membranes d'*E. coli* ; ces effets coopératifs expliqueraient l'activité antimicrobienne supérieure du lysozyme chauffé par rapport aux isoformes considérées individuellement.

Conclusions générales et perspectives

De très nombreux peptides et protéines antimicrobiens ont été étudiés au cours de ces dernières années dans le but de développer de nouvelles molécules antimicrobiennes pour des applications pharmaceutiques et/ou agro-alimentaires. Mais finalement, les molécules arrivant jusqu'au stade de la commercialisation sont très peu nombreuses, en raison du coût de leur synthèse, de la perte d'activité après digestion gastro-intestinale et/ou de leur toxicité pour les cellules eucaryotes. Parmi les différentes molécules étudiées, le lysozyme extrait d'œuf de poule présente l'avantage d'être disponible à l'échelle industrielle, et ce à un coût modéré, ce qui en fait une « base » potentiellement intéressante pour le développement de formes protéiques ou peptidiques antimicrobiennes. Son activité enzymatique a largement été étudiée depuis sa découverte et explique son effet antimicrobien vis-à-vis des bactéries à coloration de Gram positive. Mais le lysozyme est également actif contre les bactéries à coloration de Gram négative. Le mécanisme d'action est supposé être une perte d'intégrité membranaire et/ou une inhibition de la synthèse d'ARN/ADN. Jusqu'à présent les interactions lysozyme-membranes bactériennes n'étaient pas confirmées et le mécanisme d'action était peu connu.

En confrontant les résultats obtenus *in vivo* et *in vitro*, le travail rapporté dans ce manuscrit montre la perméabilisation des membranes externe et cytoplasmique d'*Escherichia coli* par le lysozyme d'œuf de poule. Cette perméabilisation est la conséquence d'un processus faisant intervenir plusieurs étapes. L'adsorption et l'insertion du lysozyme sur la membrane externe seraient tout d'abord à l'origine de la formation de pores dans cette membrane. Grâce à ces pores, le lysozyme accéderait ensuite à l'espace périplasmique où il hydrolyserait le peptidoglycane ; en raison de la taille des mailles du peptidoglycane chez *E. coli*, la simple diffusion du lysozyme au travers de la couche de peptidoglycane est également envisageable. Le lysozyme parviendrait alors jusqu'à la membrane cytoplasmique sur laquelle il s'adsorberait, provoquant sa perméabilisation. Cette perméabilisation résulterait de la formation de canaux ioniques dont l'une des conséquences est la perturbation du potentiel membranaire de la cellule.

Pour perméabiliser les membranes bactériennes, le lysozyme doit interagir avec les lipopolysaccharides (LPS) et les phospholipides (PL) qui constituent ces membranes. Les études réalisées sur monocouches lipidiques en tant que modèles des membranes bactériennes, et dont les résultats sont présentés dans ce document, ont permis de progresser dans la compréhension des mécanismes d'interaction entre le lysozyme et les lipides membranaires, et par là même dans la compréhension du phénomène de perturbation membranaire par le lysozyme.

La première barrière que le lysozyme rencontre *in vivo* est la membrane externe et plus précisément son feuillet externe, constitué de LPS. Or, nous avons pu mettre en évidence l'adsorption du lysozyme sur une monocouche de LPS, après quoi la protéine est capable de s'insérer profondément entre les lipides A qui constituent la partie hydrophobe des molécules de LPS. L'insertion du lysozyme entraîne alors une réorganisation de la monocouche qui pourrait être l'étape préliminaire à l'origine de la formation des pores. Étonnamment, l'insertion du lysozyme entre les lipides A des LPS nécessite la présence des chaînes polysaccharidiques des LPS.

Une fois la barrière de la membrane externe franchie, et le peptidoglycane hydrolysé et/ou traversé, le lysozyme peut accéder à la membrane cytoplasmique. De même qu'avec la monocouche mimant la membrane externe d'*E. coli*, il s'est avéré que le lysozyme s'adsorbe également sur une monocouche phospholipidique de composition semblable à celle de la membrane cytoplasmique d'*E. coli*. Les concentrations minimales en lysozyme nécessaires pour l'insertion dans la monocouche de PL sont cependant supérieures à celles nécessaires pour l'insertion dans la monocouche de LPS ; la capacité d'insertion est également moindre, ce qui est cohérent avec les résultats observés *in vivo* : des pores sont formés dans la membrane externe, ce qui n'est pas le cas dans la membrane cytoplasmique. L'adsorption et l'insertion du

lysozyme ont finalement pour conséquence la réorganisation de la monocouche phospholipidique. Des clusters protéine-lipides sont formés, créant des zones de moindre densité en lipides qui pourraient favoriser la formation de canaux ioniques non-spécifiques comme observés *in vivo*. Par ailleurs, l'adsorption du lysozyme pourrait expliquer la perturbation du potentiel membranaire observée *in vivo*. Le potentiel membranaire est en effet le résultat d'un équilibre de charges transversal à la membrane, et l'adsorption d'une protéine chargée positivement peut donc perturber cet équilibre.

Malgré ces nombreuses perturbations de l'intégrité membranaire, il convient de remarquer qu'il n'en résulte qu'un simple retard de croissance lorsqu'on se place à l'échelle de la population bactérienne. L'activité antimicrobienne du lysozyme vis-à-vis d' *E. coli* peut donc être qualifiée de modeste, malgré l'ampleur des modifications induites par la protéine sur les membranes. Existe-t-il un mécanisme de résistance aux attaques membranaires du lysozyme chez cette espèce bactérienne ? Une approche génomique pourrait peut-être permettre de répondre à cette question.

La modification des propriétés physicochimiques du lysozyme pour augmenter son activité antimicrobienne a été proposée par plusieurs auteurs ; des procédés variés ont été testés. Nous avons voulu pour notre part explorer les possibilités offertes par le chauffage à sec (7 jours, 80°C). Ce procédé, très simple à mettre en oeuvre, induit en effet des modifications physicochimiques potentiellement favorables à un accroissement de l'activité antimicrobienne du lysozyme. Et effectivement, nous avons pu montrer que le lysozyme chauffé à sec induit à forte concentration (3.7 g/L), non plus un simple retard de croissance comme le lysozyme natif, mais une diminution de la population d'*Escherichia coli*.

Parallèlement, l'aptitude du lysozyme à perturber les membranes externe et cytoplasmique de la bactérie se trouve accrue par le chauffage à sec. Le lysozyme chauffé est à l'origine d'un plus grand nombre de pores dans la membrane externe que le lysozyme natif, et/ou à l'origine de pores de plus grand diamètre. De plus, les fuites de potassium cytosolique et les perturbations du potentiel membranaire sont de plus grande ampleur en présence du lysozyme chauffé. Cependant, comme le lysozyme natif, le lysozyme chauffé ne crée pas de pores dans la membrane cytoplasmique ; seuls des canaux ioniques seraient formés.

Ces résultats *in vivo* ont été confortés par l'étude des interactions du lysozyme chauffé avec les membranes modèles. Le lysozyme chauffé s'adsorbe et s'insère dans la monocouche LPS de manière similaire au lysozyme natif. En revanche, dès 0.05 μM de lysozyme en solution, la pression latérale créée par l'insertion du lysozyme chauffé dans la monocouche de LPS est plus élevée que celle créée par le lysozyme natif. Ce résultat indique soit qu'un plus grand nombre de molécules de lysozyme chauffé s'insèrent dans l'interface lipidique, soit que ces molécules se déploient plus amplement à l'interface, ce qui serait cohérent avec leur plus grande flexibilité par rapport au lysozyme natif. L'affinité du lysozyme chauffé pour la monocouche de LPS est également plus élevée que celle du lysozyme natif. Les interactions entre le lysozyme et les LPS, plus fortes dans le cas du lysozyme chauffé, entrainent une réorganisation sévère de la monocouche de LPS et des agrégats lysozyme chauffé-LPS sont observés à l'interface. Ces modifications de grande ampleur pourraient constituer l'étape préliminaire de la formation des pores de grand diamètre suggérée *in vivo* dans ces conditions.

Par ailleurs, le lysozyme chauffé s'adsorbe et s'insère dans une monocouche phospholipidique à des concentrations plus faibles que le lysozyme natif. Et de nouveau, la pression latérale résultante est plus élevée qu'avec le lysozyme natif. La plus forte densité de charges positives du lysozyme chauffé par rapport à la forme native ainsi que sa plus grande flexibilité pourraient expliquer ces différences. Les interactions entre le lysozyme chauffé et une

monocouche de PL provoquent des modifications du compacité des lipides (« lipid packing ») et la formation de clusters. La composition de ces clusters est incertaine mais pourrait être le résultat d'un recrutement de lipides anioniques (PG et CL) autour de la protéine chargée positivement. Ce phénomène est fort probablement à la base des perturbations de la membrane cytoplasmique. Les techniques RMN pourraient être mises en œuvre pour confirmer (ou infirmer) l'existence de ces clusters et leur composition.

L'interaction du lysozyme avec les PL doit idéalement être sélective, c'est-à-dire limitée aux PL bactériens. L'interaction avec les PL de la membrane cytoplasmique des cellules de mammifères empêcherait en effet l'utilisation de la molécule pour des applications pharmaceutiques. Nos travaux ont permis de montrer que le lysozyme, qu'il soit natif ou chauffé à sec, n'interagit pas avec une monocouche modèle de la membrane des cellules eucaryotes. Toutefois, des études complémentaires sur des modèles plus complexes et dans des situations *in vivo* seront nécessaires pour confirmer ces premiers résultats encourageants.

Les résultats mentionnés ci-dessus ont été obtenus avec le lysozyme chauffé utilisé dans son intégralité. Or, le lysozyme chauffé est en réalité un mélange d'isoformes aux propriétés physicochimiques distinctes. La question de la spécificité éventuelle des interactions entre chacune de ces isoformes et les membranes bactériennes s'est donc posée. Indirectement, l'étude de ces isoformes prises isolément pouvait également permettre d'identifier les propriétés physicochimiques indispensables pour l'activité antimembranaire du lysozyme. Nos travaux ont permis de souligner l'importance du caractère basique de la protéine pour l'interaction avec les membranes. Cependant, ce critère ne peut expliquer à lui seul les différences de comportement observées entre les isoformes ; l'hydrophobie et la flexibilité moléculaire pourraient également intervenir. Ainsi, l'isoforme la plus basique, la plus hydrophobe et la plus flexible (lysozyme succinimidé) est non seulement la plus active sur les membranes bactériennes *in vivo* et *in vitro*, mais elle montre également l'activité antimicrobienne la plus forte. Cependant, elle n'est pas seule responsable de l'activité accrue du lysozyme chauffé. En effet, le lysozyme chauffé s'est avéré être un mélange efficace associant les activités complémentaires des différentes isoformes. L'interaction de certaines isoformes avec les membranes modifie probablement ces dernières de telle façon que les autres isoformes interagissent ensuite plus efficacement avec les membranes, aboutissant à des effets plus drastiques quand les isoformes sont en mélange. Ces observations invitent à rechercher des ratios d'isoformes différents de ceux naturellement trouvés dans le lysozyme chauffé à sec . Existe-t-il un mélange optimal, différent de celui testé ici ?

Malgré les avancées réalisées grâce à cette étude pour comprendre le mécanisme d'action du lysozyme sur les membranes bactériennes, de très nombreuses questions demeurent. Certaines d'entre elles sont présentées ci-dessous. Qu'elles soient de nature purement cognitive, ou avec des applications potentielles, toutes doivent contribuer à accroître notre connaissance de cette protéine antimicrobienne, parmi les plus étudiées des protéines, et pourtant encore si incomplètement « comprise » dans ses multiples activités biologiques.

Quels sont les changements de conformation du lysozyme à l'interface lipidique ? Existent-ils ? Quelles sont les parties de la protéine qui s'insèrent entre les lipides membranaires ? La spectrométrie infrarouge de surface (PM-IRRAS) pourrait sans doute fournir des informations sur l'organisation lipidique et la conformation de la protéine après son insertion.

Comment la protéine se positionne-t-elle à l'interface lipidique ? Des zones spécifiques d'adsorption protéique existent-elles ? Des images obtenues par spectrométrie de masse à ionisation secondaire à l'échelle nano (nano-SIMS) ont été réalisées dans l'objectif de répondre à cette question. En permettant l'identification de différents éléments de la table périodique simul-

tanément en surface et en profondeur d'un film protéines-lipides, cet outil devrait permettre de localiser verticalement les protéines à l'échelle nanométrique. Couplées aux données issues des observations AFM, ces analyses permettraient de confirmer ou d'infirmer certaines des hypothèses émises ici. Des travaux sont actuellement en cours pour interpréter les données acquises en nano-SIMS sur nos échantillons.

Afin de se rapprocher des systèmes biologiques réels, il conviendrait de tester le lysozyme et ses formes modifiées sur des bicouches membranaires, afin notamment d'évaluer les interactions du lysozyme avec les membranes en présence du deuxième feuillet. L'utilisation de sondes fluorophores spécifiques pourrait permettre d'évaluer la présence du lysozyme au cœur de la bicouche lipidique le cas échéant. Des observations par AFM de ces bicouches lipidiques pourraient éventuellement permettre de visualiser la formation des pores dans le système modèle.

Nos résultats conduisent à la conclusion que le lysozyme n'est pas capable de traverser la membrane cytoplasmique. Si tel est bien le cas, et donc si le lysozyme n'est pas capable d'atteindre le cytoplasme, comment cette protéine peut-elle inhiber la synthèse d'ARN/ADN comme suggéré par certains auteurs ? Le lysozyme modifie-t-il la membrane cytoplasmique ou interagit-t-il avec une protéine membranaire de telle manière qu'une réaction en cascade serait activée, avec un effet ultime sur la synthèse d'ARN/ADN ?

La composition lipidique étant très dépendante de l'espèce bactérienne considérée, les résultats obtenus au cours de nos travaux incitent à explorer l'effet du lysozyme, natif comme chauffé, sur d'autres espèces à coloration de Gram négative. La comparaison de la structure des lipopolysaccharides et de la composition phospholipidique des membranes des bactéries sensibles au lysozyme pourrait alors donner des informations utiles pour la compréhension du mécanisme d'interaction entre le lysozyme et les membranes.

En plus, l'activation d'autolysines et la perturbation membranaire sont suggérées comme mécanismes non-enzymatiques chez certaines bactéries à coloration de Gram positive. Comme la composition membranaire des bactéries à coloration de Gram positive est très différente de celle des bactéries à coloration de Gram négative et que la paroi membranaire n'est pas structurée de la même manière, des études supplémentaires sont nécessaires pour comprendre l'interaction du lysozyme avec ce type de membranes.

Enfin, le lysozyme chauffé et ses isoformes étant plus efficaces contre *E. coli* que le lysozyme natif, il pourrait être intéressant d'utiliser ces formes modifiées du lysozyme pour produire, par protéolyse, des peptides dont l'activité antimicrobienne pourrait être encore supérieure à celle de certains peptides issus du lysozyme natif. En particulier, en raison des résidus d'acides aminés modifiés chimiquement dans les formes iso-aspartyles et succinimides, ces formes pourraient permettre de préparer des peptides significativement différents, d'un point de vue physicochimique, des peptides du lysozyme natif. Ces différences seraient-elles favorables à l'accroissement des propriétés antibactériennes ?

Bibliographie

Abdou A., Higashiguchi S., Aboueleinin A., Kim M. & Ibrahim H. (2007). Antimicrobial peptides derived from hen egg lysozyme with inhibitory effect against *Bacillus* species. *Food Control*, 18(2) :173–178.

Abergel C., Monchois V., Byrne D., Chenivesse S., Lembo F., Lazzaroni J. & Claverie J. (2007). Structure and evolution of the Ivy protein family, unexpected lysozyme inhibitors in Gram-negative bacteria. *Proc. Natl. Acad. Sc. U.S.A.*, 104(15) :6394–6399.

Al Kayal T., Nappini S., Russo E., Berti D., Bucciantini M., Stefani M. & Baglioni P. (2012). Lysozyme interaction with negatively charged lipid bilayers : protein aggregation and membrane fusion. *Soft Matter*, 8(16) :4524–4534.

Alderton G., Ward W. & Fevold H. (1945). Isolation of lysozyme from egg white. *J. Biol. Chem.*, 157(1) :43–58.

Amiri S., Ramezani R. & Aminlari M. (2008). Antibacterial activity of dextran-conjugated lysozyme against *Escherichia coli* and *Staphylococcus aureus* in cheese curd. *J. Food Prot.*, 71(2) :411–415.

Araki Y., Nakatani T., Nakayama K. & Ito E. (1972). Occurrence of N-nonsubstituted glucosamine residues in peptidoglycan of lysozyme-resistant cell walls from *Bacillus cereus*. *J. Biol. Chem.*, 247(19) :6312–6322.

Arima H., Ibrahim H., Kinoshita T. & Kato A. (1997). Bactericidal action of lysozymes attached with various sizes of hydrophobic peptides to the C-terminal using genetic modification. *FEBS Lett.*, 415(1) :114–118.

Arnold K., Hoekstra D. & Ohki S. (1992). Association of lysozyme to phospholipid surfaces and vesicle fusion. *Biochim. Biophys. Acta*, 1124(1) :88–94.

Aström K. & Murray R. (2012). *Feedback systems :an introduction for scientists and engineers.* Princeton University Press. ISBN 978-0-691-13576-2.

Azzam R. & Bashara N. (1977). *Ellipsometry and polarized light.* North-Holland personal library. North-Holland Pub. Co. ISBN 978-0-444-87016-2.

Baron F., Cochet M., Ablain W., Grosset N., Madec M., Gonnet F., Jan S. & Gautier M. (2006). Rapid and cost-effective method for micro-organism enumeration based on miniaturization of the conventional plate-counting technique. *Lait*, 86(3) :251–257.

Bera A., Herbert S., Jakob A., Vollmer W. & Gotz F. (2005). Why are pathogenic staphylococci so lysozyme resistant ? The peptidoglycan O-acetyltransferase OatA is the major determinant for lysozyme resistance of *Staphylococcus aureus*. *Mol. Microbiol.*, 55(3) :778–787.

Berge B. & Renault A. (1993). Ellipsometry study of 2D crystallization of 1-alcohol monolayers at the water surface. *Europhys. Lett.*, 21(7) :773.

Berger L. & Weiser R. (1957). The β-glucosaminidase activity of egg-white lysozyme. *Biochim. Biophys. Acta*, 26(3) :517–521.

Bergers J., Vingerhoeds M., Van Bloois L., Herron J., Jassen L., Fisher M. & Crommeli D. (1993). The role of protein charge in protein-lipid interactions. pH-dependent changes of the electrophoretic mobility of liposomes through adsorption of watersoluble, globular proteins. *Biochem.*, 32(17) :4641–4649.

Bernkop-Schnurch A., Krist S., Vehabovic M. & Valenta C. (1998). Synthesis and evaluation of lysozyme derivatives exhibiting an enhanced antimicrobial action. *Eur. J. Pharm. Sci.*, 6(4) :301–306.

Beveridge T. & Davies J. (1983). Cellular responses of *Bacillus subtilis* and *Escherichia coli* to the Gram stain. *J. Bacteriol.*, 156(2) :846–858.

Beveridge T. & Graham L. (1991). Surface layers of bacteria. *Microbiol. Rev.*, 55(4) :684–705.

Blake C., Koenig D., Mair G., North A., Phillips D. & Sarma V. (1965). Structure of hen egg-white lysozyme. a three-dimensional fourier synthesis at 2 Angstrom resolution. *Nature*, 206(4986) :757–761.

Boisselier E., Calvez P., Demers E., Cantin L. & Salesse C. (2012). Influence of the physical state of phospholipid monolayers on protein binding. *Langmuir*, 28(25) :9680–9688.

Brandenburg K., Koch M. & Seydel U. (1998). Biophysical characterisation of lysozyme binding to LPS Re and lipid A. *Eur. J. Biochem.*, 258(2) :686–695.

Braun V. (1975). Covalent lipoprotein from the outer membrane of *Escherichia coli. Biochim. Biophys. Acta*, 415(3) :335–377.

Breeuwer P. & Abee T. (2004). Assessment of the membrane potential, intracellular pH and respiration of bacteria employing fluorescence techniques. *Molecular Microbial Ecology Manual*, 8.01 :1563–1580.

Brehm-Stecher B. & Johnson E. (2003). Sensitization of *Staphylococcus aureus* and *Escherichia coli* to antibiotics by the sesquiterpenoids nerolidol, farnesol, bisabolol, and apritone. *Antimicrob. Agents Chemother.*, 47(10) :3357–3360.

Brockman H. (1999). Lipid monolayers : why use a half a membrane to characterize protein-membrane insertion. *Curr. Opin. Struct. Biol.*, 9(4) :438–443.

Brogan D. M. & Mossialos E. (2013). Incentives for new antibiotics : the options market for antibiotics (OMA) model. *Global. Health*, 9(1) :58–68.

Brogden K. (2005). Antimicrobial peptides : Pore formers or metabolic inhibitors in bacteria ? *Nat. Rev. Microbiol.*, 3(3) :238–250.

Bruhn C. (2002). Consumer attitudes toward food additives. In Branen A., Davidson P., Salminen S. & Thorngate J., editors, *Food additives*, volume 2, pp. 111–119. Marcel Dekker Inc., New York. ISBN 0-8247-9343-9.

Callewaert L., Aertsen A., Deckers D., Vanoirbeek K., Vanderkelen L., Van Herreweghe J., Masschalck B., Nakimbugwe D., Robben J. & Michiels C. (2008). A new family of lysozyme inhibitors contributing to lysozyme tolerance in Gram-negative bacteria. *PloS Pathog.*, 4(3).

Callewaert L., Masschalck B., Deckers D., Nakimbugwe D., Atanassova M., Aertsen A. & Michiels C. (2005). Purification of Ivy, a lysozyme inhibitor from *Escherichia coli*, and characterisation of its specificity for various lysozymes. *Enzyme Microb. Tech.*, 37(2) :205–211.

Calvez P., Bussières S., Demers E. & Salesse C. (2009). Parameters modulating the maximum insertion pressure of proteins and peptides in lipid monolayers. *Biochimie*, 91(6) :718–733.

Calvez P., Demers E., Boisselier E. & Salesse C. (2011). Analysis of the contribution of saturated and polyunsaturated phospholipid monolayers to the binding of proteins. *Langmuir*, 27(4) :1373–1379.

Camesano T., Natan M. & Logan B. (2000). Observation of changes in bacterial cell morphology using tapping mode atomic force microscopy. *Langmuir*, 16(10) :4563–4572.

Canfield R. & Liu A. (1965). The disulfide bonds of egg white lysozyme (muramidase). *J. Biol. Chem.*, 240(5) :1997–2002.

Coccia C., Rinaldi A., Luca V., Barra D., Bozzi A., Giulio A., Veerman E. & Mangoni M. (2011). Membrane interaction and antibacterial properties of two mildly cationic peptide diastereomers, bombinins H2 and H4, isolated from *Bombina* skin. *Eur. Biophys. J.*, 40(4) :577–588.

Davies J., Anderson G., Beveridge T. & Clark H. (1983). Chemical mechanism of the Gram stain and synthesis of a new electron-opaque marker for electron microscopy which replaces the iodine mordant of the stain. *J. Bacteriol.*, 156(2) :837–845.

Deckers D., Masschalck B., Aertsen A., Callewaert L., Van Tiggelen C., Atanassova M. & Michiels C. (2004). Periplasmic lysozyme inhibitor contributes to lysozyme resistance in *Escherichia coli*. *Cell. Mol. Life Sci.*, 61(10) :1229–1237.

DeLisa M., Valdes J. & Bentley W. (2001a). Mapping stress-induced changes in autoinducer AI-2 production in chemostat-cultivated *Escherichia coli* K-12. *J. Bacteriol.*, 183(9) :2918–2928.

DeLisa M., Wu C., Wang L., Valdes J. & Bentley W. (2001b). DNA microarray-based identification of genes controlled by autoinducer 2-stimulated quorum sensing in *Escherichia coli*. *J. Bacteriol.*, 183(18) :5239–5247.

Demchick P. & Koch A. (1996). The permeability of the wall fabric of *Escherichia coli* and *Bacillus subtilis*. *J. Bacteriol.*, 178(3) :768–773.

Derde M., Guérin-Dubiard C., Lechevalier V., Cochet M., Jan S., Baron F., Gautier M., Vié V. & Nau F. (2014). Dry-heating of lysozyme increases its activity against *Escherichia coli* membranes. *J. Agric. Food Chem.*, 62(7) :1692–1700.

Derde M., Lechevalier V., Guérin-Dubiard C., Cochet M., Jan S., Baron F., Gautier M., Vié V. & Nau F. (2013). Hen egg white lysozyme permeabilizes the *Escherichia coli* outer and inner membranes. *J. Agric. Food Chem.*, 61(41) :9922–9929.

Desfougères Y. (2009). *Traitement thermique du lysozyme de poule à l'état solide : structures, interactions, fonctionnalités*. Ph.D. thesis, Agrocampus Ouest, Rennes.

Desfougères Y., Jardin J., Lechevalier V., Pézennec S. & Nau F. (2011a). Succinimidyl residue formation in hen egg-white lysozyme favors the formation of intermolecular covalent bonds without affecting its tertiary structure. *Biomacromol.*, 12(1) :156–166.

Desfougères Y., Lechevalier V., Pézennec S., Artzner F. & Nau F. (2008). Dry-heating makes hen egg white lysozyme an efficient foaming agent and enables its bulk aggregation. *J. Agric. Food Chem.*, 56(13) :5120–5128.

Desfougères Y., Saint-Jalmes A., Salonen A., Vié V., Beaufils S., Pézennec S., Desbat B., Lechevalier V. & Nau F. (2011b). Strong improvement of interfacial properties can result from slight structural modifications of proteins : The case of native and dry-heated lysozyme. *Langmuir*, 27(24) :14947–14957.

Diamond R. (1974). Real-space refinement of the structure of hen egg-white lysozyme. *J. Mol. Biol.*, 82(3) :371–391.

Düring K., Porsch P., Mahn A., Brinkmann O. & Gieffers W. (1999). The non-enzymatic microbicidal activity of lysozymes. *FEBS lett.*, 449(2-3) :93–100.

Eeman M. & Deleu M. (2010). From biological membranes to biomimetic model membranes. *Biotechnol. Agron. Soc. Environ.*, 14(4) :719–736.

Ellison R. & Giehl T. (1991). Killing of Gram-negative bacteria by lactoferrin and lysozyme. *J. Clin. Invest.*, 88(4) :1080–1091.

Epand R. & Epand R. (2011). Bacterial membrane lipids in the action of antimicrobial agents. *J. Pept. Sci.*, 17(5) :298–305.

Epand R., Pollard J., Wright J., Savage P. & Epand R. (2010). Depolarization, bacterial membrane composition, and the antimicrobial action of ceragenins. *Antimicrob. Agents Chemother.*, 54(9) :3708–3713.

Erickson H. (2009). Size and shape of protein molecules at the nanometer level determined by sedimentation, gel filtration, and electron microscopy. *Biol. Proced. Online*, 11(1) :32–51.

European Centre for Disease Prevention and Control/European Medicines Agency joint working group (2009). The bacterial challenge : time to react. Technical report, European Centre for Disease Prevention and Control.

European commission (2011). Action plan against the rising threats from antimicrobial resistance. Technical report, European commission.

Evran S., Yasa I. & Telefoncu A. (2010). Modification of lysozyme with oleoyl chloride for broadening the antimicrobial specificity. *Prep. Biochem. Biotechnol.*, 40(4) :316–325.

Expasy SIB Swiss (2014). Implementation of protparam tool of the expasy website for P00698. URL `http://web.expasy.org/cgi-bin/protparam/protparam1?P00698`.

Fischmann T., Bentley G., Bhat T., Boulot G., Mariuzza R., Phillips S., Tello D. & Poljak R. (1991). Crystallographic refinement of the three-dimensional structure of the FabD1.3-lysozyme complex at 2.5 A resolution. *J. Biol. Chem.*, 266(20) :12915–12920.

Fleming A. (1922). On a remarkable bacteriolytic element found in tissues and secretions. *JSTOR*, 93 :306–317.

Foschiatti M., Cescutti P., Tossi A. & Rizzo R. (2009). Inhibition of cathelicidin activity by bacterial exopolysaccharides. *Mol. Microbiol.*, 72(5) :1137–1146.

Fox J. (2013). Antimicrobial peptides stage a comeback. *Nature Biotechnol.*, 31(5) :379–382.

Gaboriaud F. & Dufrêne Y. (2007). Atomic force microscopy of microbial cells : Application to nanomechanical properties, surface forces and molecular recognition. *Colloids Surf. B-Biointerfaces*, 54(1) :10–19.

Gasteiger E., Hoogland C., Gattiker A., Duvaud S., Wilkins M. R., Appel R. D. & Bairoch A. (2005). Protein identification and analysis tools on the ExPASy server. In Walker J. M., editor, *Proteomics protocols handbook*, pp. 571–607. Humana press. ISBN 978-1-59259-890-8.

Ghuysen J. & Hackenbeck R. (1994). *Bacterial cell wall.* Elsevier. ISBN 978-0-444-88094-9.

Giacometti A., Cirioni O., Ghiselli R., Mocchegiani F., Orlando F., Silvestri C., Bozzi A., Di Giulio A., Luzi C., Mangoni M., Barra D., Saba V., Scalise G. & Rinaldi A. (2006). Interaction of antimicrobial peptide temporin L with lipopolysaccharide *in vitro* and in experimental rat models of septic shock caused by Gram-negative bacteria. *Antimicrob. Agents Chemother.*, 50(7) :2478–2486.

Gidalevitz D., Ishitsuka Y., Muresan A., Konovalov O., Waring A., Lehrer R. & Lee K. (2003). Interaction of antimicrobial peptide protegrin with biomembranes. *Proc. Natl. Acad. Sci. U.S.A.*, 100(11) :6302–6307.

Glauert A. & Thornley M. (1969). The topography of the bacterial cell wall. *A. Rev. Microbiol.*, 23 :159–198.

Gorbenko G., Ioffe V. & Kinnunen P. (2007). Binding of lysozyme to phospholipid bilayers : Evidence for protein aggregation upon membrane association. *Biophys. J.*, 93(1) :140–153.

Gram C. (1884). Uber die isolirte fdirbung der schizomyceten in schnitt-und trockenpräparaten. *Fortsch. Med.*, 2 :185–189.

Groisman E. (1994). How bacteria resist killing by host-defense peptides. *Trends Microbiol.*, 2(11) :444–449.

Gruenheid S. & Le Moual H. (2012). Resistance to antimicrobial peptides in Gram-negative bacteria. *FEMS Microbiol. Lett.*, 330(2) :81–89.

Guo L. (1998). Lipid A acylation and bacterial resistance against vertebrate antimicrobial peptides. *Cell*, 95(2) :189–198.

Hamamoto K., Kida Y., Zhang Y., Shimizu T. & Kuwano K. (2002). Antimicrobial activity and stability to proteolysis of small linear cationic peptides with D-amino acid substitutions. *Microbiol. Immunol.*, 46(11) :741–749.

Hammershøj M., Nording J., Rasmussen H., Carstens J. & Pedersen H. (2006). Dry-pasteurization of egg albumen powder in a fluidized bed. I. Effect on microbiology, physical and chemical parameters. *Int. J. Food Sci. Technol.*, 41(3) :249–261.

Hancock R. & Sahl H. (2006). Antimicrobial and host-defense peptides as new anti-infective therapeutic strategies. *Nat. Biotechnol.*, 24(12) :1551–1557.

Harkins W., Young F. & Boyd E. (1940). The thermodynamics of films : Energy and entropy of extension and spreading of insoluble monolayers. *J. Chem. Phys.*, 8(12) :954–965.

Helander I., Alakomi H., Latva-Kala K., Mattila-Sandholm T., Pol I., Smid E., Gorris L. & von Wright A. (1998). Characterization of the action of selected essential oil components on Gram-negative bacteria. *J. Agric. Food Chem.*, 46(9) :3590–3595.

Helander I. & Mattila-Sandholm T. (2000). Fluorometric assessment of Gram-negative bacterial permeabilization. *J. Appl. Microbiol.*, 88(2) :213–219.

Iacono V., Zove S., Grossbard B., Pollock J., Fine D. & Greene L. (1985). Lysozyme-mediated aggregation and lysis of the periodontal microorganism *Capnocytophaga gingivalis* 2010. *Infect. Immun.*, 47(2) :457–464.

Ibrahim H. (1998). On the novel catalytically-independent antimicrobial function of hen egg-white lysozyme : A conformation-dependent activity. *Nahrung-Food*, 42(3-4) :187–193.

Ibrahim H., Aoki T. & Pellegrini A. (2002). Strategies for new antimicrobial proteins and peptides : Lysozyme and aprotinin as model molecules. *Curr. Pharm. Des.*, 8(9) :671–693.

Ibrahim H., Hatta H., Fujiki M., Kim M. & Yamamoto T. (1994a). Enhanced antimicrobial action of lysozyme against Gram-negative and Gram-positive bacteria due to modification with perillaldehyde. *J. Agric. Food Chem.*, 42(8) :1813–1817.

Ibrahim H., Higashiguchi S., Juneja L., Kim M. & Yamamoto T. (1996a). A structural phase of heat-denatured lysozyme with novel antimicrobial action. *J. Agric. Food Chem.*, 44(6) :1416–1423.

Ibrahim H., Higashiguchi S., Koketsu M., Juneja L., Kim M., Yamamoto T., Sugimoto Y. & Aoki T. (1996b). Partially unfolded lysozyme at neutral pH agglutinates and kills Gram-negative and Gram-positive bacteria through membrane damage mechanism. *J. Agric. Food Chem.*, 44(12) :3799–3806.

Ibrahim H., Higashiguchi S., Sugimoto Y. & Aoki T. (1997). Role of divalent cations in the novel bactericidal activity of the partially unfolded lysozyme. *J. Agric. Food Chem.*, 45(1) :89–94.

Ibrahim H., Inazaki D., Abdou A., Aoki T. & Kim M. (2005). Processing of lysozyme at distinct loops by pepsin : A novel action for generating multiple antimicrobial peptide motifs in the newborn stomach. *Biochim. Biophys. Acta-General Subjects*, 1726(1) :102–114.

Ibrahim H., Kato A. & Kobayashi K. (1991). Antimicrobial effects of lysozyme against Gram-negative bacteria due to covalent binding of palmitic acid. *J. Agric. Food Chem.*, 39(11) :2077–2082.

Ibrahim H., Kobayashi K. & Kato A. (1993). Length of hydrocarbon chain and antimicrobial action to Gram-negative bacteria of fatty acylated lysozyme. *J. Agric. Food Chem.*, 41(7) :1164–1168.

Ibrahim H., Matsuzaki T. & Aoki T. (2001a). Genetic evidence that antibacterial activity of lysozyme is independent of its catalytic function. *FEBS Letters*, 506(1) :27–32.

Ibrahim H., Thomas U. & Pellegrini A. (2001b). A helix-loop-helix peptide at the upper lip of the active site cleft of lysozyme confers potent antimicrobial activity with membrane permeabilization action. *J. Biol. Chem.*, 276(47) :43767–43774.

Ibrahim H., Yamada M., Kobayashi K. & Kato A. (1992). Bactericidal action of lysozyme against Gram-negative bacteria due to insertion of a hydrophobic pentapeptide into its C-terminus. *Biosci. Biotechnol. Biochem.*, 56(8) :1361–1363.

Ibrahim H., Yamada M., Matsushita K., Kobayashi R. & Kato A. (1994b). Enhanced bactericidal action of lysozyme to *Escherichia coli* by inserting a hydrophobic pentapeptide into its C-terminus. *J. Biol. Chem.*, 269(7) :5059–5063.

Ioffe V. & Gorbenko G. (2005). Lysozyme effect on structural state of model membranes as revealed by pyrene excimerization studies. *Biophys. Chem.*, 114(2-3) :199–204.

Ishitsuka Y., Pham D., Waring A., Lehrer R. & Lee K. (2006). Insertion selectivity of antimicrobial peptide protegrin-1 into lipid monolayers : Effect of head group electrostatics and tail group packing. *Biochim. Biophys. Acta - Biomembr.*, 1758 :1450–1460.

Israelachvili J. & Mitchell D. (1975). A model for the packing of lipids in bilayer membranes. *Biochim. Biophys. Acta-Biomembranes*, 389(1) :13–19.

Ito Y., Kwon O., Ueda M., Tanaka A. & Imanishi Y. (1997). Bactericidal activity of human lysozymes carrying various lengths of polyproline chain at the C-terminus. *FEBS Lett.*, 415(3) :285–288.

Jenssen H., Hamill P. & Hancock R. (2006). Peptide antimicrobial agents. *Clin. Microbiol. Rev.*, 19(3) :491–511.

Johnston M., Hanlon G., Denyer S. & Lambert R. (2003). Membrane damage to bacteria caused by single and combined biocides. *J. Appl. Microbiol.*, 94(6) :1015–1023.

Kato A., Ibrahim H., Watanabe H., Honma K. & Kobayashi K. (1990). Structural and gelling properties of dry-heated egg white proteins. *J. Agric. Food Chem.*, 38(1) :32–37.

Kimelberg H. & Papahadjopoulos D. (1971). Interactions of basic proteins with phospholipid membranes : Binding and changes in the sodium permeability of phosphatidylserine vesicles. *J. Biol. Chem.*, 246(4) :1142–1148.

Krause R. & McCarty M. (1961). Studies on the chemical structure of the streptococcal cell wall. i. the identification of a mucopeptide in the cell walls of groups A and A-variant streptococci. *J. Exp. Med.*, 114(1) :127–140.

Krishnakumari V. & Nagaraj R. (2008). Interaction of antibacterial peptides spanning the carboxy-terminal region of human β-defensins 1–3 with phospholipids at the air–water interface and inner membrane of *E. coli*. *Peptides*, 29(1) :7–14.

Kristian S., Dürr M., Van Strijp J., Neumeister B. & Peschel A. (2003). MprF-mediated lysinylation of phospholipids in *Staphylococcus aureus* leads to protection against oxygen-independent neutrophil killing. *Infect. Immun.*, 71(1) :546–549.

Laible N. & Germaine G. (1985). Bactericidal activity of human lysozyme, muramidase-inactive lysozyme, and cationic polypeptides against *Streptococcus sanguis* and *Streptococcus faecalis* inhibition by chitin oligosaccharides. *Infect. Immun.* , 48(3) :720–728.

Lambert P. & Hammond S. (1973). Potassium fluxes, first indicators of membrane damage in microorganisms. *Biochem. Biophys. Res. Commun.*, 54(2) :796–799.

Le Brun A., Clifton L., Halbert C., Lin B., Meron M., Holden P., Lakeley J. & Holt S. (2013). Structural characterization of a model Gram-negative bacterial surface using lipopolysaccharides from rough strains of *Escherichia coli*. *Biomacromol.*, 14 :2014–2022.

Lee M., Sun T., Hung W. & Huang H. (2013). Process of inducing pores in membranes by melittin. *Proc. Natl. Acad. Sci. U.S.A.*

Lehrer R., Barton A. & Ganz T. (1988). Concurrent assessment of inner and outer-membrane permeabilization and bacteriolysis in *Escherichia coli* by multiple-wavelength spectrophotometry. *J. Immunol. Methods*, 108(1-2) :153–158.

Li A., Lee P., Ho B., Ding J. & Lim C. (2007). Atomic force microscopy study of the antimicrobial action of Sushi peptides on Gram negative bacteria. *Biochim. Biophys. Acta - Biomembranes*, 1768(3) :411–418.

Loh B., Grant C. & Hancock R. (1984). Use of the fluorescent probe 1-n-phenylnaphtylamine to study the interactions of aminoglycoside antibiotics with the outer membrane of *Pseudomonas aeruginosa*. *Antimicrobiol. Agents Chemother.*, 26(4) :546–551.

Lohner K. (2009). New strategies for novel antibiotics : peptides targeting bacterial cell membranes. *Gen. Physiol. Biophys*, 28(2) :105–116.

Lugtenberg E. & Peters R. (1976). Distribution of lipids in the cytoplasmic and outer membranes of *Escherichia coli* K12. *Biochim. Biophys. Acta*, 441(1) :38–47.

Maget-Dana R. (1999). The monolayer technique : a potent tool for studying the interfacial properties of antimicrobial and membrane-lytic peptides and their interactions with lipid membranes. *Biochim. Biophys. Acta*, 1462(1-2) :109–140.

Magonov S., Elings V. & Whangbo M. (1997). Phase imaging and stiffness in tapping-mode atomic force microscopy. *Surf. Sci.*, 375(2-3) :385–391.

Mah T. & O'Toole G. (2001). Mechanisms of biofilm resistance to antimicrobial agents. *Trends Microbiol.*, 9(1) :34–39.

Marsh D. (1996). Lateral pressure in membranes. *Biochim. Biophys. Acta*, 1286(3) :183–223.

Masschalck B., Deckers D. & Michiels C. (2002). Lytic and nonlytic mechanism of inactivation of Gram-positive bacteria by lysozyme under atmospheric and high hydrostatic pressure. *J. Food Prot.*, 65(12) :1916–1923.

Masschalck B. & Michiels C. (2003). Antimicrobial properties of lysozyme in relation to foodborne vegetative bacteria. *Crit. Rev. Microbiol.*, 29(3) :191–214.

Matias V., Al-Amoudi A., Dubochet J. & Beveridge T. (2003). Cryo-transmission electron microscopy of frozen-hydrated sections of *Escherichia coli* and *Pseudomonas aeruginosa*. *J. Bacteriol.*, 185(20) :6112–6118.

Matias V. & Beveridge T. (2006). Native cell wall organization shown by cryo-electron microscopy confirms the existence of a periplasmic space in *Staphylococcus aureus*. *J. Bacteriol.*, 188(3) :1011–1021.

Matsumura H. & Dimitrova M. (1996). A comparative study of the sorption of serum albumin, lysozyme, and cytochrome C at phospholipid membranes using surface tensiometry, electrophoresis, and leakage of probe molecules. *Colloids Surf. B : Biointerfaces*, 6(3) :165–172.

Matsuzaki K., Sugishita K., Harada M., Fujii N. & Miyajima K. (1997). Interactions of an antimicrobial peptide, magainin 2, with outer and inner membranes of Gram-negative bacteria. *Biochim. Biophys. Acta - Biomembranes*, 1327(1) :119–130.

Mattila J., Sabatini K. & Kinnunen P. (2008). Oxidized phospholipids as potential molecular targets for antimicrobial peptides. *Biochim. Biophys. Acta*, 1778(10) :2041–2050.

Meincken M., Holroyd D. & Rautenbach M. (2005). Atomic force microscopy study of the effect of antimicrobial peptides on the cell envelope of *Escherichia coli*. *Antimicrob. Agents Chemother.*, 49(10) :4085–4092.

Melo M., Ferre R. & Castanho M. (2009). Antimicrobial peptides : linking partition, activity and high membrane-bound concentrations. *Nat. Rev. Micro.*, 7(3) :245–250.

Mena C., Adenso-Diaz B. & Yurt O. (2011). The causes of food waste in the supplier–retailer interface : Evidences from the UK and Spain. *Resources, Conservation and Recycling*, 55(6) :648–658.

Meng H. & Kumar K. (2007). Antimicrobial activity and protease stability of peptides containing fluorinated amino acids. *J. Am. Chem. Soc.*, 129(50) :15615–15622.

Mengin-Lecreulx D. & Lemaitre B. (2005). Structure and metabolism of peptidoglycan and molecular requirements allowing its detection by the *Drosophila* innate immune system. *J. Endotoxin Res.*, 11(2) :105–111.

Miki T. & Hardt W. (2013). Outer membrane permeabilization is an essential step in the killing of Gram-negative bacteria by the lectin RegIIIβ. *PLoS ONE*, 8(7) :e69901.

Mine Y. (1996). Effect of pH during the dry heating on the gelling properties of egg white proteins. *Food Res. Int.*, 29(2) :155–161.

Mine Y. (1997). Effect of dry heat and mild alkaline treatment on functional properties of egg white proteins. *J. Agric. Food Chem.*, 45(8) :2924–2928.

Mine Y., Ma F. & Lauriau S. (2004). Antimicrobial peptides released by enzymatic hydrolysis of hen egg white lysozyme. *J. Agric. Food Chemistry*, 52(5) :1088–1094.

Mitchell P. (1961). Coupling of phosphorylation to electron and hydrogen transfer by a chemi-osmotic type of mechanism. *Nature*, 191 :144–148.

Miteva M., Andersson M., Karshikoff A. & Otting G. (1999). Molecular electroporation : a unifying concept for the description of membrane pore formation by antibacterial peptides, exemplified with NK-lysin. *FEBS Letters*, 462(1-2) :155–158.

Moult J., Yonath A., Traub W., Smilansky A., Podjarny A., Rabinovich D. & Saya A. (1976). The structure of triclinic lysozyme at 2-5 A resolution. *J. Mol. Biol.*, 100(2) :179–195.

Mudgil P., Torres M. & Millar T. (2006). Adsorption of lysozyme to phospholipid and meibomian lipid monolayer films. *Colloids Surf. B-Biointerfaces*, 48(2) :128–137.

Nakamura S., Kato A. & Kobayashi K. (1991). New antimicrobial characteristics of lysozyme dextran conjugate. *J. Agric. Food Chem.*, 39(4) :647–650.

Nakamura S., Kato A. & Kobayashi K. (1992). Bifunctional lysozyme galactomannan conjugate having excellent emulsifying properties and bactericidal effect. *J. Agric. Food Chem.*, 40(5) :735–739.

Nakatsuji T. & Gallo R. (2012). Antimicrobial peptides : old molecules with new ideas. *J. Investig. Dermatol.*, 132(3 Pt 2) :887–895.

Nguyen L., Haney E. & Vogel H. (2011). The expanding scope of antimicrobial peptide structures and their modes of action. *Trends Biotechnol.*, 29(9) :464–472.

Nikaido H. (2003). Molecular basis of bacterial outer membrane permeability revisited. *Microbiol. Mol. Biol. Rev.*, 67(4) :593–656.

Ohno N. & Morrison D. (1989). Lipopolysaccharide interaction with lysozyme. binding of lipopolysaccharide to lysozyme and inhibition of lysozyme enzymatic activity. *J. Biol. Chem.*, 264(8) :4434–4441.

Ohno N., Tanida N. & Yadomae T. (1991). Characterization of complex-formation between lipopolysaccharide and lysozyme. *Carbohyd. Res.*, 214(1) :115–130.

Oliveira R., Schneck E., Quinn B., Konovalov O., Brandenburg K., Gutsmann T., Gill T., Hanna C., Pink D. & Tanaka M. (2010). Crucial roles of charged saccharide moieties in survival of gram negative bacteria against protamine revealed by combination of grazing incidence x-ray structural characterizations and monte carlo simulations. *Phys. Rev. E Stat. Nonlin. Soft Matter Phys.*, 81.

Onuma K. & Inaka K. (2008). Lysozyme dimer association : Similarities and differences compared with lysozyme monomer association. *J. Cryst. Growth*, 310(6) :1174–1181.

Orlov D., Nguyen T. & Lehrer R. (2002). Potassium release, a useful tool for studying antimicrobial peptides. *J. Microbiol. Methods*, 49(3) :325–328.

Osserman E. (2012). *Lysozyme*. Elsevier Science. ISBN 978-0-323-14367-7.

Pellegrini A., Thomas U., Bramaz N., Klauser S., Hunziker P. & von Fellenberg R. (1997). Identification and isolation of a bactericidal domain in chicken egg white lysozyme. *J. Appl. Microbiol.*, 82(3) :372–378.

Pellegrini A., Thomas U., Vonfellenberg R. & Wild P. (1992). Bactericidal activities of lysozyme and aprotinin against Gram-negative and Gram-positive bacteria related to their basic character. *J. Appl. Bacteriol.*, 72(3) :180–187.

Pellegrini A., Thomas U., Wild P., Schraner E. & von Fellenberg R. (2000). Effect of lysozyme or modified lysozyme fragments on DNA and RNA synthesis and membrane permeability of *Escherichia coli*. *Microbiol. Res.*, 155(2) :69–77.

Perron G., Zasloff M. & Bell G. (2006). Experimental evolution of resistance to an antimicrobial peptide. *Proc. Biol. Sci.*, 273(1583) :251–256.

Peschel A. (2001). *Staphylococcus aureus* resistance to human defensins and evasion of neutrophil killing via the novel virulence factor MprF is based on modification of membrane lipids with L-lysine. *J. Exp. Med.*, 193(9) :1067–1076.

Podda E., Benincasa M., Pacor S., Micali F., Mattiuzzo M., Gennaro R. & Scocchi M. (2006). Dual mode of action of Bac7, a proline-rich antibacterial peptide. *Biochim. Biophys. Acta - General Subjects*, 1760(11) :1732–1740.

Posse E., Dearcuri B. & Morero R. (1994). Lysozyme interactions with phospholipid-vesicles - relationships with fusion and release of aqueous content. *Biochim. Biophys. Acta-Biomembranes*, 1193(1) :101–106.

Posse E., Vinals A., Dearcuri B., Farias R. & Morero R. (1990). Lysozyme induced fusion of negatively charged phospholipid-vesicles. *Biochim. Biophys. Acta*, 1024(2) :390–394.

Raetz C. & Whitfield C. (2002). Lipopolysaccharide endotoxins. *Annu. Rev. Biochem.*, 71 :635–700.

Roberts P., Dunkerley C., McAuley A. & Winkelman L. (2007). Effect of manufacturing process parameters on virus inactivation by dry heat treatment at 80°C in factor VIII. *Vox Sanguinis*, 92(1) :56–63.

Roes S., Seydel U. & Gutsmann T. (2005). Probing the properties of lipopolysaccharide monolayers and their interaction with antimicrobial peptide polymyxin B by atomic force microscopy. *Langmuir*, 21(15) :6970–6978.

Salton M. (1963). The relationship between the nature of the cell wall and the Gram stain. *J. Gen. Microbiol.*, 30 :223–235.

Sankaram M. & Marsh D. (1993). Protein-lipid interactions with peripheral membrane proteins. In Watts E., editor, *Protein-lipid interactions*, pp. 127–162. Elsevier. ISBN 978-0-444-81575-0.

Sarkis J., Hubert J., Legrand B., Robert E., Chéron A., Jardin J., Hitti E., Le Rumeur E. & Vié V. (2011). Spectrin-like repeats 11–15 of human dystrophin show adaptations to a lipidic environment. *J. Biol. Chem.*, 286(35) :30481–30491.

Schleifer K. & Kandler O. (1972). Peptidoglycan types of bacterial cell walls and their taxonomic implications. *Bacteriological reviews*, 36(4) :407–477.

Seltmann G. & Holst O. (2002). *The bacterial cell wall*, volume 1. Springer-Verlag Berlin Heidelberg New York. ISBN 978-3-540-42608-0.

Seo M., Won H., Kim J., Mishig-Ochir T. & Lee B. (2012). Antimicrobial peptides for therapeutic applications : A review. *Molecules*, 17(12) :12276–12286.

Shafer W., Qu X., Waring A. & Lehrer R. (1998). Modulation of *Neisseria gonorrhoeae* susceptibility to vertebrate antibacterial peptides due to a member of the resistance/nodulation/division efflux pump family. *Proc. Natl. Acad. Sci. U.S.A.*, 95(4) :1829–1833.

Shimanouchi T., Ishii H., Yoshimoto N., Umakoshi H. & Kuboi R. (2009). Calcein permeation across phosphatidylcholine bilayer membrane : Effects of membrane fluidity, liposome size, and immobilization. *Colloids Surf. B : Biointerfaces*, 73(1) :156–160.

Sieprawska-Lupa M. (2004). Degradation of human antimicrobial peptide LL-37 by *Staphylococcus aureus*-derived proteinases. *Antimicrob. Agents Chemother.*, 48(12) :4673–4679.

Silhavy T. J., Kahne D. & Walker S. (2010). The bacterial cell envelope. *Cold Spring Harb. Perspect. Biol.*, 2(5) :a000414.

Silver L. (2011). Challenges of antibacterial discorvery. *Clin. Microbiol. Rev.*, 24(1) :71–109.

Skidmore S., Pasi K., Mawson S., Williams M. & Hill F. (1990). Serological evidence that dry heating of clotting factor concentrates prevents transmission of non-A, non-B hepatitis. *J. Med. Virol.*, 30(1) :50–52.

Smith A. & Hussey M. (2005). *Gram stain protocols*. ASM Microbe Library. URL `http://www.microbelibrary.org/library/gram-stain/2886-gram-stain-protocols`.

Strahl H. & Hamoen L. (2010). Membrane potential is important for bacterial cell division. *Proc. Natl. Acad. Sci. U.S.A.*, 107(27) :12281–12286.

Strominger J. & Ghuysen J. (1967). Mechanisms of enzymatic bacteriolysis. cell walls of bacteria are solubilized by action of either specific carbohydrases or specific peptidases. *Science*, 156(3772) :213–221.

Stumpe S., Schmid R., Stephens D., Georgiou G. & Bakker E. (1998). Identification of OmpT as the protease that hydrolyzes the antimicrobial peptide protamine before it enters growing cells of *Escherichia coli*. *J. Bacteriol.*, 180(15) :4002–4006.

Teixeira V., Feio M. & Bastos M. (2012). Role of lipids in the interaction of antimicrobial peptides with membranes. *Prog. Lipid Res.*, 51(2) :149–177.

Terwilliger T. & Eisenberg D. (1982). The structure of melittin. II. Interpretation of the structure. *J. Biol. Chem.*, 257(11) :6016–6022.

TNS Opinion & Social (2010). Special eurobarometer 354 : Food-related risks. Technical report, European Comission.

Touch V., Hayakawa S. & Saitoh K. (2004). Relationships between conformational changes and antimicrobial activity of lysozyme upon reduction of its disulfide bonds. *Food Chem.*, 84(3) :421–428.

Trauble H. & Overath P. (1973). Structure of *Escherichia coli* membranes studied by fluorescence measurements of lipid phase-transitions. *Biochim. Biophys. Acta*, 307(3) :491–512.

Trusova V. (2012). Modulation of physiological and pathological activities of lysozyme by biological membranes. *Cel. Mol. Biol. Lett.*, 17(3) :349–375.

Uniprot database (2014). P00698. URL `www.uniprot.org/uniprot/P00698`.

Vaara M. (1992). Agents that increase the permeability of the outer membrane. *Microbiol. Rev.*, 56(3) :395–411.

Van der Plancken I., Van Loey A. & Hendrickx M. (2007). Effect of moisture content during dry-heating on selected physicochemical and functional properties of dried egg white. *J. Agric. Food Chem.*, 55(1) :127–135.

van Meer G., Voelker D. & Feigenson G. (2008). Membrane lipids : where they are and how they behave. *Nat. Rev. Mol. Cell Biol.*, 9(2) :112–124.

Vargaftik N., Volkov B. & Voljak L. (1983). International tables of the surface tension of water. *J. Phys. Chem. Ref. Data*, 12(3) :817–820.

Vechetti G., Dearcuri B., Posse E., Arrondo J. & Morero R. (1997). Aggregation, fusion and aqueous content release from liposomes induced by lysozyme derivatives : effect on the lytic activity. *Mol. Membr. Biol.*, 14(3) :137–142.

Vié V., Legardinier S., Chieze L., Le Bihan O., Qin Y., Sarkis J., Hubert J., Renault A., Desbat B. & Le Rumeur E. (2010). Specific anchoring modes of two distinct dystrophin rod sub-domains interacting in phospholipid Langmuir films studied by atomic force microscopy and PM-IRRAS. *Biochim. Biophys. Acta - Biomembranes*, 1798(8) :1503–1511.

Vocadlo D., Davies G., Laine R. & Withers S. (2001). Catalysis by hen egg-white lysozyme proceeds via a covalent intermediate. *Nature*, 412(6849) :835–838.

Vollmer W. & Bertsche U. (2008). Murein (peptidoglycan) structure, architecture and biosynthesis in *Escherichia coli*. *Biochim. Biophys. Acta*, 1778(9) :1714–1734.

Vollmer W., Blanot D. & de Pedro M. (2008). Peptidoglycan structure and architecture. *Fems Microbiol. Rev.*, 32(2) :149–167.

Vollmer W. & Tomasz A. (2002). Peptidoglycan N-acetylglucosamine deacetylase, a putative virulence factor in *Streptococcus pneumoniae*. *Infect. Immun.*, 70(12) :7176–7178.

Wang G. (2014). Antimicrobial peptide database. URL `http://aps.unmc.edu/AP/main.php`.

Wang L., Brauner J., Mao G., Crouch E., Seaton B., Head J., Smith K., Flach C. & Mendelsohn R. (2008). Interaction of recombinant surfactant protein D with lipopolysaccharide : Conformation and orientation of bound protein by IRRAS and simulations. *Biochem.*, 47 :8103–8113.

Wang Y., Zhou Z., Zhu J., Tang Y., Canady T., Chi E., Schanze K. & Whitten D. (2011). Dark antimicrobial mechanisms of cationic phenylene ethynylene polymers and oligomers against *Escherichia coli*. *Polymers*, 3(3) :1199–1214.

Waters C. & Bassler B. (2005). Quorum sensing : cell-to-cell communication in bacteria. *Annu. Rev. Cell Dev. Biol.*, 21 :319–346.

Wild P., Gabrieli A., Schraner E., Pellegrini A., Thomas U., Frederik P., Stuart M. & Vonfellenberg R. (1997). Reevaluation of the effect of lysoyzme on *Escherichia coli* employing ultrarapid freezing followed by cryoelectronmicroscopy or freeze substitution. *Microsc. Res. Tech.*, 39(3) :297–304.

Wu M., Maier E., Benz R. & Hancock R. (1999). Mechanism of interaction of different classes of cationic antimicrobial peptides with planar bilayers and with the cytoplasmic membrane of *Escherichia coli*. *Biochemistry*, 38(22) :7235–7242.

Xu X., Kashima O., Saito A., Azakami H. & Kato A. (2004). Structural and functional properties of chicken lysozyme fused serine-rich heptapeptides at the C-terminus. *Biosci. Biotechnol. Biochem.*, 68(6) :1273–1278.

Yasuda K., Ohmizo C. & Katsu T. (2003). Potassium and tetraphenylphosphonium ion-selective electrodes for monitoring changes in the permeability of bacterial outer and cytoplasmic membranes. *J. Microbiol. Methods*, 54(1) :111–115.

Yeagle P. (1993). *The membranes of cells*. Academic Press. ISBN 978-0-127-69041-4.

Yuan B., Xing L., Zhang Y., Lu Y., Luo Y., Mai Z. & Li M. (2007). Penetration and saturation of lysozyme in phospholipid bilayers. *J. Phys. Chem. B*, 111(22) :6151–6155.

Zasloff M. (2002). Antimicrobial peptides of multicellular organisms. *Nature*, 415(6870) :389–395.

Zhang L., Dhillon P., Yan H., Farmer S. & Hancock R. (2000a). Interactions of bacterial cationic peptide antibiotics with outer and cytoplasmic membranes of *Pseudomonas aeruginosa*. *Antimicrob. Agents Chemother.*, 44(12) :3317–3321.

Zhang L., Scott M., Yan H., Mayer L. & Hancock R. (2000b). Interaction of polyphemusin I and structural analogs with bacterial membranes, lipopolysaccharide, and lipid monolayers. *Biochem.*, 39(47) :14504–14514.

Zipperle G., Ezzell J. & Doyle R. (1984). Glucosamine substitution and muramidase susceptibility in *Bacillus anthracis*. *Can. J. Microbiol.*, 30(5) :553–559.

Zschornig O., Paasche G., Thieme C., Korb N. & Arnold K. (2005). Modulation of lysozyme charge influences interaction with phospholipid vesicles. *Colloids Surf. B-Biointerfaces*, 42(1) :69–78.

Zschornig O., Paasche G., Thieme C., Korb N., Fahrwald A. & Arnold K. (2000). Association of lysozyme with phospholipid vesicles is accompanied by membrane surface dehydration. *Gen. Physiol. Biophys.*, 19(1) :85–101.

Liste des figures

Liste des tableaux

Annexes

Annexe A : Publications acceptées

- Derde M., Lechevalier V., Guérin-Dubiard C., Cochet MF., Jan S., Baron F., Gautier M., Vié V. & Nau F. (2013). Hen egg white lysozyme permeabilizes the *Escherichia coli* outer and inner membranes, *Journal of Agricultural and Food Chemistry*, 61(41) :9922-9929

- Derde M., Guérin-Dubiard C., Lechevalier V., Cochet MF., Jan S., Baron F., Gautier M., Vié V. & Nau F. (2014). Dry-heating of lysozyme increases its activity against *Escherichia coli* membranes, *Journal of Agricultural and Food Chemistry*, 62(7) :1692-1700

- Derde M., Nau F., Lechevalier V., Guérin-Dubiard C., Paboeuf G., Jan S., Baron F., Gautier M. & Vié V. (2015) Native and dry-heated lysozyme interactions with membrane lipid monolayers : lateral reorganization of a lipopolysaccharide monolayer, model of the *Escherichia coli* outer membrane, *BBA biomembranes*, 1848 : 174-183

JOURNAL OF AGRICULTURAL AND FOOD CHEMISTRY

Article

pubs.acs.org/JAFC

Hen Egg White Lysozyme Permeabilizes *Escherichia coli* Outer and Inner Membranes

Melanie Derde,*[,†,‡] Valérie Lechevalier,[†,‡] Catherine Guérin-Dubiard,[†,‡] Marie-Françoise Cochet,[†,‡] Sophie Jan,[†,‡] Florence Baron,[†,‡] Michel Gautier,[†,‡] Véronique Vié,[#] and Françoise Nau[†,‡]

[†]Agrocampus Ouest, UMR1253 Science et technologie du lait et de l'œuf, 65 rue de St-Brieuc, F-35042 Rennes, France

[‡]INRA, UMR1253 Science et technologie du lait et de l'œuf, 65 rue de St-Brieuc, F-35042 Rennes, France

[#]Université de Rennes 1, Institut de physique de Rennes, UMR6251, CNRS, 263 Av. Général Leclerc, F-35042 Rennes, France

ABSTRACT: Natural preservatives answer the consumer demand for long shelf life foods, synthetic molecules being perceived as a health risk. Lysozyme is already used because of its muramidase activity against Gram-positive bacteria. It is also described as active against some Gram-negative bacteria; membrane disruption would be involved, but the mechanism remains unknown. In this study, a spectrophotometric method using the mutant *Escherichia coli* ML-35p has been adapted to investigate membrane disruption by lysozyme for long durations. Lysozyme rapidly increases the permeability of the outer membrane of *E. coli* due to large size pore formation. A direct delayed activity of lysozyme against the inner membrane is also demonstrated, but without evidence of perforations.

KEYWORDS: *lysozyme, antimicrobial activity, membrane permeability, Gram-negative bacteria*

INTRODUCTION

Food additives, including preservatives, worry 66% of the European consumers, and synthetic additives are perceived as more dangerous than natural additives.[1,2] On the other hand, consumers demand safer food products, with a long shelf life. Research for novel, natural food preservatives is thus stimulated, and biological resources are therefore widely screened. Special attention is given to those molecules that have a wide antimicrobial spectrum. Peptides and proteins are considered as potential candidates. One of the natural antimicrobial proteins widely studied is hen egg white lysozyme (HEWL). HEWL is well-known for its muramidase activity against Gram-positive bacteria. It is therefore used as a food additive (E1105) to control Gram-positive spoilers in winemaking and cheese refining.[3−5] Several studies suggest that HEWL also acts against some Gram-negative bacteria; mechanisms such as perturbation of DNA or RNA synthesis and membrane permeabilization would be responsible for lysozyme activity against these micro-organisms.[3,6−8] The efficacy of lysozyme against Gram-negative bacteria can be increased by modifying the protein by proteolysis to obtain small active peptides,[9−11] by fusion of chemical moieties,[12−16] or by heat-denaturation.[17−20]

Membrane disruption is a major mechanism by which antibacterial peptides and proteins act on both Gram-negative and Gram-positive bacteria. The cationic and amphipathic character of most of these peptides and proteins suggests electrostatic and hydrophobic interactions with the bacterial cell wall. Such interactions could disturb the bacterial membrane, leading to bacterial cell death, or translocation of the peptide or protein into the cytoplasm, where it interacts with intracellular targets.[21,22]

Membrane permeabilization is an attractive hypothesis to explain lysozyme activity against Gram-negative bacteria, considering the recent discovery of lysozyme inhibitors in the periplasm of species such as *E. coli*.[23,24] Gram-negative bacteria are naturally protected against lysozyme by the outer membrane, a physical barrier preventing entrance into the cell of molecules bigger than 650 Da.[25] However, the presence of periplasmic lysozyme inhibitors in some Gram-negative bacteria suggests that lysozyme is able to cross their outer membrane. Yet, very little is known about the membrane activity of lysozyme. Especially, there is no experimental evidence of the capability of lysozyme to directly act, or not, on the inner membrane of Gram-negative bacteria.

Different techniques have been used to detect bacterial membrane permeabilization, such as detection of potassium leakage, LPS monitoring, NPN uptake, $DiSC_3$ uptake, or atomic force microscopy (AFM).[26−33] One of the most popular and simple assays is a spectrophotometric method using *Escherichia coli* ML-35p. This method was first described by Lehrer in 1988 and was later optimized for smaller sample volumes by Epand in 2010.[32,33] It has been used to detect membrane activity of antibacterial peptides such as cecropin A, melittin, ceragenins, Cg-BPI, and indolicidin and of antibacterial proteins such as human defensins and HEWL.[32−35] *E. coli* ML-35p is constitutive for β-galactosidase expressed in the cytoplasm and produces a β-lactamase in the periplasm, which is encoded on a plasmid (pBR322). This bacterial strain also lacks lactose permease.[32,33] The measurement of β-lactamase and β-galactosidase activities thus enables the detection of outer and inner membrane permeabilization, respectively (Figure 1).

In the literature, membrane permeability has been measured using the *E. coli* ML-35p mutant with a contact time never

Received: July 3, 2013
Revised: September 13, 2013
Accepted: September 18, 2013
Published: September 18, 2013

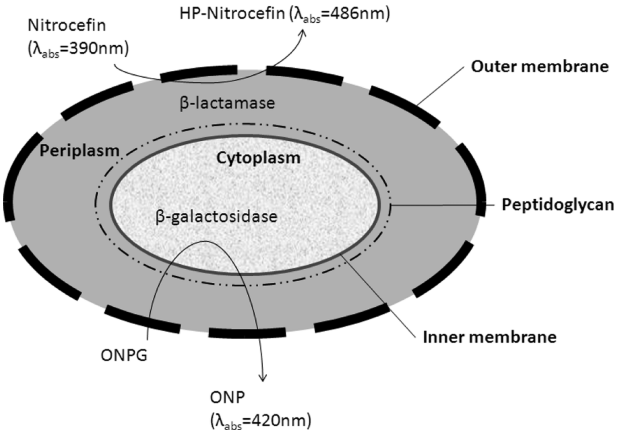

Figure 1. Schematic representation of *E. coli* ML-35p cell, with locating *β*-lactamase and *β*-galactosidase. Both enzymes become accessible to their substrates (nitrocefin and ONPG, respectively) when outer and inner membrane permeabilization occurs; the respective products HP-nitrocefin (λ_{abs} = 486 nm) and ONP (λ_{abs} = 420 nm) are then released.

exceeding 2 h between the studied antimicrobial agent and the bacterial cells. However, it is imaginable that membrane permeabilization could sometimes result from slow phenomena, especially when proteins are concerned. Indeed, the mechanisms described to explain the antimicrobial activity of peptides and binding of lysozyme upon phospolipid bilayers generally suppose conformational modifications.[21,36] Then, protein structure changes at the water/lipid interface could be slow events, because of the higher molecular mass and rigidity of proteins, compared to small and flexible antibacterial peptides. Especially, HEWL is known as a highly structured and stable protein consisting of 129 amino acids cross-linked by 4 disulfide bridges.[37] In the present study, Lehrer's protocol has thus been modified for long duration experiments to investigate membrane perturbation by lysozyme. Improvements were necessary to circumvent inconveniences such as evaporation, sedimentation, and signal instability.

MATERIALS AND METHODS

If not stated otherwise, chemicals were obtained from Sigma-Aldrich (Saint-Quentin, France).

Bacterial Strains. The bacterial strain *E. coli* ML-35p, which is lactose permease deficient and expresses *β*-lactamase and *β*-galactosidase in the periplasm and cytoplasm, respectively, was kindly provided by Destoumieux-Garzon, initially supplied by Lehrer. *E. coli* ML-35p was grown overnight (18 h) in TSB (AES, Bruz, France) with 50 *μ*g/mL ampicillin at 37 °C under stirring (130 rpm). The bacterial culture was washed twice in Tris-HCl buffer (50 mM, pH 7.0). The absorbance of the final suspension was around 1.0 at 620 nm, corresponding to about 10^9 CFU/mL. The 10^8 and 10^7 CFU/mL solutions were prepared by appropriate 10-fold dilutions of the previous culture.

Signal Stability of the Substrates and Products of *β*-Lactamase and *β*-Galactosidase. To evaluate the signal stability of ONPG, ONP, and nitrocefin (Merck Chemicals, Darmstadt, Germany), solutions of 1, 0.07, and 0.015 g/L of these three reagents, respectively, were prepared in 50 mM Tris-HCl buffer, pH 7.0. The hydrolysis product of nitrocefin (HP-nitrocefin) was produced by the enzymatic reaction (1 h, 25 °C) between nitrocefin (0.015 g/L) and penicillinase from *Bacillus cereus* (3.5 g/L) in 50 mM Tris-HCl buffer, pH 7.0. Three hundred microliter aliquots of each solution (ONPG, ONP, nitrocefin, HP-nitrocefin) were dispensed into microplate wells. The absorbance of the four substances was subsequently measured by a spectrophotometer Spectramax M2 (Molecular Devices, UK) for 10 h, after sealing or not the microplates with a Clear Seal film (4titude, Surrey, UK). The stability of ONPG and ONP was determined by ONP absorbance at 420 nm. The stability of nitrocefin and HP-nitrocefin was determined by absorbance at 390 and 486 nm, respectively.

Outer and Inner Membrane Permeability. Melittin from bee venom (85% purity) was used as a positive control in the membrane permeability experiments. Melittin is a small peptide, constituted of 26 amino acids.[38] This peptide is active on biological membranes and shows antimicrobial activity;[37] it is especially known to form pores in bacterial membranes and to permeabilize the outer and inner membranes.[33,39]

Melittin and lysozyme (Liot, Annezin, France) activity against the outer and inner membranes was measured. The sample solutions to measure their activity contained either 0.015 mg/mL melittin or 0.05 mg/mL up to 10 mg/mL of lysozyme. The sample solutions were inoculated with 10^7 or 10^8 CFU/mL of *E. coli* ML-35p. A negative control sample consisted of solutions prepared as described above, but without melittin or lysozyme.

To test outer membrane permeability, 0.015 mg/mL nitrocefin (substrate of *β*-lactamase) was added to the sample solutions. When the outer membrane was permeabilized, the periplasmic *β*-lactamase came into contact with its substrate nitrocefin, resulting in HP-nitrocefin release (Figure 1). HP-nitrocefin absorbance was measured at 486 nm, at 37 °C under stirring.

This reaction could result from nitrocefin entrance into the bacteria and/or from *β*-lactamase leakage. To test the assumption of *β*-lactamase leakage in the presence of lysozyme, a 0.25 mg/mL lysozyme solution was inoculated with 10^7 CFU/mL *E. coli* ML-35p and incubated at 37 °C for 5 h before centrifugation (5000*g*, 10 min); the *β*-lactamase activity was then measured in the supernatant by adding 0.05 mg/mL nitrocefin. HP-nitrocefin absorbance was measured at 486 nm at 25 °C under stirring.

To test inner membrane permeability, 0.7 mg/mL ONPG (substrate of *β*-galactosidase) was added to the sample solutions. When the inner membrane was permeabilized, the cytoplasmic *β*-galactosidase came into contact with its substrate ONPG, resulting in ONP release (Figure 1). ONP absorbance was measured at 420 nm at 37 °C under stirring.

Similarly to what was described above, to test the assumption of *β*-galactosidase leakage from bacteria cells in the presence of lysozyme, a 0.25 mg/mL lysozyme solution was inoculated with 10^7 CFU/mL *E. coli* ML-35p and incubated at 37 °C for 5 h before centrifugation (5000*g*, 10 min); the *β*-galactosidase activity was then measured in the supernatant by adding 1 mg/mL ONPG. ONP absorbance was measured at 420 nm at 25 °C under stirring.

Quantification of Membrane Permeabilization. The absorbance responses versus time, resulting from experiments of outer and inner membrane permeabilization, were analyzed to quantify the antibacterial efficiency of melittin and lysozyme. Absorbance curves for both outer and inner membrane permeabilization are the result of an enzymatic reaction between a substrate and the respective enzyme, which becomes accessible when the membranes are permeabilized.

For outer membrane permeabilization, the maximal slope ($\Delta AU_{486\ nm}$/30 min) was considered to quantify the velocity of the enzymatic reaction. Because the substrate concentration was fixed, this velocity was relied only on the concentration of accessible enzyme; an increase of the accessible enzyme quantity was indicative of a more severe membrane disruption. Then, the higher is the maximal slope, the more intense is the outer membrane permeabilization.

For inner membrane permeabilization, the maximal slope ($\Delta AU_{420\ nm}$/30 min) was considered to quantify the intensity of the inner membrane disruption, in a similar way as described above. Moreover, the lag time before the absorbance signal increase was considered indicative of the delay between outer and inner membrane permeabilization. The lag time was determined as the intersection between the baseline and the tangent of the curve at the maximal slope (Figure 2).

Statistical Analysis. All experiments were at least performed in triplicates. Statistical analysis was performed with R 2.15.2. Significance levels were at least 95%. Data from the normal distribution and with equal variances were treated with parametric tests. In this case, for the

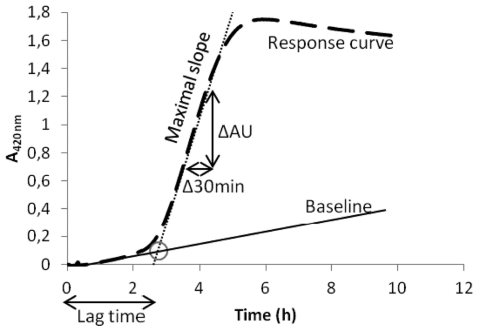

Figure 2. Quantification of inner membrane permeabilization using maximal slope and lag time.

comparison of means the Student *t* test was used. Data from other distributions or with unequal variances were treated with nonparametric tests. In this case, for the comparison of means the Wilcoxon rank sum test was used.

RESULTS

Preliminary Protocol Improvements for Reliable Measurements of Outer and Inner Membrane Disruption for Long Durations. Extension of Lehrer's method to long durations implies that substrates and products of β-lactamase and β-galactosidase are time-stable. Nitrocefin and ONPG absorbances were both stable at 37 °C for durations as long as 10 h (data not shown). On the contrary, the absorbances of HP-nitrocefin (Figure 3A) and ONP (Figure 3B) were not stable.

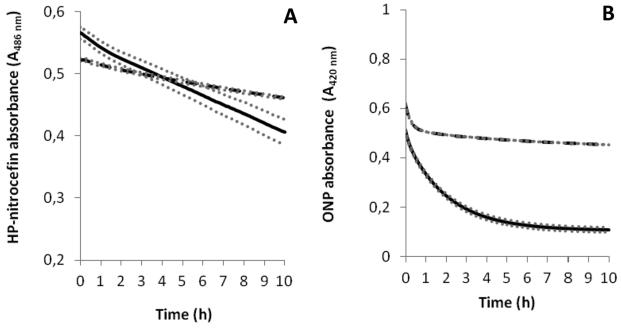

Figure 3. Absorbance stability of the reaction products of β-lactamase and β-galactosidase in nonsealed (full line) and sealed (dashed line) microplates. (A) HP-nitrocefin is detected by absorbance at 486 nm. (B) ONP is detected by absorbance at 420 nm. Standard deviation was calculated from triplicates (gray dotted line). Results were not corrected with a reference measurement, meaning that the absorbance values include the absorbance of the microplate and the buffer solution.

Sealing the microplate improved ONP stability from an 80% decrease to only 26% decrease of absorbance. Similarly, HP-nitrocefin absorbance decreased only 12% under sealed conditions compared to 28% under nonsealed conditions.

To prove the relevance of sealing microplates, melittin has been used as a reference antibacterial agent. When the outer membrane permeabilization was measured by melittin, the maximum absorbance was higher under sealed conditions, compared to nonsealed ones (Figure 4A). Moreover, a higher maximal slope was observed with a sealed microplate (Figure 4C).

When the inner membrane permeabilization was measured (Figure 4B), the absorbance signal corresponding to ONP release was dramatically different, depending on whether the microplate was sealed or not. Especially, during the first 3 h, the slope of the absorbance curve was much higher under sealed conditions. Because of this initial discrepancy, and despite an equivalent maximal slope between 3 and 5 h, the maximum absorbance was lower under nonsealed conditions (Figure 4B).

With regard to the latter results, experiments with lysozyme will be performed only with sealed microplates.

Lysozyme Activity against Outer and Inner Membranes of *E. coli*. Lehrer's method was applied to test HEWL activity, including the modifications as described above. The results exhibited that 0.25 mg/mL HEWL disturbed the outer membrane of *E. coli* because β-lactamase activity was detectable after around 0.5 h of incubation, whereas no absorbance was measured in the negative control, that is, without lysozyme (Figure 5A). Despite HP-nitrocefin content subsequently increasing in the negative control, it remained much lower than in the presence of 0.25 mg/mL lysozyme, throughout the 10 h experiment. Moreover, the supernatant of the bacterial suspension treated with lysozyme contained β-lactamase activity, unlike the supernatant of the negative control (Figure 5C).

During the first 2 h, a slight β-galactosidase activity was also measured, but in a similar way in samples with and without lysozyme (Figure 5B). On the contrary, when the experiment was extended to durations as long as 2.7 h and longer, β-galactosidase activity was much more extensive in the presence of 0.25 mg/mL HEWL, compared to the negative control (Figure 5B). However, the supernatant of the bacterial suspension treated with lysozyme did not contain β-galactosidase activity (data not shown).

Membrane Permeabilization Depending on Lysozyme Concentration and *E. coli* Inoculum. When 10^7 CFU/mL *E. coli* was inoculated, β-lactamase activity, that is, outer membrane permeabilization, remained unchanged whatever the lysozyme concentration was, from 0.05 to 10 mg/mL (maximal slope around 0.0025 $\Delta AU_{486\ nm}$/min; Figure 6A). On the contrary, when the inoculum was 10^8 CFU/mL, the intensity of outer membrane permeabilization increased when lysozyme concentration increased from 0.05 to 0.5 mg/mL; above 0.5 mg/mL HEWL, the intensity of outer membrane permeabilization decreased when the lysozyme concentration increased (Figure 6A).

For both inocula levels, β-galactosidase activity, that is, inner membrane permeabilization, increased when lysozyme concentration increased (higher maximal slope; Figure 6B). Moreover, the higher inoculum showed systematically higher maximal slopes. Considering the lag time, when 10^7 CFU/mL was inoculated, lag time strongly decreased when lysozyme concentration increased (Figure 6C). On the contrary, with 10^8 CFU/mL inoculum, the lag time first remained stable between 0.05 and 0.5 mg/mL HEWL and then slightly decreased when lysozyme concentration increased over 0.5 mg/mL HEWL (Figure 6C). Lag time was systematically shorter with 10^8 CFU/mL inoculum compared to 10^7 CFU/mL.

DISCUSSION

Membrane permeabilization is a major mechanism involved in the activity of many antimicrobial molecules, especially antimicrobial peptides and proteins.[9,10] Most of the studies aiming to highlight such bacterial membrane disruption are limited to short-time experiments (<2 h). However, it is conceivable that membrane permeabilization could sometimes need more time, especially when proteins are concerned. Indeed,

dx.doi.org/10.1021/jf4029199 | J. Agric. Food Chem. 2013, 61, 9922−9929

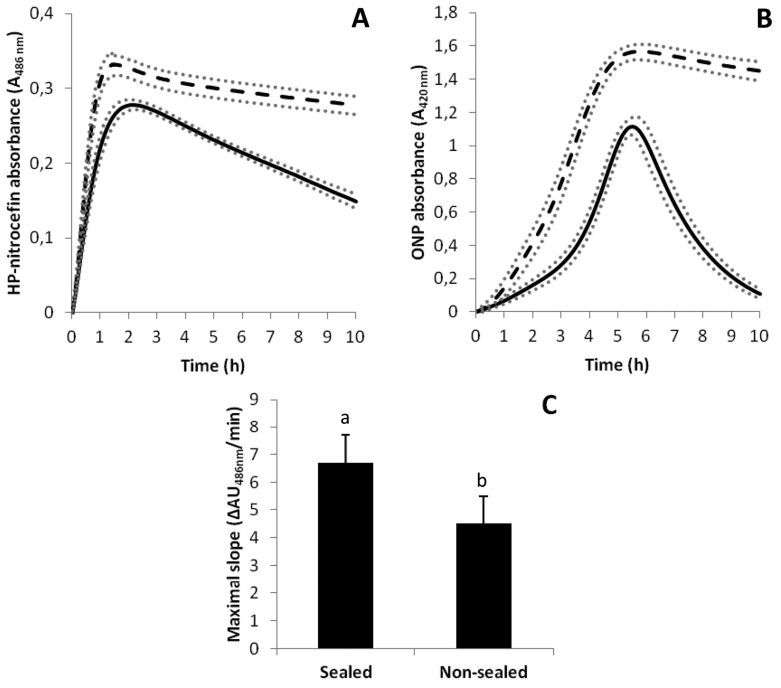

Figure 4. Permeabilization of the outer membrane (A) and inner membrane (B) of *E. coli* ML-35p (10^7 CFU/mL) by melittin (15 μg/mL) in nonsealed (full line) and sealed (dashed line) microplates, as evidenced by HP-nitrocefin and ONP release, respectively. Standard deviations were calculated from nine replicates (gray dotted line). Results were corrected with a reference absorbance including the absorbance of the microplate and the buffer solution. (C) Comparison of the maximal slopes for outer membrane permeabilization with and without sealing. Different letters (a, b) indicate significant difference ($p < 0.05$, Student t test).

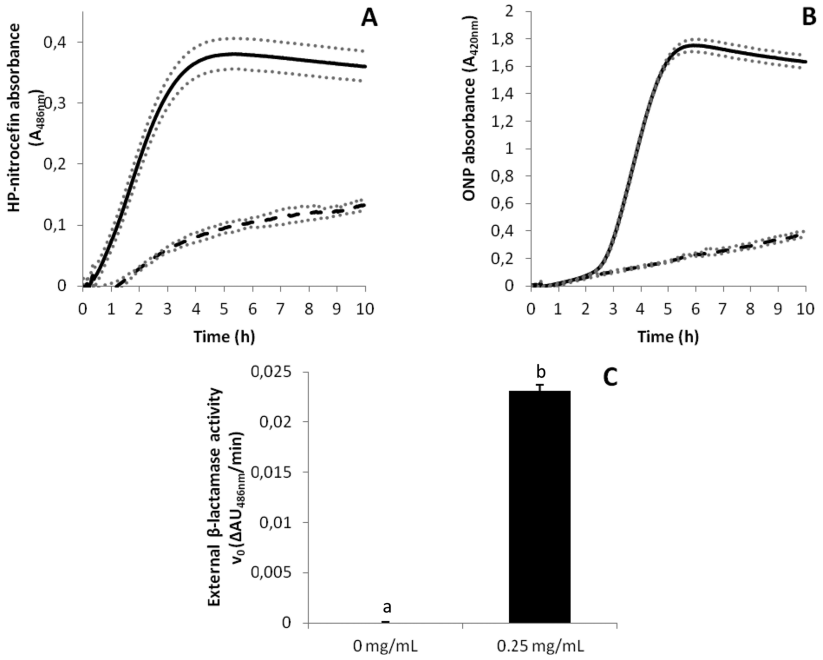

Figure 5. Permeabilization of outer membrane (A) and inner membrane (B) of *E. coli* ML-35p (10^7 CFU/mL) for 10 h, in the presence of 0.25 mg/mL HEWL (full line), and without lysozyme (dashed line). Standard deviations were calculated from triplicates (gray dotted line). Results were corrected with a reference absorbance including the absorbance of the microplate and buffer solution. (C) Externalization of β-lactamase in the absence and presence of 0.25 mg/mL of lysozyme measured by supernatant enzyme activity. Results stem from six replicates. Different letters (a,b) indicate significant difference ($p < 0.01$, Wilcoxon rank sum test).

mechanisms described to explain the antimicrobial activity of peptides and the interaction between lysozyme and lipid bilayers generally suppose conformational modifications.[21,36] Then, protein structure changes at the water/cell membrane interface might be slower than with peptides, because proteins are generally much more rigid molecules compared to peptides.

dx.doi.org/10.1021/jf4029199 | J. Agric. Food Chem. 2013, 61, 9922−9929

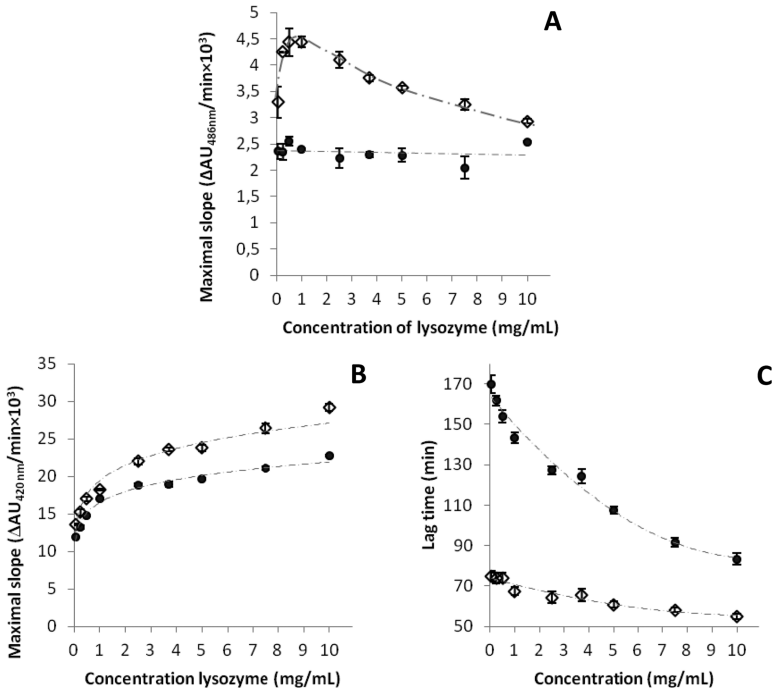

Figure 6. Membrane permeabilization as a function of lysozyme concentration for 10^7 CFU/mL (●) and 10^8 CFU/mL (◇) inocula: (A) outer membrane permeabilization as evidenced by β-lactamase activity; inner membrane permeabilization as evidenced by (B) β-galactosidase activity and (C) lag time between outer and inner membrane permeabilization. Standard deviations were calculated from triplicates.

Especially, HEWL is known as a particularly rigid protein cross-linked by four disulfide bridges.[37] The extension to long durations of the traditional methods to investigate bacterial membrane permeabilization by proteins is then a relevant challenge. The popular and simple spectrophotometric method developed by Lehrer has here been selected for such an adaptation.[32]

Sealing Microplates Is an Efficient Way To Improve the Reliability of Lehrer's Method for Long Experiments. To extend Lehrer's method to durations longer than 2 h, the substrates (ONPG and nitrocefin) and the products (ONP and HP-nitrocefin) of both enzymatic reactions need to be stable at 37 °C. This condition was not fulfilled for ONP, even for short-time experiments (Figure 3B), and to a lesser extent for HP-nitrocefin (Figure 3A). ONP, which results from ONPG hydrolysis by β-galactosidase, turns out to be especially unstable when nonsealed plates are used (Figure 3B). This is likely the result from the high volatility of this compound at 37 °C, because the ONP signal decrease is largely limited with sealed microplates. In these conditions, only a slight decrease is observed at the very beginning of the experiment (Figure 3B), probably due to the partial evaporation of ONP in the gas phase, between the liquid phase and the film, until the gas/liquid equilibrium was reached for this chemical compound. This observation suggests that a minimal headspace between the liquid phase and the film should be preferred; however, it cannot be reduced to zero, because of practical considerations such as sealing difficulty and risk of cross-contamination between adjacent wells. Although much less significant than for ONP, the HP-nitrocefin signal also decreases throughout the 10 h experiment when performed without sealing; this decrease is smaller when microplates are previously sealed (Figure 3A). Sealing microplates as proposed in this study appears then to be an easy and efficient way to improve the reliability of Lehrer's method when time extension up to 10 h is needed. Moreover, sealing avoids cross-contamination between wells, which can happen because of microplate stirring.

When the modified method (sealing microplates) was performed to measure the melittin antibacterial activity against *E. coli*, the results were significantly improved compared to the original method: higher initial rates were measured for both outer and inner membrane permeabilization (Figure 4). This indicates that the technical adjustments proposed in this study solve the underestimation induced by the original protocol. This underestimation is quite moderate for outer membrane permeabilization (Figure 4A), but a huge difference exists for the measurement of the inner membrane permeabilization (Figure 4B). In the latter case, the use of sealed microplates appears absolutely necessary, even for short-time experiments. Indeed, even in the very first moments of the test, because an extensive and quick disappearance of ONP occurs simultaneously with ONP enzymatic release, the initial rate of permeabilization is underestimated by 80% when nonsealed microplates are used.

HEWL Disrupts Outer and Inner Membranes of *E. coli*. The method adjustments proposed above enabled the investigation of lysozyme membrane activity for durations as long as 10 h. With such long experiments, the ability of HEWL to permeabilize both outer and inner membranes of *E. coli* was demonstrated. Indeed, both β-lactamase and β-galactosidase activities were detected when HEWL (0.25 mg/mL) was added to an *E. coli* culture, as indicated by HP-nitrocefin and ONP release, respectively (Figure 5). The weak absorbance signals obtained with the negative control likely result from the spontaneous lysis of bacteria that occurs during the 10 h experiments. However, both β-lactamase and β-galactosidase activities were higher when HEWL was added, undoubtedly proving the membrane permeabilization induced by lysozyme.

dx.doi.org/10.1021/jf4029199 | J. Agric. Food Chem. 2013, 61, 9922−9929

Outer membrane permeabilization has already been described by Wild et al. and Pelligrini et al. for a similar HEWL concentration.[7,40] These authors observed the outer membrane permeabilization using electron microscopy and Lehrer's membrane permeabilization assay, respectively. The original Lehrer method enabled this because outer membrane permeabilization occurs after around 30 min, for 0.25 mg/mL lysozyme. However, these authors conclude that no inner membrane permeabilization occurs due to the direct action of HEWL.

The present study highlights that, when Lehrer's method is extended to long durations, HEWL induces inner membrane permeabilization, too, but this is only detectable after 2.7 h of incubation with 0.25 mg/mL HEWL and 10^7 CFU/mL *E. coli* inoculum. It is then a slow phenomenon, compared to what is usually observed with antibacterial peptides. The delay necessary for the detection of the inner membrane permeabilization could be explained by the succession of hurdles that HEWL has to get over: passing through the outer membrane, peptidoglycan hydrolysis or diffusion through the peptidoglycan network,[41] and finally disturbance of the inner membrane.

To ensure that the inner membrane permeabilization is not the result of cell lysis caused by peptidoglycan disintegration, the presence of β-galactosidase was investigated in the supernatant of the *E. coli* cells (10^7 CFU/mL) treated with 0.25 mg/mL lysozyme (as explained under Outer and Inner Membrane Permeability). β-Galactosidase would be present in the supernatant when peptidoglycan disintegration and thus cell lysis occur.[42] However, no β-galactosidase activity could be measured in the supernatant, demonstrating that this enzyme was not leaking out of the cytoplasm; then, there was no cell lysis, and the β-galactosidase activity detected when *E. coli* cells are in the presence of lysozyme resulted from the diffusion of ONPG into the cell. This confirms that HEWL directly acts on the inner membrane of *E. coli*, modifying its permeability, and independent of the lysozyme enzymatic activity on peptidoglycan.

It is noticeable that, in opposition to β-galactosidase, β-lactamase activity was measured in the supernatant of *E. coli* cells treated with 0.25 mg/mL lysozyme (Figure 5C). This proves that HEWL disrupts the outer membrane in such a way that this enzyme of 28.9 kDa can leak out of the periplasm. Large size pores inside the outer membrane are thus induced by HEWL.

HEWL Acts by a Two-Step Process: Saturation of the Outer Membrane before Entrance into the Cell and Permeabilization of the Inner Membrane. The extent of the outer membrane permeabilization, quantified by the β-lactamase activity (Figure 6A), was unchanged between 0.05 and 10 mg/mL HEWL with inoculation of 10^7 CFU/mL. On the contrary, the outer membrane permeabilization increased when HEWL concentration increased from 0.05 to 0.5 mg/mL with inoculation of 10^8 CFU/mL. This suggests that a critical ratio for outer membrane saturation should be 0.05 mg/mL HEWL:10^7 CFU/mL *E. coli*. Indeed, β-lactamase activity did not increase when >0.05 mg/mL lysozyme was added to 10^7 CFU/mL. Moreover, the maximum β-lactamase activity when 10^8 CFU/mL was inoculated was reached at a ratio 0.5 mg/mL lysozyme:10^8 CFU/mL, that is, the same ratio as 0.05 mg/mL HEWL:10^7 CFU/mL.

As far as the inner membrane is concerned, a dose−response effect occurred for 0.05−10 mg/mL HEWL at both *E. coli* inocula (10^7 and 10^8 CFU/mL). The extent of the inner membrane permeabilization increased when HEWL concentration increased (Figure 6B). The maximal slopes obtained with 10^8 CFU/mL inoculum were systematically higher than those obtained with 10^7 CFU/mL. This is consistent with the higher quantity of β-galactosidase potentially accessible to ONPG when the bacterial inoculum was higher. Simultaneously, the lag time decreased when the HEWL concentration increased, for both *E. coli* inocula (Figure 6C). Because the lag time is the delay needed for the release of detectable quantities of ONP, a lag time decrease indicates a faster increase of ONP concentration, related to a higher β-galactosidase activity. Therefore, the lag time is consistently shorter with 10^8 CFU/mL *E. coli* compared to 10^7 CFU/mL.

When the inoculum was 10^7 CFU/mL *E. coli*, the lag time regularly and strongly decreased when HEWL increased from 0.05 to 10 mg/mL. This suggests that the higher the HEWL concentration in the bulk, the higher the quantity of HEWL reaching the inner membrane. The lag time decrease is then consistent with the assumption of the outer membrane saturation with HEWL concentration of 0.05 mg/mL or higher and 10^7 CFU/mL *E. coli*. Indeed, because of such a saturation, each additional HEWL molecule added in the bulk remains "free" (not entrapped into the outer membrane), able to cross over the disrupted outer membrane and to reach the inner membrane.

When 10^8 CFU/mL *E. coli* was inoculated, the lag time was constant between 0.05 and 0.5 mg/mL HEWL. Because the outer membrane would not be saturated with HEWL molecules in these conditions, as suggested above, each additional HEWL molecule added in the bulk would then be essentially entrapped inside the outer membrane and then unavailable for deeper penetration into the bacteria cell. On the contrary, with HEWL concentrations >0.5 mg/mL, meaning when outer membrane saturation is achieved, the lag time decreased when HEWL concentration increased, similarly to what was observed when 10^7 CFU/mL *E. coli* was inoculated; in these conditions, each additional HEWL molecule remains "free" and able to enter into the cell. However, even with the highest lysozyme concentration, that is, 10 mg/mL, the lag time remained >50 min; this could be the minimal delay for lysozyme entrance into the cell and interaction with the inner membrane.

Outer Membrane Permeabilization Is Reduced When *E. coli* Inoculum and HEWL Concentration Are Simultaneously High. At high inoculum levels, quorum sensing can play a major role in bacterial resistance against antimicrobial agents.[43] Quorum sensing is a cell-to-cell communication between bacteria by excretion of signal molecules, which can be detected by other bacteria of the same or other species.[44] In *E. coli* K12, AI-2 is one of those signal molecules that up-regulates several genes related to the outer membrane such as *rfaY*; *rfaY* controls the LPS-core biosynthesis. Stress induction of AI-2 has been demonstrated due to the addition of glucose, Fe^{3+}, NaCl, and dithiothreitol.[45,46] Thus, quorum sensing can be a stress-induced phenomenon.

In the present study, it is noticeable that *E. coli* outer membrane permeabilization decreased when HEWL concentration exceeds 1 mg/mL and when 10^8 CFU/mL was inoculated, but this was not observed when inoculum was 10^7 CFU/mL (Figure 6A). The assumption of a lysozyme stress ($\geq$1 mg/mL) could be proposed. This stress could activate quorum sensing between bacterial cells, in a dose-dependent manner. In these conditions, that is, high inoculum and high HEWL concentration, the outer membrane permeabilization of some bacterial cells may induce the expression of signal molecules, which could activate defense mechanisms by the sister cells. These defense mechanisms could include changes in the outer

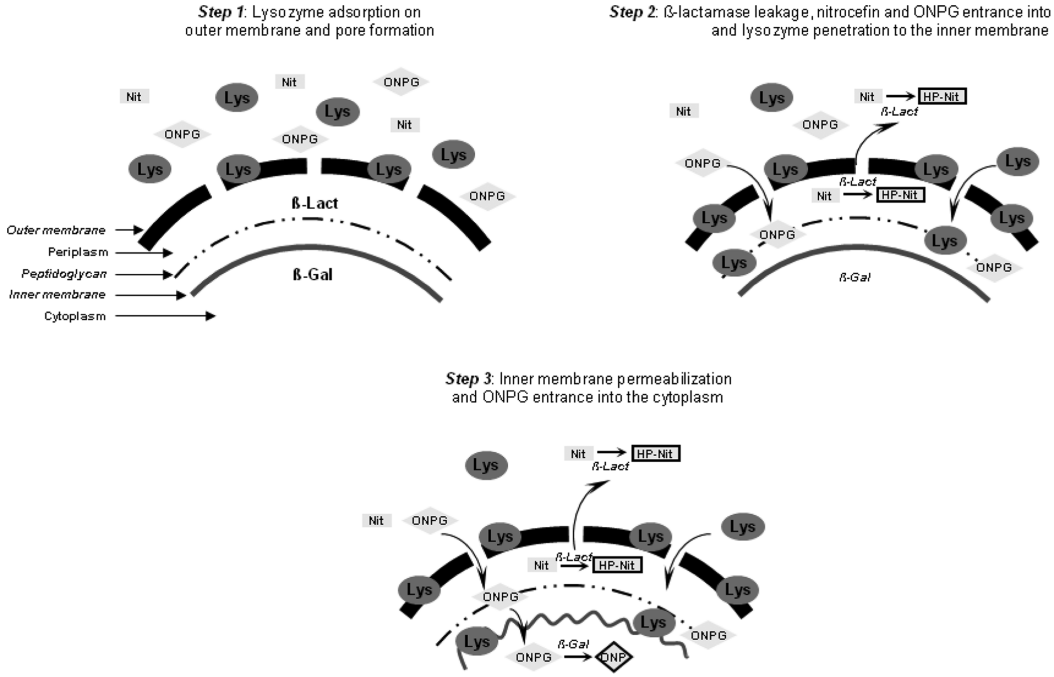

Figure 7. Hypothetical sequential events explaining the action of HEWL on outer and inner membranes of *E. coli*. Lys, lysozyme; *β*-Lact, *β*-lactamase; *β*-Gal, *β*-galactosidase; Nit, nitrocefin, and HP-Nit, HP-nitrocefin, substrate and product of *β*-lactamase, respectively; ONPG and ONP, substrate and product of *β*-galactosidase, respectively.

membrane composition, thus decreasing permeabilization by lysozyme. However, more investigations are needed to prove such hypothetical mechanisms.

This study then demonstrated that HEWL is able to permeabilize the outer and inner membranes of *E. coli*. A sequential event is proposed (Figure 7): first, entrapping of HEWL molecules inside the outer membrane, inducing its disruption with large size pore creation; then, transfer of "free" HEWL into the cell, to the inner membrane having increased permeability, but without massive cytoplasm leakage. Whereas the first step is quite rapid, the second one is a much longer phenomenon, depending on the quantity of "free" HEWL and then depending on the initial HEWL concentration in the bulk. Experiments are in progress to investigate the interactions between HEWL and *E. coli* membranes.

AUTHOR INFORMATION

Corresponding Author

*(M.D.) Mailing address: Agrocampus Ouest, UMR1253 STLO 65, rue de St-Brieuc, 35042 Rennes cedex, France. Phone: +33/2.23.48.55.74. E-mail: melanie.derde@agrocampus-ouest.fr.

Funding

This research was funded by Conseil Régional de Bretagne.

Notes

The authors declare no competing financial interest.

ACKNOWLEDGMENTS

We thank Delphine Destoumieux-Garzon for kindly providing the *E. coli* ML-35p strain.

ABBREVIATIONS USED

HEWL, hen egg white lysozyme; LPS, lipopolysaccharide; NPN, 1-*N*-phenylnaphthylamine; $DiSC_3$, 3,3-dipropylthiadicarbocyanine iodide; ONPG, *o*-nitrophenylgalactoside; ONP, *o*-nitrophenol; HP-nitrocefin, hydrolysis product of nitrocefin

REFERENCES

(1) TNS Opinion and Social. Special Eurobarometer 354: Food-related risks, 2010.

(2) Bruhn, C. M. Consumer attitudes toward food additives. In *Food Additives, 2*; Branen, A. L., Davidson, P. M., Salminen, S., Thorngate, J. H., Eds.; Dekker: New York, 2002; pp 111−119.

(3) Masschalck, B.; Michiels, C. W. Antimicrobial properties of lysozyme in relation to foodborne vegetative bacteria. *Crit. Rev. Microbiol.* **2003**, *29*, 191−214.

(4) Sonni, F.; Chinnici, F.; Natali, N.; Riponi, C. Pre-fermentative replacement of sulphur dioxide by lysozyme and oenological tannins: effect on the formation and evolution of volatile compounds during the bottle storage of white wines. *Food Chem.* **2011**, *129*, 1193−1200.

(5) Carini, S.; Mucchetti, G.; Neviani, E. Lysozyme: activity against Clostridia and use in cheese production − a review. *Microbiol., Aliments, Nutr.* **1985**, *3*, 299−320.

(6) Pellegrini, A.; Thomas, U.; Vonfellenberg, R.; Wild, P. Bactericidal activities of lysozyme and aprotinin against Gram-negative and Gram-positive bacteria related to their basic character. *J. Appl. Bacteriol.* **1992**, *72*, 180−187.

(7) Pellegrini, A.; Thomas, U.; Wild, P.; Schraner, E.; von Fellenberg, R. Effect of lysozyme or modified lysozyme fragments on DNA and RNA synthesis and membrane permeability of *Escherichia coli*. *Microbiol. Res.* **2000**, *155*, 69−77.

(8) Laible, N. J.; Germaine, G. R. Bactericidal activity of human lysozyme, muramidase-inactive lysozyme, and cationic polypeptides against *Streptococcus-sanguis* and *Streptococcus-faecalis* inhibition by chitin oligosaccharides. *Infect. Immun.* **1985**, *48*, 720−728.

(9) Mine, Y.; Ma, F.; Lauriau, S. Antimicrobial peptides released by enzymatic hydrolysis of hen egg white lysozyme. *J. Agric. Food Chem.* **2004**, *52*, 1088−1094.

(10) Ibrahim, H. R.; Thomas, U.; Pelligrini, A. A helix-loop-helix peptide at the upper lip of the active site cleft of lysozyme confers potent

antimicrobial activity with membrane permeabilization action. *J. Biol. Chem.* **2001**, *47*, 43767−43774.
(11) Ibrahim, H. R.; Imazato, K.; Ono, H. Human lysozyme possesses novel antimicrobial peptides within its N-terminal domain that target bacterial respiration. *J. Agri. Food Chem.* **2011**, *59*, 10336−10345.
(12) Ibrahim, H. R.; Kato, A.; Kobayashi, K. Antimicrobial effects of lysozyme against Gram-negative bacteria due to covalent binding of palmitic acid. *J. Agri. Food Chem.* **1991**, *39*, 2077−2082.
(13) Ibrahim, H. R.; Hatta, H.; Fujiki, M.; Kim, M.; Yamamoto, T. Enhanced antimcirobial action of lysozyme against Gram-negative and Gram-positive bacteria due to modification with perillaldehyde. *J. Agric. Food Chem.* **1994**, *42*, 1813−1817.
(14) Ibrahim, H. R.; Kobayashi, K.; Kato, A. Length of hydrocarbon chain and antimicrobial action to Gram-negative bacteria of fatty acylated lysozyme. *J. Agric. Food Chem.* **1993**, *41*, 1164−1168.
(15) Nakamura, S.; Kato, A.; Kobayashi, K. Bifunctional lysozyme galactomannan conjugate having excellent emulsifying properties and bactericidal effect. *J. Agric. Food Chem.* **1992**, *40*, 735−739.
(16) Nakamura, S.; Kato, A.; Kobayashi, K. New antimicrobial characteristics of lysozyme dextran conjugate. *J. Agric. Food Chem.* **1991**, *39*, 647−650.
(17) Ibrahim, H. R. On the novel catalytically-independent antimicrobial function of hen egg-white lysozyme: a conformation-dependent activity. *Nahrung* **1998**, *42*, 187−193.
(18) Ibrahim, H. R.; Higashiguchi, S.; Koketsu, M.; Juneja, L. R.; Kim, M.; Yamamoto, T.; Sugimoto, Y.; Aoki, T. Partially unfolded lysozyme at neutral pH agglutinates and kills Gram-negative and Gram-positive bacteria through membrane damage mechanism. *J. Agric. Food Chem.* **1996**, *44*, 3799−3806.
(19) Ibrahim, H. R.; Higashiguchi, S.; Juneja, L. R.; Kim, M.; Yamamoto, T. A structural phase of heat-denatured lysozyme with novel antimicrobial action. *J. Agric. Food Chem.* **1996**, *44*, 1416−1423.
(20) Ibrahim, H. R.; Higashiguchi, S.; Sugimoto, Y.; Aoki, T. Role of divalent cations in the novel bactericidal activity of the partially unfolded lysozyme. *J. Agric. Food Chem.* **1997**, *45*, 89−94.
(21) Nguyen, L. T.; Haney, E. F.; Vogel, H. J. The expanding scope of antimicrobial peptide structures and their modes of action. *Trends Biotechnol.* **2011**, *29*, 464−472.
(22) Jenssen, H.; Hamill, P.; Hancock, R. E. Peptide antimicrobial agents. *Clin. Microbiol. Rev.* **2006**, *19*, 491−511.
(23) Deckers, D.; Masschalck, B.; Aertsen, A.; Callewaert, L.; Van Tiggelen, C. G. M.; Atanassova, M.; Michiels, C. W. Periplasmic lysozyme inhibitor contributes to lysozyme resistance in *Escherichia coli*. *Cell Mol. Life Sci.* **2004**, *61*, 1229−1237.
(24) Callewaert, L.; Aertsen, A.; Deckers, D.; Vanoirbeek, K. G.; Vanderkelen, L.; Van Herreweghe, J. M.; Masschalck, B.; Nakimbugwe, D.; Robben, J.; Michiels, C. W. A new family of lysozyme inhibitors contributing to lysozyme tolerance in Gram-negative bacteria. *PloS Pathog.* **2008**, *4*, e1000019.
(25) Nikaido, H. Molecular basis of bacterial outer membrane permeability revisited. *Microbiol. Mol. Biol. Rev.* **2003**, *67*, 593−656.
(26) Alakomi, H.; Paananen, A.; Suihko, M.; Helander, I.; Saarela, M. Weakening effect of cell permeabilizers on Gram-negative bacteria causing biodeterioration. *Appl. Environ. Microbiol.* **2006**, *72*, 4695−4703.
(27) Vaara, M. Increased outer-membrane resistance to ethyl-enediaminetetraacetate and cations in novel lipid A mutants. *J. Bacteriol.* **1981**, *148*, 426−434.
(28) Orlov, D. S.; Nguyen, T.; Lehrer, R. I. Potassium release, a useful tool for studying antimicrobial peptides. *J. Microbiol. Methods* **2002**, *49*, 325−328.
(29) Silvestro, L.; Weiser, J. N.; Axelsen, P. H. Antibacterial and antimembrane activities of cecropin A in *Escherichia coli*. *Antimicrob. Agents Chemother.* **2000**, *44*, 602−607.
(30) Wu, M.; Maier, E.; Benz, R.; Hancock, R. E. Mechanism of interaction of different classes of cationic antimicrobial peptides with planar bilayers and with the cytoplasmic membrane of *Escherichia coli*. *Biochemistry* **1999**, *38*, 7235−7242.
(31) Meincken, A.; Holroyd, D. L.; Rautenbach, M. Atomic force microscopy study of the effect of antimicrobial peptides on the cell envelope of *Escherichia coli*. *Antimicrob. Agents Chemother.* **2005**, *49*, 4085−4092.
(32) Lehrer, R. I.; Barton, A.; Ganz, T. Concurrent assessment of inner and outer-membrane permeabilization and bacteriolysis in *Escherichia coli* by multiple-wavelength spectrophotometry. *J. Immunol. Methods* **1988**, *108*, 153−158.
(33) Epand, R. F.; Pollard, J. E.; Wright, J. O.; Savage, P. B.; Epand, R. M. Depolarization, bacterial membrane composition, and the antimicrobial action of ceragenins. *Antimicrob. Agents Chemother.* **2010**, *54*, 3708−3713.
(34) Gonzalez, M.; Gueguen, Y.; Destoumieux-Garzon, D.; Romestand, B.; Fievet, J.; Pugniere, M.; Roquet, F.; Escoubas, J. M.; Vandenbulcke, F.; Levy, O.; Saune, L.; Bulet, P.; Bachere, E. Evidence of a bactericidal permeability increasing protein in an invertebrate, the *Crassostrea gigas* Cg-BPI. *Proc. Natl. Acad. Sci. U.S.A.* **2007**, *104*, 17759−17764.
(35) Turner, J.; Cho, Y.; Dinh, N. N.; Waring, A. J.; Lehrer, R. I. Activities of LL-37, a cathelin-associated antimicrobial peptide of human neutrophils. *Antimicrob. Agents Chemother.* **1998**, *42*, 2206−2214.
(36) Gorbenko, G. P.; Ioffe, V. M.; Kinnunen, P. K. Binding of lysozyme to phospholipid bilayers: evidence for protein aggregation upon membrane association. *Biophys. J.* **2007**, *93*, 140−153.
(37) Canfield, R. E.; Liu, A. K. The disulfide bonds of egg white lysozyme (muramidase). *J. Biol. Chem.* **1965**, *240*, 1997−2002.
(38) Terwilliger, T. C.; Eisenberg, D. The structure of melittin. II. Interpretation of the structure. *J. Biol. Chem.* **1982**, *257*, 6016−6022.
(39) Lee, M. T.; Sun, T. L.; Hung, W. C.; Huang, H. W. Process of inducing pores in membranes by melittin. *Proc. Natl. Acad. Sci. U.S.A.* **2013**, DOI: 10.1073/pnas.1307010110.
(40) Wild, P.; Gabrieli, A.; Schraner, E. M.; Pellegrini, A.; Thomas, U.; Frederik, P. M.; Stuart, M. C. A.; Vonfellenberg, R. Reevaluation of the effect of lysoyzme on *Escherichia coli* employing ultrarapid freezing followed by cryoelectronmicroscopy or freeze substitution. *Microsc. Res. Tech.* **1997**, *39* (3), 297−304.
(41) Vollmer, W.; Bertsche, U. Murein (peptidoglycan) structure, architecture and biosynthesis in *Escherichia coli*. *Biochim. Biophys. Acta* **2008**, *1778*, 1714−1734.
(42) Silhavy, T. J; Kahne, D.; Walker, S. The bacterial cell envelope. *Cold Spring Harbor Perspect. Biol.* **2010**, *2*, a000414.
(43) Mah, T. F.; O'Toole, G. A. Mechanisms of biofilm resistance to antimicrobial agents. *Trends Microbiol.* **2001**, *9*, 34−39.
(44) Waters, C. M.; Bassler, B. L. Quorum sensing: cell-to-cell communication in bacteria. *Annu. Rev. Cell Dev. Biol.* **2005**, *21*, 319−346.
(45) DeLisa, M. P.; Wu, C. F.; Wang, L.; Valdes, J. J.; Bentley, W. E. DNA microarray-based identification of genes controlled by auto-inducer 2-stimulated quorum sensing in *Escherichia coli*. *J. Bacteriol.* **2001**, *183*, 5239−5247.
(46) DeLisa, M. P.; Valdes, J. J.; Bentley, W. E. Mapping stress-induced changes in autoinducer AI-2 production in chemostat-cultivated *Escherichia coli* K-12. *J. Bacteriol.* **2001**, *183*, 2918−2928.

JOURNAL OF AGRICULTURAL AND FOOD CHEMISTRY

Article

pubs.acs.org/JAFC

Dry-Heating of Lysozyme Increases Its Activity against *Escherichia coli* Membranes

Melanie Derde,*[,†,‡] Catherine Guérin-Dubiard,[†,‡] Valérie Lechevalier,[†,‡] Marie-Françoise Cochet,[†,‡] Sophie Jan,[†,‡] Florence Baron,[†,‡] Michel Gautier,[†,‡] Véronique Vié,[§] and Françoise Nau[†,‡]

[†]Agrocampus Ouest, UMR1253 Science et technologie du lait et de l'œuf, F-35042 Rennes, France

[‡]INRA, UMR1253 Science et technologie du lait et de l'œuf, F-35042 Rennes, France

[§]Institut de physique de Rennes, Université de Rennes 1, UMR6251, CNRS, F-35042 Rennes, France

ABSTRACT: For food as well as for medical applications, there is a growing interest in novel and natural antimicrobial molecules. Lysozyme is a promising candidate for the development of such molecules. This protein is largely studied and known for its muramidase activity against Gram-positive bacteria, but it also shows antimicrobial activity against Gram-negative bacteria, especially when previously modified. In this study, the activity of dry-heated lysozyme (DH-L) against *Escherichia coli* has been investigated and compared to that of native lysozyme (N-L). Whereas N-L only delays bacterial growth, DH-L causes an early-stage population decrease. The accompanying membrane permeabilization suggests that DH-L induces either larger pores or more pores in the outer membrane as compared to N-L, as well as more ion channels in the inner membrane. The strong morphological modifications observed by optical microscopy and atomic force microscopy when *E. coli* cells are treated with DH-L are consistent with the suggested disturbances of membrane integrity. The higher hydrophobicity, surface activity, and positive charge induced by dry-heating could be responsible for the increased activity of DH-L on the *E. coli* membranes.

KEYWORDS: *lysozyme, dry-heating, antimicrobial activity, membrane disruptions, Gram-negative bacteria*

INTRODUCTION

Today's society is confronted with the severe public health issue of bacterial antibiotic resistance. Decades of misuse of the available antibiotics have caused the development of multiple resistant strains such as the Gram-positive *Staphylococcus aureus* and *Enterococcus faecium* and the Gram-negative *Klebsiella pneumonia*, *Escherichia coli*, and *Pseudomonas aeruginosa*.[1] These pathogens are thus hard to treat, and remaining effective remedies are long and expensive. Research for novel active molecules is thus indispensable to ensure treatment of bacterial infections.

On the other hand, a consumer demand is observed for natural food preservatives. Consumers are concerned with the quality of ready to eat meals, which sometimes contain preservatives necessary for long food shelf life and food safety,[2,3] but consumer knowledge about these additives is often limited, and thus, perception of the preservatives used has to be considered. Especially, natural compounds sound more familiar and are perceived safer and healthier. The research for natural antimicrobial compounds is thus also stimulated by the food industry.

As a consequence, for medical as well as food applications, specific attention is devoted to natural antimicrobial molecules that can offer a broad spectrum and limit bacterial resistance development. Molecules that disturb bacterial membranes are especially relevant to achieve this latter objective, since development of microbial resistance by gene mutation is less likely with molecules acting on such generalized targets.[4,5] Moreover, these molecules must preferably not be too expensive and must be easily available.

An interesting natural antimicrobial molecule is the small protein lysozyme (14.4 kDa).[6] This protein is abundant in hen egg white and already available on the industrial scale through a quite easy purification process, resulting in a market value of about 100 €/kg. This protein has already been approved as a food preservative in cheese and wine (E 1105) by the European Union[7] and as a pharmacological product for buccal problems.

In this context, lysozyme is used for its well-known enzymatic activity against Gram-positive micro-organisms: lysozyme hydrolyzes *N*-acetylmuramic acid and *N*-acetylglucosaminic acid β-(1,4) bonds of the peptidoglycan glycosidic chain, causing cell lysis and thus cell death. Several defense strategies against this enzymatic activity have been identified in both Gram-positive and Gram-negative bacteria. In Gram-positive bacteria, O-acetylation and de-N-acetylation of the peptidoglycan cause resistance against lysozyme;[8−10] these resistance mechanisms are found in *S. aureus* and *Bacillus anthracis*, respectively. Gram-negative bacteria are protected against lysozyme by the outer membrane which physically separates the periplasm and the peptidoglycan layer from the external environment.[11] However, some Enterobacteriaceae such as *E. coli*, *P. aeruginosa*, and *Salmonella* Enteritidis express lysozyme inhibitors in the periplasm; two lysozyme inhibitors have been identified up till now in the periplasm of *E. coli:* Ivy and MliC.[12−14] This suggests that lysozyme can cross the outer membrane of these Gram-negative bacteria, accordingly with

Received: November 19, 2013
Revised: January 20, 2014
Accepted: January 22, 2014
Published: January 22, 2014

dx.doi.org/10.1021/jf405155p | *J. Agric. Food Chem.* 2014, 62, 1692−1700

the membrane disturbance assumed to explain the proven activity of lysozyme against some Gram-negative strains.[15−17]

Molecules that provoke bacterial membrane disruption are mostly positively charged, amphipathic, and hydrophobic.[4] Lysozyme possesses these physicochemical criteria at physiological pH. However, lysozyme activity against Gram-negative bacteria remains limited, but when lysozyme is modified by fusion with a chemical moiety,[18−23] heat denaturation,[24−26] or enzymatic hydrolysis,[27,28] its antimicrobial activity is enhanced. One relevant question is then to investigate the antibacterial activity against Gram-negative bacteria of lysozyme modified to increase its positive charge and/or amphipathicity and/or hydrophobicity. Dry-heating of lysozyme has been described as an easy process resulting in different lysozyme isoforms, some of them being especially more positive and more hydrophobic than native hen egg white lysozyme.[29] This modified lysozyme could then be an opportunity to create a new efficient antimicrobial, simply using a safe physical treatment.

MATERIALS AND METHODS

Materials. Native lysozyme powder (pH 3.2) was obtained from Liot (Annezin, 62-France); it was heated for 7 days at 80 °C in hermetically closed glass tubes to obtain dry-heated lysozyme. *Micrococcus lysodeikticus*, ATCC no. 4698, Trisma base, potassium phosphate monobasic, potassium phosphate dibasic, potassium chloride, ampicillin, chloramphenicol, (*o*-nitrophenyl)galactoside (ONPG), 3,3′-dipropylthiadicarbocyanine iodide ($DiSC_3$), 4-(2-hydroxyethyl)-1-piperazineethanesulfonic acid, 4-(2-hydroxyethyl)-1-piperazineethanesulfonic acid (HEPES), and glucose were obtained from Sigma-Aldrich (Saint-Quentin, France).

Nitrocefin, a standard solution of potassium (1000 mg/L), casein peptone, and yeast extract were obtained from Merck Chemicals (Darmstadt, Germany). Tryptic soy broth (TSB) was from AES (Bruz, France).

Bacterial Strains. Three different *E. coli* strains have been used (Table 1). *E. coli* K12 was obtained from the Institut Pasteur (Paris, France). *E. coli* MG1655 *ivy*::*Cm* was kindly provided by C. Michiels (Centre of Food and Microbial Technology, KU Leuven, Belgium); this bacterial strain no longer expresses the lysozyme inhibitor Ivy. The bacterial strain *E. coli* ML-35p (*LacI*$^-$ *LacY*$^-$ *LacZ*$^+$, plasmid pBR322) was kindly provided by R. Lehrer (Department of Medicine, University of California, Los Angeles) and transmitted to our laboratory by D. Destoumieux-Garzon (UMR 5119, Ecologie des systèmes marins côtiers, University of Montpellier, France). *E. coli* ML-35p lacks lactose permease and expresses *β*-lactamase and *β*-galactosidase in the periplasm and cytoplasm, respectively.

Table 1. Presence (+) or Absence (−) of Ivy, *β*-Lactamase, *β*-Galactosidase, and Lactose Permease in the Different Bacterial Strains Used for the Present Study

	Ivy	*β*-lactamase	*β*-galactosidase	Lactose permease
E. coli K12	+	−	+	+
E. coli ML-35p	+	+	+	−
E. coli MG1655 *ivy*::*Cm*	−	−	+	+

Growth Assays with *E. coli* K12 and *E. coli* MG1655 *ivy*::*Cm*. The bacterial culture *E. coli* K12 or *E. coli* MG1655 *ivy*::*Cm* was grown overnight (18 h) at 37 °C under stirring (130 rpm) in TSB containing 50 *μ*g/mL ampicillin or 30 *μ*g/mL chloramphenicol, respectively. After the incubation period, the cultures contained about 10^9 CFU/mL *E. coli*, from which 10^5 CFU/mL bacterial suspensions were prepared by performing four 10-fold serial dilutions in LB05 (Luria broth containing 10 g/L peptone of casein, 5 g/L yeast extract, and 0.5 g/L NaCl). After solubilization in demineralized water, lysozyme (native or dry-heated) was added at 0.25 or 3.7 g/L to the bacterial suspension, before incubation at 37 °C under stirring (130 rpm) for 24 h; 3.7 g/L is the natural concentration of lysozyme in hen egg white. Cell enumeration was performed by colony count after 2, 4, 6, and 24 h as previously described by Baron et al.[30] The results for cell counts are based on nine replicates (three biological replicates, each with three technical replicates).

Outer and Inner Membrane Permeability Measurements. Outer and inner membrane permeability was measured using the Lehrer method,[31] modified as described by Derde et al.[32] The *E. coli* ML-35p culture was grown overnight (18 h) in TSB containing 50 *μ*g/mL ampicillin at 37 °C under stirring (130 rpm). The bacterial culture was washed twice in 50 mM Tris−HCl buffer, pH 7.0 (5000*g*, 10 min), and diluted to obtain about 10^7 CFU/mL in solutions containing 0.25 or 3.7 g/L native or dry-heated lysozyme.

To test outer membrane permeability, 0.015 mg/mL nitrocefin (substrate of *β*-lactamase) was added to the sample solutions. When the outer membrane was permeabilized, the periplasmic *β*-lactamase hydrolyzed nitrocefin into the hydrolysis product of nitrocefin (HP-nitrocefin). HP-nitrocefin absorbance was measured at 486 nm (Spectramax M2, Molecular Devices, United Kingdom), at 37 °C under stirring.

To test inner membrane permeability, 0.7 mg/mL ONPG (substrate of *β*-galactosidase) was added to the sample solutions. When the inner membrane was permeabilized, the cytoplasmic *β*-galactosidase hydrolyzed ONPG into *o*-nitrophenol (ONP). ONP absorbance was measured at 420 nm (Spectramax M2, Molecular Devices, United Kingdom), at 37 °C under stirring.

Two parameters could then be determined: maximal slope and lag time. The maximal slope determined the maximal velocity of the enzymatic reaction of either *β*-lactamase or *β*-galactosidase. The maximal velocity is directly related to the concentration of accessible enzyme and thus to the permeability of the outer or inner membrane, respectively. The lag time was the time between outer and inner membrane permeabilization, estimated by the delay between both enzymatic reactions.

The results of lysozyme activity on membrane permeability are based on three replicates. The results were corrected for reference absorbance, i.e., the absorbance of the microplate and of the buffer solution.

Detection of *β*-Lactamase and *β*-Galactosidase Leakage out of Bacterial Cells. After overnight growth (18 h) in TSB containing 50 *μ*g/mL ampicillin at 37 °C under stirring (130 rpm), the *E. coli* ML-35p culture was washed twice with 50 mM Tris−HCl buffer, pH 7.0 (5000*g*, 10 min), and diluted to obtain 10^7 CFU/mL bacterial suspensions. These suspensions were added with lysozyme (0.25 or 3.7 g/L, native or dry-heated lysozyme) and incubated for 5 h at 37 °C under stirring, before centrifugation at 5000*g* for 10 min. *β*-Lactamase and *β*-galactosidase activities were then tested in the supernatants by adding 0.05 g/L nitrocefin and 1 g/L ONPG, respectively. The initial reaction rates of both enzymatic reactions (v_0 = ΔAU/min) were determined at 25 °C from absorbance curves (Multiskan Go, Thermo Fisher Scientific, Illkirch, France) at 486 and 420 nm, respectively.

Measurement of the Bacterial Membrane Potential Disruption. The disruption of the bacterial membrane potential was measured according to the method proposed by Wu et al.[33] The *E. coli* K12 culture was grown for 3.5 h in TSB at 37 °C under stirring (130 rpm) to reach a midlog phase. The culture was washed twice with 5 mM HEPES buffer at pH 7.2 containing 5 mM glucose (5000*g*, 10 min) and diluted to obtain an absorbance of around 0.06 at 620 nm. A 1 *μ*M concentration of $DiSC_3$ and 100 mM KCl were added to the diluted bacterial suspension, before incubation for 1 h at 30 °C in the dark. Then lysozyme (0.25 or 3.7 g/L, native or dry-heated) was added to the bacterial cells, and the samples were incubated for 30 min at 30 °C in the dark. Fluorescence was then measured at 670 nm with a fluorimeter, Perkin-Elmer LS55 (Perkin-Elmer, Courtaboeuf, France), after excitation at 622 nm; the slit width was 2.5 nm/2.5 nm, and the integration time was 6.2 s. The results are based on nine replicates (three biological replicates, each with three technical replicates).

Potassium Leakage Measurement. The measurement of potassium leakage was performed according to the method described by Orlov et al.[34] After overnight growth (18 h) in TSB at 37 °C under stirring (130 rpm), the *E. coli* K12 culture was washed twice with 10 mM Tris−acetate buffer, pH 7.0, containing 100 mM NaCl (5000*g*, 10 min), and diluted to obtain 10^8 CFU/mL bacterial suspensions. Lysozyme (0.25 or 3.7 g/L, native or dry-heated) was added to the bacterial solutions, and then the samples were incubated for 3 h at 37 °C under stirring, centrifugated (5000*g* for 10 min), and filtered with 0.22 μm filters. The K^+ concentration was measured in the filtrates using a potassium-selective electrode (DX239-K) coupled to an S50 SevenMulti meter (Mettler Toledo, Viroflay, France) and recorded with an ISE meter previously calibrated with six standard solutions containing 5.15, 10.3, 77.6, 103, 1330, and 11700 μM potassium, respectively. Calibration and measurements were performed at 25 °C.

Optical Microscopy and Atomic Force Microscopy (AFM). The *E. coli* K12 culture was grown overnight (18 h) in TSB at 37 °C under stirring (130 rpm). After the incubation period, the culture contained about 10^9 CFU/mL *E. coli*, from which 10^5 CFU/mL bacterial suspensions were prepared by performing four 10-fold serial dilutions in LB05. Then lysozyme (0.25 or 3.7 g/L, native or dry-heated) was added to the bacterial suspension before incubation at 37 °C under stirring (130 rpm) for 24 h. Samples were washed in a 0.85% NaCl solution (3000*g*, 10 min) before optical microscopy and AFM were performed.

Optical microscopy observations were performed with an Olympus BX51 (enlargement 100×). Images were taken with a digital camera, Olympus Camedia C-5050.

Samples were deposited on freshly cleaved mica. To avoid accumulation of bacteria, a dipper (Nima Technology, Cambridge, U.K.) was used to gently remove the mica from the sample solution at 2 mm/min while the solution was being stirred. The mica plate was then dried at room temperature, and shortly after that, AFM imaging was performed. Images were recorded with a Pico-plus atomic force microscope (Molecular Imaging, Phoenix, AZ) operating in tapping mode. A scanner of 100 μm was used for the measurements. Topographic and phase images, illustrating cell topography and cell heterogeneity,[35] were acquired simultaneously using silicon nitride tips (AppNano, Silicon Valley, CA) with a resonance frequency of 145−230 kHz and a nominal spring constant of 20−95 mN/m. Transversal cross sections of the bacteria were performed to illustrate height and surface roughness. The images presented in the present study are representative of several samples.

Statistical Analysis. All experiments were performed at least in triplicate. Statistical analysis was performed with R 2.15.2. Significance levels were at least 95%. Data from the normal distribution and with equal variances were treated with parametric tests. In this case, for the comparison of means the Student *t* test was used. Data from other distributions or with unequal variances were treated with non-parametric tests. In this case, for the comparison of means the Wilcoxon rank sum test was used.

RESULTS

Growth of *E. coli* in the Presence of Lysozyme. The growth of *E. coli* K12 is disturbed in the presence of both native (N-L) and dry-heated (DH-L) lysozyme during the first hours of growth (Figure 1A), but after 24 h of incubation at 37 °C, no significant difference is observed between the samples with or without lysozyme. The growth of *E. coli* K12 shows the same pattern when N-L is added, whatever the concentration (0.25 or 3.7 g/L), and when DH-L is added at low concentration (0.25 g/L): the bacterial growth is inhibited for 2 h, before it recovers, and cell counts similar to those in the control sample (without lysozyme) are finally reached. On the contrary, the addition of 3.7 g/L DH-L induces a different pattern of the *E. coli* K12 growth: 1 log reduction of the bacterial cells is observed after 2 h of incubation, after which the growth rate

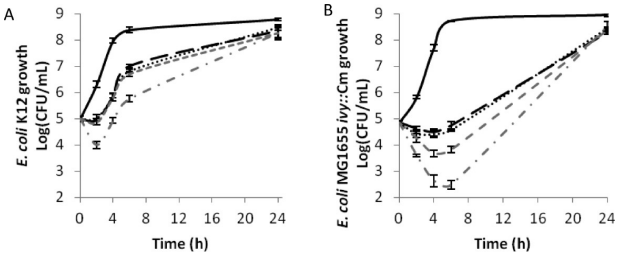

Figure 1. Growth curves of *E. coli* K12 (A) and of *E. coli* MG1655 *ivy*::*Cm* (B) in LB05 medium in the absence of lysozyme (—) or in the presence of 0.25 g/L N-L (− − −), 0.25 g/L DH-L (···), 3.7 g/L N-L (---,) or 3.7 g/L DH-L (-·-). The results are based on nine replicates.

recovers; with up to 6 h of incubation, the *E. coli* K12 population remains lower than in the other samples (control sample and samples with N-L or low-concentration DH-L).

When the same tests are performed on the *E. coli* MG1655 *Ivy*::*Cm* strain, which lacks the periplasmic lysozyme inhibitor Ivy, the impact of lysozyme on the bacterial growth pattern is stronger as compared to that for *E. coli* K12, for both N-L and DH-L and both concentrations (0.25 and 3.7 g/L) (Figure 1B). The modification of the growth pattern is dose-dependent: the higher the N-L or DH-L concentration, the higher the population decrease observed in the first hours of incubation. At high concentration (3.7 g/L), DH-L causes a population decrease which is 1.3 log higher than that of N-L, whereas no difference is observed between both types of lysozyme at low concentrations (0.25 g/L). However, the number of bacterial cells suitable for growth is the same after 24 h of incubation with N-L and DH-L.

Membrane State of *E. coli* in the Presence of Lysozyme. N-L and DH-L induce similar overall permeabilization of the outer membrane whatever the concentration, as measured by the total β-lactamase activity (Figure 2A), but externalized β-lactamase activity, i.e., activity in the supernatant resulting from centrifugation of the bacterial culture incubated with lysozyme, is higher with DH-L than with N-L at both lysozyme concentrations (Figure 2B). Moreover, it is noticeable

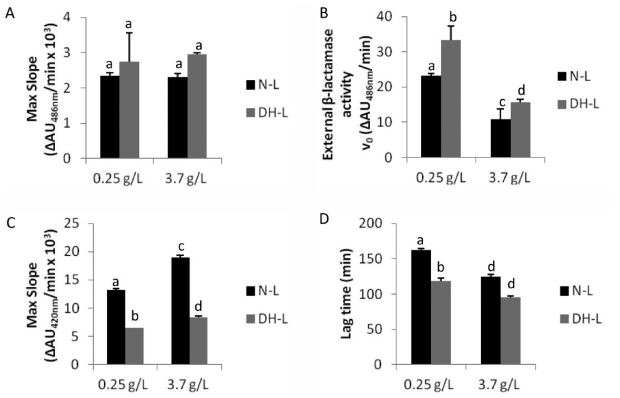

Figure 2. Comparison of the permeabilization of *E. coli* ML-35p outer (A, B) and inner (C, D) membranes by native (N-L) or dry-heated (DH-L) lysozyme as evidenced by β-lactamase and β-galactosidase activity, respectively. Different letters (a, b, c, d) indicate significant difference obtained from the Student *t* test (A, C, D) ($p < 0.01$) or Wilcoxon rank sum test (B) ($p < 0.01$).

dx.doi.org/10.1021/jf405155p | J. Agric. Food Chem. 2014, 62, 1692−1700

that a high concentration (3.7 g/L) of N-L and DH-L causes lower externalized β-lactamase activity than a low concentration (0.25 g/L) (Figure 2B).

Figure 2C shows that permeabilization of the inner membrane is stronger with N-L than with DH-L at either 0.25 or 3.7 g/L. On the other hand, the lag time before detection of the inner membrane permeabilization is shorter with DH-L than with N-L at both concentrations (Figure 2D). The intensity of inner membrane permeabilization and lag time are lysozyme concentration-dependent for both N-L and DH-L.

Disturbance of the inner membrane has also been investigated by measurement of changes of the membrane potential. N-L and DH-L similarly disturb the membrane potential of *E. coli* when added at 0.25 g/L in the bacterial culture. On the contrary, at higher concentration (3.7 g/L lysozyme), DH-L causes a stronger disruption of the membrane potential than N-L, as indicated by the 2-fold higher relative fluorescence of $DiSC_3$ (Figure 3A). For both N-L and DH-L, a dose−response effect is observed.

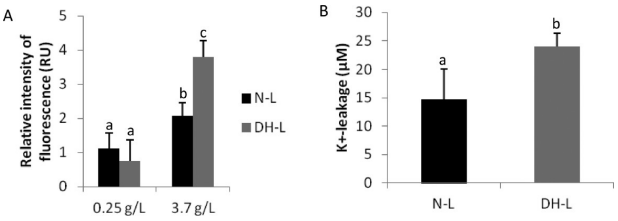

Figure 3. (A) Disruption of the membrane potential of *E. coli* K12 caused by native (N-L) or dry-heated (DH-L) lysozyme at 0.25 and 3.7 g/L. Different letters (a, b, c) indicate significant difference obtained from the Student *t* test ($p < 0.01$). Results are based on nine replicates. (B) K^+ leakage of *E. coli* K12 in the presence of 3.7 g/L N-L or DH-L after 3 h of incubation. Different letters (a, b) indicate significant difference obtained from the Student *t* test ($p < 0.01$). Results are based on six replicates.

Finally, the measurement of intracellular K^+ leakage has been used as an indicator of inner membrane disruption. K^+ leakage is not detectable in *E. coli* cultures containing 0.25 g/L N-L or DH-L (data not shown), but significant K^+ leakage is measured in the presence of 3.7 g/L lysozyme. The extent of the K^+ leakage is 75% higher with DH-L than with N-L (Figure 3B).

Morphology of *E. coli* K12 in the Presence of Lysozyme. *E. coli* K12 incubated for 24 h in the presence of 0.25 g/L lysozyme exhibits differences in cell morphology in comparison to the control sample, as shown by optical microscopy images (Figure 4). Abnormally elongated bacterial cells are observed after treatment with lysozyme; such modified bacteria are present in a larger number when DH-L is added as compared to N-L (Figure 4B,C). These elongated cells could not be observed at high concentration (3.7 g/L) of N-L and DH-L (data not shown).

Topographic AFM enables determination of the size and characterization of the shape and the surface topology of bacteria. Nontreated bacteria are about 2 μm long, with a diameter of 500 nm; the surface is smooth and regular, and flagella are observed (Figure 5A). When bacteria are treated with N-L, the size is not modified (Figure 5B,D), whereas abnormally elongated cells without a visible septum are observed when the bacteria are treated with 0.25 g/L DH-L (Figure 5C). With high-concentration N-L treatment (Figure 5D), depressions can be observed on the bacterial cells, but the bacterial morphology is more strongly disturbed when the bacteria are treated with DH-L (Figure 5C,E), with an especially irregular cell surface and depressions; the depth and the diameter of these depressions increase when the DH-L concentration increases: around 15 nm depth at 0.25 g/L DH-L versus around 26 nm at 3.7 g/L and around 128 nm diameter versus 160 nm. When the bacteria are treated with either 3.7 g/L N-L or both concentrations of DH-L, cell debris is also observed (data not shown).

Phase AFM enables visualization of homogeneity or heterogeneity of the cell surface composition.[35] Thus, the nontreated bacteria appear homogeneous (Figure 6A), whereas heterogeneity can be observed with all the treated samples, with either N-L or DH-L, and at both concentrations (Figure 6B−E). However, higher heterogeneity is observed when the bacteria are treated with DH-L as compared to N-L.

DISCUSSION

The capability of native hen egg white lysozyme to permeabilize the outer and inner membranes of *E. coli* has been previously established by Derde et al.[32] Moreover, some structural modifications of lysozyme proved to be efficient to enhance the antibacterial activity of this protein.[8] Modifying lysozyme to design a novel antimicrobial with enhanced membrane activity and thus improved antibacterial activity against *E. coli* then seems relevant. Because membrane activity of antimicrobial proteins or peptides is highly dependent on the physicochemical properties of the molecules, dry-heating could be an interesting process for lysozyme design. Indeed, dry-heated lysozyme is more hydrophobic and more surface-active, and it contains isoforms that are more positively charged than native lysozyme.[29] To test the hypothesis that dry-heated lysozyme is more active than native lysozyme against *E. coli*, because of an increased membrane activity, a comparative study is proposed.

Native Lysozyme Causes *E. coli* K12 Growth Latency. In the presence of low and high concentrations of N-L, the inhibition of *E. coli* K12 growth is observed for 2 h (Figure 1A). Lysozyme is undoubtedly the cause of this phenomenon, regarding the fact that the control sample (without lysozyme) does not induce any lag time before bacterial growth starts (Figure 1A). However, the N-L effect is rather short, and bacterial growth resumes. A bacterial concentration similar to that in the control sample is reached after 24 h of incubation (Figure 1A). This could be explained by several hypotheses: damage repair by the bacteria, activation of adaptation and defense mechanisms, and/or depletion of lysozyme in the growth medium by irreversible interaction with the bacteria.

The first possibility is that N-L causes minor damage to the bacterial cells. This damage does not lead to cell death, but the bacterial cell needs to repair the obtained cell structures. For these repair mechanisms, energy is needed and cell growth is thus retarded.

E. coli also have several defense mechanisms. The first defense mechanism of Gram-negative bacteria is the outer membrane. However, lysozyme has been shown to cross this hurdle.[32] Another present defense mechanism in *E. coli* is the lysozyme inhibitor Ivy, which neutralizes N-L in the periplasm.[36] When N-L reaches the periplasm of *E. coli*, Ivy binds to N-L. This makes N-L harmless for the *E. coli* cells (Figure 1). Enterobacteriaceae are also known for the presence of proteases on their outer membrane. *E. coli* K12 carries a protease, OmpT, which combines characteristics of serine and aspartate proteases. The OmpT of *E. coli* K12 has been

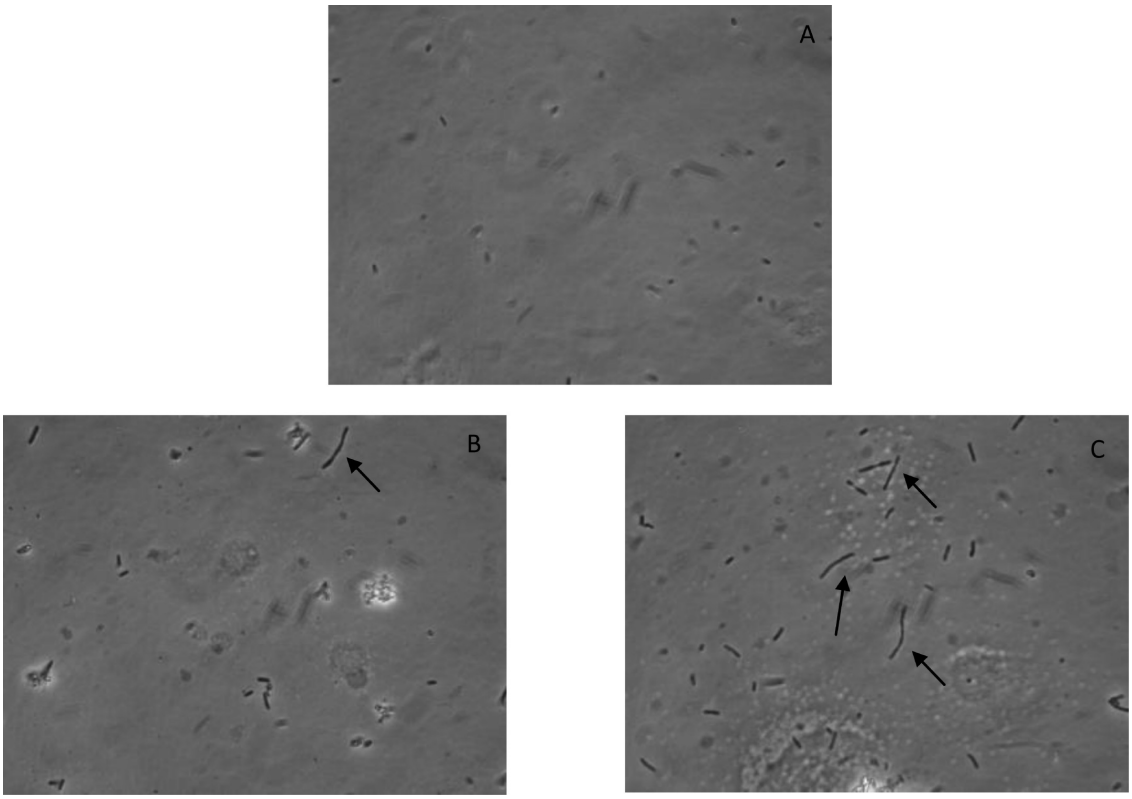

Figure 4. Observations of *E. coli* K12 with optical microscopy after 24 h of incubation in the absence of lysozyme (A) and in the presence of 0.25 g/L native lysozyme (N-L) (B) and dry-heated lysozyme (DH-L) (C).

reported to degrade the antimicrobial peptide protamine.[37] It is thus possible that OmpT also hydrolyzes lysozyme molecules. Besides the above-mentioned defense mechanisms, *E. coli* is also able to modify the lipopolysaccharides of the outer membrane, protecting the outer membrane from permeabilization and neutralizing negative charges of the lipid A moiety.[37] Finally, all these defense mechanisms could protect *E. coli* from N-L and would delay the bacterial growth in the first moments after N-L addition.

Another assumption is that lysozyme concentration in the culture medium progressively decreases until it drops below a critical concentration, because of irreversible interaction between the protein and the bacterial cell membranes.[32] Because of its amphiphilic nature, and its surface-active properties, N-L could insert itself into the outer bacterial membrane, in which it could be irreversebly entrapped, causing depletion of N-L in the medium. Moreover, regarding the N-L molecules that could pass the outer membrane, binding to the peptidoglycan and/or to the inner membrane could decrease the lysozyme concentration in the culture medium. When this decrease results in a lysozyme concentration lower than the lowest active concentration, bacterial growth will resume.

Dry-Heated Lysozyme at High Concentration (3.7 g/L) Causes an Early-Stage Population Decrease. At low concentration (0.25 g/L), DH-L acts similarly to N-L at low and high concentrations: *E. coli* growth is inhibited whether Ivy is present or not (Figure 1), but bacterial growth resumes afterward, and the same bacterial levels as in the control sample are attained after 24 h. As suggested above, three assumptions can be proposed: damage repair by the bacteria, activation of defense and adaptation mechanisms, and/or depletion of lysozyme in the growth medium by irreversible interaction with bacteria.

On the contrary, high-concentration DH-L (3.7 g/L) causes a population decrease (~1 log) in the early stages of growth. Thus, it is noticeable that whereas the presence of the Ivy inhibitor completely removes the population decrease observed when *E. coli* is treated with 3.7 g/L N-L, a slight decrease is still observed in the presence of the Ivy inhibitor when *E. coli* is treated with 3.7 g/L DH-L, even when the muramidase activity of DH-L is 22% lower than that of N-L (data not shown). This indicates that the Ivy inhibitor is not enough to defend *E. coli* cells against the effect of DH-L and that DH-L undoubtedly acts in different way compared to N-L. The physicochemical differences between both lysozymes could be responsible for such different activities. Especially, DH-L has been described more surface-active, more positively charged, and more hydrophobic than N-L.[29] This indicates that DH-L is more membrane active than N-L. To confirm this hypothesis, the *E. coli* membrane state has been tested in the presence of either DH-L or N-L.

Membrane Disruption Differs between Native and Dry-Heated Lysozyme. Both N-L and DH-L pass the outer bacterial membrane and reach the periplasm, consistently with the increased lysozyme effect in the absence of the lysozyme inhibitor Ivy (Figure 1B). Actually, the passage of N-L through the outer bacterial membrane has already been described.[32] In the present study, it is demonstrated that N-L and DH-L permeabilize the outer membrane (Figure 2A), but when *E. coli* is treated with DH-L, more β-lactamase is released from the bacterial cell than when it is treated with N-L (Figure 2B),

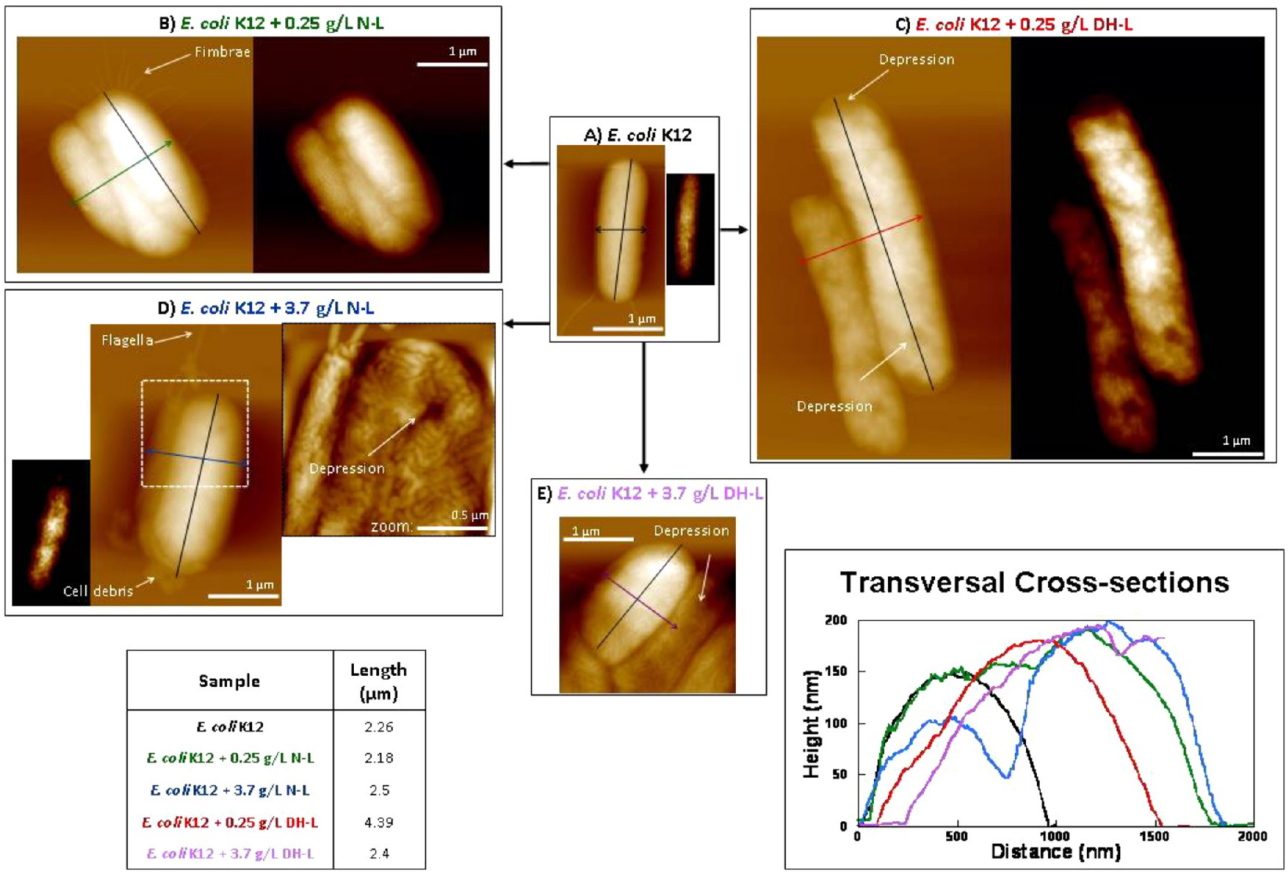

Sample	Length (µm)
E. coli K12	2.26
E. coli K12 + 0.25 g/L N-L	2.18
E. coli K12 + 3.7 g/L N-L	2.5
E. coli K12 + 0.25 g/L DH-L	4.39
E. coli K12 + 3.7 g/L DH-L	2.4

Figure 5. Topographical AFM observations: nontreated *E. coli* K12 cells (A); cells treated with native lysozyme at 0.25 g/L (B) or 3.7 g/L (D); cells treated with dry-heated lysozyme at 0.25 g/L (C) or 3.7 g/L (E). Topographical AFM images have a *z*-range from 0 to 400 nm for full-scale images and from 0 to 15 nm for the 3.7 g/L N-L zoom. Bacterial lengths and cross sections are measured as indicated by full lines on the AFM images. AFM images shown here are representative of the whole sample.

meaning that DH-L causes either larger pores or more pores in the outer membrane as compared to N-L.

Outer membrane permeabilization intensity is independent of the concentration of N-L or DH-L administered to the bacteria (Figure 2A), but higher concentrations of N-L or DH-L (3.7 g/L) cause less β-lactamase leakage in the medium (Figure 2B). This could result from a large insertion of lysozyme molecules into the outer membrane and/or surrounding of the bacteria in high-concentration conditions, causing more difficult diffusion of β-lactamase.

The permeabilization of the inner membrane by DH-L is less intense as compared to that by N-L when measured by the maximal rate of β-galactosidase activity (Figure 2C), but permeabilization occurs faster with DH-L than with N-L (Figure 2D). In both cases, β-galactosidase activity could not be observed in the medium (data not shown), meaning that neither N-L nor DH-L causes pores large enough in the inner membrane to release this cytoplasmic enzyme. High-concentration DH-L also causes higher membrane potential disturbance and K^+ leakage than N-L (Figure 3). Inner membrane disruption is also dose-dependent: the higher the lysozyme concentration, the more severe (Figures 2C and 3) and the faster (Figure 2D) the inner membrane disruption.

It thus seems that, at high concentration, the DH-L activity on *E. coli* could be related to its enhanced activity on the outer and inner membranes. DH-L forms large and/or a lot of pores in the outer membrane; afterward it penetrates into the periplasm where it could either hydrolyze the peptidoglycan layer or diffuse through this layer to finally reach the inner membrane. Once it has arrived at the inner membrane, DH-L causes severe membrane potential disturbance and cytosol leakage (K^+ leakage). These latter phenomena suggest ion channel formation, which has already been reported for native lysozyme and lysozyme-derived peptides by Kimelberg and Papahadjopoulos[38] and Ibrahim et al., respectively.[28] The presented study thus suggests that DH-L forms more ion channels in the cytoplasm membrane than N-L. Moreover, membrane potential disturbance is known to cause cellular division disturbance.[39] In combination with the pore formation, this could explain the morphological modifications observed here.

The Impact of DH-L on the Membrane Integrity of *E. coli* Is Confirmed by Severe Morphological Modifications Observed in Vivo. Not only can the effect of lysozyme, and especially of DH-L, on the membrane integrity of *E. coli* be shown in vitro as described above, it can also be highlighted in vivo. DH-L causes severe disruptions of cellular division observed by optical and atomic force microscopy: elongated cells of about 4.5 μm long could be observed without any sign of septum formation (Figures 4 and 5), as well as depressions which could be pores in the outer membrane and lateral depression which can be related to the activity of an

dx.doi.org/10.1021/jf405155p | J. Agric. Food Chem. 2014, 62, 1692−1700

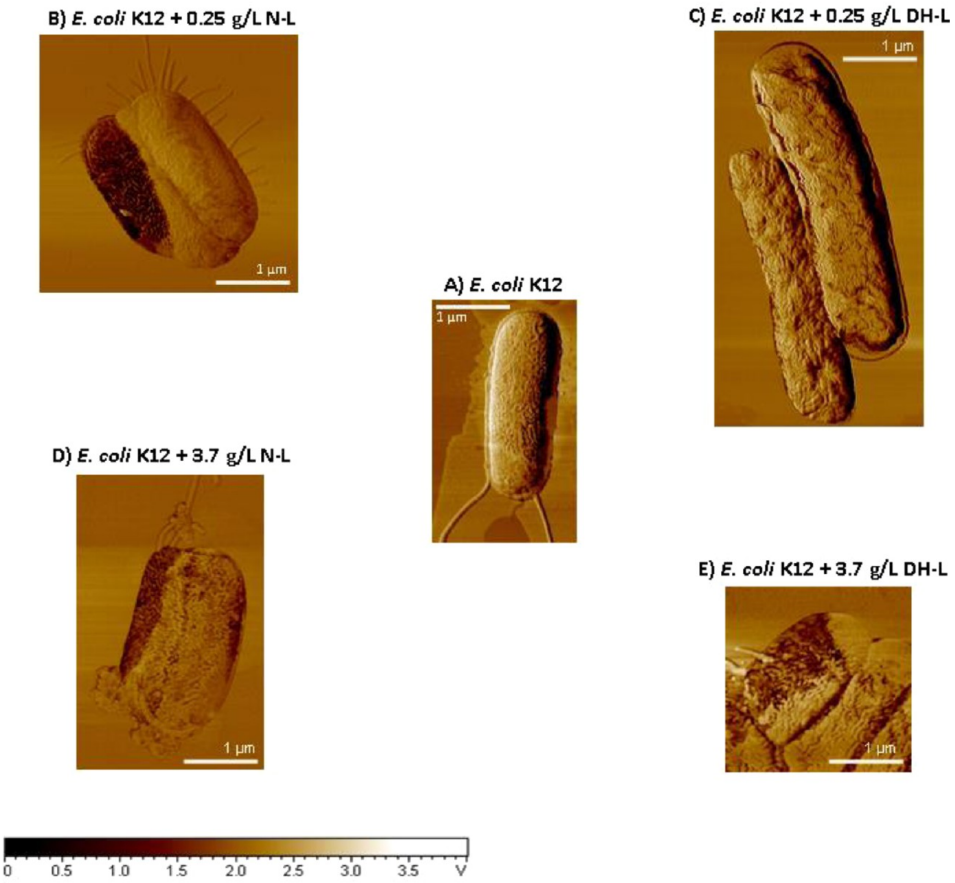

Figure 6. AFM phase imaging: nontreated *E. coli* K12 cells (A); cells treated with native lysozyme at 0.25 g/L (B) or 3.7 g/L (D); cells treated with dry-heated lysozyme at 0.25 g/L (C) or 3.7 g/L (E). The *z*-range is from 0 to 4 V. AFM images shown here are representative of the whole sample.

antimicrobial as reported by Meincken et al.[40] and Li et al.[41] (Figure 5). DH-L also homogenizes the ribs present on the bacterial cell surface at high concentrations (3.7 g/L), which could be the result of protein insertion into the bacterial cell wall as seen for *E. coli* cells treated with PGLa.[40] Then cell division and cell morphology are known to depend on the proton motive force, which itself depends on the bacterial membrane integrity.[39] In Figure 6, it is also noticeable that N-L or DH-L (0.25 and 3.7 g/L) alters the bacterial surface heterogeneity, resulting in the appearance of more rigid zones.[35,40]

These morphological modifications are consistent with the membrane integrity disturbances. Thus, the depressions formed in the presence of DH-L (Figure 5) are consistent with the higher leakage of β-lactamase, as compared to that in bacterial cells treated with N-L (Figure 2B). Perturbated cell division (Figures 4 and 5) is consistent with membrane potential disruption (Figure 3A), as recently reported by Strahl et al.[39]

To explain the differences observed between N-L and DH-L against *E. coli* membrane integrity, some assumptions can be proposed. Especially, the physicochemical modifications induced by dry-heating, and previously described by Desfougères et al.,[29] could be responsible for higher affinity of DH-L with outer and inner membranes and/or for more severe membrane disruptions. Because DH-L is more positively charged than N-L, interactions with LPS could be increased. Moreover, the higher hydrophobicity of DH-L could make it easier to interact with the lipid parts of bacterial membranes, and its higher flexibility could improve lysozyme insertion into the membranes. At last, the higher positive charge of DH-L could modify the membrane potential to a larger extent than N-L, when adsorbed on the inner membrane. However, more research has to be performed to identify the prevalent parameters responsible for the improved antibacterial activity of DH-L as compared to N-L. This is in progress by studying the behavior of DH-L at 2D model interfaces mimicking bacterial membranes.

AUTHOR INFORMATION

Corresponding Author

*E-mail: melanie.derde@agrocampus-ouest.fr.

Funding

This research was funded by Conseil Régional de Bretagne.

Notes

The authors declare no competing financial interest.

ACKNOWLEDGMENTS

We thank Delphine Destoumieux-Garzon and Chris Michiels for kindly providing the *E. coli* ML-35p strain and *E. coli* MG1655 *ivy*::*Cm*, respectively.

ABBREVIATIONS USED

ONPG, (*o*-nitrophenyl)galactoside; ONP, *o*-nitrophenol; DiSC3, 3,3′-dipropylthiadicarbocyanine; HEPES, 4-(2-hydrox-

yethyl)-1-piperazineethanesulfonic acid; TSB, tryptic soy broth; LB, Luria broth; HP-nitrocefin, hydrolysis product of nitrocefin; AFM, atomic force microscopy; N-L, native lysozyme; DH-L, dry-heated lysozyme

REFERENCES

(1) World Health Organization (WHO). *Overcoming Antimicrobial Resistance*; WHO: Geneva, Switserland, 2000.

(2) Bruhn, C. M. Consumer attitudes toward food additives. In *Food Additives*, 2nd ed.; Branen, A. L., Davidson, P. M., Salminen, S., Thorngate, J. H., Eds.; Marcel Dekker Inc.: New York, 2002; pp 111−119.

(3) *Special Eurobarometer 354: Food-Related Risks*; conducted by TNS Opinion & Social at the request of the European Food Safety Authority (EFSA): Parma, Italy, 2010.

(4) Nguyen, L. T.; Haney, E. F.; Vogel, H. J. The expanding scope of antimicrobial peptide structures and their modes of action. *Trends Biotechnol.* **2011**, *29* (9), 464−472.

(5) Peschel, A.; Sahl, H. G. The co-evolution of host cationic antimicrobial peptides and microbial resistance. *Nat. Rev. Microbiol.* **2006**, *4* (7), 529−536.

(6) Jolles, P.; Jolles, J. Whats new in lysozyme research—always a model system, today as yesterday. *Mol. Cell. Biochem.* **1984**, *63* (2), 165−189.

(7) *European Parliament and Council Directive No 95/2/EC of 20 February 1995 on Food Additives Other Than Coulors and Sweeteners*; European Union: Brussels, Belgium, 1995.

(8) Masschalck, B.; Michiels, C. W. Antimicrobial properties of lysozyme in relation to foodborne vegetative bacteria. *Crit. Rev. Microbiol.* **2003**, *29* (3), 191−214.

(9) Bera, A.; Herbert, S.; Jakob, A.; Vollmer, W.; Götz, F. Why are pathogenic staphylococci so lysozyme resistant? The peptidoglycan O-acetyltransferase OatA is the major determinant for lysozyme resistance of *Staphylococcus aureus*. *Mol. Microbiol.* **2005**, *55* (3), 778−787.

(10) Zipperle, G. F., Jr.; Ezzell, J. W., Jr.; Doyle, R. J. Glucosamine substitution and muramidase susceptibility in *Bacillus anthracis*. *Can. J. Microbiol.* **1984**, *30* (5), 553−559.

(11) Nikaido, H. Molecular basis of bacterial outer membrane permeability revisited. *Microbiol. Mol. Biol. Rev.* **2003**, *67* (4), 593−656.

(12) Callewaert, L.; Masschalck, B.; Deckers, D.; Nakimbugwe, D.; Atanassova, M.; Aertsen, A.; Michiels, C. W. Purification of Ivy, a lysozyme inhibitor from *Escherichia coli*, and characterisation of its specificity for various lysozymes. *Enzyme Microb. Technol.* **2005**, *37* (2), 205−211.

(13) Callewaert, L.; Aertsen, A.; Deckers, D.; Vanoirbeek, K. G.; Vanderkelen, L.; Van Herreweghe, J. M.; Masschalck, B.; Nakimbugwe, D.; Robben, J.; Michiels, C. W. A new family of lysozyme inhibitors contributing to lysozyme tolerance in Gram-negative bacteria. *PloS Pathog.* **2008**, *4* (3), e000019.

(14) Deckers, D.; Masschalck, B.; Aertsen, A.; Callewaert, L.; Van Tiggelen, C. G. M.; Atanassova, M.; Michiels, C. W. Periplasmic lysozyme inhibitor contributes to lysozyme resistance in *Escherichia coli*. *Cell. Mol. Life Sci.* **2004**, *61* (10), 1229−1237.

(15) Pellegrini, A.; Thomas, U.; Vonfellenberg, R.; Wild, P. Bactericidal activities of lysozyme and aprotinin against Gram-negative and Gram-positive bacteria related to their basic character. *J. Appl. Bacteriol.* **1992**, *72* (3), 180−187.

(16) Pellegrini, A.; Thomas, U.; Wild, P.; Schraner, E.; von Fellenberg, R. Effect of lysozyme or modified lysozyme fragments on DNA and RNA synthesis and membrane permeability of *Escherichia coli*. *Microbiol. Res.* **2000**, *155* (2), 69−77.

(17) Wild, P.; Gabrieli, A.; Schraner, E. M.; Pellegrini, A.; Thomas, U.; Frederik, P. M.; Stuart, M. C. A.; Vonfellenberg, R. Reevaluation of the effect of lysoyzme on *Escherichia coli* employing ultrarapid freezing followed by cryoelectronmicroscopy or freeze substitution. *Microsc. Res. Tech.* **1997**, *39* (3), 297−304.

(18) Ibrahim, H. R.; Kato, A.; Kobayashi, K. Antimicrobial effects of lysozyme against Gram-negative bacteria due to covalent binding of palmitic acid. *J. Agric. Food Chem.* **1991**, *39* (11), 2077−2082.

(19) Ibrahim, H. R.; Yamada, M.; Kobayashi, K.; Kato, A. Bactericidal action of lysozyme against Gram-negative bacteria due to insertion of a hydrophobic pentapeptide into its C-terminus. *Biosci., Biotechnol., Biochem.* **1992**, *56* (8), 1361−1363.

(20) Ibrahim, H. R.; Kobayashi, K.; Kato, A. Length of hydrocarbon chain and antimicrobial action to Gram-negative bacteria of fatty acylated lysozyme. *J. Agric. Food Chem.* **1993**, *41* (7), 1164−1168.

(21) Li, C. P.; Ibrahim, H. R.; Sugimoto, Y.; Hatta, H.; Aoki, T. Improvement of functional properties of egg white protein through phosphorylation by dry-heating in the presence of pyrophosphate. *J. Agric. Food Chem.* **2004**, *52* (18), 5752−5758.

(22) Amiri, S.; Ramezani, R.; Aminlari, M. Antibacterial activity of dextran-conjugated lysozyme against *Escherichia coli* and *Staphylococcus aureus* in cheese curd. *J. Food Prot.* **2008**, *71* (2), 411−415.

(23) Ibrahim, H. R.; Hatta, H.; Fujiki, M.; Kim, M.; Yamamoto, T. Enhanced antimicrobial action of lysozyme against Gram-negative and Gram-positive bacteria due to modification with perillaldehyde. *J. Agric. Food Chem.* **1994**, *42* (8), 1813−1817.

(24) Ibrahim, H. R.; Higashiguchi, S.; Juneja, L. R.; Kim, M.; Yamamoto, T. A structural phase of heat-denatured lysozyme with novel antimicrobial action. *J. Agric. Food Chem.* **1996**, *44* (6), 1416−1423.

(25) Ibrahim, H. R.; Higashiguchi, S.; Sugimoto, Y.; Aoki, T. Role of divalent cations in the novel bactericidal activity of the partially unfolded lysozyme. *J. Agric. Food Chem.* **1997**, *45* (1), 89−94.

(26) Ibrahim, H. R.; Higashiguchi, S.; Koketsu, M.; Juneja, L. R.; Kim, M.; Yamamoto, T.; Sugimoto, Y.; Aoki, T. Partially unfolded lysozyme at neutral pH agglutinates and kills Gram-negative and Gram-positive bacteria through membrane damage mechanism. *J. Agric. Food Chem.* **1996**, *44* (12), 3799−3806.

(27) Mine, Y.; Ma, F. P.; Lauriau, S. Antimicrobial peptides released by enzymatic hydrolysis of hen egg white lysozyme. *J. Agric. Food Chem.* **2004**, *52* (5), 1088−1094.

(28) Ibrahim, H. R.; Thomas, U.; Pellegrini, A. A helix-loop-helix peptide at the upper lip of the active site cleft of lysozyme confers potent antimicrobial activity with membrane permeabilization action. *J. Biol. Chem.* **2001**, *276* (47), 43767−43774.

(29) Desfougeres, Y.; Jardin, J.; Lechevalier, V.; Pezennec, S.; Nau, F. Succinimidyl residue formation in hen egg-white lysozyme favors the formation of intermolecular covalent bonds without affecting its tertiary structure. *Biomacromolecules* **2011**, *12* (1), 156−166.

(30) Baron, F.; Cochet, M. F.; Wilfried, A.; Noël, G.; Madec, M. N.; Gonnet, F.; Jan, S.; Gautier, M. Rapid and cost-effective method for micro-organism enumeration based on miniaturization of the conventional plate-counting technique. *Lait* **2006**, *86* (3), 251−257.

(31) Lehrer, R. I.; Barton, A.; Ganz, T. Concurrent assessment of inner and outer-membrane permeabilization and bacteriolysis in *Escherichia coli* by multiple-wavelength spectrophotometry. *J. Immunol. Methods* **1988**, *108* (1−2), 153−158.

(32) Derde, M.; Lechevalier, V.; Guerin-Dubiard, C.; Cochet, M. F.; Jan, S.; Baron, F.; Gautier, M.; Vié, V.; Nau, F. Hen egg white lysozyme permeabilizes the *Escherichia coli* outer and inner membranes. *J. Agric. Food Chem.* **2013**, *61* (41), 9922−9929.

(33) Wu, M.; Maier, E.; Benz, R.; Hancock, R. E. Mechanism of interaction of different classes of cationic antimicrobial peptides with planar bilayers and with the cytoplasmic membrane of *Escherichia coli*. *Biochemistry* **1999**, *38* (22), 7235−7242.

(34) Orlov, D. S.; Nguyen, T.; Lehrer, R. I. Potassium release, a useful tool for studying antimicrobial peptides. *J. Microbiol. Methods* **2002**, *49* (3), 325−328.

(35) Camesano, T.; Natan, M.; Logan, B. Observation of changes in bacterial cell morphology using tapping mode atomic force microscopy. *Langmuir* **2000**, *16* (10), 4563−4572.

(36) Abergel, C.; Monchois, V.; Byrne, D.; Chenivesse, S.; Lembo, F.; Lazzaroni, J. C.; Claverie, J. M. Structure and evolution of the Ivy

protein family, unexpected lysozyme inhibitors in Gram-negative bacteria. *Proc. Natl. Acad. Sci. U.S.A.* **2007**, *104* (15), 6394−6399.
(37) Gruenheid, S.; Le Moual, H. Resistance to antimicrobial peptides in Gram-negative bacteria. *FEMS Microbiol. Lett.* **2012**, *330* (2), 81−89.
(38) Kimelberg, H. K.; Papahadjopoulos, D. Interactions of basic proteins with phospholipid membranes: binding and changes in the sodium permeability of phosphatidylserine vesicles. *J. Biol. Chem.* **1971**, *246* (4), 1142−1148.
(39) Strahl, H.; Hamoen, L. W. Membrane potential is important for bacterial cell division. *Proc. Natl. Acad. Sci. U.S.A.* **2010**, *107* (27), 12281−12286.
(40) Meincken, M.; Holroyd, D. L.; Rautenbach, M. Atomic force microscopy study of the effect of antimicrobial peptides on the cell envelope of *Escherichia coli*. *Antimicrob. Agents Chemother.* **2005**, *49* (10), 4085−4092.
(41) Li, A.; Lee, P.; Ho, B.; Ding, J.; Lim, C. Atomic force microscopy study of the antimicrobial action of Sushi peptides on Gram-negative bacteria. *Biochim. Biophys. Acta, Biomembr.* **2007**, *1768* (3), 411−418.

Biochimica et Biophysica Acta 1848 (2015) 174–183

Contents lists available at ScienceDirect

Biochimica et Biophysica Acta

journal homepage: www.elsevier.com/locate/bbamem

Native lysozyme and dry-heated lysozyme interactions with membrane lipid monolayers: Lateral reorganization of LPS monolayer, model of the *Escherichia coli* outer membrane

Melanie Derde [a,b,*], Françoise Nau [a,b], Valérie Lechevalier [a,b], Catherine Guérin-Dubiard [a,b], Gilles Paboeuf [c], Sophie Jan [a,b], Florence Baron [a,b], Michel Gautier [a,b], Véronique Vié [c,**]

[a] Agrocampus Ouest, UMR1253 Science et Technologie du Lait et de l'Oeuf, F-35042 Rennes, France
[b] INRA, UMR1253 Science et Technologie du Lait et de l'Oeuf, F-35042 Rennes, France
[c] Université de Rennes 1, Institut de Physique de Rennes, UMR6251, CNRS, F-35042 Rennes, France

ARTICLE INFO

Article history:
Received 22 May 2014
Received in revised form 26 September 2014
Accepted 20 October 2014
Available online 27 October 2014

Keywords:
BAM
AFM
Langmuir film
Dry-heated lysozyme
LPS monolayer

ABSTRACT

Lysozyme is mainly described active against Gram-positive bacteria, but is also efficient against some Gram-negative species. Especially, it was recently demonstrated that lysozyme disrupts *Escherichia coli* membranes. Moreover, dry-heating changes the physicochemical properties of the protein and increases the membrane activity of lysozyme. In order to elucidate the mode of insertion of lysozyme into the bacterial membrane, the interaction between lysozyme and a LPS monolayer mimicking the *E. coli* outer membrane has been investigated by tensiometry, ellipsometry, Brewster angle microscopy and atomic force microscopy. It was thus established that lysozyme has a high affinity for the LPS monolayer, and is able to insert into the latter as long as polysaccharide moieties are present, causing reorganization of the LPS monolayer. Dry-heating increases the lysozyme affinity for the LPS monolayer and its insertion capacity; the resulting reorganization of the LPS monolayer is different and more drastic than with the native protein.

1. Introduction

Antibiotic resistance due to decades of misuse in human and veterinary medicine is causing an enormous public health problem. Several pathogens, such as *Staphylococcus aureus* and *Klebsiella pneumonia,* have developed multiple antibiotic resistance mechanisms. The consequence is difficult and expensive treatments of several diseases [1]. The number of these multi-resistant strains is increasing, but only three new antibiotic molecules against Gram-positive multiresistant strains were registered since 1970, and none for Gram-negative multiresistant strains [2]. Research for novel antimicrobial compounds is thus needed, besides the measures of the European Union to limit the spread of antibiotic resistances. Preferably, novel compounds should decrease the development rate and spread of antibiotic resistance.

Several natural proteins and peptides can be considered as potential candidates, especially the antimicrobial proteins or peptides (AMP) which act on the bacterial membranes. Their target, i.e. the bacterial cell membrane, is a generalized and vital target, and thus antimicrobial resistance development remains limited [3,4]. AMPs are mostly positively charged molecules, amphiphilic, flexible, and contain several hydrophobic residues, suggesting electrostatic and hydrophobic interactions with the bacterial cell membrane [3]. These interactions can then lead to the membrane disruption, causing bacterial cell death or translocation of the AMP into the cytoplasm where these can interact with several intracellular targets [3,5].

One of the natural antimicrobial proteins, widely studied, is hen egg white lysozyme. This small enzyme (129 amino acid residues) was for a long time only known for its antimicrobial activity against Gram-positive bacteria, due to its muramidase activity [6,7]. However, several studies suggest other mechanisms of action against both Gram-positive and Gram-negative bacteria, such as perturbation of DNA or RNA synthesis, activation of autolysin production, and membrane permeabilization [7–10]. The disruption of both the outer and cytoplasmic membranes of *Escherichia coli* by native lysozyme has been recently demonstrated in our laboratory [9]. Especially, pore formation in the outer membrane of *E. coli* has been described [11]. Moreover, pore size and/or quantity were higher with dry-heated lysozyme as compared to the native protein [11]. The physicochemical modifications

Abbreviations: AFM, Atomic force microscopy; AMP, Antimicrobial peptide or protein; BAM, Brewster angle microscopy; DH-L, Dry-heated lysozyme; HEPES, 4-(2-Hydroxyethyl) piperazine-1-ethanesulfonic acid; KLA, Lipid A-$(KdO)_2$; LPS, Lipopolysaccharides; MIP, Maximum insertion pressure; N-L, Native lysozyme

* Correspondence to: M. Derde, Agrocampus Ouest, INRA, UMR 1253 STLO, 65, rue de St-Brieuc, 35042 Rennes, France. Tel.: +33 2 23 48 55 74.
** Correspondence to: V. Vié, Université de Rennes 1, Institut de Physique de Rennes (IPR), 263, Av Général Leclerc, F-35042 Rennes Cedex. Tel.: +33 2 23 23 56 45.
E-mail addresses: melanie.derde@agrocampus-ouest.fr (M. Derde), veronique.vie@univ-rennes1.fr (V. Vié).

http://dx.doi.org/10.1016/j.bbamem.2014.10.026
0005-2736/

resulting from dry-heating are an increased positive charge at physiological pH as well as increased flexibility and hydrophobicity while preserving the secondary and tertiary structure; these modifications could be responsible for the enhanced antibacterial activity of dry-heated lysozyme, similarly to what has been described for lysozyme modification by enzyme hydrolysis, heat denaturation, or fusion with several chemical moieties [7,12–17].

However, the interactions between the outer membrane lipids of Gram-negative bacteria and both types of lysozyme (native and dry-heated) remain to be investigated. In the presently reported study, lipopolysaccharide (LPS) monolayers of *E. coli* K12 have been used as a model for the bacterial outer membrane [18,19]. These LPS monolayers were formed in a Langmuir trough at a controlled initial surface pressure ($\pi_{initial}$). Multiscale analysis of the interfacial film using tensiometry, ellipsometry, Brewster angle microscopy (BAM) and atomic force microscopy (AFM), enabled to investigate the LPS–lysozyme interactions, to study the consequences of lysozyme interaction on the LPS monolayer.

2. Materials and methods

2.1. Proteins and lipids

Native lysozyme (N-L) powder (pH 3.2) was obtained from Liot (Annezin, 62-France). It was heated for 7 days at 80 °C in hermetically closed glass tubes to obtain dry-heated lysozyme (DH-L). Lysozyme (N-L or DH-L) was solubilized (around 0.5 g/L) in 5 mM 4-(2-hydroxyethyl)piperazine-1-ethanesulfonic acid (HEPES) buffer (Sigma Aldrich, Saint-Quentin, France), pH 7.0, 150 mM NaCl (Fluka, Saint-Quentin, France). The concentration of the lysozyme stock solution was precisely determined by absorbance at 280 nm (extinction coefficient = 2.6 L/(g·cm)) [20]. The protein solution was then diluted in the HEPES buffer to obtain the desired concentration for used lysozyme solutions.

The lipopolysaccharides (LPS) of *E. coli* K12 were obtained from Invivogen (Toulouse, France). The LPS were solubilized in 2:1 chloroform/methanol mixture at 0.5 g/L. Lipid A-$(KdO)_2$ (KLA) were purchased by Avanti Polar Lipids (Alabaster, Alabama, USA) and were solubilized in a 2:1 chloroform/methanol mixture at 0.67 g/L.

2.2. Lipid/protein monolayers

The experiments were performed in a homemade TEFLON® trough of 8 ml at 20 °C. Before each use, the trough was thoroughly cleaned with successively warm tap water, ethanol, demineralized water, and then boiled for 15 min in demineralized water. After cooling the TEFLON® trough was then filled with 8 ml HEPES buffer. The LPS or KLA were spread with a high precision Hamilton microsyringe at the clean air/liquid interface to obtain an initial surface pressure between 18 and 30 mN/m. After 1 h to allow the solvent to evaporate and the lipids to organize, 50 μl N-L or DH-L solution were injected in the subphase with a Hamilton syringe to obtain a final protein concentration of 0.02, 0.03, 0.05, 0.1, 0.2, 0.3 or 1 μM.

2.3. Surface pressure measurements

The surface pressure was measured following a Wilhelmy method using a 10 mm × 22 mm filter paper as plate (Whatman, Velizy-Villacoublay, France) connected to a microelectronic feedback system (Nima PS4, Manchester, England). The surface pressure (π) was recorded every 4 s with a precision of ± 0.2 mN/m. The measured surface pressure is the result of the surface tension of water minus the surface tension of the lipid film.

2.4. Ellipsometry

Measurements of the ellipsometric angle value were carried out with an in-house automated ellipsometer in a "null ellipsometer" configuration [21,22]. A polarized He–Ne laser beam (λ = 632.8 nm, Melles Griot, Glan-Thompson polarizer) was reflected on the surface of the trough. The incidence angle was 52.12°, i.e. Brewster angle for the air/water interface minus 1°. After reflection on the liquid surface, the laser light passed through a λ/4 retardation plate, a Glan-Thompson analyzer, and a photomultiplier. The analyzer angle, multiplied by two, yielded the value of the ellipsometric angle (Δ), i.e. the phase difference between parallel and perpendicular polarization of the reflected light. The laser beam probed the 1 mm^2 surface with a depth in the order of 1 μm. Initial values of the ellipsometric angle (Δ_0) and surface pressure of buffer solutions were recorded for at least half an hour to assure that the interface is clean. Only in the case of a stable, minimal signal, experiments were performed. Values of Δ were recorded every 4 s with a precision of ± 0.5°. When measuring the pressure increase induced by lysozyme at the air/liquid interface, a lysozyme solution at 0.1 μM is deposited in the trough. When the pressure increase induced by lysozyme is measured at the LPS/liquid interface, a LPS monolayer is first created as formerly described.

For the detection of local ellipsometric angle values, an imaging ellipsometer EP3 (Nanofilm, Göttingen, Germany) in "null ellipsometer" configuration was used with a 10× objective. A solid-state laser (λ = 532 nm) was used as a light source. Delta/psi maps were recorded with the EP3 software for a 450 μm × 390 μm surface. For delta and psi maps, a polarizer and analyzer range of 20° was used. Delta/psi maps were based on 20 images taken at different polarizer and analyzer angles.

2.5. Brewster angle microscopy

An ellipsometer EP3 (Nanofilm, Berlin, Germany) with a polarized incident laser (λ = 532 nm) was used with a 10× objective in a Brewster angle configuration (angle of incidence was 53.1°). The images represented a 450 μm × 390 μm surface. Different zones of each sample were evaluated; the images here shown are representative of the whole samples.

2.6. AFM sample preparation and AFM imaging

Experiments were performed with a computer-controlled and user-programmable Langmuir TEFLON®-coated trough (type 601BAM) equipped with two movable barriers and of total surface 90 cm^2 (Nima Technology Ltd., England). Before starting the experiments, the trough was cleaned successively with ultrapure water (Nanopure-UV), ethanol, and finally ultrapure water. The trough was filled with 5 mM HEPES buffer pH 7 150 mM NaCl. LPS were spread over the clean air/liquid interface at a surface pressure of 25 mN/m or 30 mN/m. The solvent was then left to evaporate for 1 h. Then, a Langmuir–Blodgett transfer was performed onto freshly cleaved mica plates at constant surface pressure by vertically raising (1 mm/min) the mica through the air/liquid interface to obtain a sample of the initial LPS monolayer. The LPS monolayer stability was assured during the Langmuir–Blodgett transfer allowing the injection of lysozyme in the subphase.

Then, 0.1 μM lysozyme was injected in the subphase of the previously sampled LPS monolayer with a Hamilton syringe. Surface pressure variations were recorded until a stable surface pressure was reached (after ~1 h). Then, a second Langmuir–Blodgett transfer was performed onto freshly cleaved mica as described above to obtain the sample of the LPS monolayer after lysozyme interaction.

AFM imaging of Langmuir–Blodgett films was performed in contact mode using a Pico-plus atomic force microscope (Agilent Technologies, Phoenix, AZ) under ambient conditions with a scanning area of 20 × 20 μm^2 and 5 × 5 μm^2. Topographic images were acquired using

silicon nitride tips on integral cantilevers. The forces were controlled along the imaging process. Different zones of each sample were scanned; the images here shown are representative of the whole samples.

3. Results

3.1. Insertion capacity of lysozyme into a LPS monolayer

The insertion capacity of N-L and DH-L into a LPS monolayer was determined by independent tensiometry experiments at different protein concentrations. Insertion can be detected by a surface pressure increase ($\Delta\pi = \pi_{final} - \pi_{initial}$). Here, lysozyme was injected under a LPS monolayer with an initial surface pressure ($\pi_{initial}$) of 18 mN/m.

In both cases (N-L and DH-L), a surface pressure increase is demonstrated indicating lysozyme insertion into the LPS monolayer for protein concentrations above 0.02 μM (Fig. 1A). Below 0.05 μM, no difference can be observed between both lysozymes, while above this protein concentration, DH-L induces a higher surface pressure increase than N-L (Fig. 1A). When increasing the lysozyme subphase concentration, a Δπ-plateau is obtained at a lysozyme concentration of 0.2 μM for both N-L and DH-L, indicating saturation of the interface in these conditions. However, the maximum Δπ value is higher for DH-L than for N-L (12 mN/m and 8 mN/m, respectively; Fig. 1A). For further investigation of the insertion capacity of lysozyme, 0.1 μM N-L or DH-L has been used. At this concentration, differences exist between both proteins, and lipid protein interactions can be observed, while minimizing protein-protein interactions in the bulk solution (aggregation) or at the lipid interface.

3.2. Affinity of lysozyme for LPS monolayers

To evaluate the affinity of both N-L and DH-L for the LPS monolayer, Δπ was determined after lysozyme injection (0.1 μM) under LPS monolayers previously formed at different initial surface pressures ($\pi_{initial}$). Supplementary experiments demonstrated that no phase transition occurs in the π-range here used (supplementary data S3); comparisons are then valuable. Linear regression analysis of the Δπ values *versus* $\pi_{initial}$ allows calculation of three binding parameters of lysozyme: maximal insertion pressure (MIP), synergy factor, and $\Delta\pi_0$ (Fig. 1B) [23–25]. MIP is the intercept of the straight line with x-axis after extrapolation; it is thus the initial surface pressure for which no surface pressure increase occurs when lysozyme is injected in the subphase. The synergy factor is determined as the slope of the linear regression +1. The synergy factor provides information on the affinity of the protein for the lipid monolayer. High positive synergy values indicate the existence of strong protein/lipid interactions, since it means that the protein is able to insert into the lipid film even when initial surface pressure is high. $\Delta\pi_0$ is the intercept of the straight line with y-axis after extrapolation; it is thus the theoretical pressure increase in the absence of lipids ($\pi_{initial} = 0$ mN/m).

Linear regression for N-L and DH-L resulted in Eqs. (1) and (2), respectively, with respective determination coefficients (R^2) of 0.96 and 0.91.

$$y = -0.21x + 8.75 \quad (1)$$

$$y = -0.15x + 9.10 \quad (2)$$

The MIP is higher with DH-L than with N-L (59.6 and 41.5 mN/m, respectively; Table 1). The synergy factor as introduced by Boisselier et al. [24] and Calvez et al. [23] is also higher with DH-L than with N-L, and is positive for both proteins (0.85 and 0.79, respectively; Table 1) [24]. Oppositely, the $\Delta\pi_0$ are similar for N-L and DH-L (8.75 and 9.10 mN mN/m, respectively; Table 1). It is noticeable that these latter values are smaller than the experimental surface pressure increase observed for N-L and DH-L lysozymes at the air/liquid interface at the same subphase concentration (10 and 11 mN/m, respectively).

The rate constant of adsorption k_{ads} ($M^{-1}\ s^{-1}$) of a lysozyme solution with a concentration (c) of 0.1 μM at the air/liquid interface and the LPS/liquid interface can be evaluated by fitting the Langmuir Eq. (3) for adsorption to the surface pressure measurements. The rate constant of desorption k_{des} ($M^{-1}\ s^{-1}$) can here be considered negligible.

$$\pi(t) = \pi_{final}(1 - \exp(-\sigma t)) \quad (3)$$

$$\sigma = k_{ads}c + k_{des} \quad (4)$$

At the air/liquid interface, N-L and DH-L have a k_{ads} value of $6.6 \cdot 10^2\ M^{-1}\ s^{-1}$ and 6.4 · 102 M-1·s-1, respectively. The rate constants of adsorption for N-L and DH-Lat the LPS/liquid interface of 1.7 103 M-1·s-1 and 1.3 103 M-1·s-1, respectively, are higher than the rate constants of adsorption at the air/liquid interface. Thus, lysozyme adsorption at the air/liquid interface is slower than adsorption at the LPS/liquid interface. The differences in k_{ads} for N-L and DH-L forboth the air/liquid and the LPS/liquid interface are not significant.

3.3. Changes of surface pressure (π) and ellipsometric angle (Δ) of LPS monolayer in the presence of lysozyme

Kinetics of the π and Δ changes after injection of N-L and DH-L in the subphase was recorded using a LPS monolayer with an initial surface

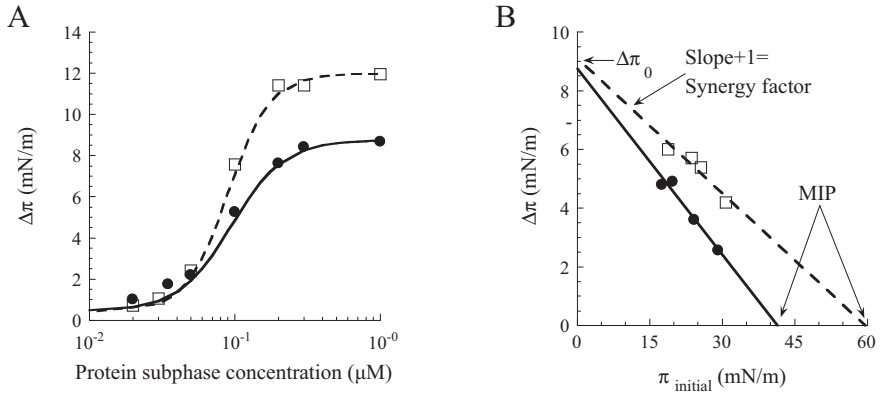

Fig. 1. A) Surface pressure increase (Δπ) of a LPS monolayer ($\pi_{initial} = 18$ mN/m) induced by different subphase concentrations of native lysozyme (N-L) (●) and dry-heated lysozyme (DH-L) (□). B) Surface pressure increase of a LPS monolayer induced by 0.1 μM N-L (●) and DH-L (□), depending on the initial surface pressure ($\pi_{initial}$); the maximal insertion pressure (MIP) and the theoretical pressure increase in the absence of lipids ($\Delta\pi_0$) are indicated by arrows.

Table 1
Binding parameters calculated for N-L and DH-L adsorption at a LPS monolayer: maximal insertion pressure (MIP), synergy factor, and theoretical pressure increase in the absence of lipids ($\Delta\pi_0$); these parameters were extrapolated from the $\Delta\pi$ *vs.* $\pi_{initial}$ plots for 0.1 μM lysozyme. For comparison, the surface pressure increase resulting from 0.1 μM lysozyme adsorption at the air/liquid interface is indicated ($\Delta\pi_{final}$).

		N-L	DH-L
LPS/liquid interface	MIP (mN/m)	41.5	59.6
	Synergy factor	0.79	0.85
	Theoretical $\Delta\pi_0$ (mN/m)	8.75	9.10
Air/liquid interface	$\Delta\pi_{final}$ (mN/m)	10	11

pressure of 25 mN/m and 30 mN/m, respectively. Different initial surface pressures of the LPS monolayers were chosen because of the different insertion capacities of N-L and DH-L for this experiment. The aim of this study is to evaluate the effects of N-L or DH-L on the LPS monolayer after a similar insertion of proteins, i.e. a similar Δπ. The initial surface pressures which correspond to this prerequisite is 25 mN/m and 30 mN/m for a concentration of 0.1 μM N-L and DH-L, respectively (Fig. 1B); more so, LPS monolayers with an initial surface pressure of 25 mN/m and 30 mN/m have similar Δ values (supplementary data S1). The injection of N-L and DH-L under the LPS monolayer in these conditions results in a surface pressure increase of 2.9 mN/m and 3.5 mN/m, respectively (Fig. 2A), and induces an increase of ellipsometric angle of 8° and 12°, respectively (Fig. 2B).

3.4. Changes of surface pressure (π) and ellipsometric angle (Δ) of KLA monolayer in the presence of lysozyme

To estimate the influence of the polysaccharide moieties on lysozyme interactions with LPS monolayer, KLA lipids were used. KLA lipids are derivative forms of LPS from which the polysaccharide moiety besides two 3-deoxy-D-manno-octulosonic acid (KdO) groups are missing (Fig. 3). The use of KLA was also relevant to test the role of electrostatic interactions between lysozyme and the negative charge at the interface by making the access to the charge easier. KLA monolayers are homogeneous lipid films on the contrary to LPS monolayers. This was confirmed by AFM imaging (supplementary data S2).

Kinetics of the π and Δ changes after injection of N-L and DH-L in the subphase was recorded for a KLA monolayer with an initial surface pressure of 25 mN/m and 30 mN/m, respectively. For N-L, the surface pressure of the KLA monolayer is stable for the first half hour and then decreases after 3 h (−2.1 mN/m) (Fig. 4A). Oppositely, DH-L injection induces an immediate and more intense decrease (−5 mN/m after 3 h) (Fig. 4A). Both N-L and DH-L interact with the KLA monolayer in such a way that the ellipsometric angle increases slightly after injection of both proteins: +0.65° and +1.5° after 3 h, respectively (Fig. 4B).

3.5. Microscopic observations of LPS monolayer in the presence of lysozyme

Brewster angle microscopy (BAM) and ellipsometry were performed to visualize the LPS monolayer organization on a μm-scale before and after lysozyme injection in the subphase. BAM-images give information on the thickness and refraction index of the LPS monolayer. Thick and/or high refraction index zones will appear lighter (white) than thin and low index zones (black). Delta maps show the same information as the BAM images, but the differences in height and/or refraction index are more precisely measured. Blue is the baseline color of the delta maps and correspond to a small delta value. High delta zones will be represented from green till red.

Before lysozyme injection, the LPS monolayer is heterogeneous, with black and white zones, at both initial surface pressures (25 mN/m and 30 mN/m), as evidenced by BAM-imaging (Fig. 5A and E). In the absence of literature references, the black colored zones are assumed to correspond to LPS with short polysaccharide chains (low refractive index and low thickness), while the white regions are assumed to correspond to LPS with long polysaccharide chains (high refractive index and high thickness). Such domain-organization is likely considering the optimal thermodynamic configuration that suggests segregation of LPS with similar polysaccharide chain lengths. The same information is provided by the delta-maps (Fig. 5C and G).

One hour after injection of 0.1 μM N-L, the BAM-images and delta-maps do not show any significant change of the heterogeneity as compared to the initial LPS monolayer (Fig. 5B and D), despite a slight increase of the background Δ-value in the delta-map (Fig. 5D). On the contrary, after injection of DH-L, an unequivocal change of the LPS monolayer organization is observed in both BAM-images and delta-maps (Fig. 5F and H). Especially, the small high Δ-domains make place for bigger ones, and the background Δ-value increases (Fig. 5H).

Atomic force microscopy (AFM) enables to investigate the LPS monolayer at a nanoscale with a high resolution. Thus, this technique was used to study more precisely the organization of the lipid monolayer observed in the background of BAM-images (black zones).

The resulting AFM-images show the heterogeneity of the initial LPS monolayer at a nanoscale at both initial surface pressures (25 mN/m and 30 mN/m; Fig. 6A, C, E and G). The height difference between the lower (zone 1) and higher (zone 2) lipid zones is 1.2 to 2.0 ± 0.2 nm. By grating the LPS (data not shown), the monolayer thickness could be measured and corresponds to 5 nm. The monolayer thickness is in coherence with the one found by Le Brun et al. [26].

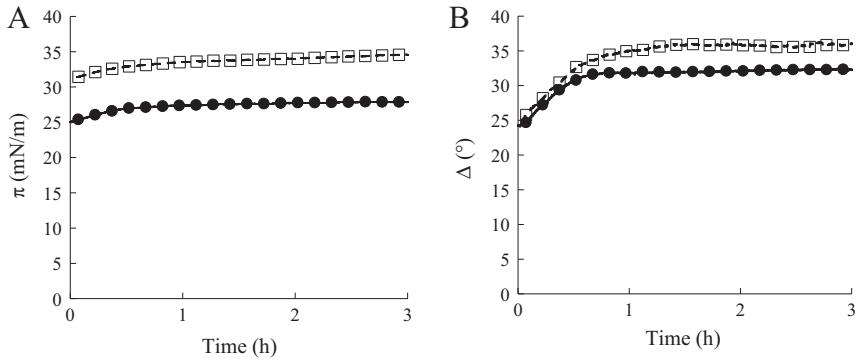

Fig. 2. Surface pressure π (A) and ellipsometric angle Δ (B) changes during N-L (●) and DH-L (□) adsorption at a LPS monolayer having an initial surface pressure of 25 mN/m and 30 mN/m, respectively.

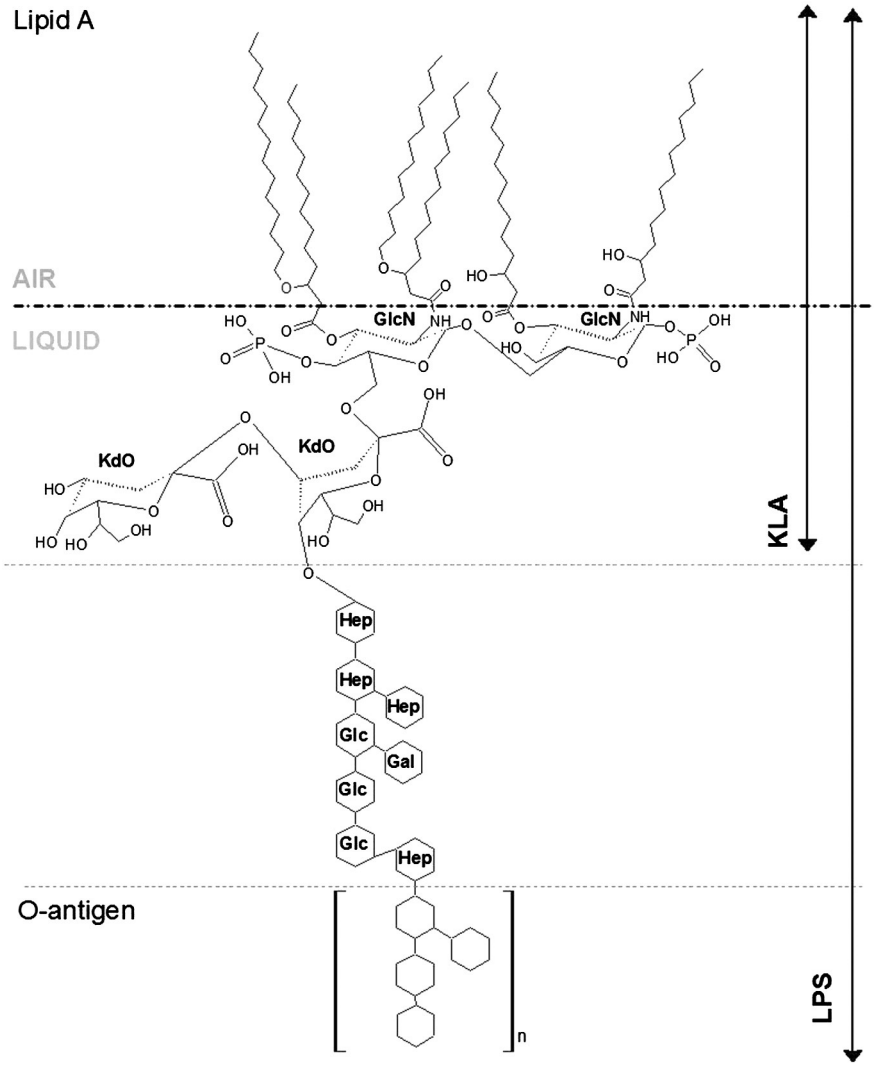

Fig. 3. Schematic representation of *E. coli* K12 LPS and KLA lipids. GlcN (*N*-acetylglucosamine); KdO (3-deoxy-D-manno-octulosonic acid); Hep (L-gycero-D-manno heptose); Gal (galactose); Glc (glucose).

The impact of N-L and DH-L on the lipid monolayer can also be studied by AFM, enabling to study more carefully the reorganization of the low Δ-domains present in the BAM-images.

AFM shows that the injection of 0.1 μM N-L or DH-L does not significantly modify the heterogeneous appearance of the LPS monolayer (Fig. 6B, D, F and H). However, the insertion and adsorption of 0.1 μM N-L gives rise to the formation of small domains (object 1) with a height of 1.4 ± 0.4 nm (Fig. 6B and D). The height of these domains is equivalent to the height of the dense domains observed in absence of lysozyme (Fig. 6A and C). The adsorption and insertion of 0.1 μM

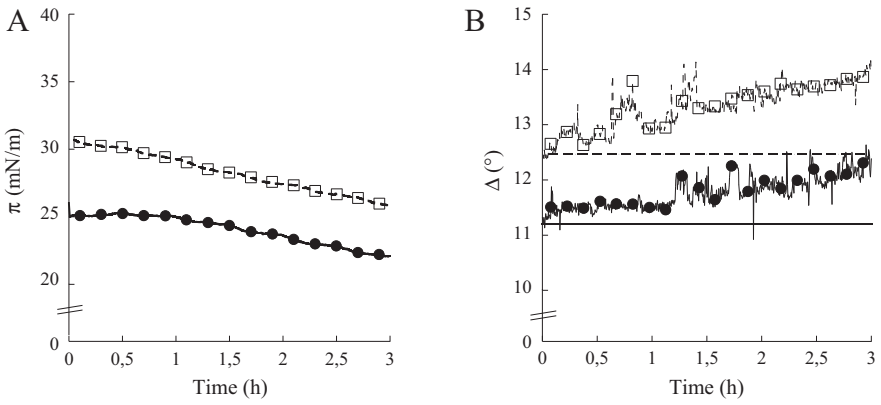

Fig. 4. Surface pressure π (A) and ellipsometric angle Δ (B) changes during N-L (●) and DH-L (□) adsorption at a KLA monolayer having an initial surface pressure of 25 mN/m and 30 mN/m, respectively. The initial Δs of the KLA lipids at 25 mN/m and 30 mN/m are shown as full and dashed lines, respectively.

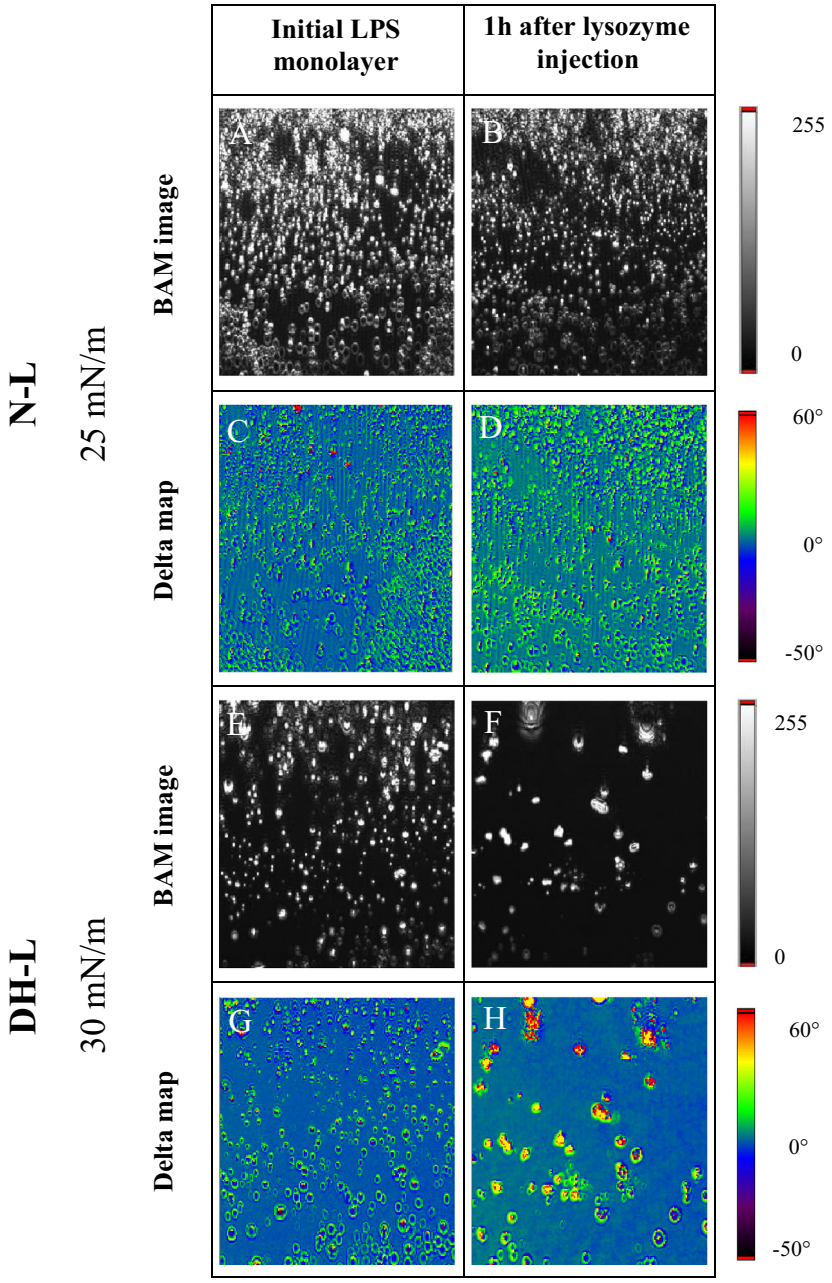

Fig. 5. BAM-images and delta-maps (450 μm × 390 μm) before (A, C, E, G) and after N-L (B, D) or DH-L (F, H) injection under the LPS monolayer. The initial surface pressure was 25 mN/m or 30 mN/m, for N-L or DH-L, respectively.

DH-L induces the formation of two types of clusters (objects 2 and 3 with a height of 25 ± 5 and 57 ± 12 nm, respectively) and small domains (object 4) (1.4 ± 0.3 nm height) (Fig. 6F and H).

Topographical information shown in the AFM images is representative for the whole sample. However, the size and shape of the different domains is irregular and heterogeneously distributed over the sample, making it impossible to quantify the effect of lysozyme on the domain size and shape.

4. Discussion

Native lysozyme (N-L) has been shown active against Gram-negative bacteria such as *E. coli* [11,27]. Membrane permeabilization has been suggested as one of the mechanisms responsible for this activity [8,28]. This assumption was recently confirmed by our group who demonstrated that N-L causes the formation of pores and ion channels in the outer and cytoplasmic membranes, respectively [9,11]. Pore formation due to N-L implies that interactions occur between the protein and the *E. coli* outer membrane. Nevertheless, the mode of insertion of lysozyme into the outer membrane remains unknown.

Moreover, dry-heated lysozyme (DH-L) has a higher antimicrobial activity and higher membrane disruption potential than N-L [11]. This improved activity is supposed to be related to the modified physicochemical properties of DH-L. DH-L is more hydrophobic, flexible and surface active than N-L, but its secondary and tertiary structures remain intact [29,30]. It is thus relevant to compare the interaction of native and dry-heated lysozymes with LPS, the lipid components of the outer leaflet of the outer membrane of Gram negative bacteria.

Interfacial monolayers are considered as good models to study interactions between antimicrobial peptides and bacterial membranes [18,

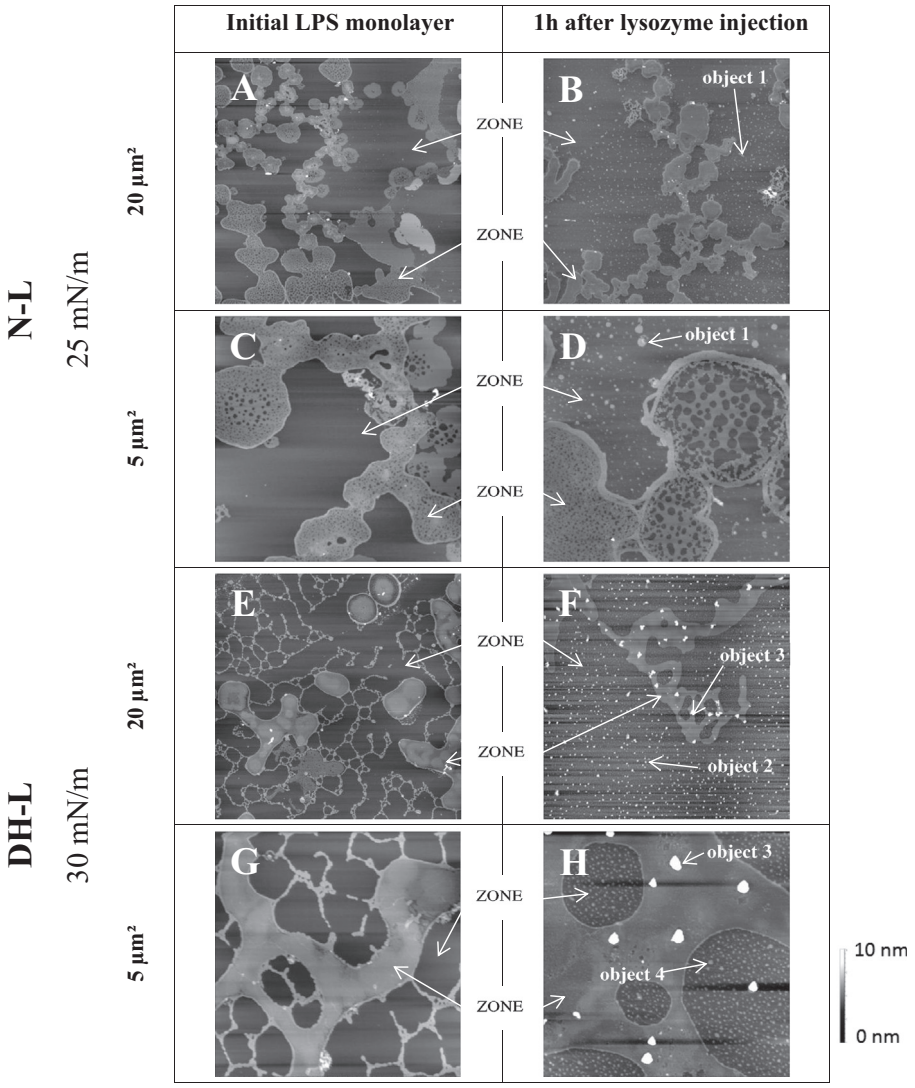

Fig. 6. Topographic AFM-images before (A, C, E, G) and after N-L (B, D) or DH-L (F, H) injection under the LPS-monolayer. The initial surface pressure was 25 mN/m or 30 mN/m, for N-L or DH-L, respectively. The Z-range is 10 nm.

19]. In the presently reported study, a LPS monolayer was used to mimic the outer leaflet of the *E. coli* K12 outer membrane, in order to explore the first step of lysozyme interaction with bacterial membrane. It is noticeable that wild-type LPS was here used for the first time to investigate protein-LPS interactions at a macroscopic and mesoscopic level, using biophysical tools such as tensiometry, ellipsometry, AFM and BAM.

4.1. The affinity of N-L for LPS is very high and makes possible the insertion of the protein into a LPS monolayer

For the first time, protein insertion into a wild type LPS monolayer is here demonstrated. Until now, protein insertion was only recorded for LPS-derivative monolayers and lung surfactant protein D. [31]. The

Table 2
Surface pressure increase (Δπ) of LPS or LPS-derivative monolayers measured after adsorption of antimicrobial peptides and N-L or DH-L. The initial surface pressure was 18 mN/m for both peptides and protein.

	Peptide or protein	Concentration (μM)	Δπ (mN/m)	Bacterial species	LPS type	Reference
Peptides	Polymyxin B (1.4 kDa)	0.5	17.5	*S. enterica*	Re-LPS	[32]
	Polymyxin E1 (1.2 kDa)	0.5	21	*S. enterica*	Re-LPS	[32]
	Colymycin (1.8 kDa)	0.5	0.5	*S. enterica*	Re-LPS	[32]
	Gramicidin S (1.1 kDa)	0.15	17	*S. enterica*	Re-LPS	[32]
	Temporin L (1.6 kDa)	0.1	7.5	*E. coli*	Wild-type LPS	[33]
Lysozyme	N-L (14.4 kDa)	0.1	5.2	*E. coli*	Wild-type LPS	This study
	N-L (14.4 kDa)	0.1	−2.1	*E. coli*	KLA ~ Re-LPS	This study
	DH-L (14.4 kDa)	0.1	7.8	*E. coli*	Wilt-type LPS	This study
	DH-L (14.4 kDa)	0.1	−5	*E. coli*	KLA ~ Re-LPS	This study

surface pressure increase measured when N-L is injected into the subphase demonstrates that N-L is able to insert into a LPS monolayer (Fig. 1A). The ability of lysozyme to interact with LPS is consistent with the surface activity of the protein at the air/liquid interface [30]. However, insertion of N-L into the LPS monolayer remains lower than for antimicrobial peptides such as temporin L, as suggested by the lower surface pressure increase (Table 2) [32,33]. The larger molecular size and higher rigidity of lysozyme [34], as compared to peptides, could be responsible for the lower efficiency of the protein.

The maximal insertion pressure (MIP), determined from measurements of N-L insertion at different initial pressures, is high (41.5 mN/m, Table 1) and similar to MIP recorded for antimicrobial peptides and phospholipid monolayers (25–45 mN/m) [23,33]. Especially, it is remarkable that the MIP value is higher than the lateral pressure which is supposed to exist in natural membrane systems in eukaryotic cells (~30 mN/m) [35]. Unfortunately, no measurements or theoretical deductions of the lateral pressure in the outer and cytoplasmic membranes of prokaryotes are available in literature then no comparison is possible with the here observed MIP value. Moreover, the N-L synergy factor (0.79, Table 1) is extremely high as compared to reported values for protein insertion into phospholipid monolayers (from 0.3 to 0.5) [24]. It can thus be concluded that the protein has a high affinity for the LPS interface between 18 and 30 mN/m and strikingly lysozyme insertion is almost not impacted by the lateral cohesion of the LPS molecules. These observations suggest a mode of action that is unusual compared to the interaction between protein and phospholipids. This could result from the LPS inherent molecular structure and from the specificities of a LPS monolayer compared to a phospholipid monolayer; the LPS molecules have heterogeneous polysaccharide chains in length, thus the monolayer has a variable thickness induced by the auto-assemblage of similar LPS molecules observed by BAM and AFM microscopy (Figs. 5 and 6). Indeed, a LPS monolayer can be divided into two distinct zones, i.e. a polysaccharide zone and a phospholipid-like zone, on the contrary to a phospholipid monolayer which is composed of a unique zone.

4.2. The polysaccharide moieties of LPS are needed for N-L insertion

When LPS molecules are depleted from their polysaccharide moieties (KLA), lysozyme is no longer able to insert into the lipid monolayer, since no increase of the surface pressure occurs (Fig. 4A). However, lysozyme adsorption is evidenced by the increase of the ellipsometric angle (Δ) (Fig. 4B). Lysozyme adsorption could involve hydrogen bonds between the protein and the remaining two sugar moieties, or electrostatic interactions between the positive lysozyme and the negative KLA. The latter assumption is reinforced by the immediate and higher adsorption of DH-L which is more positively charged than N-L (Fig. 2B). It is also in accordance with Brandenburg et al. who reported electrostatic interactions between *Salmonella minnesota* Re-LPS and lysozyme in solution [36].

Actually, while N-L adsorption is proceeding for 3 h (Fig. 4B), the surface pressure of the lipid monolayer is decreasing (Fig. 4A). This could be due to a destabilization and partial solubilization of the lipid monolayer as has been previously described for the antimicrobial peptide protegrin-1 at a lipid A monolayer [37]; another hypothesis is the reorganization or reorientation of the lipid headgroups induced by lysozyme presence beneath the monolayer, similar to what has been previously reported for a dystrophin subdomain R20-24 at a DOPC/DOPS monolayer [38]. If a partial solubilization of the KLA occurs, this should be reflected in a decrease of the ellipsometric angle (Δ), due to the loss of matter at the interface. Here, the ellipsometric angle increases (Fig. 4), meaning that rather than a solubilization of the KLA monolayer, a reorganization of the KLA head groups takes place leading to a relaxation of the lipid film. Lysozyme molecules are trapped beneath the KLA monolayer caused by strong electrostatic attractive forces between lysozyme and the KLA lipids.

On the contrary, when N-L interacts with a LPS monolayer, i.e. including polysaccharide moieties, surface pressure and ellipsometric angle simultaneously increase (Fig. 2A and B). Undoubtedly, N-L is thus able to insert deeply in the interface, up to the hydrophobic zone of the LPS monolayer. A hypothesis can be the effect of steric hindrance of the polysaccharides which prevents total coverage of the interface by the lipid headgroups, thus leaving free space for lysozyme insertion. Moreover, the polysaccharide chains can also cause simultaneously partial shielding of the negative charges on the headgroups and therefore prevent the entrapment of the positive lysozyme molecules at the level of these negative charges as it is the case for KLA lipids. The decreased interaction of the negative charges with positive lysozyme could enable insertion of the protein between the LPS headgroups. At last, lysozyme and the polysaccharides moieties could interact and create compact zones as LPS/lysozyme domains and complexes (Fig. 6) resulting in lesser density in other areas enabling the remaining free lysozyme to attain the interface. Such strong hydrophobic interactions have already been reported between LPS and lysozyme in solution [39], and LPS/lysozyme complexes have been observed [36,40].

4.3. N-L interaction with LPS causes a slight reorganization of the LPS monolayer

At the same time as the surface pressure increases when N-L is injected under a LPS monolayer, a strong increase of the ellipsometric angle Δ (+7°, Fig. 2B) is observed, which is higher than the ellipsometric angle increase for protein/phospholipid monolayers [41]. This unusually high Δ increase can be explained by the LPS/lysozyme complex formation, polysaccharide reorganization, and/or the presence of N-L at the interface, since the ellipsometric angle depends on the refraction index and the film thickness.

BAM and AFM imaging were performed to evaluate the different hypotheses explaining the Δ increase. BAM and AFM imaging show the heterogeneity of the initial LPS monolayer at micrometer and nanometer scales, respectively (Figs. 4A, C and 5A, C), as a result of the variable lengths of the polysaccharides chains. After N-L injection and interaction with LPS, this heterogeneity is maintained as can be observed in the BAM (Fig. 5B and D) and AFM images (Fig. 6B and D). But N-L injection also results in a slight increase of the background Δ-value in the delta-map (Fig. 5D), and in the formation of small domains on the background zones in AFM-imaging (Fig. 6B and D). It can thus be concluded that N-L reorganizes the LPS monolayer, even if this reorganization remains limited. The reorganization of the LPS monolayer and the LPS/lysozyme complex formation could possibly be the preliminary steps for pore formation by N-L as observed *in vivo* by Derde et al. [9].

4.4. DH-L has a stronger affinity for LPS than N-L, and causes more radical reorganization of the LPS monolayer

Similarly to N-L, DH-L insertion into the LPS monolayer is enabled by the polysaccharides moieties, and DH-L reorganizes the LPS monolayer. However, differences in the behavior of DH-L *versus* N-L with the LPS monolayer can be noticed. This modified behavior could be related to its different physico-chemical properties such as increased hydrophobicity, surface-activity, positive charge and flexibility [29,30].

DH-L insertion into the LPS monolayer is more efficient than N-L at concentrations higher than 0.05 μM (Fig. 1A). This could be due to the higher flexibility of DH-L as compared to N-L [29], which could allow more DH-L molecules to insert into the LPS monolayer, and/or to restructure more efficiently the interface. The increased insertion capacity of DH-L is consistent with its slight increased interfacial behavior (π_{final}, Table 1). Especially, it is noticeable that the surface pressure increase induced by DH-L insertion into the LPS-monolayer is similar to that measured with an antimicrobial peptide, i.e. temporin L, in equivalent

conditions (Table 2). DH-L has also more affinity for the LPS monolayer than N-L, demonstrated by its higher MIP and synergy factor (59.6 mN/m and 0.85, respectively; Table 1) [23,33]. The drastically different reorganization of the LPS monolayer by DH-L is highlighted by BAM and AFM imaging (Figs. 5 and 6). The BAM-images show that the many small domains with a high Δ-value visible in the presence of N-L (Fig. 5B and D) are replaced by larger and fewer high Δ-value domains in the presence of DH-L (Fig. 5F and H). Concurrently, more or less thick, and more or less large clusters appear in the presence of DH-L, as evidenced by AFM images (Fig. 6F and H). These clusters could be protein aggregates caused by high local concentration of DH-L at the LPS-monolayer, consistently with the higher sensitivity to aggregation of DH-L as compared to N-L, previously established by Desfougères et al. [30].

5. Conclusions

The presently reported study demonstrates the strong interaction between N-L and a LPS monolayer, usually considered as a relevant model of the outer membrane of Gram-negative bacteria. Even more, N-L is able to insert leading to a lateral reorganization of the LPS monolayer, which can explain pore formation into the *E. coli* outer membrane, previously observed *in vivo* [11]. An original and unexpected result is that lysozyme insertion between the lipid A of LPS monolayers requires the presence of the polysaccharide moieties. This reveals specific interactions between lysozyme and the polysaccharide moieties leading to better insertion and decreased electrostatic attraction. Further experiments are needed in order to settle between the different hypotheses that could explain this finding.

Moreover, dry-heating modifies lysozyme properties in such a way that its affinity for LPS, its insertion capacity, and its ability for LPS monolayer reorganization are emphasized. These results are thus consistent with *in vivo* experiments that demonstrated larger and/or more numerous pores induced by DH-L into the *E. coli* outer membrane, as compared to N-L [11].

The interaction of N-L and DH-L with the outer membrane lipids is now well established and consistent with the pore formation previously demonstrated *in vivo*. Self-uptake mechanism is then imaginable meaning that lysozyme molecules involved in pore formation and stabilization could enable the entrance of free lysozyme in the bacterial cell. Then, it is relevant to further study the interaction of lysozyme with the cytoplasmic membrane, the final hurdle before access to the cytoplasm. The findings resulting from this study are currently analyzed and will soon be published.

Acknowledgment

The authors thank “Conseil Regional de Bretagne” for the funding of this work.

Appendix A. Supplementary data

Additional experimental data on the ellipsometric angle of a LPS monolayer (S1), atomic force images of LPS or KLA monolayers (S2) and isothermal compression of LPS and KLA monolayers (S3). This material is available free of charge via the Internet at http://pubs.acs.org. Supplementary data related to this article can be found online at DOI: http://dx.doi.org/10.1016/j.bbamem.2014.10.026.

References

[1] World Health Organization, Overcoming antimicrobial resistance, Geneva, Zwitserland, 2000.
[2] A. Rosbach, Report on the microbial challenge—Rising threats from antimicrobial resistance (2012/2041(INI)), European parliament, commitee on the environment, public health and food safety, 2012.
[3] L.T. Nguyen, E.F. Haney, H.J. Vogel, The expanding scope of antimicrobial peptide structures and their modes of action, Trends Biotechnol. 29 (2011) 464–472.
[4] A. Peschel, H.G. Sahl, The co-evolution of host cationic antimicrobial peptides and microbial resistance, Nat. Rev. Microbiol. 4 (2006) 529–536.
[5] H. Jenssen, P. Hamill, R.E. Hancock, Peptide antimicrobial agents, Clin. Microbiol. Rev. 19 (2006) 491–511.
[6] P. Jolles, J. Jolles, Whats new in lysozyme research—always a model system, today as yesterday, Mol. Cell. Biochem. 63 (1984) 165–189.
[7] B. Masschalck, C.W. Michiels, Antimicrobial properties of lysozyme in relation to foodborne vegetative bacteria, Crit. Rev. Microbiol. 29 (2003) 191–214.
[8] A. Pellegrini, U. Thomas, P. Wild, E. Schraner, R. von Fellenberg, Effect of lysozyme or modified lysozyme fragments on DNA and RNA synthesis and membrane permeability of *Escherichia coli*, Microbiol. Res. 155 (2000) 69–77.
[9] M. Derde, V. Lechevalier, C. Guérin-Dubiard, M.F. Cochet, S. Jan, F. Baron, et al., Hen egg white lysozyme permeabilizes the *Escherichia coli* outer and inner membranes, J. Agric. Food Chem. 61 (2013) 9922–9929.
[10] K. During, P. Porsch, A. Mahn, O. Brinkmann, W. Gieffers, The non-enzymatic microbicidal activity of lysozymes, FEBS Lett. 449 (1999) 93–100.
[11] M. Derde, C. Guérin-Dubiard, V. Lechevalier, M.-F. Cochet, S. Jan, F. Baron, et al., Dry-heating of lysozyme increases its activity against *Escherichia coli* membranes, J. Agric. Food Chem. 62 (2014) 1692–1700.
[12] Y. Mine, F.P. Ma, S. Lauriau, Antimicrobial peptides released by enzymatic hydrolysis of hen egg white lysozyme, J. Agric. Food Chem. 52 (2004) 1088–1094.
[13] A.M. Abdou, S. Higashiguchi, A. Aboueleinin, M. Kim, H.R. Ibrahim, Antimicrobial peptides derived from hen egg lysozyme with inhibitory effect against *Bacillus* species, Food Control 18 (2007) 173–178.
[14] H.R. Ibrahim, S. Higashiguchi, L.R. Juneja, M. Kim, T. Yamamoto, A structural phase of heat-denatured lysozyme with novel antimicrobial action, J. Agric. Food Chem. 44 (1996) 1416–1423.
[15] M. Hoq, I.K. Mitsuno, Y. Tsujino, T. Aoki, H.R. Ibrahim, Triclosan-lysozyme complex as novel antimicrobial macromolecule: a new potential of lysozyme as phenolic drug-targeting molecule, Int. J. Biol. Macromol. 42 (2008) 468–477.
[16] H.R. Ibrahim, A. Kato, K. Kobayashi, Antimicrobial effects of lysozyme against Gram-negative bacteria due to covalent binding of palmitic acid, J. Agric. Food Chem. 39 (1991) 2077–2082.
[17] H.R. Ibrahim, M. Yamada, K. Kobayashi, A. Kato, Bactericidal action of lysozyme against Gram-negative bacteria due to insertion of a hydrophobic pentapeptide into its C-terminus, Biosci. Biotechnol. Biochem. 56 (1992) 1361–1363.
[18] H. Brockman, Lipid monolayers: why use half a membrane to characterize protein-membrane interactions? Curr. Opin. Struct. Biol. 9 (1999) 438–443.
[19] S. Roes, U. Seydel, T. Gutsmann, Probing the properties of lipopolysaccharide monolayers and their interaction with the antimicrobial peptide polymyxin B by atomic force microscopy, Langmuir 21 (2005) 6970–6978.
[20] ExPASy, P00698 (Chicken lysozyme), (n.d.). http://web.expasy.org/cgi-bin/protparam/protparam1?P00698@19-147@ (accessed April 2, 2014).
[21] B. Berge, A. Renault, Ellipsometry study of 2D crystallization of 1-alcohol monolayers at the water surface, EPL Europhys. Lett. 21 (1993) 773.
[22] R.M.A. Azzam, N.M. Bashara, Ellipsometry and polarized light, North-Holland Pub. Co., 1977
[23] P. Calvez, S. Bussières, Éric Demers, C. Salesse, Parameters modulating the maximum insertion pressure of proteins and peptides in lipid monolayers, Biochimie 91 (2009) 718–733.
[24] É. Boisselier, P. Calvez, É. Demers, L. Cantin, C. Salesse, Influence of the physical state of phospholipid monolayers on protein binding, Langmuir 28 (2012) 9680–9688.
[25] P. Calvez, E. Demers, E. Boisselier, C. Salesse, Analysis of the contribution of saturated and polyunsaturated phospholipid monolayers to the binding of proteins, Langmuir 27 (2011) 1373–1379.
[26] A.P. Le Brun, L.A. Clifton, C.E. Halbert, B. Lin, M. Meron, P.J. Holden, et al., Structural characterization of a model Gram-negative bacterial surface using lipopolysaccharides from rough strains of *Escherichia coli*, Biomacromolecules 14 (2013) 2014–2022.
[27] A. Pellegrini, U. Thomas, R. Vonfellenberg, P. Wild, Bactericidal activities of lysozyme and aprotinin against Gram-negative and Gram-positive bacteria related to their basic character, J. Appl. Bacteriol. 72 (1992) 180–187.
[28] P. Wild, A. Gabrieli, E.M. Schraner, A. Pellegrini, U. Thomas, P.M. Frederik, et al., Reevaluation of the effect of lysoyzme on *Escherichia coli* employing ultrarapid freezing followed by cryoelectronmicroscopy or freeze substitution, Microsc. Res. Tech. 39 (1997) 297–304.
[29] Y. Desfougères, J. Jardin, V. Lechevalier, S. Pézennec, F. Nau, Succinimidyl residue formation in hen egg-white lysozyme favors the formation of intermolecular covalent bonds without affecting its tertiary structure, Biomacromolecules 12 (2011) 156–166.
[30] Y. Desfougères, A. Saint-Jalmes, A. Salonen, V. Vié, S. Beaufils, S. Pézennec, et al., Strong improvement of interfacial properties can result from slight structural modifications of proteins: the case of native and dry-heated lysozyme, Langmuir 27 (2011) 14947–14957.
[31] L. Wang, J.W. Brauner, G. Mao, E. Crouch, B. Seaton, J. Head, et al., Interaction of recombinant surfactant protein D with lipopolysaccharide: conformation and orientation of bound protein by IRRAS and simulations, Biochemistry 47 (2008) 8103–8113.
[32] L. Zhang, P. Dhillon, H. Yan, S. Farmer, R.E.W. Hancock, Interactions of bacterial cationic peptide antibiotics with outer and cytoplasmic membranes of *Pseudomonas aeruginosa*, Antimicrob. Agents Chemother. 44 (2000) 3317–3321.
[33] A. Giacometti, O. Cirioni, R. Ghiselli, F. Mocchegiani, F. Orlando, C. Silvestri, et al., Interaction of antimicrobial peptide temporin L with lipopolysaccharide *in vitro* and in experimental rat models of septic shock caused by Gram-negative bacteria, Antimicrob. Agents Chemother. 50 (2006) 2478–2486.
[34] R.E. Canfield, A.K. Liu, The disulfide bonds of egg white lysozyme (muramidase), J. Biol. Chem. 240 (1965) 1997–2002.
[35] D. Marsh, Lateral pressure in membranes, Biochim. Biophys. Acta 1286 (1996).

[36] K. Brandenburg, M.H. Koch, U. Seydel, Biophysical characterisation of lysozyme binding to LPS Re and lipid A, Eur. J. Biochem. 258 (1998) 686–695.
[37] Y. Ishitsuka, D. Pham, A. Waring, R. Lehrer, K. Lee, Insertion selectivity of antimicrobial peptide protegrin-1 into lipid monolayers: effect of head group electrostatics and tail group packing, Biochim. Biophys. Acta BBA-Biomembr. 1758 (2006) 1450–1460.
[38] V. Vié, S. Legardinier, L. Chieze, O. Le Bihan, Y. Qin, J. Sarkis, et al., Specific anchoring modes of two distinct dystrophin rod sub-domains interacting in phospholipid Langmuir films studied by atomic force microscopy and PM-IRRAS, Biochim. Biophys. Acta BBA-Biomembr. 1798 (2010) 1503–1511.
[39] N. Ohno, D.C. Morrison, Lipopolysaccharide interaction with lysozyme. Binding of lipopolysaccharide to lysozyme and inhibition of lysozyme enzymatic activity, J. Biol. Chem. 264 (1989) 4434–4441.
[40] N. Ohno, N. Tanida, T. Yadomae, Characterization of complex-formation between lipopolysaccharide and lysozyme, Carbohydr. Res. 214 (1991) 115–130.
[41] J. Sarkis, J.-F. Hubert, B. Legrand, E. Robert, A. Chéron, J. Jardin, et al., Spectrin-like repeats 11–15 of human dystrophin show adaptations to a lipidic environment, J. Biol. Chem. 286 (2011) 30481–30491.

Annexe B : Publications soumises/Preuves de soumission

- Derde M., Nau F., Guérin-Dubiard C., Lechevalier V., Paboeuf G., Jan S., Baron F., Gautier M. & Vié V. Native and dry-heated lysozyme interactions with membrane lipid monolayers : lipid packing modifications of a phospholipid monolayer, model of the *Escherichia coli* cytoplasmic membrane, soumis *BBA biomembranes*, en revision

- Derde M., Vié V., Lechevalier V., Guérin-Dubiard C., Cochet MF., Paboeuf G., Bertović T., Jan S., Baron F., Gautier M. & Nau F. Dry-heated lysozyme, a mixture of complementary lysozyme isoforms acting on the *Escherichia coli* membranes, soumis *International Journal of Biological Macromolecules*, en revision

Elsevier Editorial System(tm) for BBA - Biomembranes
Manuscript Draft

Manuscript Number: BBAMEM-14-365

Title: Native and dry-heated lysozyme interactions with membrane lipid monolayers: lipid packing modifications of a phospholipid mixture, model of the E. coli cytoplasmic membrane.

Article Type: Regular Paper

Keywords: dry-heating, monolayer membrane models, cytoplasmic membrane, Escherichia coli, antimicrobial protein

Corresponding Author: Mrs. Melanie Derde,

Corresponding Author's Institution:

First Author: Melanie Derde

Order of Authors: Melanie Derde; Françoise Nau; Catherine Guérin-Dubiard; Valérie Lechevalier; Gilles Paboeuf; Sophie Jan; Florence Baron; Michel Gautier; Véronique Vié

Abstract: Antimicrobial resistance is an important public health issue nowadays. The need for novel antimicrobials is thus growing. The novel, ideal antimicrobial compounds should limit antimicrobial resistance. Antimicrobial peptides or proteins such as hen egg white lysozyme are promising molecules acting on the bacterial membranes. Hen egg white lysozyme has recently by identified active on Gram negative bacteria due to disruption of the outer and cytoplasmic membranes integrity. Moreover, dry-heating (7 days and 80°C) improves the membrane activity of lysozyme resulting in higher antimicrobial activity. These in vivo findings suggest interactions between lysozyme and the membrane lipids. This is consistent with the findings of several authors showing lysozyme interaction with bacterial phospholipids such as phosphatidylglycerol and cardiolipin. However, up till now the mechanism of interaction between lysozyme and the bacterial cytoplasmic phospholipids still needs elucidation. In the here presented study, the use of a monolayer model with a realistic bacterial phospholipid composition and in physiological conditions is proposed. The lysozyme/phospholipid interactions have been studied by surface pressure measurements, ellipsometry and atomic force microscopy. Native lysozyme revealed able to adsorb onto and insert into a bacterial phospholipid monolayer resulting in lipid packing reorganization leading to lateral cohesion decrease between phospholipids. Dry-heating of lysozyme increased insertion capacity and ability to induce lipid packing modifications. These in vitro findings are then consistent with increased membrane disruption potential of dry-heated lysozyme in vivo compared to native lysozyme. Moreover, lysozyme/phospholipid interactions have been shown specific for bacterial cytoplasmic membranes lipids after a eggPC monolayer study.

Suggested Reviewers: Maria Luisa Mangoni Prof. Dr.
Biochemical Sciences, Sapienza University of Rome
marialuisa.mangoni@uniroma1.it

Robert Hancock Prof. Dr.
Microbiology and Immunology, University of British Columbia
bob@hancocklab.com

Thomas Gutsmann Prof. Dr.
Division of Biophysics, Research center Borstel
tgutsmann@fz-borstel.de

Yolanda Cayal Prof. Dr.
Physical Chemistry, University of Barcelona
ycajal@ub.edu

Elsevier Editorial System(tm) for International Journal of Biological Macromolecules
Manuscript Draft

Manuscript Number: IJBIOMAC-D-14-01439

Title: Dry-heated lysozyme, a complementary mixture of lysozyme isoforms acting on the E. coli membranes

Article Type: Research Report

Keywords: Membrane permeabilization, Membrane depolarization, Monolayer models, Iso-aspartyle lysozyme, Succinimide lysozyme

Corresponding Author: Mrs. Melanie Derde,

Corresponding Author's Institution:

First Author: Melanie Derde

Order of Authors: Melanie Derde; Véronique Vié, Dr.; Valérie Lechevalier, Dr.; Cathérine Guérin-Dubiard, Dr.; Marie-Françoise Cochet; Gilles Paboeuf; Tanja Bertovic; Sophie Jan, Dr.; Florence Baron, Dr.; Michel Gautier, Prof. Dr.; Françoise Nau, Prof. Dr.

Abstract: Because of increasing bacteria resistance towards antibiotics, research for novel antimicrobials is stimulated. Proteins acting on bacterial membranes could be a solution. Lysozyme proved active against E. coli by disruption of both outer and cytoplasmic membranes. Moreover, dry-heating increases lysozyme activity. Since dry-heated lysozyme is a mixture of isoforms (iso-aspartyle, native-like and succinimide lysozymes), the question arises of what are the individual effects of each isoform. This issue was here investigated in vivo and in vitro. Each isoform appears less efficient than DH-L against E. coli, but their combination results in a more efficient mixture. The membrane modifications induced by one isoform could facilitate the subsequent action of the other isoforms. Positive charges, hydrophobicity and molecular flexibility of the isoforms seem key parameters for their interaction with E. coli membranes. Succinimide lysozyme, the most positive, flexible and hydrophobic isoform, shows the highest antimicrobial activity and induces the strongest membrane disruption.

Annexe C : Communications scientifiques

- **Communications orales**

  - Derde M., Guérin-Dubiard C., Lechevalier V., Jan S., Baron F., Gautier M., Vié V. & Nau F. Bacterial membrane perturbation by native versus dry-heated lysozyme. Présenté au congrès BioMicroWorld 2013 (2-4 octobre), Madrid, Espagne

  - Derde M., Nau F., Lechevalier V., Guérin-Dubiard C., Paboeuf G., Jan S., Baron F., Gautier M. & Vié V. Exploring the membrane insertion of native and dry-heated lysozymes into *E. coli* lipopolysaccharide monolayers. Présenté au congrès Rencontres Biologie-Physique du Grand Ouest 2014 (3-4 juin), Le Mans, France

- **Communications par affiche**

  - Derde M. Modifications biochimiques du lysozyme : Des opportunités pour le développement de nouvelles molécules bactéricides ? Affiché à INRA UMR1253 STLO, Rennes, France

  - Derde M., Nau F., Lechevalier V., Guérin-Dubiard C., Jan S., Baron F., Gautier M. & Vié V. Evidence by AFM-imaging of morphological differences between *E. coli* K12 cells treated with native and dry-heated lysozyme. Présenté au Forum des microscopie à sonde locale 2013 (25-29 mars), Spa, Belgique

  - Derde M., Lechevalier V., Guérin-Dubiard C., Cochet MF., Jan S., Baron F., Gautier M., Vié V. & Nau F. Bacterial membrane disruption by native versus dry-heated lysozyme. Présenté au GEM/GERLI 2013 (10-14 novembre), St-Jean Cap Ferrat, France

  - Derde M., Nau F., Lechevalier V., Guérin-Dubiard C., Paboeuf G., Jan S., Baron F., Gautier M. & Vié V. Exploring the membrane insertion of native and dry-heated lysozymes into *E. coli* lipopolysaccharide monolayers. Présenté au Symposium AMP 2014 (4-6 juin), Lorient, France

Bacterial membrane perturbation by native *versus* dry-heated lysozyme

M. Derde[1,2], C. Guérin-Dubiard[1,2], V. Lechevalier[1,2], S. Jan[1,2], F. Baron[1,2], M. Gautier[1,2], V. Vié[3] and F. Nau[1,2]

[1] Agrocampus Ouest, UMR 1253 STLO, rue de St-Brieuc 65, 35042 Rennes, France
[2] INRA,UMR 1253 STLO, rue de St-Brieuc 65, 35042 Rennes, France
[3] Université de Rennes 1, UMR CNRS 6251, Institut de Physique de Rennes, 35042 Rennes, France

Antimicrobial drug resistance causes public health problems worldwide. Scientific research for the discovery of novel antimicrobial molecules is thus highly stimulated [1]. Particular attention is given to antimicrobial molecules that limit drug resistance development and have a large spectrum. Antimicrobial peptides and proteins are thus good candidates. Some of them act on the bacterial cell wall because of their physico-chemical properties; when amphiphilic and positively charged, these molecules are able to interact with the negatively charged bacterial surface[2]. These antimicrobial peptides and proteins can thus perturb the bacterial cell envelope, enter the cell, and/or act on intracellular targets [2, 3]. Hen egg white lysozyme is a marketed protein, available at an affordable price (100€/kg). This small protein (14.4 kDa) is largely studied and widely known for its muramidase activity against the peptidoglycan of Gram-positive bacteria, the Gram negative bacteria being protected by their outer membrane [4]. However, lysozyme is also described as being active against some Gram-negative bacteria, especially because it permeabilizes the bacterial membranes [4, 5]. But few is known about this activity, and the consequences on the bacterial membranes remains quite limited. Since dry-heated lysozyme, composed of a mixture of several isoforms, *i.e.* iso-aspartyle, native-like and succinimide lysozymes [6], is more positively charged, more hydrophobic and more tensio-active than native lysozyme [6], dry-heating could be a way to increase lysozyme activity against the bacterial membranes, and especially against Gram-negative bacteria.

To investigate the membrane activity of both native and dry-heated lysozyme, membrane permeability measurements using a mutant *E. coli* ML-35p and measurements of membrane potential perturbation were performed. These experiments revealed that native and dry-heated lysozyme induce different consequences on the bacterial membranes. Native lysozyme permeabilizes both outer and inner membranes. Pore formation could be observed for the outer membrane, but not for the inner membrane. Moreover, the membrane potential of the inner membrane is modified in the presence of native lysozyme. Dry-heated lysozyme induces an overall stronger disturbance than native lysozyme, by giving rise to the formation of more and/or larger pores in the outer membrane, by permeabilizing more rapidly the inner membrane, and by leading to a stronger disturbance of membrane potential. We could also establish that each of the dry-heated lysozyme isoforms affords a specific disturbance of either the outer or the inner membrane. Succinimide lysozyme strongly increases the outer membrane permeability, but mildly modifies the permeability of the inner membrane. On the contrary, iso-aspartyle lysozyme modifies more strongly the inner than the outer membrane permeability. This was confirmed by membrane potential perturbation caused by iso-aspartyle lysozyme. Both isoforms thus prove complementary.

Keywords: Lysozyme; Gram-negative bacteria, Bacterial membrane perturbation

[1] WHO. Overcoming antimicrobial resistance. **2000**, Geneva, Zwitserland

[2] Nguyen, NT et al. The expanding scope of antimicrobial peptide structures and their modes of action. Trends Biotechnol. **2011**, 29(9):464-472

[3] Jenssen, H et al. Peptide antimicrobial agents. Clin.Microbiol.Rev. **2006**, 19(3):491-511

[4] Masschalck, B et al. Antimicrobial properties of lysozyme in relation to foodborne vegetative bacteria. Crit.Rev.Microbiol. **2003**, 29(3): 191-214

[5] Pellegrini, A et al. Effect of lysozyme or modified lysozyme fragments on DNA and RNA synthesis and membrane permeability of *Escherichia coli*. Microbiol. Res. **2000**, 155(2): 69-77

[6] Desfougères, Y. et al. Succinimidyl Residue Formation in Hen Egg-White Lysozyme Favors the Formation of Intermolecular Covalent Bonds without Affecting Its Tertiary Structure. Biomacromol. **2011**, 12(1): 156-166

EXPLORING THE MECHANISMS OF MEMBRANE INSERTION OF NATIVE AND DRY-HEATED LYSOZYME: USE OF *E. COLI* LIPOPOLYSACCHARIDE MONOLAYERS

Melanie Derde[1,2], Françoise Nau[1,2], Valérie Lechevalier[1,2], Catherine Guérin-Dubiard[1,2], Gilles Paboeuf [3], Sophie Jan[1,2], Florence Baron[1,2], Michel Gautier[1,2], Véronique Vié[3]

1) Agrocampus Ouest, UMR1253 Science et technologie du lait et de l'œuf, F-35042 Rennes, France
2) INRA, UMR1253 Science et technologie du lait et de l'œuf, F-35042 Rennes, France
3) Université de Rennes 1, Institut de physique de Rennes, UMR6251, CNRS, F-35042 Rennes, France

Antibiotic resistance causes public health problems and stimulates research for novel antimicrobials. Particular attention is given to molecules that limit drug resistance development.[1] Hen egg white lysozyme acting on the bacterial cell envelope through its physico-chemical properties is thus a good candidate.[2,3] However, its antimicrobial effect caused by membrane permeabilization on Gram-negative bacteria remains limited. But some physico-chemical modifications of the lysozyme can modify its membrane activity, increasing lysozyme antimicrobial properties against *E. coli*; dry-heating is able to induce such modifications.[4] Especially, we previously highlighted that native (N-L) and dry-heated lysozyme (DH-L) disrupt the outer membrane of *E. coli*, but in different ways.[3,4] The mode of insertion into the bacterial outer membrane and molecular interactions remains unknown.

This was thus investigated using an *E. coli* lipopolysaccharide monolayer (LPSM) membrane model, mimicking the outer leaflet of the bacterial outer membrane. The interactions between lysozyme and LPSM were studied by tensiometry, ellipsometry, atomic force microscopy (AFM) and Brewster angle microscopy (BAM). Both N-L and DH-L are able to insert into a LPSM. As expected, electrostatic interactions between the negatively charged LPSM and both positively charged forms of lysozyme were observed. Furthermore, we could establish that N-L and DH-L insertion into the LPSM depends on the presence of the polysaccharide moieties. These polysaccharide chains might increase the space between the lipid headgroups, enabling lysozyme insertion. Moreover, dry-heating increases the lysozyme affinity for the LPSM. Microscopic observations (BAM and AFM) show that the LPSM reorganizes and reorients in the presence of DH-L, in contrast to N-L. Dry-heating thus improves the lysozyme insertion, which might explain the increased activity on the outer membrane of *E. coli*, resulting in a higher antimicrobial effect.

Références:
[1]Nguyen et al., The expanding scope of antimicrobial peptide structures and their modes of action, Trends Biotechnol.,29, 9, 464-472, **2011**
[2]Masschalck et al., Antimicrobial properties of lysozyme in relation to foodborne vegetative bacteria, Crit.Rev.Microbiol., 29, 3, 191-214, **2003**
[3]Derde et al., Hen egg white lysozyme permeabilizes *Escherichia coli* outer and inner membranes, JAFC, 61, 9922-9929, **2013**
[4]Derde et al., Dry-heating of lysozyme increases its activity against *Escherichia coli* membranes, JAFC, 62, 7, 1692-1700, **2014**

Melanie DERDE

Bourse de thèse Région Bretagne
•
2011-2014

UMR INRA - Agrocampus Ouest
Science et technologie
du lait et de l'œuf

Equipe BN
Bioactivité et nutrition

Mots-clés
Lysozyme
Activité bactéricide
Modification biochimique
Interface phospholipidique

Modifications biochimiques du lysozyme : Des opportunités pour le développement de nouvelles molécules bactéricides ?

Contexte socio-économique

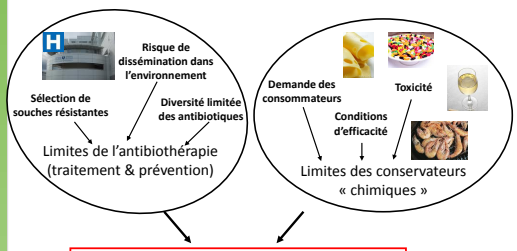

Recherche de molécules antibactériennes d'origine naturelle (diversité structurale, large spectre)

Contexte scientifique

- Le lysozyme : un antibactérien dont l'activité peut être modulée par « design moléculaire »
- Le chauffage en poudre du lysozyme : un procédé simple induisant des modifications biochimiques à l'origine d'une augmentation de ses propriétés interfaciales

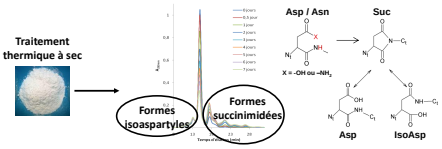

(Desfougères, et al. 2011)

Questions de recherche

- Les formes modifiées originales obtenues par chauffage en poudre du lysozyme induisent-elles des perturbations spécifiques des interfaces phospholipidiques ?

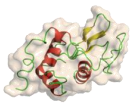

Lysozyme

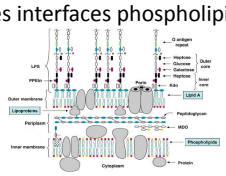

Représentation paroi *E. coli* K12
(Raetz and Withfield , 2002; Kubelt, et al. 2004)

- Quelles conséquences sur les cellules bactériennes *in vivo* en termes d'efficacité bactéricide et de spectre d'action ?

Résultats attendus

- Explorer de nouvelles pistes en matière de fonctionnalisation du lysozyme
  - pour la modulation / amélioration des propriétés bactéricides
  - par le recours à un procédé simple directement industrialisable

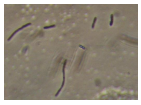

Microscopie optique *E. coli* K12 après traitement au Lysozyme chauffé (0,25 g.L^{-1})

- Enrichir les données concernant le lien entre caractéristiques structurales des protéines et comportement aux interfaces phospholipidiques, modèles des membranes biologiques.

Perspectives

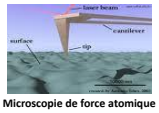

Microscopie de force atomique

Ellipsométrie

- Transfert des connaissances acquises concernant les relations entre les caractéristiques structurales du lysozyme et son comportement interfacial vers le développement de formes « designées » pour des propriétés bactéricides modulées / améliorées
- Utilisation de ces connaissances pour la compréhension, voire l'amélioration d'autres molécules antibactériennes de nature protéique ou peptidique

Références

Desfougères, Y., Jardin, J., Lechevalier, V., Pezennec, S., and Nau, F. (2011) Succinimidyl residue formation in hen egg-white lysozyme favors the formation of intermolecular covalent bonds without affecting its tertiary structure. *Biomacromolecules* **12:** 156-166.

Kubelt, J. (2004) Investigations on the rapid transbilayer movement of phospholipids in biogenic membranes, *PhD thesis Berlin University*

Raetz and Whitfield (2002) Lipopolysaccharide endotoxins, *Annu Rev Biochem* **71:**635-700.

Financeurs

Région Bretagne

Collaborateurs

INRA Rennes

STLO Science et Technologie du Lait et de l'Oeuf

INRA AGRO CAMPUS OUEST

Evidence by AFM-imaging of morphological differences between *E. coli* K12 cells treated with native and dry-heated lysozyme

Melanie Derde[1,2], Françoise Nau[1,2,] Valérie Lechevalier[1,2], Catherine Guérin-Dubiard[1,2], Sophie Jan[1,2], Florence Baron[1,2], Michel Gautier[1,2], Véronique Vié[3]

[1]*Agrocampus Ouest, UMR1253 Science et technologie du lait et de l'œuf, F-35042 Rennes, France*
[2]*INRA, UMR1253 Science et technologie du lait et de l'œuf, F-35042 Rennes, France*
[3]*Université de Rennes 1, Institut de physique de Rennes, UMR CNRS 6251, F-35042 Rennes, France*

Research in the domain of antimicrobial molecules is nowadays a hot topic because of the increasing bacterial resistance against antibiotics; moreover, consumers demand for natural food preservatives is growing. Proteins and peptides from different origins, such as hen egg white lysozyme, seem promising candidates for the discovery of novel and natural antimicrobial compounds. The understanding of the mechanism by which these compounds are active could help goal-oriented screening and design of antimicrobial peptides and proteins. Membrane permeabilization is an interesting mechanism because it causes bacterial cell death, while limiting the development of bacterial resistance [1, 2, 3]. Several tools can be used to investigate membrane perturbations such as spectrophotometric methods using mutant *E. coli* ML-35p, fluorescent probes and AFM-imaging [4, 5, 6].

Lysozyme is a major natural antimicrobial molecule widely used for food and pharmaceutical applications. This small protein (14400 Da) is especially known for its capacity to hydrolyze the peptidoglycan of Gram-positive bacteria [3, 7]. On the other hand, because of the outer membrane of Gram-negative bacteria, lysozyme is almost inactive against these microorganisms. However, some structural modifications of lysozyme are efficient to increase and broaden the antimicrobial activity of lysozyme; thus modified lysozyme would operate by disturbing the bacterial membrane [2, 8]. Dry-heating of lysozyme (80°C for 7 days) could be an interesting way to increase the lysozyme antimicrobial activity, since this process makes the protein much more tensio-active than the native form [9].

Native and dry-heated lysozymes have been compared for their activity against *E. coli* K12, a model Gram-negative bacteria. Bacterial growth has been measured for 24 h in Luria Broth containing 0.5 g/L NaCl at 37°C, in the presence of native or dry-heated lysozyme with concentrations ranging from 0.05 g/L to 3.7 g/L. The inner and outer membrane permeabilization has been measured using the mutant *E. coli* ML-35p. The morphological characteristics of the bacteria have been investigated by AFM after 24 h of contact with native or dry-heated lysozyme.

E. coli K12 growth is disturbed in the presence of both native and dry-heated lysozyme, but the inhibition is larger at high concentration (3.7 g/L) of dry-heated lysozyme. Similarly, permeabilization of the outer and inner membranes was observed with both native and dry-heated lysozyme, in a concentration-dependant way. On the contrary, AFM-imaging enables to distinguish between bacterial cells which were non-treated, treated with native lysozyme, or with dry-heated lysozyme. The size of non-treated cells is about 2 µm long x 500 nm diameter; the surface is quite smooth and regular, and flagella can be observed (figure 1). When treated with 0.25 g/L native lysozyme, only small differences such as higher rigidity of cells are observed, compared to the non-treated cells (figure 2); similar images are obtained with 3.7 g/L native lysozyme. But when treated with 0.25 g/L dry-heated lysozyme, bacteria cells appear strongly disturbed, with especially irregular cell surface, local depressions, and disturbance of cell division (figure 3); besides well defined bacteria cells, cell debris are also observed (figure 4). Equivalent images are obtained after incubation with 3.7 g/L dry-heated lysozyme. This underlines that AFM is a relevant and efficient tool to investigate antibacterial activity of native and modified lysozymes, since it highlights differences that are not easily detectable with usual microbiological and biochemical methods.

References

[1] Nguyen, L.T. ; Haney, E.F. and Vogel, H.J. *Trends in Biotechnology,* **2011**, *29*, 464
[2] Masschalk, B. and Michiels, C.W. *Critical Reviews in Microbiology* **2003**, *29*, 191
[3] Mine, Y. and Kovacs-Nolan, J. *Journal of Poultry Science* **2004**, *41*, 1
[4] Lehrer, R.I.; Barton, A. and Ganz, T. *Journal of Immunological Methods* **1988**,*108*,153
[5] Wu, M.; Maier, E.; Benz, R.; Hancock, R.E.W. *Biochemistry* **1999**, *38*, 7235
[6] Braga, P.C. and Ricci, D. *Antimicrobial Agents and Chemotherapy* **1998**, *42*, 18
[7] Jolles, P. and Jolles, J. *Molecular and Cellular Biochemistry* **1984**, *63*, 165
[8] Ibrahim, H.R. *Molecular and Cellular Biochemistry* **1984**, *63*, 165
[9] Desfougères, Y; Jardin, J; Lechevalier, V. Pezennec, S. and Nau, F. *Biomacromolecules* **2011**, *12*, 156

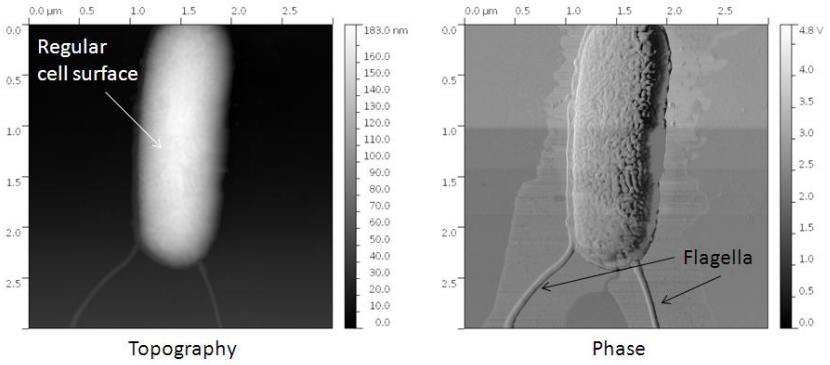

Figure 1: AFM-images of untreated *E. coli* K12 after 24 h incubation

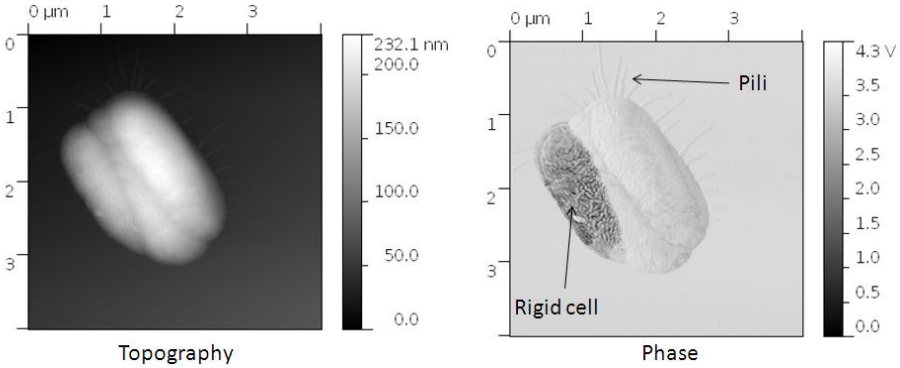

Figure 2: AFM-images of *E. coli* K12 treated with 0.25 g/L native lysozyme for 24 h

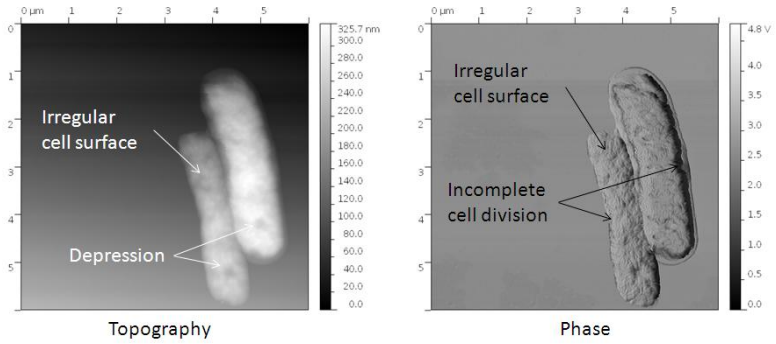

Figure 3: AFM-images of E. coli K12 treated with 0.25 g/L dry-heated lysozyme for 24 h

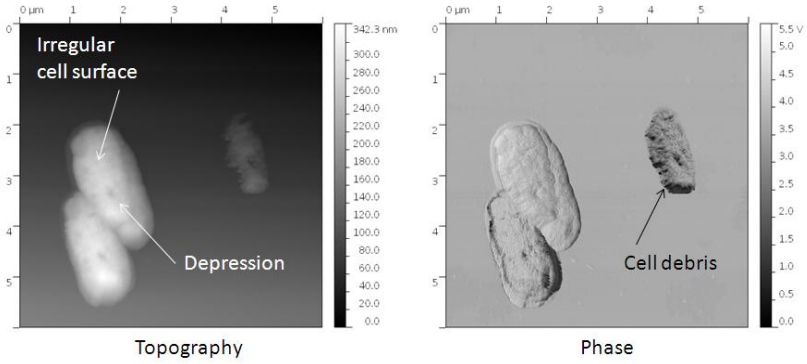

Figure 4: AFM-images of E. coli K12 treated with 0.25 g/L dry-heated lysozyme for 24 h

Evidence by AFM-imaging of morphological differences between *E. coli* K12 cells treated with native and dry-heated lysozyme

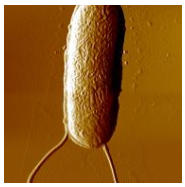

M. Derde[1,2], F. Nau[1,2], V. Lechevalier[1,2], C. Guérin-Dubiard[1,2], S. Jan[1,2], F. Baron[1,2], M. Gautier[1,2], V. Vié[3]

[1] *Agrocampus Ouest, UMR1253 Science et technologie du lait et de l'oeuf, F-35042 Rennes, France*
[2] *INRA, UMR1253 Science et technologie du lait et de l'oeuf, F-35042 Rennes, France*
[3] *Université de Rennes 1, Institut de physique de Rennes, UMR CNRS 6251, F-35042 Rennes, France*
melanie.derde@agrocampus-ouest.fr

Dry-heating of hen egg white lysozyme

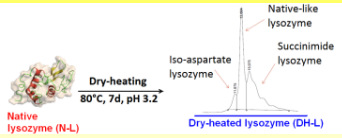

Dry-heated lysozyme contains three different lysozyme entities, separated by cation exchange chromatography

Influence of dry-heating on the biochemical characteristics of lysozyme

Secondary and tertiairy protein structures remain unchanged

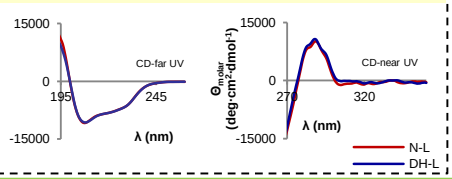

Surface hydrophobicity is increased

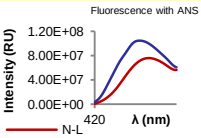

Muramidase activity is decreased

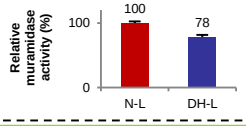

Dry-heated lysozyme: an opportunity for a natural, large spectrum antimicrobial protein ?

Growth of *E. coli* K12 in the presence of N-L and DH-L

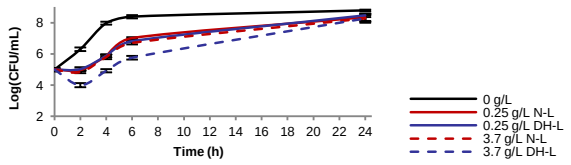

Dry-heated lysozyme inhibits the growth of the Gram-negative bacterium *E. coli* more efficiently than native lysozyme at high protein concentrations.

Is higher membrane activity the cause of the increased antimicrobial activity of dry-heated lysozyme on *E. coli* K12 ?

Different tools for the detection of bacterial membrane perturbation mechanisms

1) Quantification of changes in the bacterial membrane potential

Dry-heated lysozyme at 3.7 g/L disturbs the membrane potential of *E. coli* K12 more than native lysozyme.

2) Quantification of outer/ inner membrane permeabilization using E. coli ML-35p

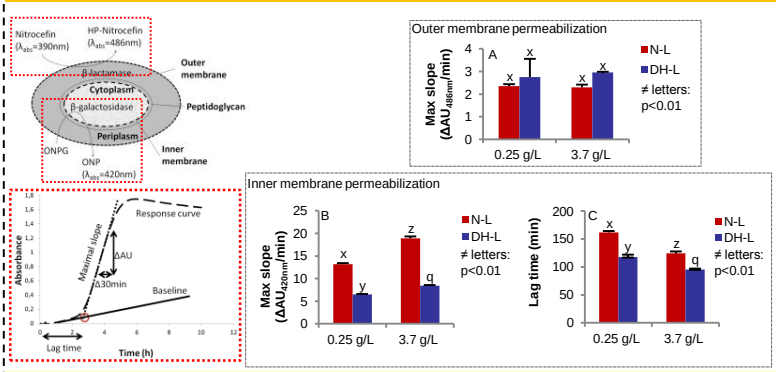

Native and dry-heated lysozyme permeabilize the outer and inner membrane of *E. coli* ML-35p. Outer membrane permeabilization is equivalent for native and dry-heated lysozyme (A). Inner membrane permeabilization is more pronounced for native lysozyme (B). However dry-heated lysozyme permeabilizes more rapidly the inner membrane (C).

3) Observations of the bacterial morphology by Atomic Force Microscopy (AFM)

Observations of mean length, width and height of multiple imaged bacterial cells with different treatments. (0.25 g/L DH-L contained multiple cell morphologies (individual cell /cell showing perturbated cell division/ highly deteriorated cell), the mean was thus not calculated)

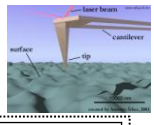

	0 g/L	N-L 0.25 g/L	N-L 3.7 g/L	DH-L 0.25 g/L	DH-L 3.7 g/L
Length (µm)	2.39	2.18	2.43	2.43/4.39/1.6	2.37
Width (nm)	722	593	1228	867/995/700	878
Height (nm)	170	113	49	175/186/35.6	71

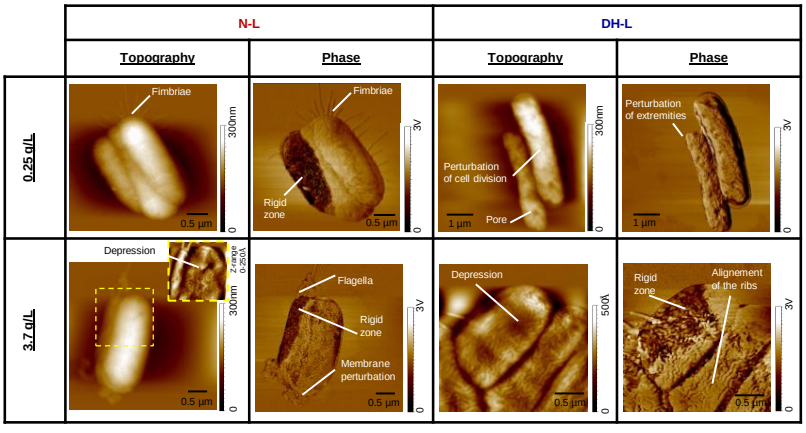

E. coli K12 morphology is highly affected when treating the bacterial cells with lysozyme:

- high concentrations of lysozyme decrease cell height
- pores have been detected for a 0.25 g/L DH-L and 3.7 g/L N-L treatment
- 0.25 g/L DH-L treatment causes perturbation of cell division
- 3.7 g/L DH-L causes the alignment of the ribs present on the bacterial cell surface
- fimbriae and flagella were present independently of the lysozyme doses or type

These results show that AFM is a very powerful and useful tool to study the damage caused by antimicrobial molecules on the bacterial cell. This technique can show differences left unnoticed by other more classically used methods.

VIII / Presentation solicited: POSTER

BACTERIAL MEMBRANE PERTURBATION BY NATIVE *VERSUS* DRY-HEATED LYSOZYME

Melanie Derde[1,2], Catherine Guérin-Dubiard[1,2], Valérie Lechevalier[1,2], Sophie Jan[1,2], Florence Baron[1,2], Michel Gautier[1,2], Véronique Vié[3] and Françoise Nau[1,2]

1 Agrocampus Ouest, UMR 1253 STLO, rue de St-Brieuc 65, 35042 Rennes, France ; [2] INRA,UMR 1253 STLO, rue de St-Brieuc 65, 35042 Rennes, France ; [3] Université de Rennes 1, UMR CNRS 6251, Institut de Physique de Rennes, 35042 Rennes, France (melanie.derde@agrocampus-ouest.fr)

Keywords: Lysozyme; Gram-negative bacteria, Bacterial membrane perturbation

Antimicrobial drug resistance causes public health problems worldwide and stimulates research for novel antimicrobials.[1] Particular attention is given to antimicrobial molecules that limit drug resistance development and have a large spectrum. Antimicrobial peptides and proteins are thus good candidates acting on the bacterial cell wall because of their physico-chemical properties[2] These antimicrobial peptides and proteins can thus perturb the bacterial cell envelope, enter the cell, and/or act on intracellular targets.[2,3] Hen egg white lysozyme is largely studied and widely known for its muramidase activity against the peptidoglycan of Gram-positive bacteria.[4] However, lysozyme is also described as being active against some Gram-negative bacteria, especially because it permeabilizes the bacterial membranes.[4,5] But few is known about this activity, and the consequences remain quite limited. Since dry-heated lysozyme (DHL) is more positively charged, more hydrophobic and more tensio-active than native lysozyme (NL)[6], dry-heating could be a way to increase lysozyme activity against the bacterial membranes, and especially against Gram-negative bacteria.

To investigate the membrane activity of both NL and DHL, membrane permeability measurements using a mutant *E. coli* ML-35p and measurements of membrane potential perturbation were performed. These experiments revealed that NL and DHL induce different consequences on the bacterial membranes. NL permeabilizes both outer (OM) and inner (IM) membranes. Pore formation could be observed for OM, but not for IM. Moreover, the membrane potential of IM is modified in the presence of NL. DHL induces an overall stronger disturbance than NL, by giving rise to the formation of more and/or larger pores in OM, by permeabilizing more rapidly IM, and by leading to a stronger disturbance of membrane potential.

[1]WHO. Overcoming antimicrobial resistance. **2000;** [2]Nguyen, NT et al. Trends Biotechnol. **2011**, 29:464-472; [3]Jenssen, H et al. Clin.Microbiol.Rev. **2006**, 19:491-511; [4]Masschalck, B et al. **2003**, 29: 191-214; [5]Pellegrini, A et al. Microbiol. Res. **2000**, 155: 69-77 ; [6]Desfougères, Y. et al. Biomacromol. **2011**, 12: 156-166

Bacterial membrane disruption by native *versus* dry-heated lysozyme

M. Derde[1,2], C. Guérin-Dubiard[1,2], V. Lechevalier[1,2] S. Jan[1,2], F. Baron[1,2], M. Gautier[1,2] , V. Vié[3] and F. Nau[1,2]

[1] *Agrocampus Ouest, UMR1253 Science et Technologie du Lait et de l'Oeuf, F-35042 Rennes, France*
[2] *INRA, UMR1253 Science et Technologie du Lait et de l'Oeuf, F-35042 Rennes, France*
[3] *Université de Rennes 1, Institut de Physique de Rennes, UMR CNRS 6251, F-35042 Rennes, France*
melanie.derde@agrocampus-ouest.fr

Dry-heating of lysozyme and its physico-chemical properties

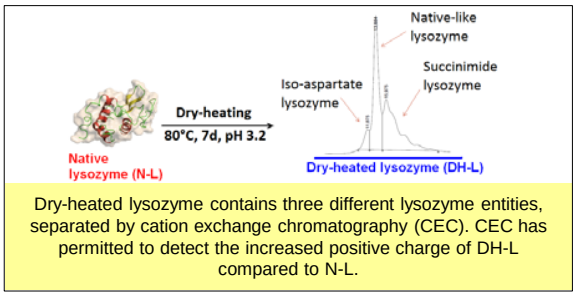

Dry-heated lysozyme contains three different lysozyme entities, separated by cation exchange chromatography (CEC). CEC has permitted to detect the increased positive charge of DH-L compared to N-L.

Secondary and tertiairy protein structures remain unchanged

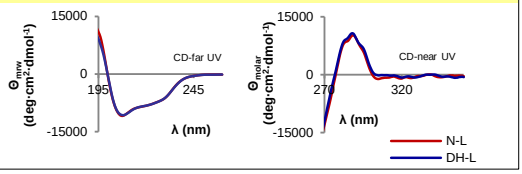

Surface hydrophobicity ↗

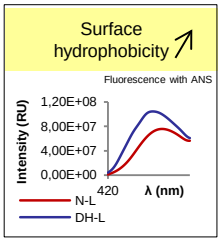

AND

Tensio-activity increase and muramidase decrease

Disruption of the *E. coli* outer and inner membranes by N-L

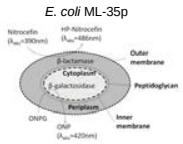

* Measured by HP-nitrocefin absorbance at 486 nm
** Externalised β-lactamase is an indication of pore formation, measured by its enzyme activity (absorbance of HP-nitrocefin at 486 nm)
***Measured by ONP absorbance at 420 nm

Outer membrane

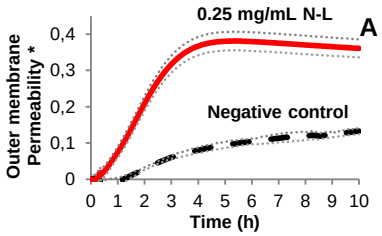

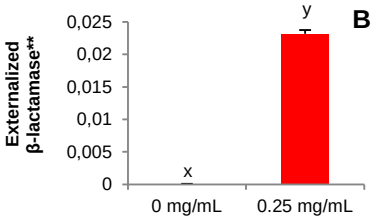

N-L permeabilizes the outer membrane (A) and provokes pore formation (B)

Inner membrane

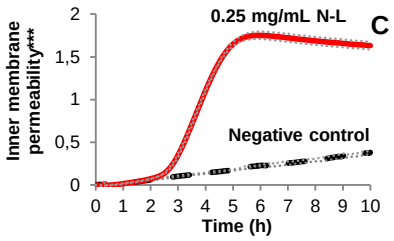

N-L permeabilizes the inner membrane (C)

Disruption of the *E. coli* outer and inner membranes by DH-L compared to N-L

Outer membrane

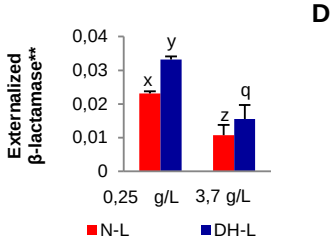

DH-L causes larger and/or more pores than N-L (D)

Inner membrane

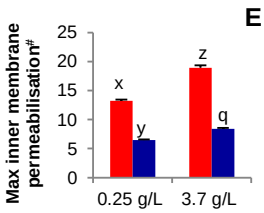

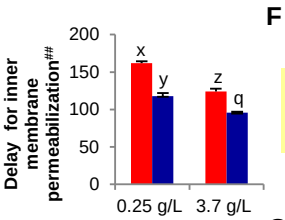

DH-L permeabilizes less severly (E) but more rapidly (F) the inner membrane and without perforations

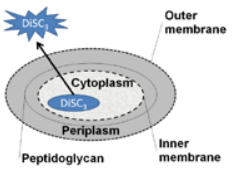

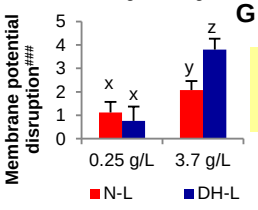

DH-L disrupts more severly the bacterial membrane potential at 3.7 g/L (G)

The maximal inner membrane permeabilization is the maximal slope of the absorbance of ONP at 420 nm in function of time

Measured by the delay between the detection of HP-nitrocefin and ONP by absorbance at 486 nm and 420 nm respectively

Measured by the fluorescence intensity of $DiSC_3$

Conclusions

Native lysozyme permeabilizes the outer and inner membranes of *E. coli.* Dry-heating changes the physico-chemical properties of lysozyme and increases its activity against the outer and inner *E. coli* membranes.

Derde, M. et al, Hen egg white lysozyme permeabilizes *Escherichia coli* outer and inner membranes, *J. Agri. Food. Chem.*, DOI:jf4029199

Exploring the mechanisms of membrane insertion of native and dry-heated lysozyme: use of *E. coli* lipopolysaccharide monolayers

Melanie Derde[1,2](#), Françoise Nau[1,2], Valérie Lechevalier[1,2], Catherine Guérin-Dubiard[1,2], Gilles Paboeuf [3], Sophie Jan[1,2], Florence Baron[1,2], Michel Gautier[1,2], Véronique Vié[3]

[1]Agrocampus Ouest, UMR1253 Science et technologie du lait et de l'œuf, F-35042 Rennes, France

[2]INRA, UMR1253 Science et technologie du lait et de l'œuf, F-35042 Rennes, France

[3]Université de Rennes 1, Institut de physique de Rennes, UMR6251, CNRS, F-35042 Rennes, France

Antibiotic resistance causes public health problems and stimulates research for novel antimicrobials. Particular attention is given to molecules that limit drug resistance development.[1] Hen egg white lysozyme acting on the bacterial cell envelope through its physico-chemical properties is thus a good candidate.[2,3] However, its antimicrobial effect caused by membrane permeabilization on Gram-negative bacteria remains limited. But some physico-chemical modifications of the lysozyme can modify its membrane activity, increasing lysozyme antimicrobial properties against *E. coli*; dry-heating is able to induce such modifications.[4] Especially, we previously highlighted that native (N-L) and dry-heated lysozyme (DH-L) disrupt the outer membrane of *E. coli*, but in different ways.[3,4] The mode of insertion into the bacterial outer membrane and molecular interactions remains unknown.

This was thus investigated using an *E. coli* lipopolysaccharide monolayer (LPSM) membrane model, mimicking the outer leaflet of the bacterial outer membrane. The interactions between lysozyme and LPSM were studied by tensiometry, ellipsometry, atomic force microscopy (AFM) and Brewster angle microscopy (BAM). Both N-L and DH-L are able to insert into a LPSM. As expected, electrostatic interactions between the negatively charged LPSM and both positively charged forms of lysozyme were observed. Furthermore, we could establish that N-L and DH-L insertion into the LPSM depends on the presence of the polysaccharide moieties. These polysaccharide chains might increase the space between the lipid headgroups, enabling lysozyme insertion. Moreover, dry-heating increases the lysozyme affinity for the LPSM. Microscopic observations (BAM and AFM) show that the LPSM reorganizes and reorients in the presence of DH-L, in contrast to N-L. Dry-heating thus improves the lysozyme insertion, which might explain the increased activity on the outer membrane of *E. coli*, resulting in a higher antimicrobial effect.

[1]Nguyen et al., Trends Biotechnol., **2011**

[2]Masschalck et al., Crit.Rev.Microbiol., **2003**

[3]Derde et al., JAFC, **2013**

[4]Derde et al., JAFC, **2014,** accepted

Exploring the membrane insertion of native and dry-heated lysozymes into *E. coli* lipopolysaccharide monolayers

M. Derde[1,2], F. Nau[1,2], V. Lechevalier[1,2], C. Guérin-Dubiard[1,2], G. Paboeuf[3], S. Jan[1,2], F. Baron[1,2], M. Gautier[1,2] and V. Vié[3]

[1] *Agrocampus Ouest, UMR1253 Science et Technologie du Lait et de l'Oeuf, F-35042 Rennes, France*
[2] *INRA, UMR1253 Science et Technologie du Lait et de l'Oeuf, F-35042 Rennes, France*
[3] *Université de Rennes 1, Institut de Physique de Rennes, UMR CNRS 6251, F-35042 Rennes, France*
melanie.derde@agrocampus-ouest.fr

Pore formation in the *E. coli* outer membrane

E. coli ML-35p

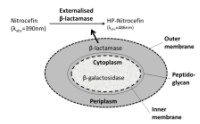

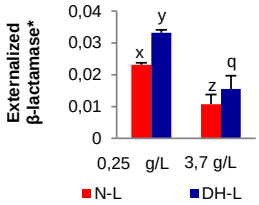

*Externalised β-lactamase is an indication of pore formation, measured by its enzyme activity after elimination of the bacterial cells by centrifugation (absorbance of HP-nitrocefin at 486 nm)

DH-L causes larger and/or more pores than N-L.

In vivo testing has its limitations for the observation of the interaction mechanism of both lysozymes and the outer membrane.
Therefore, a LPS monolayer mimicking the outer membrane of *E. coli* will be used.

E. coli LPS structure

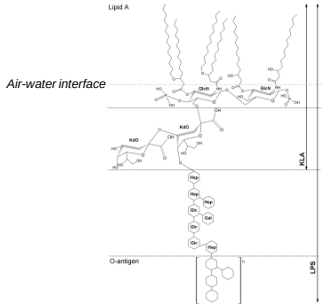

Insertion capacity and affinity for the LPS monolayer

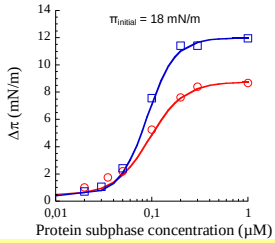

The insertion capacity of DH-L is higher than that of N-L at concentrations above 0,05 µM

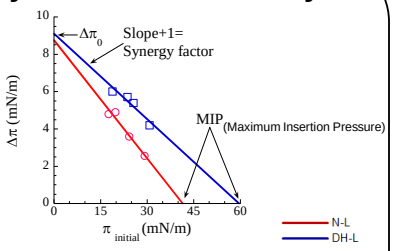

The affinity of DH-L for LPS monolayers is higher than that of N-L

Lysozyme insertion needs the presence of polysaccharide moieties

KLA monolayer

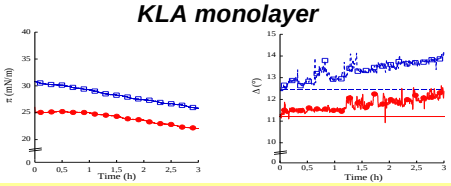

N-L and DH-L do not insert into the KLA monolayer…

…however they are present at the KLA/liquid interface

LPS monolayer

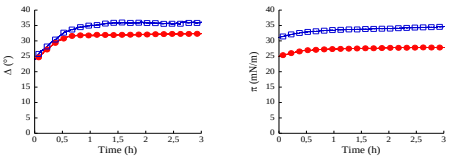

N-L and DH-L adsorb to the LPS monolayer…

…and insert into the LPS monolayer

LPS organization after lysozyme injection

BAM ellipsometry

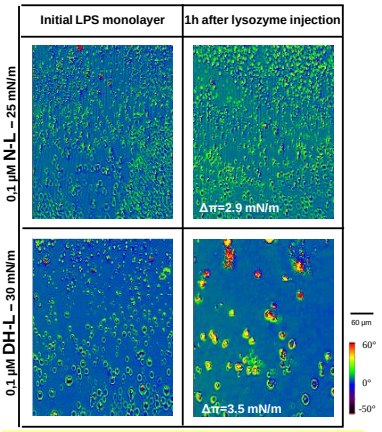

DH-L reorganizes the LPS monolayer at a µm-scale by creating large high-delta-angle zones

AFM imaging

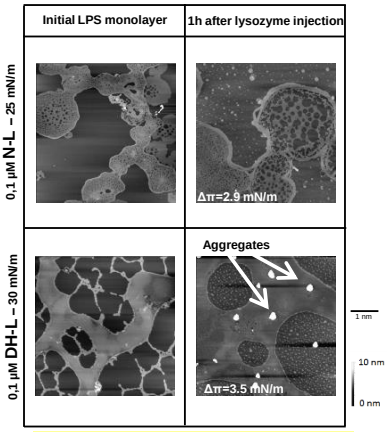

DH-L reorganizes the LPS monolayer at a nm-scale by creating large aggregates

DH-L reorganizes the LPS monolayer more severly than N-L

Conclusions

Native and dry-heated lysozymes are able to insert and to reorganize a LPS monolayer.
Dry-heated lysozyme acts more severely than native lysozyme.

Résumé

La recherche de nouveaux composés antimicrobiens naturels est un enjeu important pour répondre d'une part à la problématique des bactéries multirésistantes et d'autre part à la demande croissante de conservateurs naturels. Les protéines et peptides antimicrobiens agissant sur les membranes bactériennes semblent de bons candidats. Une des premières protéines antimicrobiennes découvertes est le lysozyme, connu depuis longtemps pour son activité muramidase contre les bactéries à coloration de Gram positive. Récemment, le lysozyme s'est avéré également actif contre les bactéries à coloration de Gram négative. L'activité membranaire du lysozyme est considérée comme un des mécanismes possibles responsables de cette activité.
Dans ce travail, l'activité du lysozyme vis-à-vis des membranes d'*E. coli* a été évaluée. Le lysozyme affecte l'intégrité des deux membranes : des pores et des canaux ioniques sont formés respectivement dans les membranes externe et cytoplasmique. Des monocouches de LPS et de phospholipides ont été utilisées pour mimer respectivement les membranes externe et cytoplasmique. Le lysozyme peut s'adsorber à, s'insérer dans et réorganiser les deux monocouches de manière dose-dépendante. Ces résultats obtenus sur membranes modèles sont cohérents avec les observations de perturbations membranaires *in vivo*.
Le lysozyme chauffé à sec, plus flexible, hydrophobe et basique que la protéine native, a une activité antimicrobienne accrue par rapport au lysozyme natif. Cette activité peut être reliée à sa plus grande capacité de perturbation des membranes *in vivo*. De même, le lysozyme chauffé à sec induit une réorganisation des monocouches plus drastique que le lysozyme natif. En fait, le lysozyme chauffé à sec se révèle être un mélange efficace d'isoformes agissant différemment et de manière complémentaire sur les membranes d'*E. coli*.

Mots clés : Lysozyme, Chauffage à sec, Isoformes du lysozyme, Escherichia coli, Activité membranaire, Monocouche de LPS, Monocouche de phospholipides, Interaction lysozyme/lipides

---

Abstract

Research for novel natural antimicrobial compounds is highly stimulated because of the growing number of multi-resistant bacteria on the one hand and the growing consumer demand for natural conservatives on the other hand. Antimicrobial peptides or protein acting on the bacterial membranes could answer this demand. One of the first discovered antimicrobial proteins is lysozyme, is widely known for its muramidase activity against several Gram positive bacteria. Recently, lysozyme was also shown active against Gram negative bacteria. Membrane activity of lysozyme is suggested as one of the possible mechanisms involved.
In this work, lysozyme activity on both the outer and cytoplasmic membranes of *Escherichia coli* is evaluated *in vivo* and *in vitro*. Lysozyme has been shown to affect the integrity of both membranes ; pores and ion channels are formed in the outer and cytoplasmic membranes, respectively. LPS and phospholipid monolayers have been used to mimic the *E. coli* outer and cytoplasmic membranes, respectively. Lysozyme is able to adsorb onto, to insert into and to reorganize LPS and phospholipid monolayers in a dose-dependent manner. These findings on lipid membrane models are consistent with the membrane disruption observed *in vivo*.
Dry-heated lysozyme, more flexible, hydrophobic and basic than the native protein, has here been shown to exhibit an increased antimicrobial activity compared to native lysozyme. This activity could be related to its increased membrane disruption capacity *in vivo*. As well dry-heated lysozyme is able to reorganize LPS and phospholipid monolayers in a larger extent than native lysozyme. Actually, dry-heated lysozyme appears to be a efficient, mixture of complementary lysozyme isoforms acting differently on the *E. coli* membranes.

Keywords : Lysozyme, Dry-heating, Lysozyme isoforms, Escherichia coli, Membrane activity, LPS monolayer, Phospholipid monolayer, Lysozyme-lipid interaction